D-MEM
PhD-UNIMI

Doctorate program
Milan
EXPERIMENTAL
MEDICINE

Università degli Studi di Milano

PhD Course in
Experimental Medicine

CYCLE XXXIV

PhD thesis

LIPIDOMIC CHARACTERIZATION OF CELL SECRETOME COMBINED WITH THE STUDY OF SELECTED BIOACTIVE LIPIDS IN AN OSTEOARTHRITIS MODEL

Candidate: **Dr. Sara Casati**
Matr. R12182

Tutor: **Prof. Anna T. Brini**

Supervisor: **Dr. Chiara Giannasi & Prof. Marica Orioli**

Director: **Prof. Nicoletta Landsberger**

Academic Year 2020-2021

Table of contents

Abstract

Lipidomics is the large-scale identification and quantification of lipids and their variations in various physio-pathological conditions. This recent "-omic" area is rapidly developing as an emerging field, and it sustains the advancement of current knowledge in the realm of lipid biology. Indeed, if lipids are conventionally considered as structural components of cellular membranes, they have emerged recently as key players in a wide range of biological processes such as signaling events and trafficking. However, their precise physio-pathological function is still poorly understood and a comprehensive characterization of lipids in each cell type can provide pivotal information to better understand the roles exercised by these compounds in several biological phenomena. In this project, the attention was focused on the roles of specific bioactive lipids families, as polyunsaturated fatty acids (PUFA), PUFA-derived molecules (known as eicosanoids), endocannabinoids (EC) and EC-related compounds N-acylethanolamines (NAE), and their involvement in the mesenchymal stem/stromal cells (MSC)-related inflammatory context. Indeed, MSC have attracted much attention for their capacity in regulating inflammation and reparative roles. Since it is known that MSC therapeutic action largely depends on paracrine mechanisms, the scientific interest has shifted to the study of their secretome, namely conditioned medium (CM). The therapeutic potential of the CM, derived from MSC in disparate medical fields (from immunology to orthopedics), has been extensively endorsed by *in vitro* and *in vivo* evidence. However, lipidomics knowledge in the MSC field and their secretome remain rather limited and a broadly characterization of lipids is still missing. In recent years, our group have investigated and characterized the adipose-derived stem/stromal cells (ASC)-CM content, in terms of both soluble factors and vesicular components (extracellular vesicles – EV), through different approaches (i.e.Raman spectroscopy and proteomic analysis), highlighting substantial differences in the total lipid content and inflammatory factors between CM and EV. In this project, two advanced mass spectrometry (MS) analytical methods for the absolute quantification of 32 bioactive lipid molecules - belonging to PUFA, eicosanoids and EC/NAE families and highly implicated in the inflammatory scenario - were developed and validated according to the Food and Drug Administration guidelines. A double liquid-liquid extraction step was set up, starting from a single sample, in different mixture of organic solvents, to cover the broad polarity range of selected analytes. Linearity was observed in the range of 0.1-2.5ng/ml (1-25ng/ml for PUFA) with a r^2>0.991. Regarding precision and accuracy, the methods showed good performance in terms of both repeatability and

reproducibility, showing CV values below 15%, while lowest limits of quantitation (LLOQ) were <0.1ng/ml. Extraction recovery, matrix effect and post-extraction stability values were within acceptance limits. The analytical methods were applied to the secretome (in terms of CM and EV) derived from MSC, isolated either from human bone marrow (BMSC) or adipose tissue (ASC), and from dermal fibroblasts (DF), since they share common characteristics with MSC, and they have started to be considered a convenient alternative. A total of 9 lipid molecules in MSC and DF-derived CM and EV samples were quantified. In detail, the presence of 5 EC/NAE (including 2-arachidonoilglycerol -2AG- and N-palmitoylethanolamide -PEA) and 3 PUFA were reported in both preparations. Prostaglandin E2 (PGE2) was found only in CM samples. An enrichment in lipid content were displayed in almost all MSC-CM and DF-CM rather than coupled MSC- and DF-derived EV. Then, the biological function of 2 lipid compounds quantified in ASC-CM - 2AG and PEA – was assessed in a well-established *in vitro* model of osteoarthritis (OA), based on the administration of 10ng/ml tissue necrosis factor alfa (TNFα) to human primary articular chondrocytes (CH). The CH were isolated by femoral head of 14 patients and treated with TNFα alone or in association with 2AG and PEA at observed ASC-CM concentrations (0.05 and 0.02 ng/mL per million cells, respectively). The expression of both CB1 and CB2 on primary articular CH was confirmed by western blot (WB) analysis. TNFα increases the extracellular concentration of the inflammatory lipid prostaglandin E2 (PGE2) analyzed by MS and an additional increment was highlighted when CH were treated with the combination of TNFα and 2AG. In contrast, PEA showed a protective effect on the PGE2 release, providing a downmodulation up to the levels quantified in inactivated CH. Accordingly, TNFα increased the expression of cyclooxygenase 2 (COX2) especially when in association with 2AG, while PEA partly blunts TNFα-induced COX2. In parallel, also the nitric oxide (NO) production in CH cell media was significantly enhanced under TNFα as well as TNFα+2AG treatments, while PEA was able to blunt NO release. Finally, the targeted MS analysis, using previously described analytical methods, showed a significant decrease in PUFA induced by TNFα, suggesting a possible implication in PUFA-derived mediators effect. Our results allowed a first partial lipids characterization of MSC and DF secretome, demonstrating a specific lipid profile for CM and EV and supporting a possible implication of some bioactive lipids molecules in the OA scenario and in the future use of this cell-free products therapeutic approach.

Disclosure for research integrity

This research was conducted following the European Code of Conduct for Research Integrity, which includes the values of reliability, rigor, honesty, respect and transparency.

Abbreviations

2AG 2-arachidonoilglycerol

AA arachidonic acid

ACN acetonitrile

AEA anandamide

ASC adipose-derived stem cells

BM bone marrow

BMSC bone marrow-derived stem cells

CB cannabinoid receptors

CB1 cannabinoid receptor 1

CB2 cannabinoid receptor 2

CBD cannabidiol

CDMEM complete culture medium

CH chondrocytes

CM conditioned medium

COX cyclooxygenases

COX1 cyclooxygenases 1

COX2 cyclooxygenase 2

CS calibration standards

CV coefficient of variation

DAGL diacylglycerol lipase

DCM dichloromethane

DF dermal fibroblasts

DHA docosahexaenoic acid

DHEA N-docosahexaenoylethanolamine;

EC endocannabinoids

ECM extracellular matrix

EET epoxyeicosatrienoic acids

EPA eicosapentaenoic acid

EPEA N-eicosapentaenoylethanolamine

ESI electrospray ionization

ETE epoxyeicosatrienoids

EtOAc ethyl acetate

EV extracellular vesicles

FA fatty acyls

FAAH fatty acid amide hydrolase

GC gas chromatography

GL glycerolipids

GP glycerophospholipids

GPCR G protein-coupled receptor

HCL hydrochloride acid

HETE hydroxyeicosatetraenoic acids

HPLC high-performance liquid chromatography

HPLC-MS high-performance liquid chromatography coupled to mass spectrometry

IFNγ interferon gamma

IL1a interleukin-1a

IL1β interleukin-1beta

iNOS inducible nitric oxide synthase

IPA isopropanol

IS internal standards

ISEV International Society for Extracellular Vesicles

LC liquid chromatography

LGP lysoglycerophospholipids

LLE liquid-liquid extraction

LMSD LIPID MAPS Structure Database

LOD limits of detection

LOQ lowest limits of quantitation

LOX lipoxygenases

LP lysophospholipids

LPC lysophosphatidylcholines

LT leukotrienes

LX lipoxins

LXA4 lipoxin A4

MaR maresins

MeOH methanol

MMP matrix metalloproteinases

MRM multiple reaction monitoring

MS mass spectrometry

MS/MS tandem mass spectrometry

MSC mesenchymal stem cells

MUFA monounsaturated fatty acids

NADA N-arachidonoyldopine

NAE N-acylethanolamines

NAGly N-arachidonoylglycine

NLS neutral loss scan

NO nitric oxide

NP normal-phase

NSAID non-steroidal anti-inflammatory drugs

OA osteoarthritis

p38-MAPK P38 mitogen activated protein kinases

PBS phosphate buffer

PC phosphatidyl choline

PD protectin

PEA N-palmitoylethanolamide

PG prostaglandins

PGE2 prostaglandin E2

PGJ2 prostaglandin J2

PI phosphatidylinositols

PIS precursor ion scan

PK polyketides

PPARα receptor peroxisome proliferator-activated receptor alpha

PR prenol lipids

PUFA polyunsaturated fatty acids

ROS reactive oxygen species

RP reversed-phase

RT retention times

Rv resolvins

S1P sphingosine 1-phosphate

S1PR1 sphingosine 1-phosphate receptor 1

SEA N-stearoylethanolamide

SFA saturated fatty acids

SK sphingosine kinases

SL saccharolipids

SP sphingolipids

SM starving medium

SP sphingolipids

SPE solid phase extraction

SPM specialized pro-resolving mediators

SRM selective reaction monitoring

ST sterols

THC delta9-tetrahydrocannabinol

TIMP tissue inhibitors of metalloproteinases

TLC thin-layer chromatography

TNFα tumor necrosis factor alpha

TRPV1 transient receptor potential vanilloid type 1

TX thromboxanes

UHPLC ultra-high-performance liquid chromatography

UHPLC−ESI-MS/MS ultra-high-performance liquid chromatography-ESI-tandem-MS

WB western blot

1. Introduction

1.1 Lipidomics

In the last decades, lipidomics has evolved rapidly due to its capability to offer new opportunities for studying the roles of lipids in cellular biology as well as in health and disease (1). The lipidome is the complete set of lipid molecules within a cell, a tissue or an organism that regulates cell membranes dynamics, energy storage for cellular maintenance and/or serves as precursors of intra- and intercellular bioactive signaling molecules (2,3). Research focused in this field highlighted how the lipidome, as well as the transcriptome and the proteome, is in a dynamic balance and changes in diet, physio-pathological conditions and external stimuli can affect its stability (4,5). The diverse functions of lipids are highly dependent on their structures, their concentration levels, and their inter- and intracellular temporal e spatial distributions. Since 2005, lipids have been classified in eight main categories: (a) fatty acyls (FA), (b) glycerolipids (GL), (c) glycerophospholipids (GP), (d) sphingolipids (SP), (e) sterols (ST), (f) prenol lipids (PR), (g) saccharolipids (SL), and (h) polyketides (PK) (Fig. 1) (6). Further subclassifications, based on structural moieties and physio-chemical features (e.g., charge, polarity, size, shape etc.) characterizing each of these eight lipid categories, has lead to a total of 46,090 lipids in the LIPID MAPS Structure Database (LMSD), among which 24,145 molecules are curated and 21,945 are computationally generated lipids (August 2021).

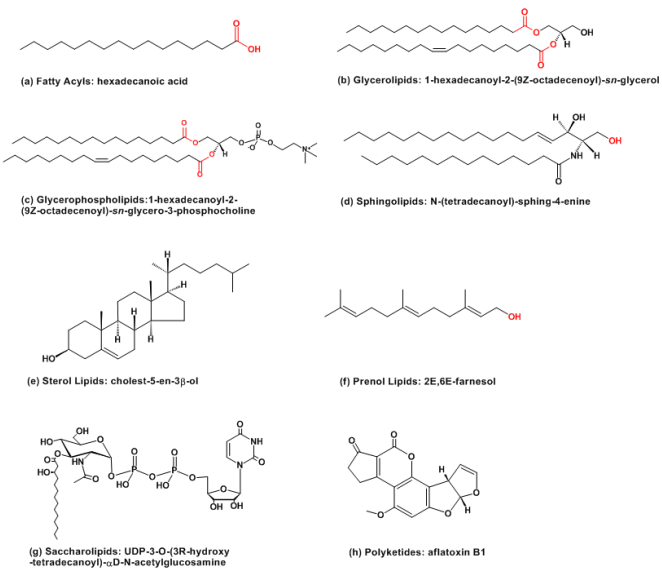

Fig 1. Lipid classification according to the International Lipids Classification and Nomenclature Committee: one representative structure is shown for each category (7)

1.1.1 Advances in mass spectrometry (MS) based lipidomics

Over the last three decades, technical advances in analytical method development have enabled large-scale investigations on cellular lipids. With analytical approaches, such as thin-layer chromatography (TLC) and gas chromatography (GC), lipidomics provides new diagnostic tools and therapeutic strategies (8); but more considerable enhancements have been driven by the advent of the next-generation mass spectrometry (MS) (9–14). Nowadays, there are two MS strategies to analyze lipids: (i) targeted and (i) non-targeted lipid analysis. The targeted approach is addressed on known lipids and develops a specific method with a high sensitivity for the quantitative analysis. On the other hand, non-targeted approach aims to identify every lipid species concurrently (qualitative or semi-quantitative analysis). Additionally, the development of “soft” ionization techniques (for example the electrospray ionization (ESI) and the exact mass resolution (high resolution mass spectrometers)) have lead to significant advances in the field of lipidomics (15). Indeed, mass analyzers are characterized by different mass accuracy, resolution, detection range and capability to perform tandem-MS (MS/MS) experiments. While higher mass accuracy and resolution enhance the identification of analytes and improve the number of lipids that can be separated by mass to charge ratio (m/z), the triple quadrupole MS-based approach, coupled to ultra-high-performance liquid chromatography-ESI-tandem-MS (UHPLC−ESI-MS/MS) with Multiple Reaction Monitoring (MRM) data acquisition strategies, continue to be the most used for targeted identification and quantitation of lipids studies, where the retention times (RT) and the product ions formed during tandem-MS experiments are used for an exact assignment of the specific lipid identities and concentrations (16).

1.1.2 Lipidomics from sample preparation to data analysis: overview of lipidomic workflow and techniques

A typical lipidomic workflow analysis of biological samples includes (i) sample preparation, (ii) MS-based analysis and (iii) data processing (Fig. 2).

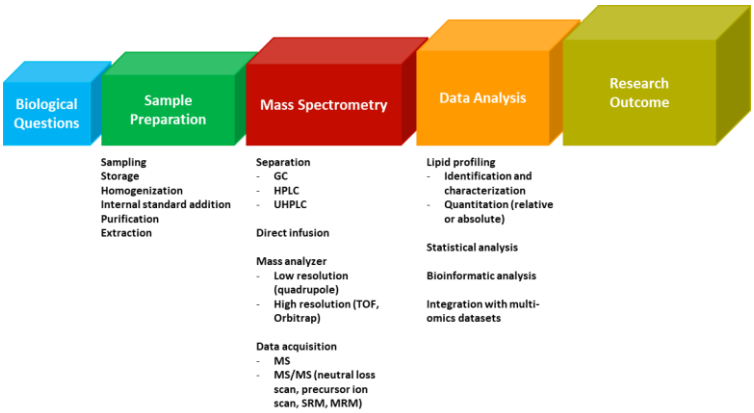

Fig 2. Analytical techniques and workflows for mass spectrometry-based lipidomic analysis. These workflows comprised 3 main components, namely, (i) Sample Preparation, (ii) Mass Spectrometry, and (iii) Data Analysis. The analytical options and commonly used techniques within each component are listed below. Legend: gas chromatography (GC), high-performance liquid chromatography (HPLC), (ultra-high-performance liquid chromatography (UHPLC), mass spectrometry (MS), tandem mass spectrometry (MS/MS), selective reaction monitoring (SRM), multiple reaction monitoring (MRM)

1.1.2.1 Sample preparation

At first, an appropriate sampling and sample storage at fixed temperature is required for any lipidomic analysis (17). Once collected, sample should be immediately processed or frozen at -20 or -80 °C to prevent the enzymatic and chemical processes that might metabolize the lipids (18,19). Moreover, since lipids are prone to hydrolysis and oxidation it is highly advisable to restrict the period of storage. Another crucial issue is the sample homogenization, since it ensures that lipids are equally accessible to the organic extraction solvents. In details, the cell membrane wall needs to be destroyed to reach the intracellular compartments. The most common cells homogenization methods are the shear-force based or frozen based approaches. The lipid extraction is preceded by the addition of appropriate internal standards (IS), which are usually added during the earliest sample preparation step to normalize and correct the matrix effect. The structures and the physicochemical properties of IS must be representative of the endogenous lipid species of interest. Any extraction procedure in lipidomics serve for two main purposes: (i) it reduces the complexity of the sample by removing unwanted compounds of different nature (mainly proteins) (ii) it enhances the lipids of interest in the sample, leading to a better signal-to-noise ratio. Indeed, another critical issue could be the achievement of sufficient efficiency and unbiased recovery

of lipid molecules from the biological matrices. Multiple lipid extraction techniques based on different chemical or physical properties, have been set up for either targeted or non-targeted analysis. Some criteria must be considered in order to develop an efficient extraction method: the lipid category and its physical-chemical properties, sample recovery, repeatability, capability to remove interfering components. Other factors that should be considered are the possibility of automation and cost- and time-saving. Lipids are mainly extracted by liquid-liquid extraction (LLE) or solid phase extraction (SPE) procedures. The LLE is the most implemented technique, particularly the Bligh−Dyer and Folch method (20) continue to be used with some adjustment or modification (i.e. organic and aqueous solvent ratios or acidification/basification in order to enhance the recovery of specific classes of lipids) for peculiar applications (21,22). Some extraction methods replacing ether or chloroform with other less toxic organic solvents. Moreover, the polarity of solvents has been demonstrated to influence the efficiency of the recovery within specific category or class (23), given the range of lipid polarity very wide. SPE is based on reversed-phase (RP), normal-phase (NP) or ion exchange interactions. Available in single column or 96-well plate-based format, SPE is mainly performed in class-specific or targeted lipid class extraction due to their ability to purify the sample and enrich the low abundant analytes.

1.1.2.2 MS-based analysis

Lipid extracts are analyzed by direct infusion into a mass spectrometer (technique known as “shotgun” lipidomics), or separated by liquid (LC) or gas chromatography (GC) prior to detection by MS. These two approaches are complementary : the “shotgun” method allows a larger lipid profiling by simultaneously identifying several classes of lipids, meanwhile LC and GC/MS enable a more targeted analysis through the detection of lipids with similar structures belonging to a single class (1,24,25). Although GC/MS continues to be used for the analysis of fatty acids, LC/MS is the primary chromatographic separation-based technique of choice in the current lipid scenario. Significant improvement in this field continues to be made, mainly providing faster and more efficient separations as well as lower sample consumption (i.e., UHPLC). The HPLC and UHPLC are the most used separation strategies. They allow to separate the molecules of interests depending on the strength of their interaction between the solid stationary phase and the liquid mobile phase. In lipidomics, RP is the most used analysis techniques, and, for this reason, mainly nonpolar and medium-polar lipids have been investigated. A linear or second-degree dependence on

the number of double bonds in the lipid and the total number of carbon elements were found to influence the retention times of lipids (26). Several RP-HPLC separation approaches have been performed for targeted lipidomic analysis using retention time-dependent SRM, MRM, precursor ion scan (PIS) and neutral loss scan (NLS)-mode MS/MS data acquisition methods. Fekete et al. demonstrated that UHPLC permits a good separation efficiency of lipid at slow flow through 2 µm sized particle (27). This discovery determined an exponential growth of UHPLC and UHPLC-MS publications in the field of lipids after its publication.

1.1.2.3 Data processing

Data analysis strategies depend on the availability of libraries for the identification of lipid structures or appropriate processing methods and software tools for “relative” or “absolute” quantitation of their abundances (1,28,29). Finally, statistical and bioinformatic analysis approaches are required to investigate biologically relevant findings from the data to answer the initial research question (29–31) Recently, also integrative analysis of lipidomics data sets with those from their interacting biomolecules (e.g., genomics, transcriptomics, proteomics, and metabolomics) are performed in order to characterize the overall phenotype of the system of interest and to elucidate the functional roles of lipids in complex biomolecular network interactions (32,33).

1.2 Functional lipids in inflammation

Endogenous bioactive lipids and their alteration play a crucial role in different clinical course and pathogenesis, such as inflammation (34,35). Inflammation is an immune response that involves an extensive network of cellular and molecular processes based on multiple preformed or newly synthesized mediators. Based on their structure and biochemical functions, bioactive lipids can be grouped into three different families (Table 1): polyunsaturated fatty acids (PUFA)-derived mediators (known as eicosanoids), endocannabinoids (EC) and lysophospholipids (LP) (36). Additional two subclasses can be identified for bioactive lipids derived from PUFA: one is represented by ω6 arachidonic acid (AA)-derived lipid mediators, including prostaglandins (PG), leukotrienes (LT), thromboxanes (TX), and lipoxins (LX); the other comprises ω3-PUFA-derived lipid mediators (i.e., eicosapentaenoic acid -EPA- and docosahexaenoic acid -DHA-) such as E-series and D-series resolvins (Rv), protectins (PD), and maresins (MaR), collectively termed “specialized pro-resolving mediators” (SPM). EC and EC-like compounds originate from ω6-

and ω3-PUFA metabolism, but also from saturated and monounsaturated fatty acids (SFA and MUFA). Finally, membrane-derived bioactive lipids from LP are grouped into lysoglycerophospholipids (LGP) and lysosphingophospholipids (LSP), based on the glycerol or sphingosine backbone.

Categories	Eicosanoids	Endocannabinoids and related compounds	Lysophospholipids
Structures	Carboxylic acid + hydrocarbon chain; synthesized by chain elongation of an acetyl-CoA with malonyl-CoA	Ethanolamide or other head groups + fatty acids	Polar head group + glycerol or sphingosine backbone
Roles	Cell signaling	Cell signaling	Cell membrane and lipoprotein composition, cell signaling
Sub-classes or examples	PG, TX, LT, LX	AEA, 2AG, PEA, OEA, SEA, DHEA	LGP, LSP

Table 1. Structures, roles and sub-classes or examples of the different categories of bioactive lipids. Adapted by (37)

1.2.1 Eicosanoids

Eicosanoids represent the widest family of bioactive lipids and contain several derivatives of fatty acids with 20-carbon chain, such ω6 AA, or 22-carbon chain, such as ω3 EPA and DHA. AA is released from membrane phospholipids both *via* phospholipase A2 and phospholipase C and is the substrate for three different enzymes, leading to the generation of pleiotropic compounds: (i) cyclooxygenases 1 and 2 (COX1 and COX2) drive the synthesis of PG, prostacyclins, and TX (38,39); (ii) 5-, 12- and 15-lypooxygenases (5/12/15-LOX) produce LT (40,41), LXs (42) and hydroxyeicosatetraenoids (HETE) (43); (iii) P450 epoxygenase generates also HETE and epoxyeicosatrienoids (ETE) (43). ω3 PUFA-derived bioactive products are Rv, PD and MaR. EPA or DHA generate Rv that and can be divided into E-series or D-series, respectively. DHA acts also as a precursor for the biosynthesis of PD and MaR (Fig 3). Generally, the ω6 eicosanoids play is responsible for different inflammatory responses (35). PG seem to promote inflammation by increasing the release of the pro-inflammatory cytokines (44–46), enhancing the innate immunity response (47), recruiting the leukocytes and activating T helper cells (48,49). Vasoconstriction and

vasodilatation are promoted by TX and prostacyclins, respectively (50). On the other hand, the ω3 mediators exert a beneficial action on inflammation, for example by working as substrate competitors that inhibit the conversion of AA into pro-inflammatory eicosanoids or by serving as an alternative substrate in the production of less potent LT, PG and TX. Moreover, ω3 PUFA-derived lipids found in the inflammatory exudate (RvE1 and PD1) show anti-inflammatory and pro-resolving actions both *in vitro* and *in vivo* (44,51).

1.2.2 Endocannabinoids (EC) and related compounds

EC are a group of endogenous lipids that can activate cannabinoid receptors 1 (CB1) and 2 (CB2) in the same way as tetrahydrocannabinol (THC), the major psychoactive component of *Cannabis sativa*. For many years, *Cannabis sativa*-based preparations are being used for recreational and medical purposes (52). THC and the non-psychoactive cannabidiol (CBD) possess anti-inflammatory and analgesic properties, along with anti-emetic (THC) and anxiolytic (CBD) actions (53). Studies performed on cannabis plants and their chemicals lead to the discovery of the endocannabinoid system. The EC system is composed by CB receptors, their endogenous ligands (i.e., EC) and the enzymes involved in the synthesis and degradation of these lipids (54). CB1 and CB2 are G-protein-coupled receptors with seven transmembrane domains associated with the inhibitory Gi/o protein (55). However, several evidences support the existence of other receptors that bind EC, such as GPR55 (56). CB1 and CB2 are differently distributed in the CNS and peripheral tissues (57). CB1 is mainly expressed in the brain, in particular in glutamatergic and c-aminobutyric acid neurons (58), and its distribution has been well characterized in rodents (59) and humans (60). CB1 is also expressed in peripheral organs, including adipocytes, pancreatic cells, lungs, smooth muscle, gastrointestinal tract, liver, reproductive organs, immune system, peripheral sensory nerves, sympathetic nerves, chondrocytes and bone cells (61). CB2 is mainly expressed in the immune system cells such as macrophages, neutrophils, monocytes, B-lymphocytes, T-lymphocytes and microglial cells, but also in skin nerve fibres and keratinocytes, liver, bone cells and chondrocytes (61,62). The main endogenous ligands for CB1 and CB2 are N- arachidonoyl-ethanolamide (AEA) (63) and 2-arachidonoyl-glycerol (2AG) (64,65): AEA is the first isolated EC, represents a partial agonist of CB receptors, while 2AG is a full agonist (Fig 3). Different biosynthetic pathways are responsible for the on demand biosynthesis of both AEA and 2AG from cell membrane lipids: 2AG from diacylglycerol by diacylglycerol lipase (DAGL), while AEA from the

phosphatidylethanolamine by N-acyltransferase and phospholipase D (66). The EC system is involved in an extensive variety of physio-pathophysiological processes: it presents a low tonic activity under physiological conditions, and it is mainly activated in order to maintain the homeostatic equilibrium in the CNS and peripheral tissues (67). Findings suggest the involvement of ECS also in the peripheral regulation of nociception in different inflammatory pain models (68). In detail, AEA exhibits anti-inflammatory properties (69), while 2AG shows both pro- and anti-inflammatory characteristics (70,71). Alterations in homeostasis and progression of the chronic inflammatory status might be responsible for dysfunctions that lead to changes in concentration levels, metabolism, and receptors of EC (72). Moreover, ω3-FA ethanolamides, N-eicosapentaenoylethanolamine (EPEA) and N-docosahexaenoylethanolamine (DHEA) (73,74) could be additional CB receptor agonists (75), and they have been shown to possess anti-inflammatory properties in macrophages (76) and adipocytes (77). In addition to CB1 and CB2 receptors, EC can be actioned also by different receptors. Indeed, besides AEA, other ethanolamides coming from various long-chain fatty acids were discovered, and collectively known as N-acylethanolamines (NAE). Ethanolamides of SFA and MUFA such as palmitic, stearic, and oleic acids, which are more abundant than AEA in mammals, show less activity on CB receptors, but act also on other receptors, like the nuclear receptor peroxisome proliferator-activated receptor-α (PPARα), leading to the trigger of biological events including anti-inflammation and appetite suppression (78,79). In detail, the PPARα-mediated actions of N-palmitoylethanolamide (PEA) include anti-inflammatory, analgesic, anti-epileptic, and neuroprotective properties (80,81). Moreover, PEA could also activate the orphan G protein-coupled receptor GPCR55 (82). Another saturated NAE, N-stearoylethanolamide (SEA), was reported to act as an anti-inflammatory/immunomodulatory agent and cell growth controller, through still unknown targets (83–85). Finally, a variety of EC-related compounds, containing FA chains conjugated with different polar heads, have been discovered as a result of advancements of the analytical techniques (86,87). Within the novel group of lipids generally known as lipoamino acids, N-arachidonoylglycine (NAGly) possesses anti-inflammatory effects by targeting the G-protein coupled receptor GPCR18 (88,89), vasorelaxant properties (90) and seems to be involved in cell migration (91), and inhibition of the fatty acid amide hydrolase (FAAH) (92), the AEA inactivating enzyme. Moreover, NAgly might have either a physiological role in the resolution of acute inflammatory response and become a potential therapeutic candidate for the resolution of chronic inflammation, by increasing the production

of prostaglandin J_2 (PGJ_2) and lipoxin A_4 (LXA_4), reducing the migration of inflammatory cells into areas of acute inflammation and inducing the death of inflammatory cells (88).

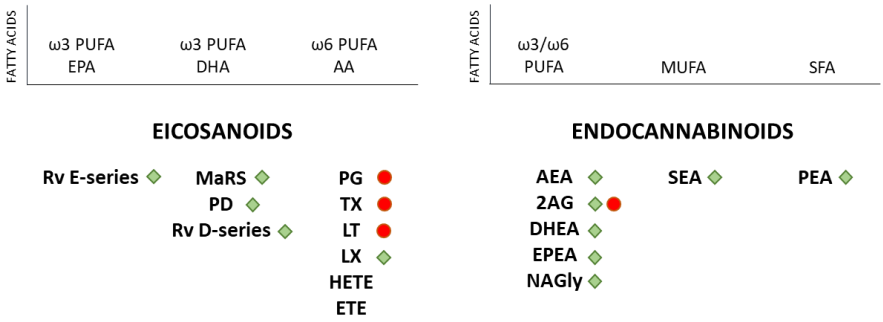

Fig 3. Eicosanoids and endocannabinoids involved in inflammation. The green squares and the red dots indicate lipids with anti- and pro-inflammatory properties, respectively. Legend: PUFA: polyunsaturated fatty acids; MUFA: monounsaturated fatty acids; SFA: saturated fatty acids; EPA: eicosapentaenoic acid; DHA: docosahexaenoic acid; AA: arachidonic acid; Rv: resolvins; MaR: maresines; PD: protectins; PG: prostaglandins; TX: thromboxanes; LT: leukotrienes; LX: Lipoxins; HETE: hydroxyeicosatetraenoids; ETE: epoxyeicosatetraenoids AEA: anandamide; 2AG: 2-arachidonoilglycerol; DHEA: N-docosahexaenoylethanolamine; EPEA: N-eicosapentaenoylethanolamine; SEA: N-stearoylethanolamide; PEA: N-palmitoylethanolamide, N-arachidonoylglycine (NAGly). Adapted by (37)

1.3 Functional lipids in the mesenchymal stem cells (MSC)-related inflammatory scenario

1.3.1 MSC and MSC-secretome: dialogue with inflammation

MSC are adult multipotent progenitor cells with self-renewal potential and the ability to differentiate into different mesodermal lineages including osteoblasts, chondrocytes, and adipocytes (93,94). Since no single biomarker is available for human MSC identification, the International Society for Cellular Therapy defines a set of minimal criteria: (i) MSC show plastic-adherent growth under standard culture conditions; (ii) expression of CD105, CD73 and CD90 and lacking expression of the hematopoietic cell surface markers CD45, CD34, CD14 and human leukocyte antigen-DR; (iii) differentiation into osteoblasts, adipocytes and chondrocytes up on a proper stimulation (95,96). Firstly expanded from human bone marrow (BM), MSC can also be collected and cultured from several sources including adipose tissue (108,109). Compared to BMSC, adipose-derived stem cells (ASC) grow faster and easier in

culture, age slower, maintain the mesenchymal pluripotency and stem cell phenotype even after a high number of passages and show a great proliferative rate with a consequent relatively high yield (about 2500-fold higher than BMSC) (94,95,110,111). ASC differentiate into several cellular lineages and have a good stability throughout long-term cultures (109). Several studies have largely demonstrated the immunomodulatory potential of MSC and their ability to resolve inflammation and promote tissue repair in various diseases (97–99). MSC do not always have immunosuppressive, indeed, they can move to a pro-inflammatory state under certain conditions. For example, the presence of low levels of interferon gamma (IFNγ) and tumor necrosis factor alpha (TNFα) can enhance the MSC immunostimulatory potential, suggesting that variations in levels of pro-inflammatory cytokines affect the immunoregulatory mode of MSC. The MSC immunomodulatory phenotype can be affected not only by inflammatory stimuli but also by other environmental factors, including hypoxia and the extracellular matrix (ECM) composition (100).

Furthermore, originally considered as whole-cell therapy, it is now well known that transplanted MSC do not survive in situ for long time and thus the effects of MSC-based therapies are largely mediated by the paracrine action of a broad array of secreted bioactive factors, collectively referred to as the secretome (known also as conditioned medium - CM) (101). The recognition that MSC-CM is responsible for the therapeutic effect of MSC on tissue repair or regeneration allowed to minimize the risk linked to cell therapies such immune reactions or tumor growth (102). In general, the secretome is a mixture of soluble factors as well as molecules shuttled with extracellular vesicles (EV). EV are lipid bilayer delimited particles of various dimensions and complexities containing proteins, nucleic acids and metabolites released into the extracellular space from cells and having both endosomal and plasma membrane origin (103). Recently, EV have been divided into small (< 200 nm) and large (> 200 nm) particles by the International Society for Extracellular Vesicles (ISEV); previously, they were known as exosomes and microvesicles based on their endosomal or plasma membrane origin (104). Soluble components, such as nucleic acids, proteins and lipids, can all be detected in the cell secretome, at different concentrations and activity levels depending on the cell type and environment (105). In detail, the human MSC secretome contains both EV and a multitude of proteins including growth factors, cytokines, peptides and hormones with a promising potential in regenerative applications (106) (Fig. 4). Up to now, lipid mediators are less well documented but have been described as bioactive factors released by human MSC (107). Our recently ASC-CM and ASC-EV characterizations

performed by Raman spectroscopy have demonstrated not only specific bands for nucleic acids and proteins, but also a considerable lipid content, suggesting substantial differences between the two MSC byproducts (108). Moreover, the analysis of ASC-CM and ASC-EV by a differential proteomic data analysis showed a clear distinction between the two derivatives, also considering inflammatory factors (109). For this reason, a solid understanding of the individual bioactive factors secreted by MSC, including lipids, and the mechanisms underlying their effect are indispensable to refine MSC secretome-based therapies in several disorders such as inflammation (99,105,110).

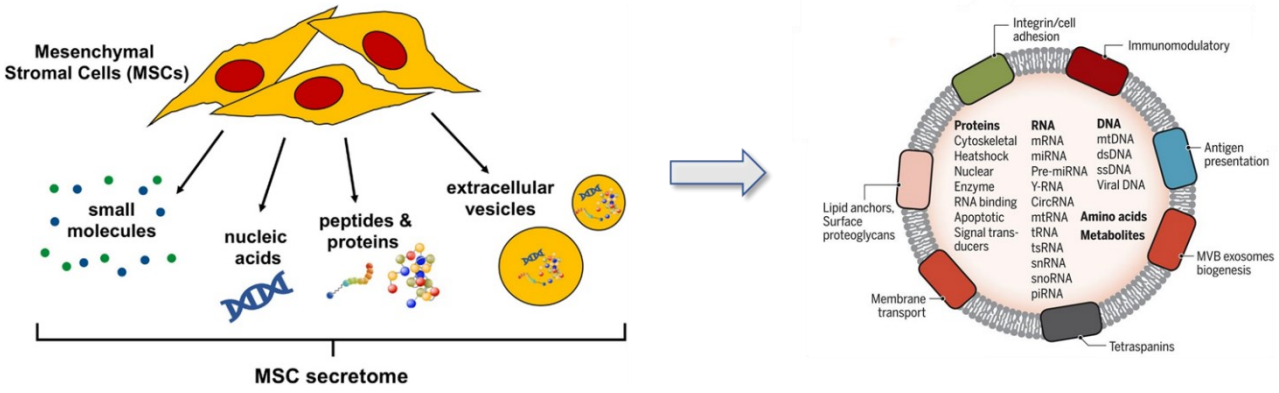

Fig 4. Bioactive components of the complete MSC-secretome and MSC-EV. Adapted from (111,112)

1.3.2 MSC-related functional lipids

Since MSC are physiologically recruited at the damaged site, they are often submitted to a strong pro-inflammatory microenvironment. Immunomodulation, together with trophic factor release, has been attributed as pivotal components of MSC-mediated repair. Further, inflammation and injury derived signals are essential to trigger MSC based immunemodulation (113,114). Campos et al. (115) have performed a comprehensive lipidomic analysis of MSC under pro-inflammatory conditions by 10ng/ml TNFα and 500U/ml IFNγ to better understand the involvement of lipid compounds in the MSC pro- or anti-inflammatory properties and underlying their mechanisms of action; they demonstrated significant changes in MSC phospholipid profile. Higher levels of molecular phosphatidylcholine (PC) species with longer FA chains and lower levels of molecular PC species with shorter FA chains were assessed. Moreover, a peculiar expressions of specific phospholipids and sphingomyelins were found, including the lysophosphatidylcholines 18:0 (LPC 18:0) that has already been correlated with anti-inflammatory properties (116,117). The lipidome of

untreated MSC described by Campos et al. was consistent with previous results (118), with the exception of the presence of sphingomyelins (115) which have not been previously identified, and some derivatives (i.e., sphingosine 1-phosphate - S1P) that are bioactive and mediate essential cell functions (119). However, PG are the widely investigated lipids due to their key role in the immunosuppressive activity of MSC (120). The release of PG (including PGE_1, PGE_2, PGE_3, 6-keto $PGF_{1\alpha}$, $PGF_{2\alpha}$ and PGJ_2) by human heart-derived MSC (121) were documented in the CM by HPLC-MS/MS. Although PGE_2 has been linked to the immunosuppressive effects of MSC since the production of their inhibitors attenuate MSC-mediated immunomodulation (120), PG mediate vasodilatation that allows immune cells to invade inflamed tissue. Indeed, recent evidence suggests that Th1 differentiation might be facilitated by PGE_2, which may have an immunostimulatory role also by expanding the Th17 T-cells population (48). Prostaglandins act through paracrine and autocrine mechanisms in the local environment because of their short half-life and the MSC themselves express receptors for prostaglandins. However, the effects triggered by the stimulation of these receptors on MSC are still unknown. The dual and controversial immunomodulatory properties of MSC seem to depend on the local environment, where IFNγ and TNFα play a crucial role in promoting immunosuppressive function of MSC (122,123).

In the presence of PGE_2, also a higher expression of the PG receptor EP3, which is involved in the stimulation of angiogenesis, was observed in MSC suggesting a possible correlation with the early phases of inflammation (124). Finally, recent studies have evidenced also the roles of LX, and in particular of LXA_4, as regulators of the resolution phase of inflammation (125) and of Rv as key players in the MSC immunoregulation (126,127).

1.4 MSC as an alternative treatment of inflammatory diseases: focus on osteoarthritis

Osteoarthritis (OA) is an age-related condition affecting millions of people in the world. It is a complex and heterogeneous disease characterized by the degradation of articular cartilage, subchondral bone erosion and inflammation (128). In OA, the catabolic and anabolic activities result unbalanced, and the joint cartilage damage seems to be one of the earliest disease promoting events (129). Indeed, articular chondrocytes (CH) modify their phenotype from quiescent to hypertrophic. This shift is characterized by an enhanced cell proliferation and an altered activity of specific enzymes that are able to degrade the matrix (130). The aberrant regulation of hypertrophy-inducing factors leads to the over-expression

of collagen X and matrix metalloproteinases (MMP) such as MMP1, MMP3 and MMP13. These proteinases are secreted from the cells in a latent form, requiring activation extracellularly, and are inhibited by tissue inhibitors of metalloproteinases (TIMP) (131). In OA, there is an imbalance between the proteinases and TIMP that, at least in part, accounts for the cartilage degradation. In vivo studies have suggested the arrest of CH hypertrophy as a valid therapeutic approach since the down-modulation of factors involved in the hypertrophic shift postpones the OA progression (132). Additionally, our and other studies reported as CH treatments with interleukin-1 β (IL-1β) or tissue necrosis factor α (TNFα), principal players in OA physiopathology, leaded to the develop of in vitro models of osteoarthritic CH (133,134). Also the nitric oxide (NO) production, from L-arginine oxidation by inducible nitric oxide synthase (iNOS), resulted abnormally high in OA (i.e., when stimulated by IL-1 or lipopolysaccharide) (135,136). The destructive action of NO is mediated by inhibiting the formation of ECM components such as type II collagen. Furthermore, NO is implicated in the inhibition of synthesis of proteoglycan and acts as a proinflammatory and destructive mediator increasing the production of PGE2 and other inflammatory cytokines (137). It has been reported that IL-1β and TNF-α induce the production of NO as well as reactive oxygen species (ROS) (138).

Recent findings on the involvement of lipids in OA development and progression indicate a possible role for ω3 PUFA and their anti-inflammatory SPM derivatives (139). Since ω3 PUFA/SPM seem to target all the processes that OA course and the chronic wound both show (such as cell death, inflammation and pain (140)), it is reasonable to believe that these lipids could be effective therapeutic agents for OA. In the context of this disease, few studies have investigated the FA presence in OA affecting patients and their relationship to clinical symptoms. These studies indicated that increases of ω3 FAs levels could be associated with a reduced cartilage loss while the increase of the increase of ω6 FA levels with enhanced synovitis (141). Additionally, ω3 PUFA seem to counteract the proinflammatory and catabolic actions of interleukin-1a (IL1a) on cartilage *in vitro* models (142). Accordingly, both *in vitro* and *in vivo* in a rat model of OA, DHA seems to downregulate MMP13 through a P38 mitogen activated protein kinases (p38-MAPK)-mediated mechanism (143). Apart from direct effects of ω3 PUFAs on OA, ω3-derived oxylipins could be generated *in vitro* for example by CH, mediating the observed effects. Other lipid molecules as PG and LT have been detected in plasma and synovial fluid of OA patients showing proinflammatory and catabolic effects (144). Hardy et al. (145) and Shimpo et al. (146) have studied the role of

PGE_2 in osteoarthritic CH showing higher levels of PGE_2 , related to the increased expression of the COX2 gene and the microsomal prostaglandin E synthase-1 at molecular level, under interleukin-1 beta (IL1β) stimulation. By contrast, Rv D1, belongs to the family of D-series Rv, was found to inhibit the IL1β-mediated upregulation of COX-2, PGE_2, MMP13 and nitric oxide in human osteoarthritis CH (147).

Also EC are showing to be effective mediators for controlling joint inflammation and pain associated with OA (61). A functional role of CB1 and CB2 was demonstrated in joint tissues of rodents (148,149) and humans (150). After tissue damage, EC levels rise, but they are then rapidly degraded by the catabolic enzymes FAAH and monoacylglycerol lipase (MAGL) (151). Both AEA and 2AG were detected in the synovial fluid of OA patients, but not in healthy volunteers, providing further evidence for a functional role of EC system in osteoarthritic joints (150). In addition, COX2 pathway can metabolize 2AG, leading to the formation of pro-inflammatory and pain-producing prostaglandins that could counteract the analgesic effects of 2AG (66). Synthetic cannabinoids showed protective effects toward cytokine-induced ECM degradation in cartilage through the inhibition of the synthesizing enzymes of inflammatory mediators, such as PGE_2 and NO (62). Therefore, cannabinoids could have a modulatory effect on the early stages and progression of OA disease.

The most common surgical approaches, e.g., microfracture, subchondral drilling or autologous cartilage implantation, often lead to the development of low-quality fibrocartilage, since cartilage does not regenerate spontaneously. Concerning pharmacological treatments, they cannot reverse OA, but only help relieve its symptoms. The most common medications are corticosteroids, non-steroidal anti-inflammatory drugs (NSAID), duloxetine, and acetaminophen, often accompanied by physiotherapy and life style modification (152)

Although the quality of life in OA patients is improved by the available treatments reducing pain and promoting joint mobility, the achievement of adequate tissue regeneration and the development of drugs able to modify the course of the disease is still needed. In this context, orthobiologics (including intra-articular injection of platelet-rich plasma and biografts, such as autologous chondrocyte implantation, bone marrow concentrate, and ASC therapy) are emerging as alternative therapeutic tools, thanks to their regenerative potential and cost-effectiveness (153,154). In the last years, the use of MSC has emerged to be effective in the treatments of cartilage repair (155,156). Its efficacy has been demonstrated both in vitro

(157,158) and in vivo studies (159,160). Since the widely recognized MSC paracrine effect, the researcher's interest has shifted to the study of their secretome, the CM. MSC-CM has been successfully tested in several preclinical models, e.g., (161–163), suggesting its promising therapeutic action on cartilage, subchondral bone and synovium. As previously described (paragraph 1.3.1), among other MSC sources, adipose tissue presents several advantages in terms of harvesting procedure, cell isolation, and expansion. Efficacy and safety of ASC in vitro and in vivo have been studied and they have been confirmed also by clinical trials (164,165). We recently demonstrated the therapeutic potential of ASC secretome and EV both *in vitro* on TNFα-stimulated articular chondrocytes (134,166), and *in vivo* in a mouse model of OA (167), providing evidences of MSC mediated anti-inflammatory and immunomodulatory action. Moreover, MSC-derived EV stimulate tissue regeneration (168), homing to the inflammatory site and transfer proteins/peptides, mRNA, microRNA, lipids, or organelles with reparative and anti-inflammatory activities (169,170). Lipids are essential components of the EV membranes, and it is well-known that some EV are enriched in specific lipids compared to their parent cells. (171,172). Human CH co-cultured with MSC-EV showed enhanced proliferation and decreased apoptosis induced by IL1β, also known as one of the main inflammatory mediators for arthritis through the S1P/S1P receptor 1 (S1PR1) signaling pathway activation suggesting the implication of specific lipids into the clinical application of MSC-secretome to the treatment of articular cartilage defect (173).

2. Aim of the thesis

The aim of the present thesis included the development and optimization of advanced analytical MS techniques in lipidomic field, in order to better elucidate the bioactive lipids composition of MSC secretome (CM and EV) and also the study of their functional role in an *in vitro* model of OA.

At first, fast and sensitive quantitative UHPLC-MS/MS analytical methods, using a double LLE procedure, for a simultaneous investigation of the four major signaling lipid families (polyunsaturated fatty acids, eicosanoids, endocannabinoids and N-acyl-ethanolamines) from small amounts of different bio-matrices (including cellular byproducts such as CM and EV, but also urine and serum) were set-up and validated, providing a powerful tool for the lipidomic translational research.

Secondly, due to the extreme complexity of secretome composition and the necessity of an extensively characterization in the perspective of a future clinical translation, the lipid fraction of the CM and EV from BMSC, ASC and DF were investigated, by previously developed analytical methods, in order to highlight analogies and differences in their lipid content.

At last, since previous evidence obtained by our laboratory, in an in vitro OA model support the thesis of the effectiveness of ASC-CM in contrasting the TNFα-induced hypertrophy, catabolic processes and inflammatory markers, the functional activity of two lipid compounds, quantified in ASC-CM - 2AG and PEA, was studied in a well-established *in vitro* model of OA based on the administration of 10ng/ml TNFα to human primary articular CH.

3. Material and Methods

3.1 Targeted MS analytical methods development and validation

3.1.1 Chemicals

Ultrapure water, acetonitrile (ACN), dichloromethane (DCM), isopropanol (IPA), methanol (MeOH), ethyl acetate (EtOAc), n-hexane and hydrochloride acid were of analytical grade and purchased from Carlo Erba (Milan, Italy). Formic acid (98%–100%) was purchased from Sigma–Aldrich (Milan, Italy). The reference materials N-arachidonoylethanolamide (AEA), N-linolenoylethanolamide (LNEA), N-linoleoylethanolamide (LEA), N-oleoylethanolamide (OEA), N-palmitoylethanolammide (PEA), N-stearoylethanolamide (SEA), and N-stearoylethanolamide-d4 (SEA-d4) were synthesized and completely characterized as previously described (174,175). The reference materials N-docosahexaenoylethanolamide (DHEA), N-eicosapentaenoylethanolamide (EPEA), N-arachidonoyldopamine (ADA), N-oleoyldopamine (ODA), N-arachidonoylglycine (AGly), N-oleoylglycine (OGly), N-palmitoylglicine (PalGly), N-arachidonoylserine (ASer), N-arachidonoylserotonine (A5HT), N-oleoylserotonine (O5HT), N-palmitoylserotonine (Pal5HT), 2-arachidonoylglycerylether (2AGE), 2-arachidonoyglycerol (2AG), N-arachidonoyl-3-hydroxy-γ-aminobutyric acid (AGABA), arachidonoyl acid (AA), eicosapentaenoyl acid (EPA), docosahexaenoyl acid (DHA), thromboxane-B_2 (TXB_2), prostaglandin-$F_{2\alpha}$ ($PGF_{2\alpha}$), 6α-keto-prostaglandin-F1α (6α-keto-$PGF_{1\alpha}$), prostaglandin-E_2 (PGE_2), prostaglandin-D_2 (PGD_2), leukotriene-B4 (LTB_4), 5-hydroxyeicosatetraenoic acid (5(S)-HETE), 15-hydroxyeicosatetraenoic acid (15(S)-HETE), (±)14(15)-epoxyeicosatrienoic acid (14,15-EET) and internal standards N-arachidonoylethanolamide-d8 (AEA-d8), N-oleoylethanolamide-d2 (OEA-d2), N-palmitoylethanolammide-d5 (PEA-d5), N-eicosapentaenoylethanolamide-d4 (EPEA-d4), N-arachidonoyldopamine-d8 (ADA-d8), N-arachidonoylglycine-d8 (AGly-d8), N-arachidonoylserine-d8 (AS-d8), N-oleoylserotonine-d17 (O5HT-d17), eicosapentaenoyl acid-d5 (EPA-d5), thromboxane-B_2-d4 (TXB_2-d4), prostaglandin-$F_{2\alpha}$-d4 ($PGF_{2\alpha}$-d4), leukotriene-B_4-d4 (LTB_4-d4) were purchased from Cayman Chemical (Ann Arbor, USA).

3.1.2 Cell cultures

Saos-2 and MG-63 cell lines (ATCC, Rockville, MD) were plated in tissue culture vessels (Corning, New York, USA) at a density of $5x10^3$ cells/cm^2 in complete culture medium (CDMEM) (176): DMEM (Euroclone, Milan, Italy) supplemented with 10% fetal bovine serum

(Euroclone), penicillin 50 U/ mL, 50 µg/ mL streptomycin (Sigma Aldrich, Milan, Italy) and 2 mM L-glutamine (L-Glu, Euroclone). Cultures were maintained at 37 °C in a humidified atmosphere, containing 5% CO_2. After 48 h culture, non-adherent cells were removed, and the medium replaced. At 70–80% confluence, the cells were detached with 0.5% trypsin/0.2% EDTA (Sigma Aldrich) and expanded.

3.1.3 Sample collection

3.1.3.1 Cell samples

Once at 80–90% confluence, cells were washed twice with PBS and kept for one h in starving medium (SM) (phenol red-free DMEM supplemented with 2 mM L-glutamine, 50 U/ mL penicillin, 50 µg/ mL streptomycin without fetal bovine serum) for additional washing. Medium was replaced by fresh SM and cells were starved for 72 h following optimized procedures (177).

Concentrated conditioned media (CM)

CM were collected from approximately 6 × 10^6 cells in starving conditions, centrifuged for 15 min at 2,500 g, 4°C to remove debris and large apoptotic bodies, and concentrated through Amicon Ultra-15 Centrifugal Filter Devices with 3 kDa cut-off (Merck Millipore) for 90 min at 4,000 g, 4°C (134). The final product was concentrated about 40–50 folds. This procedure allows the retention of the vesicular component of cell secretome, as previously demonstrated in (108,109,166).

Extracellular vesicles (EV)

EV were isolated from cell conditioned medium using differential centrifugation, as previously described (178,179). In brief, after 72 h of starvation, the conditioned medium from approximately 15 × 10^6 cells was centrifuged for 15 min at 2,500 g, 4°C, and then ultracentrifuged for 70 min at 100,000 g (L7–65; Rotor 55.2 Ti; Beckman Coulter, Brea, CA, USA) at 4 °C. Pellet was resuspended in sterile phosphate buffer (PBS, composed of NaCl 137 mM, KCl 2.7 mM, Na_2HPO_4 x $2H_2O$ 8.1 mM, KH_2PO_4 1.7 mM - pH 7.4) and ultracentrifuged again under the same conditions. The resulting EV pellet was kept at -20 °C for MS analysis.

3.1.3.2 Serum and urine samples

Control human urine and serum samples, used for purification and extraction studies and for validation experiments, were obtained from healthy volunteers, which gave informed consent to offer their biological samples for research intent. Blood samples were collected in Vacuette® 6-mL non-gel serum separator tubes and aliquots of 1-2 mL serum were stored at −20 °C. Human urine specimens, obtained from volunteer colleagues, were collected after a circadian cycle and aliquots of 1-2 mL were stored at -20 °C until analysis.

3.1.4 Standard solutions, calibrators and quality control (QC) samples

Stock solutions of reference materials and internal IS were prepared at the final concentration of 10 µg/mL by appropriate dilution with ACN under a stream of nitrogen. All solutions were stored in the dark at – 20 °C. Working solutions were prepared in ACN from stock solutions and used for the preparation of calibration curves and quality QC samples at 100 ng/mL, except for AA, DHA, EPA and EPA-d5 (1 µg/mL).

3.1.4.1 Cell samples

Calibration standards (CS) containing 0, 0.1, 0.25, 0.5, 1.25, 2.5, 5 ng/mL for all compounds; 0, 1, 2.5, 5, 12.5, 25 ng/mL for AA, DHA and EPA; 1 ng/mL for ISs and 10 ng/mL for EPA-d5 were prepared daily for each analytical batch by adding suitable amounts of working solutions to 500 µL of SM. QC samples were prepared in SM at three different concentration levels (low, intermediate and high).

3.1.4.2 Serum and urine samples

CS and QC samples were prepared by adding ISs at same concentration levels (see paragraph 2.1.4.1) to 500 µL of PBS, serum and urine. Pooled serum and urine CS and QC used for validation experiments were prepared combining 20 and 5 different samples, respectively.

3.1.5 Sample preparation

EV, stored at -20°C, were resuspended in 500 µL of SM and strongly vortexed three times for 1 minute. Prior to extraction, 10 µL IS and 1 mL of ice-cold ACN were added to 500 µL CM (as well as for serum and urine) and EV suspension and centrifuged for 10 minutes at 350 g at 4°C degrees. The clear supernatant was then transferred into glass test tubes and extracted with 4 mL of DCM/IPA (8:2; v/v). After centrifugation at 350 g for 10 minutes, the organic layer was separated and dried under a stream of nitrogen. The dried residue was

reconstituted with 60 µL methanol and a 3 µL aliquot was injected into UHPLC-MS/MS system for EC and NAE analysis. The remaining aqueous solution was used for PUFA and eicosanoids extraction, by adding 500 µL hydrochloride acid (HCl, 0.125 N) and 4 mL EtOAc/n-hexane (9:1; v/v). The organic phase was dried, and the residue was reconstituted with 60 µL ACN. A 30 µL aliquot of methanol obtained from the neutral extraction and a 30 µL aliquot from acid extraction were merged and transferred into an autosampler vial. A 10 µL aliquot was injected into UHPLC/MS-MS system for PUFA and eicosanoids determination.

3.1.6 Equipment

Analyses were performed on 1290 Infinity UHPLC system (Agilent Technologies, Palo Alto, CA, USA) coupled to a Q Trap 5500 triple quadrupole linear ion trap mass spectrometer (Sciex, Darmstadt, Germany) equipped with an electrospray (ESI) source. Compounds were separated on a Kinetex UHPLC XB-C18 column (100 mm x 2.1 mm i.d, 2.6 p.s.) (Phenomenex, CA, USA) using 0.1% formic acid in water (mobile phase A) and MeOH/ACN (5:1; v/v) (mobile phase B). For EC and NAE analysis, solvent A and B were 75% and 25% at 1.00 min, respectively. Solvent B was increased to 70% from 1.00 to 1.50 min, then increased to 85% from 1.50 to 6.00 min and to 100% from 6.00 to 7.00, held at 100% from 7.00 to 9.00 min, and then decreased back to 25% from 9.00 to 9.20 min and held at 25% from 9.20 to 11.0 min for re-equilibration. For PUFA and eicosanoids analysis, solvent A and B were 75% and 25% at 1.00 min, respectively. Solvent B was increased to 40% from 1.00 to 3.00 min, then increased to 95% from 3.00 to 5.50 min and to 100% from 5.50 to 7.00, held at 100% from 7.00 to 8.00 min, and then decreased back to 25% from 8.00 to 8.20 min and held at 25% from 8.20 to 10.0 min for re-equilibration. The flow rate was 0.60mL/min and the column thermostatic oven was kept at 40 °C. The working conditions and parameters of the MS were optimized by direct infusion (flow rate 7µL/min) of a standard mix solution (100ng/ml) as follows: the acquisitions were performed in positive mode for the EC/NAE and in negative mode for PUFA/eicosanoids analysis; the resolution of Q1 and Q3 was set to 0.7 ± 0.1 amu; the curtain gas, ion gas 1, ion source gas 2 were set at 25, 45 and 10 psi, respectively; the source temperature was 550 °C; the ionization voltage was 5500 eV (positive mode) and -4500 eV (negative mode); the entrance potential was 10 eV; dwell time was fixed 70 msec for each MRM transitions. The MRM conditions and parameters including ion transitions, de-clustering potential (DP) and relative collision energy (CE) are

provided in Table 2. In detail, the following transitions parent ions > product ions were applied:

- AEA, LNEA, LEA, PEA, OEA, SEA → m/z 62 relative to the protonated ethanolamine moiety;
- 2AG → m/z 287 relative to glycerol neutral loss;
- ODA, ADA → m/z 154 relative to the protonated dopamine moiety;
- A5HT, O5HT, Pal5HT → m/z 160 relative to the protonated dehydroxy-5HT moiety;
- ASer → m/z106 relative to the protonated serine moiety;
- AGly, OGly, PalGly → m/z 76 relative to the protonated glycine moiety.

Compound	Precursor ion (m/z)	Product ions (m/z)	DP (eV)	CE (eV)
AA (20:4)	303.1	59.1	-45	-42
		259.6	-45	-20
EPA (20:5)	301.4	59.1	-55	-42
		203.1	-55	-20
DHA (22:6)	327.3	283.3	-80	-10
		59.1	-80	-35
TXB_2	369	177	-50	-22
		195	-50	-20
PGE_2	351.5	315	-50	-25
		271.1	-50	-25
PGD_2	351.5	271	-50	-30
		189	-50	-30
$PGF_{2\alpha}$	353	291	-50	-35
		193	-50	-35
6αKeto-$PGF_{1\alpha}$	369.5	245	-50	-35
		163	-50	-35
LTB_4	335	273	-45	-23
		195	-45	-23
5(S)-HETE	319.5	115	-50	-18
		301.1	-50	-18
15(S)-HETE	319.5	219	-50	-15
		301.2	-50	-15
14,15-EET	319.,5	219.1	-50	-22
		301	-50	-40
AEA	348	62	76	42
		133	76	33
2AG	379.4	287.3	76	18
		203	76	25
LNEA	322.3	62.2	85	35

		81.2	85	35
LEA	324.3	62.2	85	35
		109	85	32
PEA	300.1	62	98	19
		283	98	36
OEA	326.3	62.2	85	35
		309	85	21
SEA	328.3	62.2	85	35
		311.1	85	22
DHEA	372.3	62	85	18
		67	85	36
AGly	362.3	287	85	18
		76	85	18
ADA	440.5	137	95	34
		154	95	23
2AGE	365.3	273	85	10
		121	85	20
ODA	418.3	137	85	24
		154	85	35
EPEA	346.3	62	85	35
		135	85	35
ASer	392.5	106	85	35
		137.3	85	33
OGly	340.5	76	85	35
		265	85	35
PalGly	314.5	76	85	35
		239	85	20
AGABA	406.5	287.4	85	24
		84.1	85	55
A5HT	463.3	160.4	85	35
		132.2	85	35
O5HT	441.7	160.4	85	35
		132.2	85	35
Pal5HT	415.7	160.4	130	47
		132.2	130	47
TXB_2-d4	373	199	-50	-22
		173	-50	-22
PGF_{2a}-d4	357	295	-50	-35
		197	-50	-35
LTB_4-d4	339	197	-45	-23
		277	-45	-23
EPA-d5	306.3	59.1	-50	-35
		208.1	-50	-18
AEA-d8	356.3	62	76	35
		70	76	35
SEA-d4	332.3	66.2	85	35
		62	85	18
EPEA-d4	350.3	66	85	35

		135	85	35
OEA-d2	328.3	62	85	35
		311	85	35
PEA-d5	305.1	62	85	35
		288	85	35
ADA-d8	448.5	137	85	35
		154	85	35
AGly-d8	370.6	76	85	20
		84	85	20
ASer-d8	400.6	106	85	35
		70	85	35
O5HT-d17	458.7	160.4	130	47
		132.2	130	47

Table 2 MRM parameters: precursor and product ion transitions (quantifier underlined) for all the analytes and IS, de-clustering potential (DP) and collision energy (CE)

3.1.7 Data evaluation

Data acquisition and processing were performed using Analyst®1.6.2 and MultiQuant®2.1.1 software (Sciex, Darmstadt, Germany), respectively. Calculations for validation assessment, which includes linearity, precision, accuracy, sensibility, recovery, and stability were performed using Microsoft Office Excel 2013.

3.1.8 Validation procedure

Assay validation was carried out in accordance with the recommendations endorsed by FDA guideline referred to drugs and non-endogenous compounds (180) and specific issues for endogenous compounds (181) were addressed. A full validation was performed in the analyte-free SM and the following parameters were assessed: linearity, precision and accuracy, sensitivity in terms of limits of detection (LOD) and limits of quantitation (LOQ), specificity, recovery, matrix effect and stability. Additionally, the described method was partially validated in serum and urine. Surrogate analyte-free matrices (i.e. water and/or appropriate buffer) are usually used for the preparation of CS and QC when validation has to be performed for endogenous compounds, to overcome the lack of analyte-free matrix (181). For this reason, to avoid the interference of endogenous analytes, linearity, slope, recovery, and the influence of matrix effect were obtained by spiking serum and urine with ISs at the same concentrations' levels (see paragraph 2.1.4.2), whereas LOD and LOQ evaluation was achieved on PBS.

3.1.8.1 Calibration range and linearity

The 7-point calibration curve (*n = 6*) were obtained by spiking analyte-free SM with appropriate amounts of working solutions in the range 0.1 – 2.5 ng/mL and 1 – 25 ng/mL (EPA, AA and DHA), as described at paragraph 2.4. A linear model was used to describe the relation between analyte concentration and instrument response (analyte peak area/internal standard peak area). Linearity was considered satisfactory for each curve if $R^2 \geq 0.990$. Additionally, to evaluate linearity and slope, CS were also prepared in the analyte-free PBS, as well as in urine and serum, by spiking IS at the same concentration levels.

3.1.8.2 Sensitivity and specificity

Reagents and consumables were extracted, following the procedures described before, and analyzed in triplicate to evaluate and exclude interferences and false positive responses derived from sample preparation. The specificity of the method and matrix-to-matrix reproducibility was evaluated by analyzing SM in triplicate from different lots number (n=3). Sensitivity was expressed in terms of LOD and LOQ, defined as the ratio between the standard deviation of the response and the slop of the calibration curve, and correspondent to 3.3 and 10 times, respectively. LOD and LOQ were calculated on calibration curves prepared in the analyte-free SM for cell samples quantification. Additionally, LOD and LOQ were also tested in the analyte-free PBS in order to quantify serum and urine samples.

3.1.8.3 Precision and accuracy

Precision and accuracy of the method were determined by analyzing six independent replicates of QC materials, extracted from the analyte-free SM at three concentration levels (low, intermediate, and high). Precision was denoted by percent coefficient of variation (CV%), while the accuracy was expressed as bias (BIAS%), the percent deviation of the mean determined concentration from the accepted reference value. The accuracy and precision were required to be ≤15% CV (Table S1 and S2).

3.1.8.4 Recovery and matrix effects

Extraction recovery (%) was measured by comparing the peak area of the analyte-free SM (n=3) fortified with standards at three concentration levels, prior and after extraction. Peak areas of pre- and post-extraction samples were used for calculations, considering the analytes area in post-extraction spiked samples as 100% recovery. The matrix effects (%) was determined by comparing the analytes peak area in PBS and in the analyte-free SM, fortified in the low, intermediate, and high concentration range after extraction. Concerning

the extraction recovery evaluation in human, serum and urine, matrices containing endogenously all the analytes, we spiked them with ISs before and after LLE. The matrix effect was assessed by comparing the peak area of ISs spiked in eluate from serum and urine to those in PBS. As for SM, the extraction recovery and matrix effect were evaluated at three concentration levels.

3.1.8.5 Stability studies

The stability was assessed in QC samples at low, intermediate and high concentration, by analyzing them the initial day (T0) as well as 24h later at 4°C and -20 °C. The response factor at each concentration was compared to the original vial at T0 and a mean deviation below 15 % from day 0 was considered acceptable.

3.1.9 Efficiency evaluation in real samples

The proposed method was firstly applied to Saos-2- and MG-63-derived CM, EV and cell lysates to identify and quantify lipids belonging to PUFA/eicosanoids and EC/NAE groups, as described at paragraph 2.1.3. Each sample was injected into UHPLC-MS/MS three times (n=3 analytical replicates).

3.2 Mesenchymal stem cells (MSC) and dermal fibroblasts (DF) secretome characterization by UHPLC-MS/MS analysis

3.2.1 ASC, BMSC and DF isolation and maintenance

Human primary cell cultures were obtained from waste tissues deriving from aesthetic and prosthetic surgery performed at IRCCS Istituto Ortopedico Galeazzi upon Institutional Review Board approval. Written informed consent was provided from all donors.

Adipose tissue derived MSC (ASC)

Human ASC were isolated from the subcutaneous adipose tissue of 8 non obese (BMI<30) donors (females, 44±12 years old) who underwent total hip replacement surgery or liposuction. Adipose tissue samples were shredded with a sterile scalpel, digested for 30 min with 0.75 mg/ml type I Collagenase (Worthington Biochemical Corporation, Lakewood, NJ, USA) and filtered with a 100 µm cell strainer (Corning Incorporated, Corning, NY, USA). ASC were cultured in a CDMEM composed by high glucose DMEM (Sigma-Aldrich, St. Louis, MO, USA), 10% Fetal Bovine Serum (FBS, Euroclone, Pero, Italy), 2mM L-glutamine,

50 U/ml penicillin, and 50 µg/ml streptomycin (Sigma-Aldrich, St. Louis, MO, USA) at 37°C, 5% CO_2.

Bone marrow derived MSC (BMSC)

Human BMSC were isolated from the bone marrow blood of 5 donors (2 males and 3 females, 64±11 years old) who underwent total hip replacement surgery. The blood was centrifuged at 510 g for 10 min and the pellet resuspended in PBS and centrifuged again. The pellet was resuspended in CDMEM. BMSC were cultured in CDMEM at 37°C, 5% CO_2.

Dermal fibroblasts (DF)

Human DF were obtained from the deepidermised dermis of 3 donors (females, 46±11 years old) undergoing abdominoplasty. Dermis tissue samples were fragmented with a sterile scalpel, digested with 0.1% type I Collagenase (Worthington Biochemical Corporation, Lakewood, NJ, USA) and filtered with a 100 µm cell strainer (Corning Incorporated, Corning, NY, USA). DF were cultured and maintained in a humidified atmosphere at 37°C, 5% CO_2 in CDMEM.

For all primary cell cultures, the medium was replaced every other day and, at 70–80% confluence, cells were detached with 0.5% trypsin/0.2% EDTA, plated at a density of 10,000 cells/cm^2 for ASC and BMSC, 5000 cells/cm^2 for DFs, and expanded.

3.2.2 CM and EV production

ASC, BMSC and DF from IV to XI passage at ~ 90% of confluence were incubated in starving conditions for 72 h (absence of FBS). No signals of cell suffering were ever observed during the period. The CM and EV were collected as previously described (paragraph 2.3.1.1) and the resulting products were kept at -20 °C until MS analysis.

3.2.3 Secretome characterization by targeted lipidomic analysis

The previously set-up and validated methods (paragraph 2.1) were applied to ASC (*n=8*), BMSC (*n=5*) and DF (*n=3*)-derived CM and EV in order to partially characterize the lipid profile related to PUFAs/eicosanoids and EC/NAE groups.

3.2.4 Statistics

Statistical analysis was performed one-way analysis of variance (ANOVA) followed by Tukey's post hoc test. Differences were considered significant at $P \leq 0.05$. Data for the three

groups are presented as box and whisker plots. The box represents the 25 to 75 interquartile range, and the horizontal line represents the median value. The whiskers represent the extremes values. All values are presented in ng/ml per million cells (CM) or ng per million cells (EV). All the analyses were performed using Prism 7 (GraphPad Software, La Jolla, CA, USA).

3.3 Evaluation of the functional activity of two ASC-CM bioactive lipids – 2AG and SEA – in an in vitro model of osteoarthritis (OA)

3.3.1 Human primary cells

All the waste tissue was collected at IRCCS Galeazzi Orthopaedic Institute following Institutional procedure. Written informed consent was obtained from all the patients. Human ASC were isolated from the adipose tissue of 5 healthy donors (2 males and 3 females; 49±13 y/o) undergoing total hip replacement surgery, following previously described protocol (paragraph 2.2.1). All ASC donors were normal-weight subjects (BMI < 30, no documented diagnosis of obesity) Human CH derived from the articular cartilage of the femoral heads collected from 14 patients (3 males and 11 females; 67±12 y/o) who underwent total hip replacement surgery at the same Clinical Institute. The areas of macroscopically healthy cartilage (white, shiny, elastic, and firm) were harvested through a scalpel and digested overnight at 37 °C with 1.5 mg/ml type II Collagenase (Worthington Biochemical Corporation, Lakewood, NJ, USA) (182,183). The areas characterized by irregular surface, discoloration or softening were never collected in order to exclude any experimental bias linked to the use of compromised cartilage. Cells were cultured in CDMEM added by 110 µg/ml sodium pyruvate for CH maintenance at 37 °C in a humidified atmosphere with 5% CO2.

3.3.2 ASC-CM production

Conditioned medium was collected from ~ 90% confluent ASC from V to VIII passage were incubated in starving conditions for 72 h. No signs of cell suffering were ever recorded during the period. The CM was collected as previously described (paragraph 2.3.1.1) and the resulting products were kept at -20 °C until use.

3.3.3 *In vitro* OA induction and treatments

In our experimental set up, CH were employed at 1st culture passage in order to prevent their dedifferentiation (184). CH were seeded at the density of 10^4 cells/cm^2 in tissue culture treated 6-well plates (Corning Incorporated, Corning, NY, USA) and cultured in CDMEM until the full confluence was reached (185), then shifted in a complete medium containing 1% FBS and treated with 10 ng/ml TNFα for 3 days to mimic OA microenvironment (134,186), without any media change. Concurrently, CH were treated with ASC-CM from 5 × 10^5 cells, 2AG and PEA at real (1 and 0.5 pg/ml, respectively) and increasing concentration levels (0.1, 1 and 0.05, 0.5 ng/ml, respectively). CH culture media were collected and centrifuged for 5 min at 2000 g, 4 °C, to remove dead cells and debris and aliquoted. CH supernatants and cells lysates were stored at − 20 °C for further analyses.

3.3.4 Western blotting of CH samples

CH were lysed in 50 mM Tris-HCl (pH 7.5), 150 mM NaCl, 1% NP-40, and 0.1% SDS supplemented with protease inhibitor cocktail (PIC) and 2 mM PMSF. Upon incubation on ice for 30 min, lysates were centrifuged for 15 min at 15,000 g, 4 °C, in order to eliminate cell membranes. The protein content of each sample was quantified through BCA Assay (Thermo Fisher Scientific, Waltham, MA, USA). Measurements were performed in technical duplicates. Samples were analyzed by 10% SDS-PAGE and Western blotting (WB), using standard protocols (134). For each sample, 10 µg of protein extract were loaded and probed with the following primary antibodies: rabbit anti-COX2 (Cell Signaling, Danvers, MA, USA, 1:1000 diluted), mouse anti-MMP13 (Thermo Fisher Scientific, Waltham, MA, USA, 0.4 µg/µl, 1:100 diluted), rabbit anti-MMP3 (Cell Signaling, Danvers, MA, USA, 1:1000 diluted), rabbit anti-CB1 (Cayman Chemical, Ann Arbor, USA, 1:1000 diluted), rabbit anti-CB2 (Cayman Chemical, Ann Arbor, USA, 1:1000 diluted) and goat anti-GAPDH (Santa Cruz Biotechnology, 0.1 µg/µl, 1:1000 diluted). Specific bands were revealed upon incubation with appropriate secondary antibodies conjugated to horseradish peroxidase (Rabbit IgG Secondary antibody, Thermo Fisher Scientific, Waltham, MA, USA, dilution 1:10,000; Mouse IgG Secondary Antibody, Thermo Fisher Scientific, Waltham, MA, USA, dilution 1:6000; Goat IgG Secondary Antibody, Santa Cruz Biotechnology, CA, USA; 0.1 µg/µl, 1:6000 diluted) followed by detection with ECL Westar Supernova (Cyanagen, Bologna, Italy). After image acquisition with ChemiDoc Imaging System, protein expression was quantified through Image Lab Software (Bio-Rad, Milan, Italy). To normalize target protein expression, the band intensity of each sample was divided by the intensity of the loading control protein

GAPDH. Then, the fold change was calculated by dividing the normalized expression from each lane by the normalized expression of the control sample (CTR=1).

3.3.5 Nitric oxide (NO) determination in culture medium

NO was measured in CH culture media following reduction of nitrate to nitrite using an improved Griess method (Abcam, Cambridge, Regno Unito). Absorbance was measured at 540 nm. Nitrite concentration was then determined from a nitrite standard curve (0–200 μM).

3.3.6 Targeted lipidomic UHPLC-MS/MS analysis of CH culture medium and cell lysates

500 μl CH supernatants and 40±15μl CH cell lysates were analyzed by UHPLC-MS/MS analysis for lipids determination by previously described methods (paragraph 2.1). The protein content of each cell lysate sample was quantified through BCA Assay (Thermo Fisher Scientific, Waltham, MA, USA). Measurements were performed in technical duplicates.

3.3.7 Statistics

Statistical analysis was performed by student's *t*-test or one-way analysis of variance (ANOVA) followed by Tukey's post hoc test in case of normally distributed measures, otherwise by Friedman's test followed by Dunn's multiple comparison. Differences were considered significant at $P \leq 0.05$. Unless otherwise stated, data are expressed as mean ± SD of independent experiments. All the analyses were performed using Prism 7 (GraphPad Software, La Jolla, CA, USA).

4. Results

4.1 Targeted MS analytical methods development and validation

4.1.1 Instrumental parameters

Mass spectrometry parameters were optimized by infusing a standard mix solution (100 ng/ml in MeOH). Positive and negative transitions were selected for the EC/NAE and PUFA/eicosanoids, respectively, as described in paragraph 3.1.6. The source/gas parameters, CE and DP, were varied from 0 to ±60 eV and 0 to ±150 eV, respectively. Parents and product ions, CE and DP, shown in table 1, were selected for analytes quantification. The optimization of the chromatographic separation lead to obtain two different elution gradients, performed on a Kinetex UHPLC XB-C18 column, providing the best analytes sensitivity and peak shape. The mobile phase was 0.1% formic acid in water and MeOH/ACN (5:1; v/v), the total runtime was 11.0 min, comprising cleaning and reconditioning of the column.

4.1.2 Method validation

4.1.2.1 Calibration range and linearity

The 7-point calibration curve (*n = 6*) were obtained by adding 500 µL analyte-free SM and PBS (for lipids quantification in human serum and urine) aliquots with a mix of standard solution, as described at paragraph 3.1.5. The calibration ranges were set as follow: 0.1-2.5 ng/mL for all the compounds except for AA, EPA and DHA (1-25 ng/mL). All calibration curves displayed good linearity ($R^2 > 0.991$) for all the analyzed compound over the entire investigated range, when using linear correlation. No interfering peaks were observed in either the blank SM or PBS, at the retention times of our analytes of interest. The LOD and LOQ have been calculated for all analytes both in the analyte-free SM and PBS and are listed in table 3.

Compound	R^2	Analytical range ng/ml	LOD (SM) ng/ml	LOQ (SM) (ng/mL)	LOD (PBS) (ng/mL)	LOQ (PBS) (ng/mL)
AA	1.000	1-25	0.259	0.864	0.014	0.046
EPA	1.000	1-25	0.039	0.132	0.007	0.024
DHA	0.999	1-25	0.013	0.042	0.022	0.073
TXB_2	0.991	0.1-2.5	0.021	0.070	0.022	0.073
PGE_2	1.000	0.1-2.5	0.018	0.061	0.010	0.035
PGD_2	0.999	0.1-2.5	0.008	0.028	0.031	0.103
$PGF_{2\alpha}$	1.000	0.1-2.5	0.008	0.028	0.018	0.059
6aKeto-$PGF_{1\alpha}$	1.000	0.1-2.5	0.006	0.020	0.014	0.048
LTB_4	0.999	0.1-2.5	0.011	0.037	0.033	0.110
5(S)-HETE	0.998	0.1-2.5	0.031	0.100	0.016	0.053
15(S)-HETE	0.999	0.1-2.5	0.012	0.041	0.021	0.070
14,15-EET	0.999	0.1-2.5	0.002	0.006	0.027	0.090
AEA	0.996	0.1-2.5	0.013	0.045	0.027	0.088
2AG	0.992	0.1-2.5	0.004	0.015	0.027	0.089
2AGE	0.999	0.1-2.5	0.008	0.026	0.015	0.049
LNEA	0.997	0.1-2.5	0.033	0.109	0.019	0.064
LEA	0.992	0.1-2.5	0.030	0.100	0.028	0.094
PEA	0.995	0.1-2.5	0.030	0.101	0.027	0.090
OEA	0.999	0.1-2.5	0.020	0.076	0.025	0.084
SEA	0.999	0.1-2.5	0.005	0.018	0.013	0.045
DHEA	0.996	0.1-2.5	0.020	0.081	0.028	0.092
EPEA	0.998	0.1-2.5	0.010	0.033	0.005	0.017
ADA	0.998	0.1-2.5	0.018	0.059	0.029	0.099
ODA	0.999	0.1-2.5	0.031	0.106	0.029	0.099
ASer	0.996	0.1-2.5	0.019	0.064	0.023	0.081
AGly	0.999	0.1-2.5	0.030	0.101	0.029	0.099
OGly	0.998	0.1-2.5	0.028	0.094	0.035	0.100
PalGly	0.999	0.1-2.5	0.006	0.019	0.026	0.099
AGABA	0.999	0.1-2.5	0.021	0.084	0.017	0.057
A5HT	0.998	0.1-2.5	0.008	0.028	0.007	0.024
O5HT	0.994	0.1-2.5	0.002	0.073	0.013	0.043
Pal5HT	0.998	0.1-2.5	0.007	0.023	0.012	0.042

Table 3. Calibration parameters

4.1.2.2 Precision and accuracy

The coefficients of variance (CV) and accuracy (BIAS) were always under 15%. Precision and accuracy levels, for all compounds, were displayed in the supplementary tables S1 and S2. A representative chromatogram of a SM sample spiked at intermediate concentration level for PUFA/eicosanoids and EC/NAE groups is reported in Fig. 5 and 6, respectively.

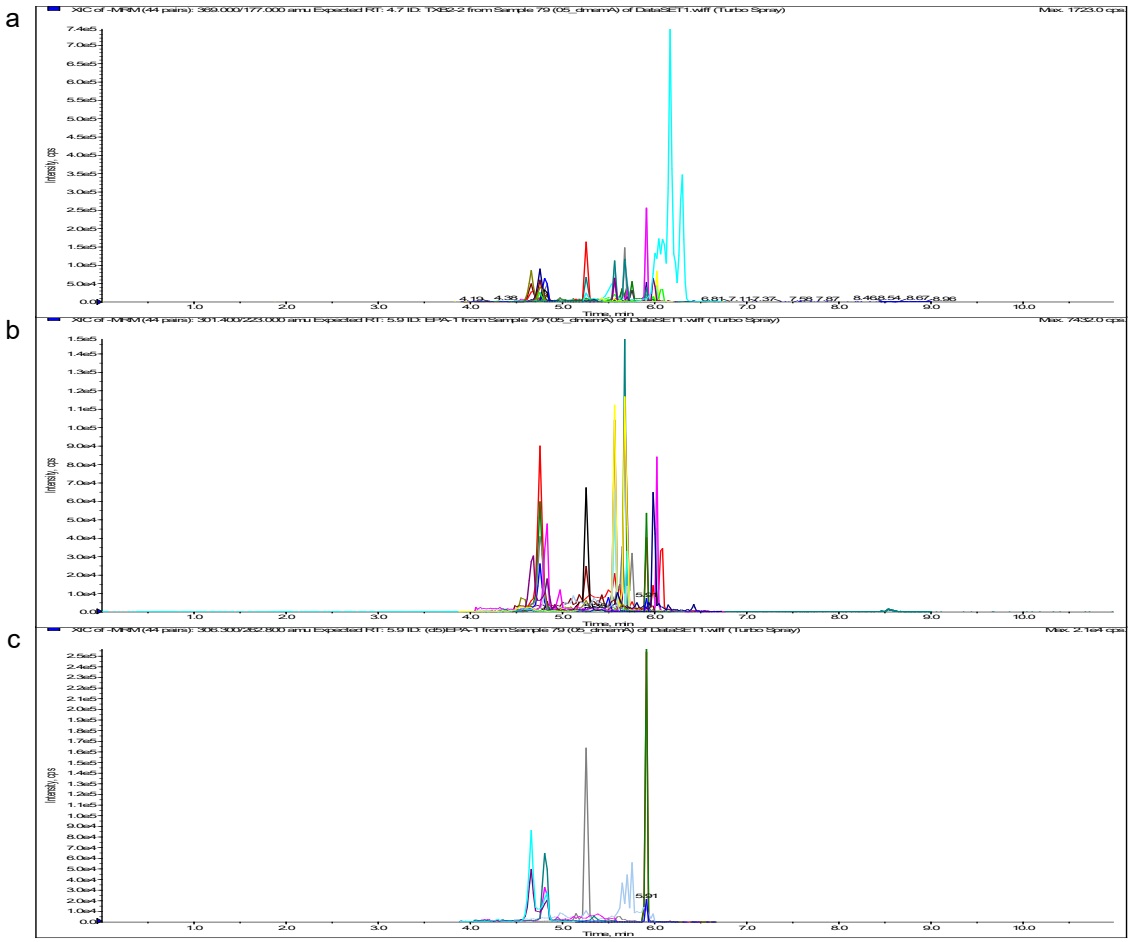

Fig 5. MRM chromatogram of PUFA/eicosanoids extract. From the top: Total ion Current (a), selected ion monitoring relative to standard molecules standard (0.5 ng/mL and 5 ng/mL for AA, EPA and DHA) (b), and to IS (c)

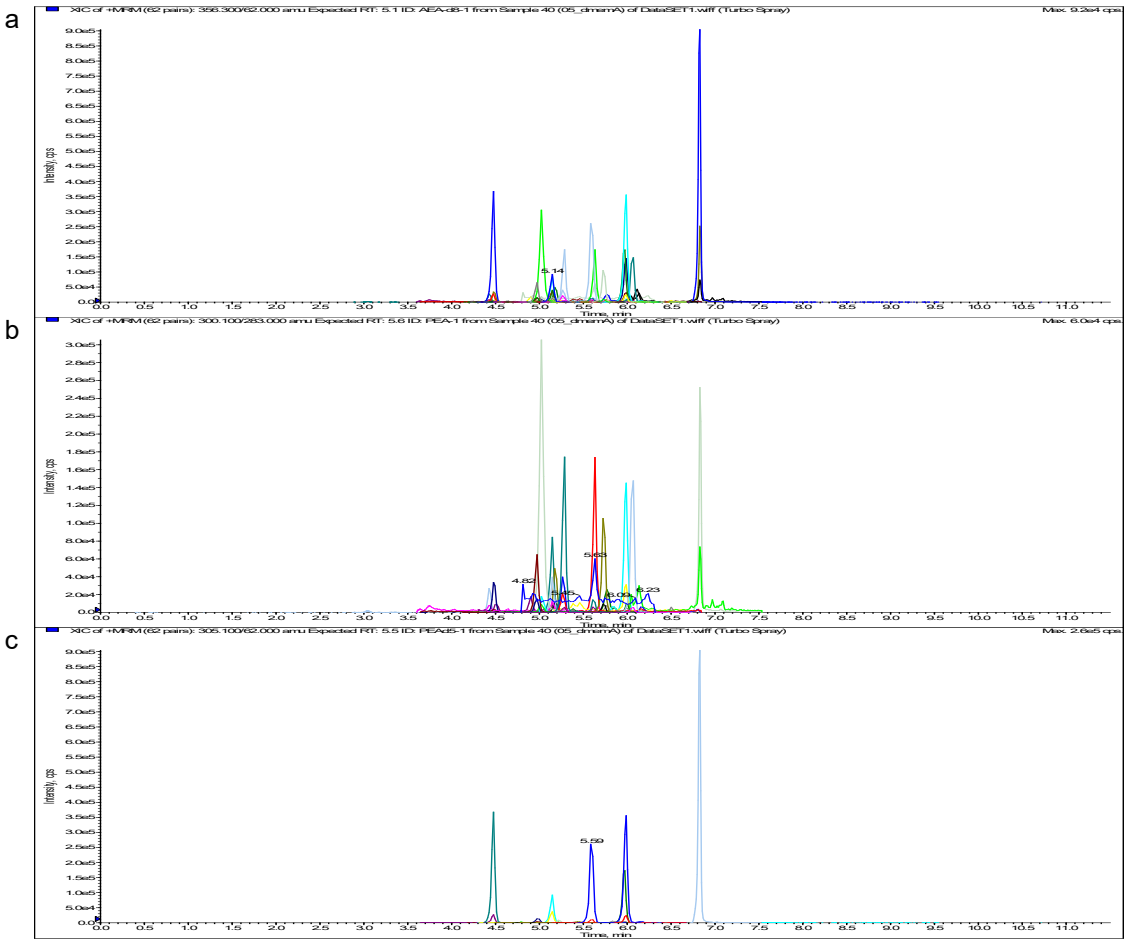

Fig 6. MRM chromatogram of EC/NAE extract. From the top: Total ion Current (a), selected ion monitoring relative to standard molecules standard (0.5 ng/mL) (b), and to IS (c)

4.1.2.3 Recovery and matrix effect

The mean extraction recovery in analyte-free SM was satisfactory, being over 41% for all the compounds belonging to PUFA/eicosanoids class (Figure 7a) and 52% for the EC/NAE class (Figure 7b), except for the basic compounds A5HT, O5HT e Pal5HT. Matrix effects ranged from ±20% for both lipids groups, except for PGF2α, 5(S)-HETE and O5HT (Figure 7c and 7d). To avoid the interference of serum and urine endogenous analytes on the evaluation of recovery and matrix effect, the peak area of ISs, spiked in these eluates, was compared to those in the extract and PBS, respectively. These results for PUFA/eicosanoids and EC/NAE are showed in the supplementary materials Table S3 and S4, respectively.

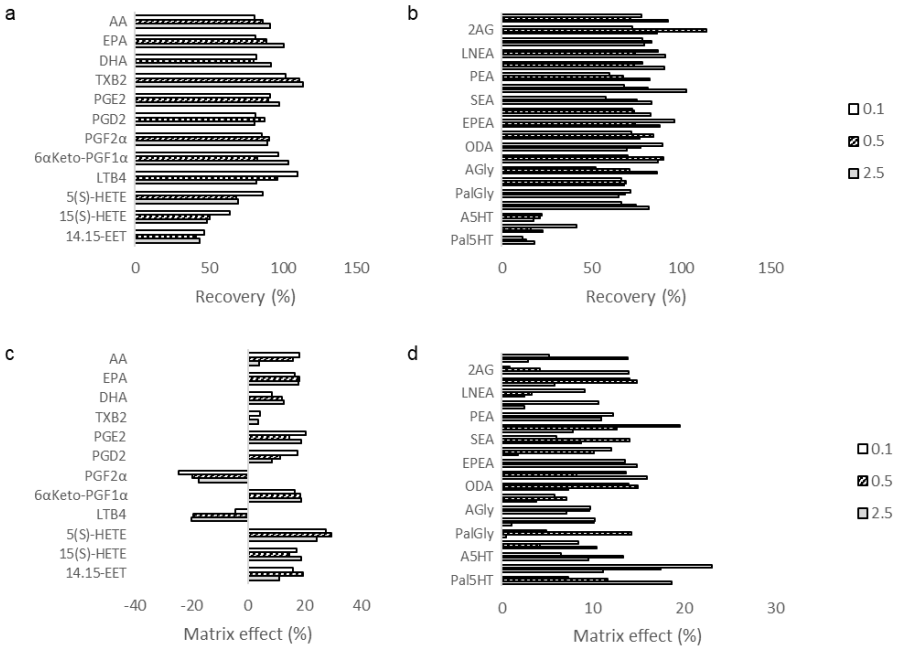

Fig 7. Extraction ecovery and matrix effect (%) values of PUFA/eicosanoids (a and c, respectively) and EC/NAE (b and d, respectively)

4.1.2.4 Stability studies

The analytes concentration in QC samples was not altered when kept at 4 °C and -20°C for 24 h, except for PGD_2, 5(S)-HETE¸15(S)-HETE e 14,15-EET, especially at -20°C (Supplementary material Table S5). The response factor did not show unacceptable differences compared with the first determination (mean deviation from day 0 < 15%).

4.1.2.5 Efficiency evaluation in real samples: CM and EV from 2 OS cell lines

The bioanalytical assays were applied to 2 OS cell lines-derived secretome (CM and EV) providing the absolute quantitation (> LOQs) of 3 PUFA (AA, EPA, DHA) and 7 EC/NAE (2AG, LEA, OEA, SEA, DHEA, PEA, PalGly), as displayed in Table 4.

	Saos-2				MG-63			
	CM pg/ml x10^6 cells		EV pg x10^6 cells		CM pg/ml x10^6 cells		EV pg x10^6 cells	
Compound	Mean	DS	Mean	DS	Mean	DS	Mean	DS
AA	0.26	0.02	0.78	0.06	nd	nd	nd	nd
EPA	0.14	0.002	0.16	0.003	nd	nd	nd	nd
DHA	0.18	0.01	0.14	0.01	nd	nd	nd	nd
2AG	78.4	3.78	73.9	3.57	5.37	0.26	1.77	0.09
LEA	3.18	0.29	1.31	0.12	22.5	2.07	3.13	0.29

OEA	1.91	0.09	3.88	0.18	nd	nd	3.33	0.15
SEA	6.34	0.51	10.4	0.85	11.3	0.92	12.1	0.90
DHEA	2.84	0.16	2.47	0.14	nd	nd	nd	nd
PEA	nd	nd	9.43	0.68	nd	nd	16.1	1.15
PalGly	nd	nd	21.5	1.10	nd	nd	nd	nd

Table 4. Lipids quantitation in CM and EV samples from Saos-2 and MG-63

4.2 MSC and DF secretome lipidomic characterization by UHPLC-MS/MS analysis

CM and EV preparations were obtained, as previously described, from the culture medium harvested from confluent BMSC, ASC and DF, cultured for 3 days in serum-free conditions: in brief, CM was concentrated by centrifugal filter devices of about 60 times, while EV were isolated by differential centrifugation at 100,000 g. A total of 32 lipids belonging to eicosanoids and EC were analyzed by MS techniques in CM and EV samples using the previously described analytical methods. MS data were acquired for all the CM and EV samples from ASC (*n=8*), BMSC (*n=5*) and DF (*n=3*), obtained from the cells of eight, five and three different donors, respectively. Cells and donor features are listed in table 5.

Primary cell type	Cell passage	Gender	Age	Surgery
ASC-1	IX	F	39	Total hip replacement
ASC-2	VII	F	35	Plastic surgery
ASC-3	VII	F	58	Plastic surgery
ASC-4	VIII	F	56	Total hip replacement
ASC-5	X	F	56	Total hip replacement
ASC-6	XI	F	26	Plastic surgery
ASC-7	V	F	46	Plastic surgery
ASC-8	VIII	F	34	Plastic surgery
BMSC-1	VI	M	47	Total hip replacement
BMSC-2	VI	F	69	Total hip replacement
BMSC-3	VII	F	60	Total hip replacement
BMSC-4	VIII	F	73	Total hip replacement
BMSC-5	VI	M	74	Total hip replacement
DF-1	V	F	46	Abdominoplasty

DF-2	IV	F	46	Abdominoplasty
DF-3	V	F	26	Abdominoplasty

Table 5. Cell passage and donor features

Data analysis allowed to quantify a total of 9 lipid molecules in MSC and DF-derived CM and EV samples. In detail, the presence of 2AG – PEA – OEA – SEA – DHEA belonging to EC/NAE and AA – EPA – DHA belonging to PUFA were reported in both preparations. PGE2 was found only in CM samples. An enrichment in lipid content were displayed in almost all MSC-CM and DF-CM rather than coupled MSC- and DF-derived EV. According to our previous findings (108), this result could be explained by the lower number of particles/10^6 cells found in EV preparations in comparison with coupled CM samples. Mean values and confidential interval 95% (CI95) were reported in table 6.

After a logarithmic transformation of lipids concentration levels found in CM and EV preparations to improve normality, all groups passed the Shapiro–Wilk test for normality. The lipids content from BMSC, ASC and DF groups were analyzed by a completely random ANOVA followed by post hoc Tukey's test. Measured lipids concentration for each group are shown in the box and whisker plots in Figure 9 and 10. Interestingly, the major differences were observed between BMSC and ASC/DF groups, suggesting similar lipid profile between ASC and DF-derived secretome. By a differential proteomic analysis, we have recently demonstrated a degree of similarity between ASC and DF secretome also at protein levels (109). In detail, 2AG – PEA – SEA and OEA were significantly different among BMSC-EV and both ASC-EV and DF-EV groups, but they did not differ between ASC-EV and DF-EV (Figure 9). Moreover, a significant difference was reported also for DHEA between BMSC-EV and DF-EV. In contrast, nonsignificant differences were found for PUFA and eicosanoids between MSC and DF-derived EV (Figure 9). Regarding CM samples, generally higher levels of lipids were displayed in BMSC group (Figure 8 and 9). 2AG and PGE2 were significantly different between BMSC and ASC, while PEA between BMSC and DF.

	BMSC				ASC				DF			
	CM pg/ml x10^6 cells		EV pg x10^6 cells		CM pg/ml x10^6 cells		EV pg x10^6 cells		CM pg/ml x10^6 cells		EV pg x10^6 cells	
Compound	Mean	IC95	Mean	IC95	Mean	IC95	Mean	IC95	Mean	IC95	Mean	IC95
AA	43.1	32.9	2.68	1.99	16.7	13.8	1.37	1.00	2.64	2.80	1.20	1.65
EPA	0.70	0.61	0.04	0.03	0.93	0.29	0.03	0.02	-	-	-	-
DHA	3.34	2.04	0.10	0.08	1.58	1.10	0.07	0.04	0.70	0.98	0.01	0.01
PGE2	163	145	-	-	38.1	14.5	-	-	28.8	12.5	-	-
2AG	287	159	118	59.2	53.2	28.3	18.7	14.9	16.2	3.69	10.9	4.94
OEA	55.4	39.3	14.5	6.41	3.14	0.77	2.46	1.03	4.96	3.24	2.53	1.66
SEA	549	577	59.7	38.9	81.2	36.6	12.0	10.1	31.3	20.5	9.27	11.02
DHEA	12.7	6.51	3.40	2.43	15.5	11.2	1.04	0.80	17.2	13.1	0.13	0.13
PEA	259	319	62.3	27.9	23.1	12.7	14.4	8.69	4.42	3.81	13.6	17.6

Table 6. Lipids quantitation in CM and EV samples from BMSC, ASC and DF

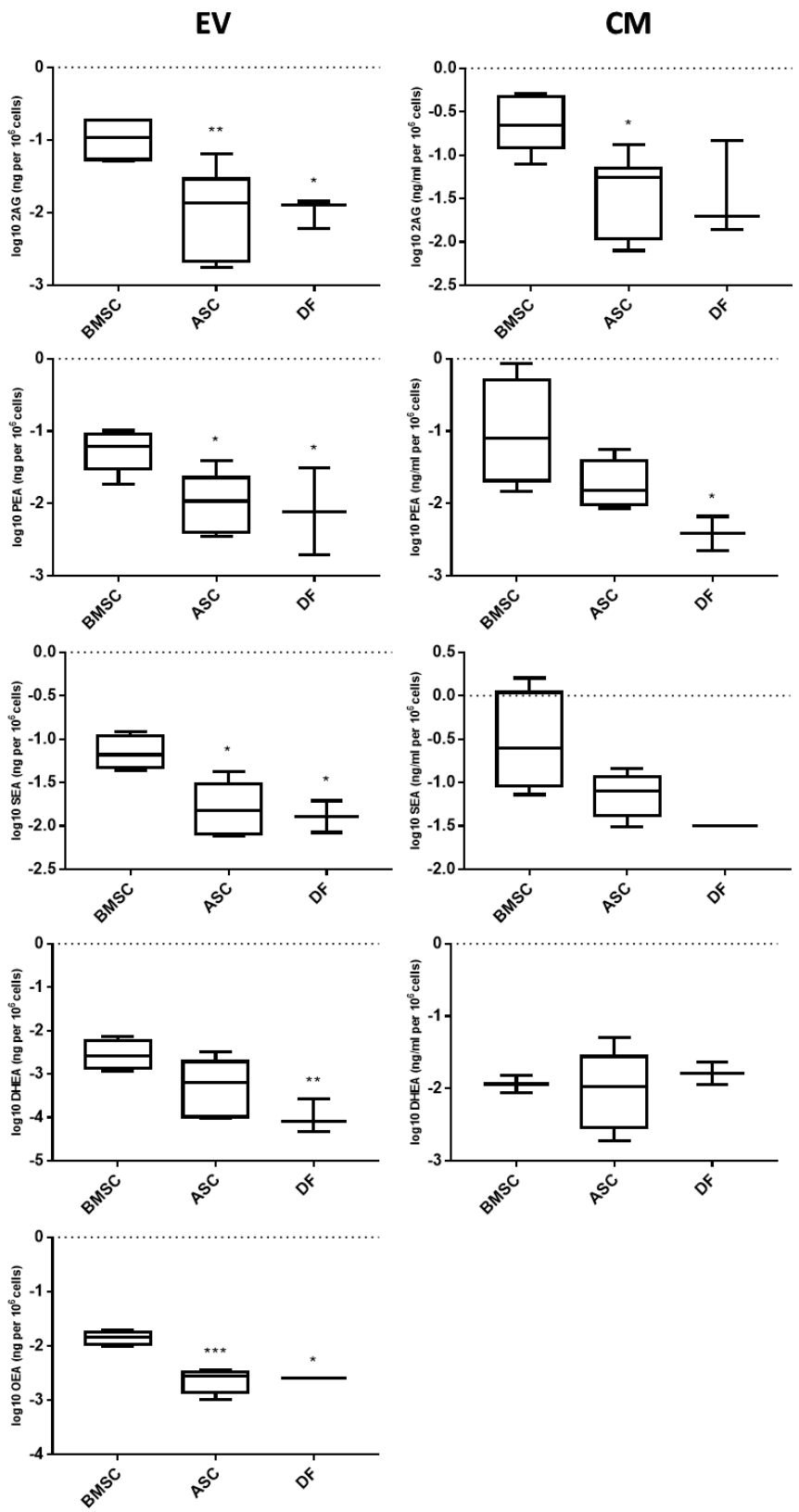

ANOVA followed by post-hoc Tukey's test: * p<0.05, ** p<0.001, *** p<0.0001 vs BMSC

Fig 8. Box and whisker plots referred to EC and NAE levels in EV (ng per 10^6 cells) and CM (ng/ml per 10^6) cells from BMSC, ASC and DF

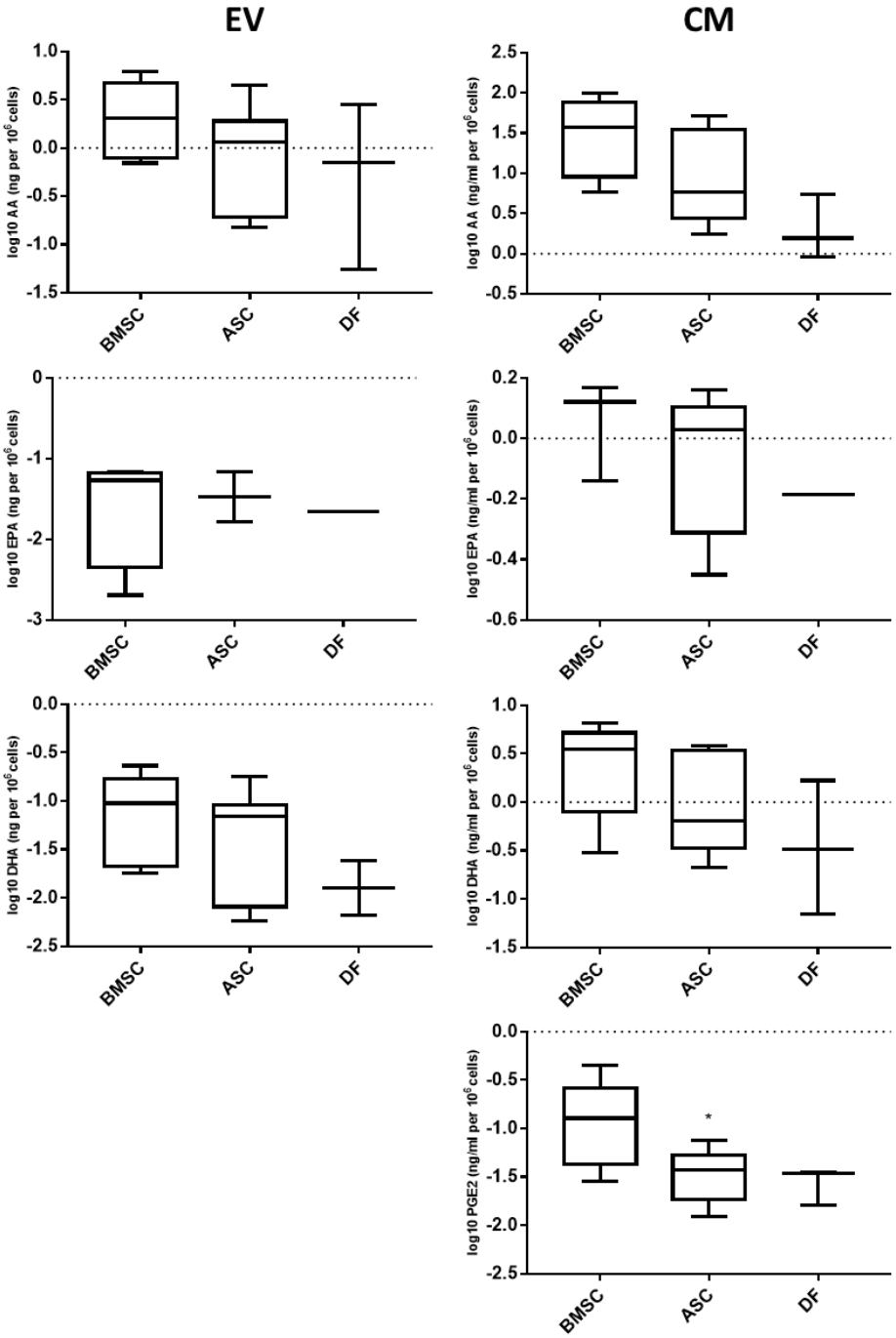

ANOVA followed by post-hoc Tukey's test: * p<0.05 vs BMSC

Fig 9. Box and whisker plots referred to PUFA and PGE2 levels in EV (ng per 10^6 cells) and CM (ng/ml per 10^6) from BMSC, ASC and DF

4.3 Evaluation of the functional activity of two ASC-CM bioactive lipids – 2AG and PEA – in an in vitro model of osteoarthritis (OA)

Considering MSC-CM future clinical translation and its promising anti-inflammatory therapeutic potential, here, the role of 2 bioactive lipids previously detected in MSC-CM samples was investigated *in vitro* in a model of OA. In detail, ASC-CM contains 2AG at the mean and median concentration value of 53.2 and 56.2 pg/ml x10^6 cells, respectively, and PEA at 23.1 and 15.3 pg/ml x10^6 cells, respectively.

4.3.1 CB1 and CB2 expression in primary articular CH

Initially, in order to study the involvement of EC system in the OA context, we assessed the CB1 and CB2 expression in untreated primary CH. Both CB1 and CB2 were expressed in all considered isolated CH, as reported in Figure 10 (c and d, respectively). Additionally, the 10ng/ml TNFα-treated CH as well as the effect of ASC-CM on TNFα-treated CH were assessed. The inflammatory stimulus significantly reduced the expression of both cannabinoid receptors after 3 days. ASC-CM did not affect TNFα-reduced CB receptors expression (Figure 10). Despite a decrease of CB1 and CB2 in TNFα-treated CH, we could observe their expression in all considered samples.

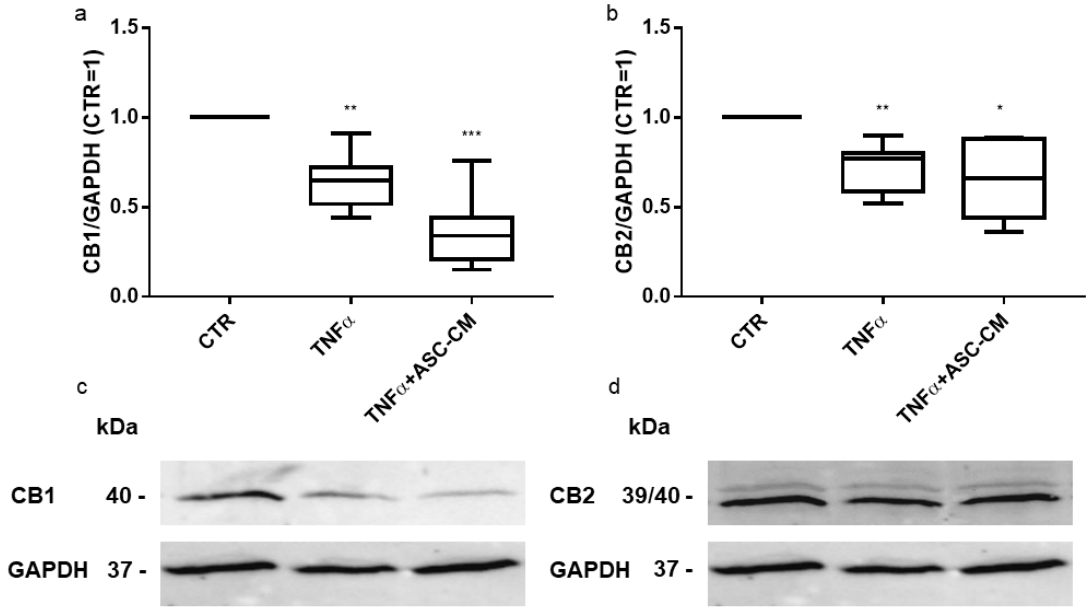

ANOVA followed by post-hoc Tukey's test: * p<0.05, ** p<0.01, *** p<0.001 vs CTR

Fig 10. Quantification of CB1 (a) and CB2 (b) expression in untreated, TNFα and TNFα+ASC-CM stimulated CH at day 3 analyzed by Western blot. Data (n=7 independent experiments) were normalized on GAPDH and expressed as relative values (CTR=1). (c-d) Representative Western

Blots of CB1 (c) and CB2 (d) expression by TNFα-stimulated and ASC-CM-treated CH. GAPDH was used as internal control and CB1 or CB2 densitometric evaluation was normalized on it.

4.3.2 2AG and PEA differently modulate inflammation in TNFα-treated CH

The PGE2 release and the protein expression of COX2, MMP3 and MMP13 were tested in in TNFα-stimulated CH in order to investigate a possible effect of the 2AG and PEA lipid mediators. As expected, 10 ng/ml TNFα raises the extracellular concentration of the inflammatory mediator PGE2 analyzed by MS (Figure 11a). In our previous study, we have demonstrated a possible counteracting effect of ASC-CM in decreasing PGE2 upregulation (166). In this case, an additional increment in PGE2 content was highlighted when CH were treated with the combination of TNFα and 2AG. In contrast, PEA showed a protective effect on the PGE2 release, providing a downmodulation up to the levels quantified in inactivated CH. Accordingly, TNFα increased the expression of COX2 especially when in association with 2AG (1pg/ml) (Figure 11b). By contrast, PEA (0.5pg/ml) partly blunts TNFα effect on the production of COX2.

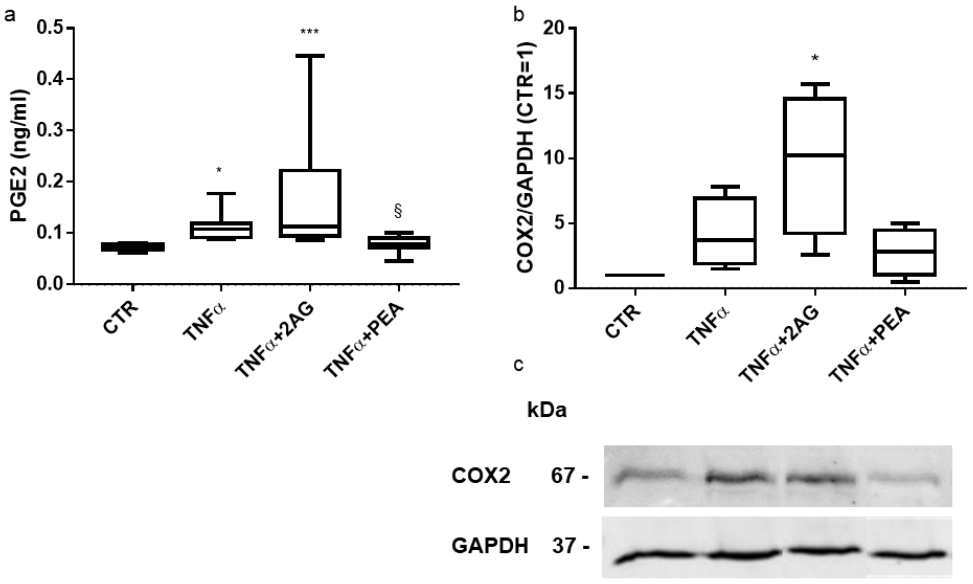

ANOVA followed by post-hoc Tukey's test: * p<0.05, *** p<0.001 vs CTR; § p<0.05 vs TNFα+2AG

Fig 11. Modulation of PGE2 (a) and COX2 (b) by 2AG (1pg/ml) and PEA (0.5pg/ml). (a) PGE2 release, analyzed by UHPLC-MS/MS in CH culture medium (n=8 independent experiments) 3 days

after treatments. (b) Quantification of the COX2 expression in TNFα-stimulated and 2AG or PEA-treated CH at day 3 analyzed by Western blot. Data (n=4 independent experiments) were normalized on GAPDH and expressed as relative values (CTR=1). (c) Representative Western Blots of COX2 expression by TNFα-stimulated and 2AG- or PEA-treated CH. GAPDH was used as internal control and COX2 densitometric evaluation was normalized on it.

At last, the expression of MMP3 and MMP13, two matrix-degrading enzymes involved in OA, were investigated. Our previous study showed that no significant effects were exerted on their expression by ASC-CM treatment on TNFα-stimulated CH (134,166). Consistently, also 2AG and PEA exert no effect on MMP3 and MMP13 expression (Supplementary materials F1).

4.3.3 ASC-CM and PEA, but not 2AG, reduce NO production in CH culture medium

Unstimulated CH produce low levels of NO, but its production is strongly enhanced by the inflammatory stimulus TNFα after 3 days (Figure 12). In addition, also the co-treatment of CH with TNFα and 2AG significantly increased NO production compared to untreated cells. By contrast, PEA seems to partially counteract TNFα-induced production showing no statistically significant difference if compared with unstimulated CH. Differently, ASC-CM significantly reverts TNFα effect.

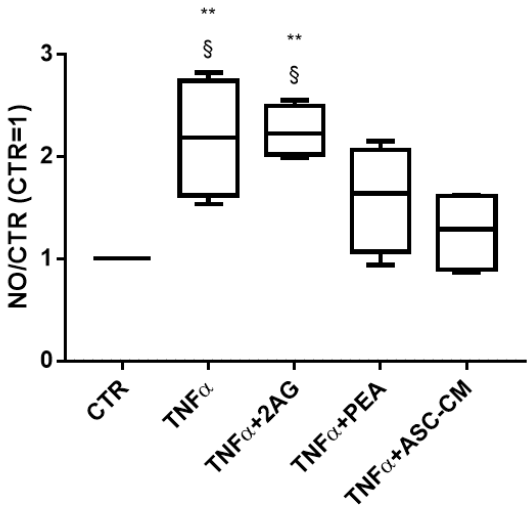

ANOVA followed by post-hoc Tukey's test:
** p<0.01 vs CTR, § p<0.05 vs TNFα+ASC-CM

Fig 12. Quantification of NO by 2AG (1pg/ml), PEA (0.5pg/ml) and ASC-CM treatments NO production, analyzed in CH culture medium (n=4 independent experiments) at day 3, is expressed as [nitrite] μM. Data were expressed as relative values (CTR=1)

4.3.4 Modulation of PUFA lipid precursors in untreated and TNFα-stimulated CH cell media

Given the involvement of lipid precursors in inflammation and OA progression, a lipidomic analysis of PUFA in CH culture media was performed by previously developed UHPLC-MS/MS methods. At first, PUFA levels were analyzed in the culture media of untreated CH as well as 2AG, PEA and ASC-CM treated CH without TNFα. No significant differences were showed among treatments (Figure 13).

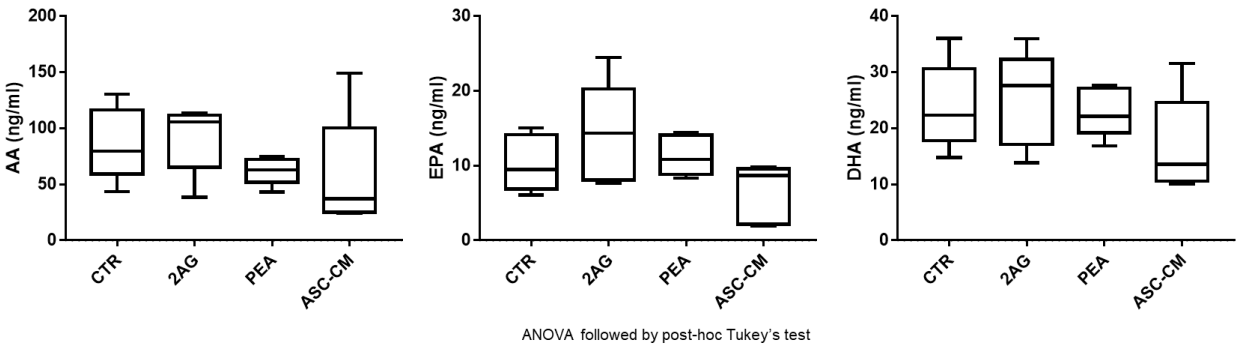

Fig 13. Quantification of AA, EPA and DHA in untreated and 2AG, PEA, ASC-CM treated CH cell media (absence of TNFα) at day 3 analyzed by UHPLC-MS/MS analysis. Data (n=5 independent experiments) were expressed in ng/ml

Differently, TNFα significantly decreases PUFA lipid precursors expression in CH culture media. Despite the inter-donor variability due to the use of patient-derived articular CH, a clear effect of TNFα on PUFA expression was always determined, as displayed in Figure 14. A significant reduction of AA, EPA and DHA were displayed under TNFα stimulation. Conversely, 2AG, PEA and ASC-CM did not affect TNFα-reduced PUFA levels (supplementary materials F2). At intracellular level, TNFα did not exert a downmodulation of PUFA (supplementary materials F3).

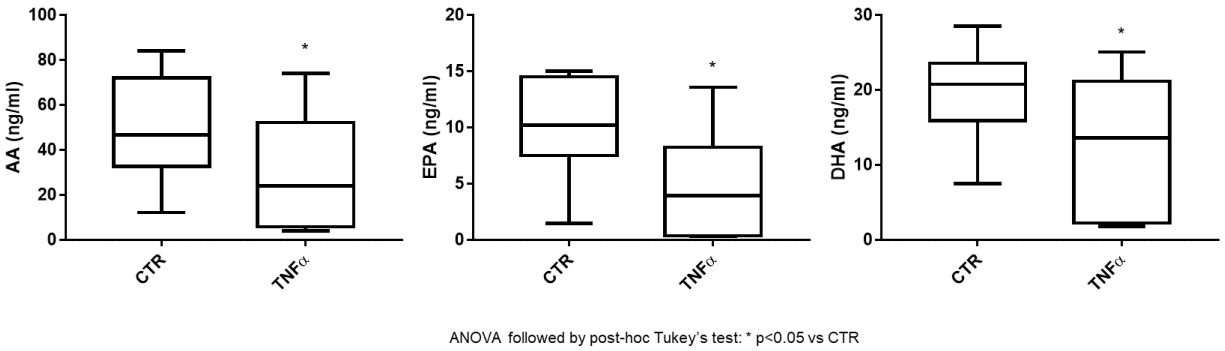

Fig 14. Quantification of AA, EPA and DHA in TNFα-stimulated CH cell media at day 3 analyzed by UHPLC-MS/MS analysis. Data (n=9 independent experiments) were expressed in ng/ml

4.3.5 Pro and anti-inflammatory lipids determination in CH culture media and lysates

Lipidomic data analysis of eicosanoids and EC/NAE confirms the presence of specific lipid profiles both in CH cell media and lysates. Unstimulated CH secrete low levels of PGE2, as previously reported at paragraph 4.3.2, but also PGD2, PGF2α, PEA, SEA and DHEA were detected in the cell media of 2AG, PEA and ASC-CM treated CH without TNFα (Figure 15).

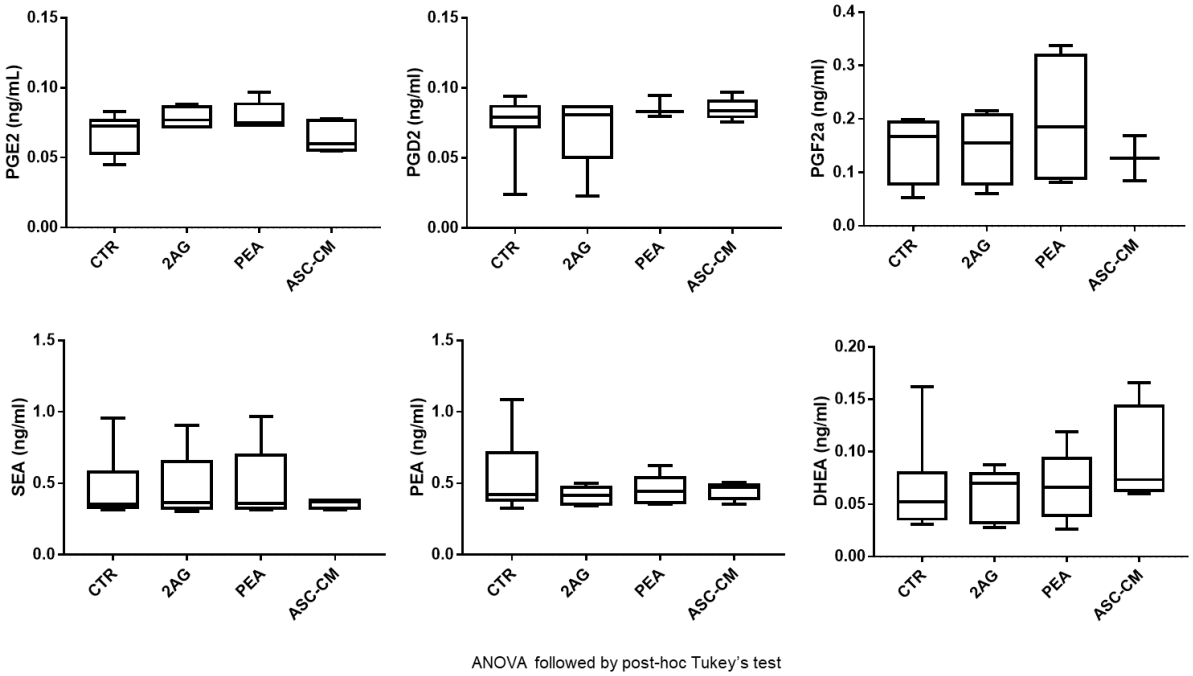

Fig 15. Quantification of lipids in untreated and 2AG, PEA, ASC-CM treated CH cell media (absence of TNFα) at day 3 analyzed by UHPLC-MS/MS analysis. Data (n=5 independent experiments) were expressed in ng/ml

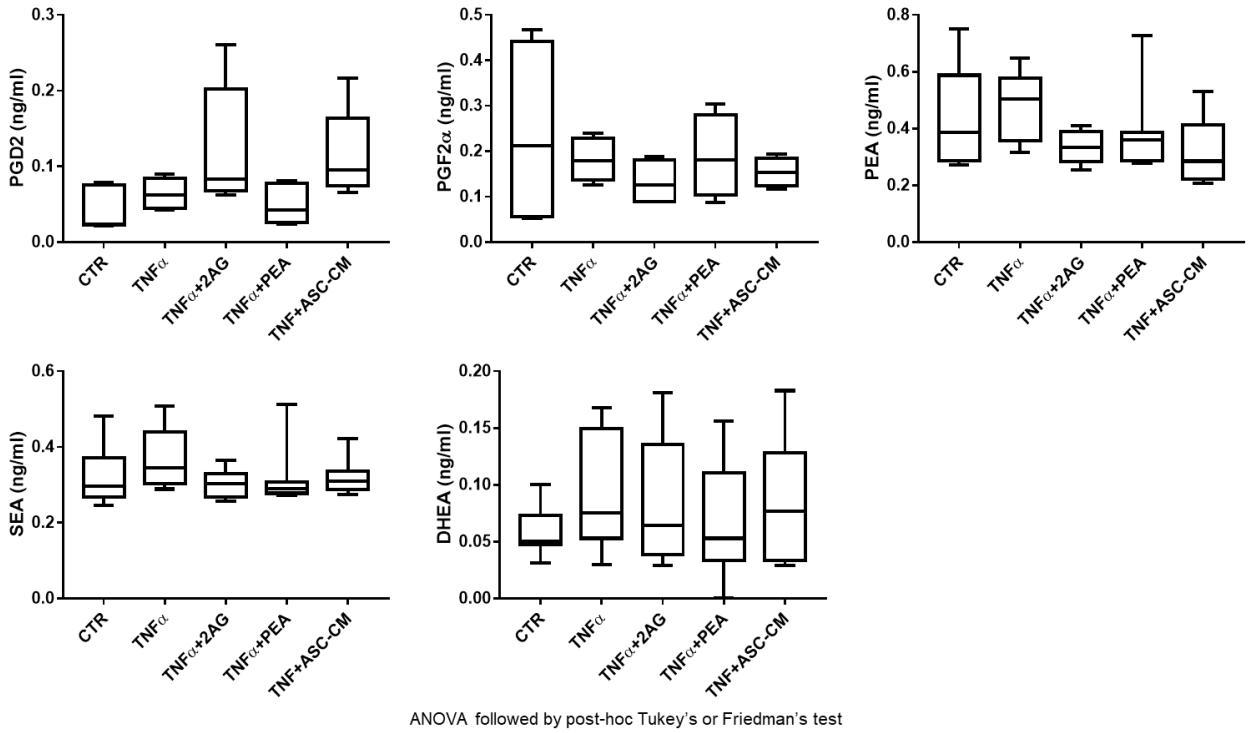

Fig 16. Quantification of lipids in CH cell media at day 3 analyzed by UHPLC-MS/MS analysis. Data (n=7 independent experiments) were expressed in ng/ml

However, except for PGE2 (Figure 11a), no significant differences were displayed also by all considered TNFα treatments (Figure 16), while 2AG was quantifiable only under TNFα alone and in combination with 2AG or ASC-CM treatments. Similar results were reported at intracellular levels. Picomolar concentrations of 2AG, PEA, SEA and DHEA were found in CH cell lysates, but no modulation was displayed among treatments (supplementary materials F4).

5. Discussion and conclusions

5.1 Targeted MS analytical methods development and validation

Lipid analysis is challenging because of the very low concentrations of lipids in biological samples (pg to ng per ml or mg), their different physio-chemical properties, the *in vitro* metabolism and the autoxidation. For an efficient extraction recovery of lipids like PUFA, eicosanoids, EC and NAE from biomatrices, an optimized solvent combination is necessary to cover the whole polarity and pKa ranges of these metabolites, including for example the polar PG and the less polar PUFA. Several protocols for the extraction and the subsequent analysis of either EC and NAE, mainly AEA and 2AG, or PUFA and eicosanoids have been previously published (187–189): the majority of LLE protocols according to Bligh and Dyer or Folch (20,190) are limited by the distribution of analytes in both water and chloroform layers. However, application of ternary solvent combinations including polar as well as nonpolar solvents seems to be a way to overcome these problems (21,188,189). In this work, different protocols for the purification and several combinations of solvents over the expected polarity range were examined for the extraction of the considered analytes. The highest lipids count was obtained through a double step extraction preparation with DCM/IPA (8:2; v/v) and EtOAc/n-hexane (9:1; v/v), respectively. Despite SPE is largely used for its capability to provide concentrated and free-interfering-matrix components extracts (187,191–193), there are some drawbacks, such as the fact that it's money- and time-consuming, due to the necessity of column cartridges and multiple steps. Contrarily, LLE is an easier and faster procedure, if compared to the most commonly SPE procedures, and these features could represent an advantage for studies that involve a huge number of samples. One critic issue of LLE (but also SPE) could be the toxicity of the organic solvents used. In the extraction protocol we applied, a simple and fast pretreatment, consisting of proteins exclusion with ACN followed by a first extraction with DCM/IPA (8:2; v/v) and a second one with EtOAc/n-hexane (9:1; v/v), was used: these solvents are surely less toxic than others commonly used, such as toluene, chloroform or tert-methyl-butyl ether (Figure 17). In general, the combination of two or more sample preparation techniques, such as protein precipitation and LLE, improves method selectivity (189,191,192). Additionally, the second extraction is preceded by a pH adjustment step, which is crucial since some eicosanoids present a lower pKa value than EC. Indeed, a lower pH leads to a decreased protein binding and the protonation of carboxylate anions, which both allow improved

extraction by the organic solvent. Otherwise, greater acidification may lead to eicosanoid alteration (194), and therefore an extremely low pH should be avoided. The optimized solvent mixture, combined with the pH adjustment, which allows a lower protein binding and an enhanced extraction of the non-ionized forms, was necessary to cover the whole polarity range of these numerous metabolites. Moreover, the two sequential extraction steps, from a single sample, allow to analyze limited amount of samples, a very useful feature for in vitro and preclinical studies.

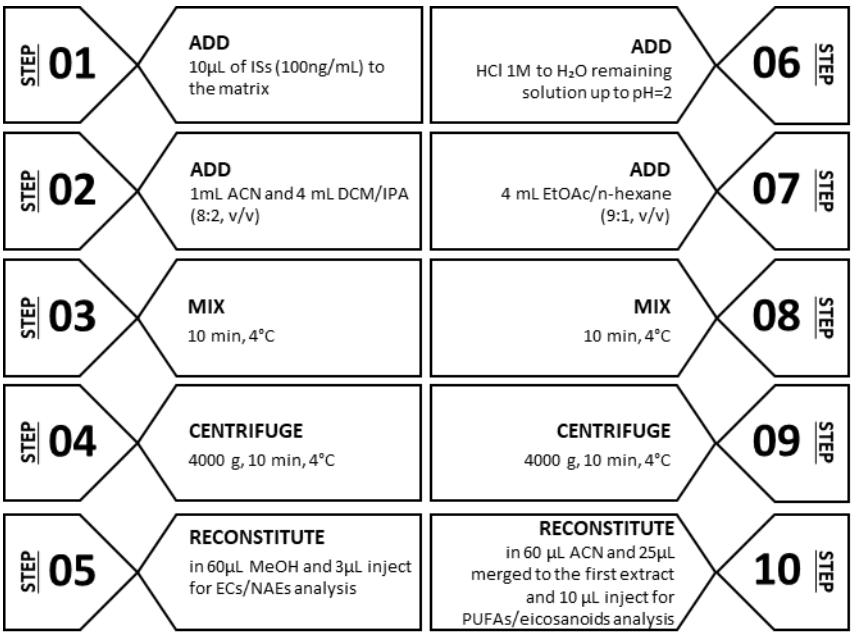

Fig 17. Scheme of the LLE protocol for EC/NAE (step 1-5) and PUFA/eicosanoids (step 6-10)

After the extraction procedure set-up, the instrumental UHPLC and MS parameters were optimized as previously described (paragraph 4.1.1). Several reversed phase columns (i.e., C18, C8, phenyl, biphenyl), mobile phases and elution gradients have been tested in order to improve the responses of the target compounds and to reduce the analysis time. Finally, two different elution gradients, performed on a Kinetex UHPLC XB-C18 column and characterized by the same mobile phases and a moderate runtime, were developed. This allowed the consequential analysis of the two classes of interest without changing either the elution column or mobile phases, and therefore without operator assistance.

According to the FDA guidelines, the major issue of analytical methods validation for biologics were satisfied, as previously described (paragraph 4.1.2). Methods specificity was achieved by the selection of the parent ion, followed by detection and quantification of product ions. The calibration curves were performed in SM and PBS, the latter in order to allow the lipid quantification also in different biomatrices such as serum and urine that may contain analytes of interest. To do this, we compared the calibration curves prepared spiking IS, at the same concentration levels, in PBS and in human serum/urine (see paragraph 3.1.8.1). We obtained parallel curves, with a standard deviation of correlation coefficients below than 0.0001. For this reason, calibration lines obtained from CS spiked in PBS may be used for lipids quantification. Specificity tests, performed on all reagents and consumables used, have shown not to interfere with the detection or quantification of the analytes. To avoid the interference of endogenous analytes on the evaluation of recovery and matrix effect, the peak area of IS, spiked in serum and in urine eluates, was compared to those obtained in the extract and in PBS, providing results within the acceptance criteria, except for the PEA-d5, OEA-d2, and AGly-d8 matrix effect in human serum, whose percentage mean was 59% ± 8%, and TXB2-d4 in both serum and urine, which was 56% ± 7% (supplementary materials). Concerning SM matrix, as previously displayed, a full method validation was performed, showing satisfactory values for all the considered parameters (LOD, LOQ, precision, accuracy, recovery, matrix effect and stability). At first, the developed analytical methods efficiency was evaluated in EV and CM samples from two osteosarcoma (OS) cell lines, Saos-2 and MG-63, as described at paragraph 3.1.9. Quantitative data are presented in table 2. Three PUFA (AA, EPA, DHA) and seven EC/NAE (2AG, LEA, OEA, SEA, DHEA, PEA, PalGly) were quantified (> LOQ). PUFA and the AA-related metabolite 2AG were found to be more expressed in Saos-2-derived samples than in MG-63-derived ones. Surprisingly, no PUFA/eicosanoid was detectable in MG-63 samples. Among ECs, PalGly is the only compound, belonging to N-acylglycines, which was found in Saos-2-derived EV only. 2AG, LEA and SEA were quantified in all the considered samples. LEA, PEA and SEA were found more abundant in MG-63-derived samples, with PEA detectable only in EV. Interestingly, 2AG and DHEA were more abundant and/or quantified only in Saos-2-derived samples, as well as their related compounds AA and DHA, respectively. It is well known that eicosanoids and EC/NAE are biologically active lipid mediators that play a critical role in different pathological processes, however little is still known about their release in OS secretome. Our results provided evidence of a different lipid secretion

between the two considered OS cell lines. Other peculiar characteristics that clearly differentiate this two bone tumor cell lines, including differences in growth, gene expression and immunohistochemical profiles, have already been demonstrated (195,196). Indeed, Saos-2 cells display a more mature osteoblastic phenotype with a stronger alkaline phosphatase activity and a larger expression of osteoblastic markers (osteocalcin, bone sialoprotein, decorin and procollagen-I) than MG-63. The latter exhibit both mature and immature osteoblastic features, with only a small subpopulation expressing the typical osteoblastic markers. In conclusion, we demonstrated that the methods we set-up in this work provide enough sensibility and specificity to analyze low amount of lipids in cell secretome like CM and EV, and this procedure could represent a useful tool to investigate other components of inflammatory microenvironment, relevant for the cellular crosstalk among injured tissues and mesenchymal stem/stromal cells, which are already under investigation in our laboratory by a proteomic approach.

5.2 MSC and DF secretome lipidomic characterization by UHPLC-MS/MS analysis

The therapeutic potential of the MSC secretome in disparate medical fields, from immunology to orthopedics, has been widely suggested by in vitro and in vivo evidences. Recently, in the context of cell therapy, also DF, the major cell type in the human dermis, have started to be considered a suitable alternative to MSC. Indeed, they share common characteristics including positivity to the same mesenchymal markers and multi-differentiative potential towards mesodermal lineage and, additionally, they exert anti-inflammatory, immunomodulatory and regenerative effects (197,198). Their therapeutic potential is similar and, in comparison to MSC, DF are easier to expand in vitro. Moreover, while the DF canonical therapeutic applications include skin regeneration and wound healing, our recent investigation have provided evidences of pro-osteogenic action of their secretome (177).

Despite the overall success obtained in clinical trials, cell therapy presents several challenges, such as safety/regulatory concerns and technical aspects (harvesting procedure, cell expansion, and storage of the final product). However, nowadays it is widely accepted that MSC action is largely mediated by paracrine mechanisms (199), thus for this reason and due to the extreme complexity of their secretome/conditioned medium (MSC-CM) composition, a great multidisciplinary scientific effort and an extensively

characterization are needed in the perspective of the future clinical translation. Our recent research has identified key ingredients, including lipids, of ASC secretome that may be involved in its therapeutic action and whose consistent levels among different ASC-CM batches may represent promising quality control criteria (200).

In this context, we aim at partially disclosing the lipid content of the two most common secretome formulas, i.e. CM and EV, from primary BMSC, ASC and DF. The lipidomic MS developed methods have demonstrated their usefulness in assessing a total of 9 lipid molecules in MSC and DF-derived CM and EV samples. 2AG, PEA, OEA, SEA, DHEA belonging to EC/NAE and AA, EPA, DHA, PGE2 belonging to PUFA/eicosanoids were detected and quantified. The present data confirm previously findings obtained by analyzing the secretome of different cell sources (OS cell lines) (25).

With this work we showed that (i) detected lipids are more enriched in CM samples than coupled isolated EV (ii) lipid content in CM and EV can distinguished BMSC from ASC and DF, but not ASC from DF and (iii) inflammatory factor PGE2 is expressed specifically by CM samples. An enrichment in lipid content was displayed in almost all MSC-CM and DF-CM rather than coupled MSC- and DF-derived EV. This result appears in accordance with our previous work demonstrating a 3–4 times higher number of particles per million donor cells in CM preparations compared to EV ones (108). This data could be explained by a suboptimal yield of the ultracentrifugation procedure, as already reported in the literature (201,202). However, our isolation procedure through ultracentrifugation did not affect EV quality in terms of size distribution and antigen profile (108).

Interestingly, the major differences related to cell type were observed between both BMSC-ASC and BMSC-DF groups, suggesting a more similar lipid profile between ASC and DF-derived secretome. Accordingly, a Raman spectroscopy profile on ASC and DF secretomes demonstrates that CM from these cell types share also common proteomic patterns (177). In order to confirm these data, we have recently performed a quantitative proteomics to explore the protein composition of CM and EV from these two cell types providing evidences that multiple biological processes were shared between ASC and DF-derived (109).

Finally, the levels of the inflammatory mediator PGE2 were found significantly lower in ASC-CM than BMSC-CM. This PG is generally known to exert multiple opposed functions based on its concentration; its quantification in CM could be remarkable in several pathological and inflammatory context.

5.3 Evaluation of the functional activity of two ASC-CM bioactive lipids – 2AG and PEA – in an in vitro model of osteoarthritis (OA)

Among other MSC sources, adipose tissue presents several advantages in terms of harvesting procedure, cell isolation, and expansion (203). In the last years, the safety and the efficacy of ASC in counteracting OA have been proved both *in vitro* (134,166) and *in vivo* (161,167), and confirmed by clinical trials (164). Since ASC act mainly through paracrine mechanisms, their secretome represents a promising therapeutic alternative. Two papers have been recently published, reviewing the MSC-CM therapeutic action on cartilage, subchondral bone and synovium (204,205). As previously described, ASC-CM is a complex cocktail of proteins, nucleic acids, and lipids released as soluble factors and/or conveyed into EV. In this way, CM represents a promising complete product characterized by an easier manufacturing procedure and a minor manipulation, accounting for a more feasible scale up, in comparison to ultracentrifuge-isolated EV. Additionally, it is well known that ASC-CM preparations allow also a complete retention of the vesicular component (134,206). Considering future clinical applications in the OA management and the previously promising results obtained in OA context by ASC-CM treatment, we investigated the potential role of two bioactive lipids, quantified in ASC-CM -i.e., 2AG and PEA-, whose action is widely documented in others inflammatory diseases (72,207), in an *in vitro* model of OA (Figure 18). The experimental settings were realized on the lipid concentrations found in ASC-CM: a mean concentration level of 53.2 pg/ml x10^6 cells for 2AG and of 23.1 x10^6 cells for PEA.

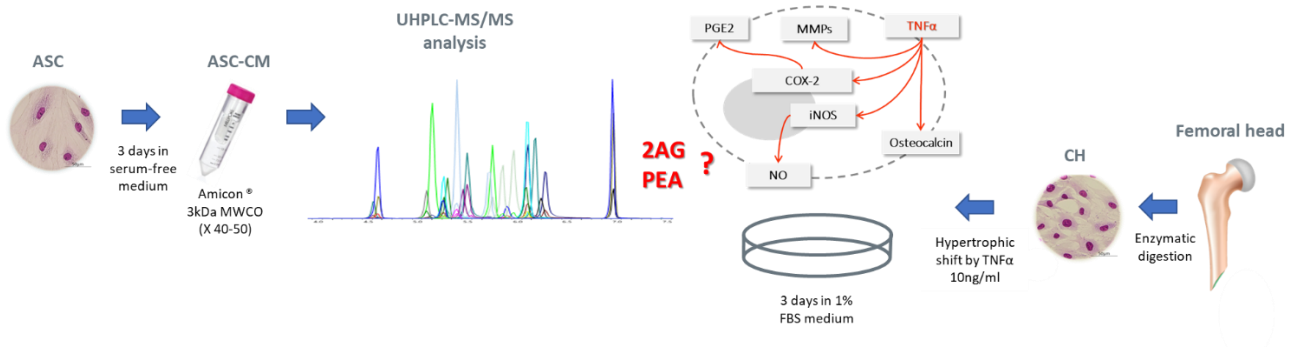

Fig 18. Experimental *in vitro* model of OA

Although CB signaling and the regulation of cytokines by some cannabinoids are well documented (208,209), only few studies have looked so far at the effects of inflammatory cytokines on the cannabinoid system (210,211). Thus, at first, in order to study the interaction between the ECS and the inflammatory cytokine TNFα in articular CH, we found that CB1 and CB2 expression levels were most significantly reduced by TNFα treatment (Figure 10). In the literature, conflictingly results on the CB receptor modulation by TNFα and other cytokines are reported (212,213). This may be attributed to the different concentrations used or to the cell origin. However, both CB receptors were always detected in untreated and TNFα-treated CH. No significant differences were showed by ASC-CM treatment on TNFα-reduced CB receptors expression (Figure 10).

An opposite modulation of inflammatory factors (i.e., PGE2 and COX2) by 2AG and PEA was reported in TNFα-treated CH. Our data confirm a PGE2 extracellular concentration enhancement under a 10 ng/ml TNFα treatment (Figure 11a). Indeed, we have recently demonstrated a possible counteracting effect of ASC-CM in decreasing PGE2 upregulation by TNFα-stimulated CH (166). Here, an additional increment in PGE2 content was highlighted when CH were treated with the combination of TNFα and 2AG. By contrast, PEA reduced the PGE2 production, providing a downmodulation up to 0.08±0.02 ng/ml and restoring its physiological levels linked to a healthy CH phenotype (0.07±0.01 ng/ml). Gabrielsson et al. proposed a linkage between reduced levels of PG and the blockage of hydrolysis of PEA to palmitic acid (214).

Generally, unstimulated CH release low amounts of PGE2 that are consistent with the concentrations known to inhibit collagen cleavage and the expression of hypertrophy markers (215), while increasing PGE2 levels exerts a pro-catabolic and anti-anabolic effect on articular CH (216,217). Recently, a potential effect of CM in reducing TNFα-related inflammation by CH was linked to COX2 expression. Indeed, TNFα treatment induces PGE2 release through the activation of COX2 transcription via NF-κB (218). Also, in this context, TNFα increased the expression of COX2 especially when in association with 2AG, suggesting a possible interconnection (Figure 11b). By contrast, PEA partly blunts TNFα effect on the production of COX2. The ability of PEA to reduce COX2 expression and/or PG release was determined in other in vivo studies using models of pain and/or inflammation (219–221), while a reduction in COX2 activity was observed in a macrophage cell line, but without a direct effect of PEA on COX2 levels (214).

Another promising result related to ASC-CM in OA context is the blunting of the TNFα-mediated hypertrophic shift. We previously demonstrated that ASC-CM is able to mediate a reduction of MMPs activity, correlated to the abundance of TIMPs in ASC secretome, rather than to a direct down-modulation of the expression and/or release of these proteases (134). Consistently, in this case, neither 2AG nor PEA exert any effect on MMP3 and MMP13 expression (Supplementary materials F1).

Moreover, it is well known that inflammatory CH produce large quantities of NO by iNOS, for example when stimulated by IL-1 or LPS (135). NO is a signaling molecule produced in the oxidative deamination of L-arginine catalyzed by a NOS. During an inflammatory process, the inducible isoform of this enzyme (iNOS or NOS2), which is not expressed in non-pathological situations, is up regulated. This up-regulation can be initiated by different stimuli including lipopolysaccharide (LPS), inflammatory cytokines or IFN-γ. Also, cartilage obtained from arthritic patients produces significant amounts of NO ex vivo, even in the absence of IL-1 or LPS (135). NO produced by iNOS has been shown to be a key inflammatory mediator in tissue injury in a variety of pathological conditions and there are increasing evidences that excess NO production could be a pivotal factor in the early stages of OA (222–224). Here, while unstimulated CH produce low levels of NO, its release is strongly enhanced by the TNFα inflammatory stimulus. Indeed, in cytokine-stimulated CH, NO sustains nuclear translocation of NF-kB, maintaining the NF-kB-dependent transcription persistently activated (225). This may be the mechanism through which NO promotes cartilage degradation. In this way, NO may promote expression of proteinases (i.e., MMPs) responsible for the degradation of the ECM. Indeed, the selective inhibition of NF-kB blocks inflammatory bone destruction (226). Our results show that both ASC-CM and low doses of PEA (pg/ml) reduced NO formation in TNFα-stimulated CH (Figure 12). The PEA effect on NO production seems to be in line with previous investigations published by Mejerink et al, who reported comparable results by other anti-inflammatory NAE including DHEA (76). Moreover, Mbvundula et al. showed that a synthetic cannabinoid is more potent in inhibiting IL-1a-induced NO production in bovine articular CH than the endogenous AEA. It may be attributed to its readily metabolization by the FAAH.

By contrast, we found that 2AG significantly increases NO production compared to untreated CH (Figure 12). 2AG may also be metabolized via COX2 pathway, leading to the formation of pro-inflammatory PG (67). Thus, PEA, but not 2AG, appear to have potential as cartilage

protective agent by abrogating cartilage matrix degradation through its ability to inhibit NO production. However, further studies are required to elucidate the mechanisms by which this occurs, for example by involving PEA antagonists receptors or FAAH inhibitors.

At last, since it is well documented the PUFA involvement in inflammatory context, the cell medium of untreated and TNFα-treated CH was analyzed by previously developed analytical methods for lipids determination.

Although previous studies support a role PUFA in modifying OA severity, data on the effect of TNFα on these lipid precursors are still missing. Here, we showed a clear reduction of all secreted PUFA, both ω6 and ω3, by CH under the inflammatory stimulus (Figure 14). In this case, all considered treatment were not able to revert the TNFα down-regulation. By contrast, no significant differences were displayed for PUFA derivatives (PGD2 and PGF2α) and NAE (PEA, SEA, DHEA) in the cell media from untreated and treated CH, suggesting there is no-influence by the different treatments including TNFα.

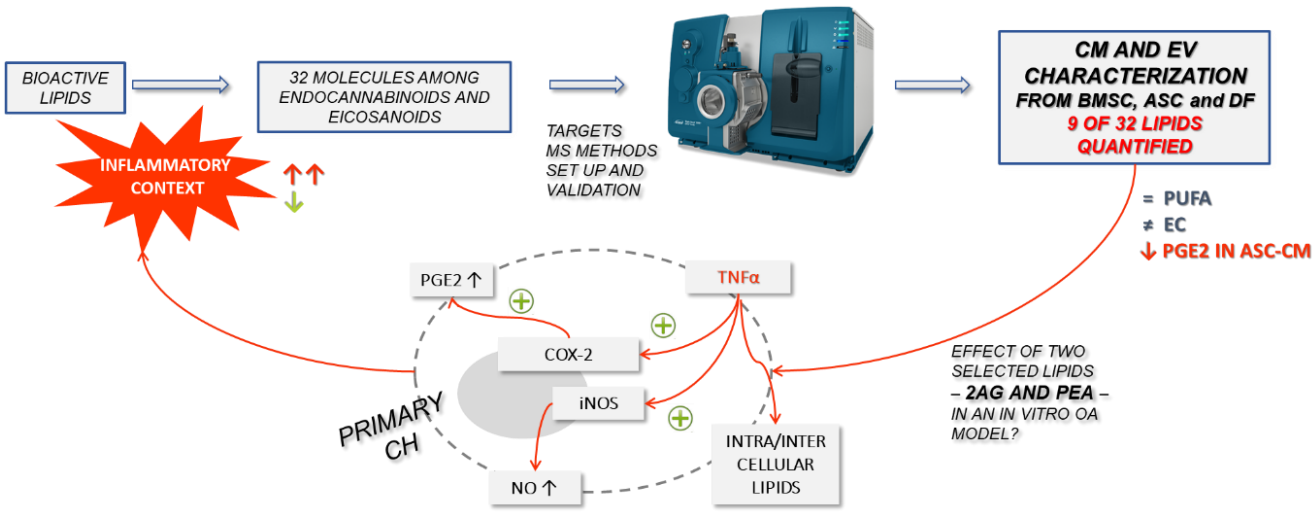

Fig 19. Experimental design: from lipid MS analysis to their functional roles in an *in vitro* model of OA

In conclusion (Figure 19), in this thesis, two targeted UHPLC-MS/MS analytical methods for the identification and quantification of 32 lipid molecules, belonging to PUFA, eicosanoids, EC and NAE families, were developed and fully validated in several bio-matrices, according to the FDA guidelines. We first applied the methods to the secretome from BMSC, ASC and DF in order to provide a partial characterization of their lipid content. This allowed to define a peculiar bioactive lipid profile of the secretome from different sources, giving evidence of differences between the two byproducts CM and EV. In our opinion, a clear identification of

the key ingredients, including lipids, of MSC secretome that may be involved in its therapeutic action could be pivotal for investigating its clinical potential At last, considering the future clinical applications in the OA management and the previously promising results obtained in OA context by ASC-CM treatment, we investigated the potential role of two bioactive lipids quantified in ASC-CM -i.e., 2AG and PEA- in an in vitro model of OA. Our results showed a possible protective effect of PEA and a pro-inflammatory activity and/or lack of effectiveness for 2AG in counteracting TNFα. All data were assessed after 3 days treatments of 1pg/ml PEA or 0.5pg/ml 2AG, since previous studies conducted by our laboratory revealed a beneficial action of ASC-CM at the same time point, including anti-inflammatory properties, in the OA context. Our findings support a possible implication of some bioactive lipids and their related pathways in the OA scenario and in the future use of these cell-free products therapeutic approach. For this reason, future studies may be addressed to more complex systems, including organoids or 3D models, and/or osteochondral explants.

Acknowledgments

I acknowledge Università degli Studi di Milano for granting my PhD course in Experimental Medicine and I would like to thank for the given opportunity to attend this three-years PhD fellowship.

References

1. Yang K, Han X. Lipidomics : Techniques , Applications , and Outcomes Related to Biomedical Sciences. Trends Biochem Sci [Internet]. 2016;41(11):954–69. Available from: http://dx.doi.org/10.1016/j.tibs.2016.08.010

2. Fahy E, Subramaniam S, Murphy RC, Nishijima M, Raetz CRH, Shimizu T, et al. Update of the LIPID MAPS comprehensive classification system for lipids. J Lipid Res [Internet]. 2009;50(Supplement):S9–14. Available from: http://www.jlr.org/lookup/doi/10.1194/jlr.R800095-JLR200

3. Fahy E, Cotter D, Sud M, Subramaniam S. Lipid classification, structures and tools. Biochim Biophys Acta. 2011;1811(11):637–47.

4. Garc JC, Peris-d MD, Donato MT. A lipidomic cell-based assay for studying drug-induced phospholipidosis and steatosis. Electrophoresis. 2017;38:2331–40.

5. Lydic TA, Goo YH. Lipidomics unveils the complexity of the lipidome in metabolic diseases. Clin Trans Med. 2018;7(4).

6. Fahy E, Subramaniam S, Brown HA, Glass CK, Merrill AH, Murphy RC, et al. A comprehensive classification system for lipids. 2005;46.

7. LIPID MAPS® Lipidomics Gateway [Internet]. [cited 2021 Aug 17]. Available from: https://www.lipidmaps.org/data/classification/lipid_cns.html

8. Nguyen VL, Haber PS, Seth D. Applications and Challenges for the Use of Phosphatidylethanol Testing in Liver Disease Patients (Mini Review). Alcohol Clin Exp Res. 2017;42(2):238–43.

9. Avela HF, Sirén H. Advances in lipidomics. Clin Chim Acta [Internet]. 2020;510(November 2019):123–41. Available from: https://doi.org/10.1016/j.cca.2020.06.049

10. German JB, Gillies LA, Smilowitz JT, Zivkovic AM, Watkins SM. Lipidomics and lipid profiling in metabolomics. Curr Opin Lipidol. 2007;18:66–71.

11. Wenk MR. The emerging field of lipidomics. Nat Rev Drug Discov. 2005;4(7):594–610.

12. Wenk MR. Lipidomics: New tools and applications. Cell [Internet]. 2010;143(6):888–95. Available from: http://dx.doi.org/10.1016/j.cell.2010.11.033

13. Schwudke D, Shevchenko A, Hoffmann N, Ahrends R. Lipidomics informatics for life-science. J Biotechnol. 2017;261(February):131–6.

14. Shevchenko A, Simons K. Lipidomics: coming to grips with lipid diversity. Nat Publ Gr. 2010;11:593–8.

15. Rustam YH, Reid GE. Analytical Challenges and Recent Advances in Mass Spectrometry Based Lipidomics. Anal Chem. 2018;90(1):374–97.

16. Sethi S, Brietzke E. Recent advances in lipidomics: Analytical and clinical perspectives. Prostaglandins Other Lipid Mediat [Internet]. 2017;128–129:8–16. Available from: http://dx.doi.org/10.1016/j.prostaglandins.2016.12.002

17. Hyötyläinen T, Ore M. Optimizing the lipidomics workflow for clinical studies — practical considerations. 2015;4973–93.

18. Liebisch G, Drobnik W, Lieser B, Schmitz G. High-throughput quantification of lysophosphatidylcholine by electrospray ionization tandem mass spectrometry. Clin Chem. 2002;48(12):2217– 24.

19. Scherer M, Schmitz G, Liebisch G. High-throughput analysis of sphingosine 1-phosphate, sphinganine 1-phosphate, and lysophosphatidic acid in plasma samples by liquid chromatography-tandem mass spectrometry. Clin Chem. 2009;55(6):1218–22.

20. Bligh EG, J. DW. A rapid method of total lipid extraction and purification. Can J Psychiatry. 1979;24(5):422–422.

21. Breil C, Abert Vian M, Zemb T, Kunz W, Chemat F. “Bligh and Dyer” and Folch methods for solid–liquid–liquid extraction of lipids from microorganisms. Comprehension of solvatation mechanisms and towards substitution with alternative solvents. Int J Mol Sci. 2017;18(4):1–21.

22. Zhang H, Gao Y, Sun J, Fan S, Yao X, Ran X, et al. Optimization of lipid extraction and analytical protocols for UHPLC-ESI-HRMS-based lipidomic analysis of adherent mammalian cancer cells. Anal Bioanal Chem. 2017;409(22):5349–58.

23. Cajka T, Fiehn O. Toward Merging Untargeted and Targeted Methods in Mass Spectrometry-Based Metabolomics and Lipidomics. Anal Chem. 2016;88(1):524–545.

24. Li L, Han J, Wang Z, Liu J, Wei J, Xiong S, et al. Mass spectrometry methodology in lipid analysis. Int J Mol Sci. 2014;15(6):10492–507.

25. Casati S, Giannasi C, Minoli M, Niada S, Ravelli A, Angeli I, et al. Quantitative Lipidomic Analysis of Osteosarcoma Cell-Derived Products by UHPLC-MS / MS.

Biomolecules. 2020;10:1–22.

26. Lísa M, Cífková E, Khalikova M, Ovčačíková M, Holčapek M. Lipidomic analysis of biological samples: Comparison of liquid chromatography, supercritical fluid chromatography and direct infusion mass spectrometry methods. J Chromatogr A. 2017;1525:96–108.

27. Fekete S, Schappler J, Veuthey JL, Guillarme D. Current and future trends in UHPLC. TrAC - Trends Anal Chem. 2014;63:2–13.

28. Koelmel JP, Kroeger NM, Ulmer CZ, Bowden JA, Patterson RE, Cochran JA, et al. LipidMatch : an automated workflow for rule-based lipid identification using untargeted high-resolution tandem mass spectrometry data. 2017;1–11.

29. Han X. In Lipidomics: Comprehensive Mass Spectrometry of Lipids. John Wiley & Sons, Inc: Hoboken, NJ. 2016. Chapter 5, pp 121−150.

30. Goracci L, Tortorella S, Tiberi P, Pellegrino RM, Veroli A Di, Valeri A, et al. Lipostar, a Comprehensive Platform-Neutral Cheminformatics Tool for Lipidomics. 2017;(4).

31. Gross RW. The evolution of lipidomics through space and time. Biochim Biophys Acta - Mol Cell Biol Lipids [Internet]. 2017;1862(8):731–9. Available from: http://dx.doi.org/10.1016/j.bbalip.2017.04.006

32. Stefely JA, Kwiecien NW, Freiberger EC, Richards AL, Jochem A, Rush MJP, et al. Mitochondrial protein functions elucidated by multi-omic mass spectrometry profiling. Nat Biotechnol. 2016;34(11).

33. Kopczynski D, Coman C, Zahedi RP, Lorenz K, Sickmann A, Ahrends R. Multi-OMICS : a critical technical perspective on integrative lipidomics approaches ☆. Biochim Biophys Acta - Mol Cell Biol Lipids - Mol Cell Biol Lipids [Internet]. 2017;1862(8):808–11. Available from: http://dx.doi.org/10.1016/j.bbalip.2017.02.003

34. Shimizu T. Lipid Mediators in Health and Disease: Enzymes and Receptors as Therapeutic Targets for the Regulation of Immunity and Inflammation. Annu Rev Pharmacol Toxicol. 2009;49(1):123–50.

35. Leuti A, Fazio D, Fava M, Piccoli A, Oddi S, Maccarrone M. Bioactive lipids , inflammation and chronic diseases. Adv Drug Deliv Rev. 2020;159:133–69.

36. Chiurchiù V, Leuti A, Maccarrone M. Bioactive lipids and chronic inflammation: Managing the fire within. Front Immunol. 2018;9(JAN).

37. Casati S, Giannasi C, Niada S, Bergamaschi RF, Orioli M, Brini AT. Bioactive Lipids in MSCs Biology : State of the Art and Role in Inflammation. 2021;

38. Smith WL, Dewitt DL, Garavito RM. CYCLOOXYGENASES: Structural, Cellular, and Molecular Biology. Annu Rev Biochem. 2000;69:145–82.

39. Stitham J, Midgett C, Martin KA, Hwa J. Prostacyclin: An inflammatory paradox. Front Pharmacol. 2011;MAY(May):1–8.

40. Mandal AK, Jones PB, Bair AM, Christmas P, Miller D, Yamin TTD, et al. The nuclear membrane organization of leukotriene synthesis. Proc Natl Acad Sci U S A. 2008;105(51):20434–9.

41. Murphy RC, Gijón MA. Biosynthesis and metabolism of leukotrienes. Biochem J. 2007;405(3):379–95.

42. Serhan CN. Pro-resolving lipid mediators are leads for resolution physiology. Nature. 2014;510(7503):92–101.

43. Dennis EA, Norris PC. Eicosanoid storm in infection and inflammation. Nat Rev Immunol. 2015;15(8):511–23.

44. Aoki T, Narumiya S. Prostaglandins and chronic inflammation. Trends Pharmacol Sci [Internet]. 2012;33(6):304–11. Available from: http://dx.doi.org/10.1016/j.tips.2012.02.004

45. Narumiya S, Furuyashiki T. Fever , inflammation , pain and beyond : prostanoid receptor research during these 25 years. 1897;813–8.

46. Honda T, Segi-nishida E, Miyachi Y, Narumiya S. Prostacyclin-IP signaling and prostaglandin E2 -EP2/EP4 signaling both mediate joint infl ammation in mouse collagen-induced arthritis. J Exp Med. 2006;203(2):325–35.

47. Hirata T, Narumiya S. Chapter Five - Prostanoids as Regulators of Innate and Adaptive Immunity. Vol. 116, Advances in Immunology. 2012. 143–174 p.

48. Yao C, Sakata D, Esaki Y, Li Y, Matsuoka T, Kuroiwa K, et al. Prostaglandin E2 – EP4 signaling promotes immune inflammation through T H 1 cell differentiation and T H 17 cell expansion. Nat Med. 2009;15(6):633–41.

49. Chen Q, Muramoto K, Masaaki N, Ding Y, Yang H, Mackey M, et al. RESEARCH PAPER A novel antagonist of the prostaglandin E 2 EP 4 receptor inhibits Th1 differentiation and Th17. 2010;292–310.

50. Gilroy DW, Bishop-Bailey D. Lipid mediators in immune regulation and resolution. Br J Pharmacol. 2019;176(8):1009–23.

51. Basil MC, Levy BD. Specialized pro-resolving mediators: Endogenous regulators of infection and inflammation. Nat Rev Immunol. 2016;16(1):51–67.

52. Ligresti A, Petrocellis L De, Marzo V Di. FROM PHYTOCANNABINOIDS TO CANNABINOID RECEPTORS AND ENDOCANNABINOIDS : PLEIOTROPIC PHYSIOLOGICAL AND PATHOLOGICAL ROLES THROUGH COMPLEX PHARMACOLOGY. Physiol Rev. 2016;96:1593–659.

53. Pertwee RG. Cannabidiol as a potential medicine. 2005;47–8.

54. Di Marzo V. Targeting the endocannabinoid system: To enhance or reduce? Nat Rev Drug Discov. 2008;7(5):438–55.

55. Childers S., Deadwyler S. Role of cyclic AMP in the actions of cannabinoid receptors. Biochem Pharmacol. 1996;52:819–27.

56. Baker D, Pryce G, Davies WL, Hiley CR. In silico patent searching reveals a new cannabinoid receptor. Trends Pharmacol Sci. 2006;27:1–4.

57. Pertwee RG, Howlett AC, Abood ME, Alexander SPH, Marzo V Di, Elphick MR, et al. Cannabinoid Receptors and Their Ligands : Beyond CB 1 and CB 2. Pharmacol Rev. 2010;62(4):588–631.

58. Rodriguez MJ, Robledo P, Andrade C, Mahy N. In vivo co-ordinated interactions

between inhibitory systems to control glutamate- mediated hippocampal excitability. J Neurochem. 2005;95:651–661.

59. Tsou K, Brown S, Sanudo-Pena MC, Mackie K, Walker JM. Immunohistochemical distribution of cannabinoid CB1 receptors in the rat central nervous system. Neuroscience. 1998;83:393–411.

60. Westlake TM, Howlett AC, Bonner TI, Matsuda LA, Herkenham M. Cannabinoid receptor binding and messenger RNA expression in human brain: an in vitro receptor autoradiography and in situ hybridiza- tion histochemistry study of normal aged and Alzheimer's brains. Neuroscience. 1994;63:637–652.

61. Porta C La, Bura SA, Negrete R, Maldonado R. Involvement of the endocannabinoid system in osteoarthritis pain. 2014;39:485–500.

62. Mbvundula EC, Bunning RAD, Rainsford KD. Effects of cannabinoids on nitric oxide production by chondrocytes and proteoglycan degradation in cartilage. Biochem Pharmacol. 2005;69(4):635–40.

63. Devane WA, Hanuš L, Breuer A, Pertwee RG, Stevenson LA, Griffin G, et al. Isolation and structure of a brain constituent that binds to the cannabinoid receptor. Science (80-). 1992;258(5090):1946–9.

64. Sugiura T, Kondo S, Sukagawa A, Nakane S, Shinoda A, Itoh K, et al. 2-arachidonoylglycerol: A possible endogenous cannabinoid receptor ligand in brain. Biochem Biophys Res Commun. 1995;215(1):89–97.

65. Mechoulam R, Ben-Shabat S, Hanus L, Ligumsky M, Kaminski NE, Schatz AR, et al. Identification of an endogenous 2-monoglyceride, present in canine gut, that binds to cannabinoid receptors. Biochem Pharmacol. 1995;50(1):83–90.

66. Di Marzo V. Endocannabinoids: synthesis and degradation. Rev Physiol Biochem Pharmacol. 2008;160:1–24.

67. Bisogno T, Di Marzo V. Cannabinoid receptors and endocannabi- noids: role in neuroinflammatory and neurodegenerative disorders. CNS Neurol Disord Dr. 2010;9:564–573.

68. Guindon J, Hohmann AG. The endocannabinoid system and pain. CNS Neurol Disord Dr. 2009;8:403–421.

69. Ribeiro A, Pontis S, Mengatto L, Armirotti A, Chiurchiu V, Capurro V, et al. A Potent Systemically Active N - Acylethanolamine Acid Amidase Inhibitor that Suppresses In fl ammation and Human Macrophage Activation. 2015;

70. Maestroni GJM. The endogenous cannabinoid 2-arachidonoyl glycerol as in vivo chemoattractant for dendritic cells and adjuvant for Th1 response to a soluble protein. FASEB J. 2004;15(4):1–16.

71. Gallily R, Breuer A, Mechoulam R. 2-Arachidonylglycerol, an endogenous cannabinoid, inhibits tumor necrosis factor-a production in murine macrophages, and in mice. Eur J Pharmacol. 2000;406:1997–9.

72. Barrie N, Manolios N. The endocannabinoid system in pain and inflammation : Its relevance to rheumatic disease. Eur J Rheumatol 2017; 2017;1(13):210–8.

73. Artmann A, Petersen G, Hellgren L, Boberg J, Skonberg C, Nellemann C, et al. Influence of Dietary Fatty Acids on Endocannabinoid and N-acylethanolamine Levels in Rat Brain, Liver and Small Intestine. Biochim Biophys Acta. 1781(4):200–12.

74. Lucanic M, Held JM, Vantipalli MC, Klang IM, Graham JB, Gibson BW, et al. N-acylethanolamine signallingmediates the effect of diet on lifespan in Caenorhabditis elegans. Nature. 2011;473:226–31.

75. Brown I, Cascio MG, Wahle KWJ, Smoum R, Mechoulam R, Ross RA, et al. Cannabinoid receptor-dependent and -independent anti-proliferative effects of omega-3 ethanolamides in androgen receptor-positive and -negative prostate cancer cell lines. Carcinogenesis. 2010;31(9):1584–91.

76. Meijerink J, Plastina P, Vincken J, Poland M, Attya M, Balvers M, et al. The ethanolamide metabolite of DHA , docosahexaenoylethanolamine , shows immunomodulating effects in mouse peritoneal and RAW264 . 7 macrophages : evidence for a new link between fish oil and inflammation. Br J Nutr. 2011;105:1798–807.

77. Piomelli D. Neuropharmacology More surprises lying ahead . The endocannabinoids keep us guessing. NP [Internet]. 2014;76:228–34. Available from: http://dx.doi.org/10.1016/j.neuropharm.2013.07.026

78. Laleh P, Yaser K, Alireza O. Oleoylethanolamide : A novel pharmaceutical agent in the management of obesity - an updated review. J Cell Physiol. 2019;234:7893–902.

79. Tutunchi H, Saghafi-Asl M, Alireza O. A systematic review of the effects of oleoylethanolamide , a high-affinity endogenous ligand of PPAR- α , on the management and prevention of obesity. Clin Exp Pharmacol Physiol. 2020;47:543–52.

80. Raso GM, Russo R, Calignano A, Meli R. Palmitoylethanolamide in CNS health and disease. Pharmacol Res [Internet]. 2014;86:32–41. Available from: http://dx.doi.org/10.1016/j.phrs.2014.05.006

81. Petrosino CS, Biomolecolare C, Nazionale C. The pharmacology of palmitoylethanolamide and fi rst data on the therapeutic ef fi cacy of some of its new formulations. 2017;1349–65.

82. Hjorth S, Hermansson N, Leonova J, Elebring T, Ryberg E, Larsson N, et al. The orphan receptor GPR55 is a novel cannabinoid receptor. 2007;(September):1092–101.

83. Hansen HS. Palmitoylethanolamide and other anandamide congeners . Proposed role in the diseased brain. Exp Neurol [Internet]. 2010;224(1):48–55. Available from: http://dx.doi.org/10.1016/j.expneurol.2010.03.022

84. Maccarrone M, Cartoni A, Parolaro D, Margonelli A, Massi P, Bari M, et al. Degradation of Stearoylethanolamide within the Mouse Central Nervous System. Mol Cell Neurosci. 2002;140:126–40.

85. Carbonare MD, Giudice E Del, Stecca A, Colavito D, Fabris M, Arrigo AD, et al. A Saturated N-Acylethanolamine Other than N-Palmitoyl Ethanolamine with Anti-inflammatory Properties : a Neglected Story …. J Neuroendocrinol. 2008;20:26–34.

86. Balvers MGJ, Verhoeckx KCM, Witkamp RF. Development and validation of a

quantitative method for the determination of 12 endocannabinoids and related compounds in human plasma using liquid chromatography – tandem mass spectrometry. J Chromatogr B. 2009;877:1583–90.

87. Han B, Wright R, Kirchhoff AM, Chester JA, Cooper BR, Jo V, et al. Quantitative LC – MS / MS analysis of arachidonoyl amino acids in mouse brain with treatment of FAAH inhibitor. Anal Biochem [Internet]. 2013;432(2):74–81. Available from: http://dx.doi.org/10.1016/j.ab.2012.09.031

88. Burstein SH, Mcquain CA, Ross AH, Salmonsen RA, Zurier RE. Resolution of Inflammation by N-Arachidonoylglycine. J Cell Biochem. 2011;3233(July):3227–33.

89. Burstein SH, Adams JK, Bradshaw HB, Fraioli C, Rossetti G, Salmonsen RA, et al. Potential anti-inflammatory actions of the elmiric (lipoamino) acids. Bioorg Med Chem. 2007;15(10):3345–55.

90. Parmar N, Ho WV. N -arachidonoyl glycine , an endogenous lipid that acts as a vasorelaxant via nitric oxide and large conductance calcium-activated potassium channels Abbreviations : Br J Pharmacol. 2010;160(August 2009):594–603.

91. Mchugh D, Hu SSJ, Rimmerman N, Juknat A, Vogel Z, Walker JM, et al. N - arachidonoyl glycine , an abundant endogenous lipid , potently drives directed cellular migration through GPR18 , the putative abnormal cannabidiol receptor. BMC Neurosci. 2010;11(44).

92. Cascio MG, Minassi A, Ligresti A, Appendino G, Burstein S, Di V. A structure–activity relationship study on N-arachidonoyl-amino acids as possible endogenous inhibitors of fatty acid amide hydrolase. Biochem Biophys Res Commun. 2004;314:192–6.

93. Locke M, Windsor J, Dunbar PR. Human adipose-derived stem cells: isolation, characterization and applications in surgery. ANZ J Surg. 2009;79:235–44.

94. Strem BM, Hicok KC, Zhu M, Wulur I, Alfonso Z, Schreiber RE, et al. Multipotential differentiation of adipose tissue-derived stem cells. Keio J Med. 2005;54(3):132–41.

95. Dominici M, Le Blanc K, Mueller I, Slaper-Cortenbach I, Marini F., Krause DS, et al.

Minimal criteria for defining multipotent mesenchymal stromal cells. The International Society for Cellular Therapy position statement. Cytotherapy. 2006;8(4):315–7.

96. Horwitz EM, Le Blanc K, Dominici M, Mueller I, Slaper-Cortenbach I, Marini FC, et al. Clarification of the nomenclature for MSC: The International Society for Cellular Therapy position statement. Cytotherapy. 2005;7(5):393–5.

97. Glassberg MK, Minkiewicz J, Toonkel RL, Simonet ES, Rubio GA, DiFede D, et al. Allogeneic Human Mesenchymal Stem Cells in Patients With Idiopathic Pulmonary Fibrosis via Intravenous Delivery (AETHER): A Phase I Safety Clinical Trial. Chest [Internet]. 2017;151(5):971–81. Available from: http://dx.doi.org/10.1016/j.chest.2016.10.061

98. Lindsay JO, Allez M, Clark M, Labopin M, Ricart E, Rogler G, et al. Autologous stem-cell transplantation in treatment-refractory Crohn's disease: an analysis of pooled data from the ASTIC trial. Lancet Gastroenterol Hepatol. 2017;2(6):399–406.

99. Shi Y, Wang Y, Li Q, Liu K, Hou J, Shao C, et al. Immunoregulatory mechanisms of mesenchymal stem and stromal cells in inflammatory diseases. Nat Rev Nephrol [Internet]. 2018;14(8):493–507. Available from: http://dx.doi.org/10.1038/s41581-018-0023-5

100. Taylor CT, Colgan SP. Regulation of immunity and inflammation by hypoxia in immunological niches. Nat Rev Immunol. 2017;17:774–785.

101. Gowen A, Shahjin F, Chand S, Odegaard KE, Yelamanchili S V. Mesenchymal Stem Cell-Derived Extracellular Vesicles : Challenges in Clinical Applications. Front Cell Dev Biol. 2020;8(March):1–8.

102. Sun D, Abelson B, Babbar P, Damaser M. Harnessing the Mesenchymal Stem Cell Secretome for Regenerative Urology. Nat Rev Urol. 2019;16(6):363–75.

103. Van Niel G, D'Angelo G, Raposo G. Shedding light on the cell biology of extracellular vesicles. Nat Rev Mol Cell Biol [Internet]. 2018;19(4):213–28. Available from: http://dx.doi.org/10.1038/nrm.2017.125

104. Théry C, Witwer KW, Aikawa E, Alcaraz MJ, Anderson JD, Andriantsitohaina R, et

al. Minimal information for studies of extracellular vesicles 2018 (MISEV2018): a position statement of the International Society for Extracellular Vesicles and update of the MISEV2014 guidelines. J Extracell Vesicles. 2018;7(1).

105. Daneshmandi L, Shah S, Jafari T, Bhattacharjee M, Momah D, Saveh-Shemshaki N, et al. Emergence of the Stem Cell Secretome in Regenerative Engineering. Trends Biotechnol [Internet]. 2020;38(12):1373–84. Available from: https://doi.org/10.1016/j.tibtech.2020.04.013

106. Abbasi-Malati Z, Roushandeh AM, Kuwahara Y, Roudkenar MH. Mesenchymal Stem Cells on Horizon: A New Arsenal of Therapeutic Agents. Stem Cell Rev Reports. 2018;14(4):484–99.

107. Vasandan AB, Jahnavi S, Shashank C, Prasad P, Kumar A, Jyothi Prasanna S. Human Mesenchymal stem cells program macrophage plasticity by altering their metabolic status via a PGE 2 -dependent mechanism. Sci Rep. 2016;6(December):1–17.

108. Carlomagno C, Giannasi C, Niada S, Bedoni M. Raman Fingerprint of Extracellular Vesicles and Conditioned Media for the Reproducibility Assessment of Cell-Free Therapeutics. 2021;9(April):1–9.

109. Niada S, Giannasi C, Magagnotti C, Andolfo A, Brini T. Proteomic analysis of extracellular vesicles and conditioned medium from human adipose-derived stem / stromal cells and dermal fibroblasts. J Proteomics [Internet]. 2021;232:104069. Available from: https://doi.org/10.1016/j.jprot.2020.104069

110. Eleuteri S, Fierabracci A. Insights into the secretome of mesenchymal stem cells and its potential applications. Int J Mol Sci. 2019;20(18).

111. Harman RM, Marx C, Van de Walle GR. Translational Animal Models Provide Insight Into Mesenchymal Stromal Cell (MSC) Secretome Therapy. Front Cell Dev Biol. 2021;9(March):1–23.

112. Kalluri R, LeBleu VS. The biology, function, and biomedical applications of exosomes. Science (80-). 2020;367(6478).

113. Ren G, Zhang L, Zhao X, Xu G, Zhang Y, Roberts AI, et al. Mesenchymal Stem Cell-Mediated Immunosuppression Occurs via Concerted Action of Chemokines and Nitric Oxide. Cell Stem Cell. 2008;2(2):141–50.

114. Liu Y, Wang L, Kikuiri T, Akiyama K, Chen C, Xu X, et al. Mesenchymal Stem Cell-Based Tissue Regeneration is Governed by Recipient T Lymphocyte via IFN-γ and TNF-α. Nat Med. 2012;17(12):1594–1601.

115. Campos AM, Maciel E, Moreira ASP, Sousa B, Melo T, Domingues P, et al. Lipidomics of Mesenchymal Stromal Cells: Understanding the Adaptation of Phospholipid Profile in Response to Pro-Inflammatory Cytokines. J Cell Physiol. 2016;231(5):1024–32.

116. Cunningham TJ, Yao L, Lucena A. Product inhibition of secreted phospholipase A2 may explain lysophosphatidylcholines ' unexpected therapeutic properties. J Inflamm. 2008;10:1–10.

117. Chen G, Li J, Qiang X, Czura CJ, Ochani M, Ochani K, et al. Suppression of HMGB1 release by stearoyl lysophosphatidylcholine : an additional mechanism for its therapeutic effects in experimental sepsis. J lipid rese. 2005;46:623–7.

118. Kilpinen L, Tigistu-sahle F, Oja S, Greco D, Parmar A, Saavalainen P, et al. Aging bone marrow mesenchymal stromal cells have altered membrane glycerophospholipid composition and functionality. J Lipid Res. 2013;54.

119. Olivera A, Rivera J. Sphingolipids and the Balancing of Immune Cell Function: Lessons from the Mast Cell. J Extra Corpor Technol. 2005;174:1153–8.

120. Aggarwal S, Pittenger MF. Human mesenchymal stem cells modulate allogeneic immune cell responses. Blood. 2005;105(4):1815–22.

121. Masoodi M, Nicolaou A. Lipidomic analysis of twenty-seven prostanoids and isoprostanes by liquid chromatography / electrospray tandem mass spectrometry. RAPID Commun MASS Spectrom. 2006;20:3023–9.

122. English K, Barry FP, Field-corbett CP, Mahon BP. IFN-g and TNF-a differentially regulate immunomodulation by murine mesenchymal stem cells. Immunol Lett.

2007;110:91–100.

123. Renner P, Eggenhofer E, Rosenauer A, Popp FC, Steinmann JF, Slowik P, et al. Mesenchymal Stem Cells Require a Sufficient , Ongoing Immune Response to Exert Their Immunosuppressive Function. Transplant Proc [Internet]. 2009;41(6):2607–11. Available from: http://dx.doi.org/10.1016/j.transproceed.2009.06.119

124. Ern C, Frasheri I, Berger T, Kirchner HG, Heym R, Hickel R, et al. Effects of prostaglandin E2 and D2 on cell proliferation and osteogenic capacity of human mesenchymal stem cells. Prostaglandins Leukot Essent Fat Acids [Internet]. 2019;151(May):1–7. Available from: https://doi.org/10.1016/j.plefa.2019.09.005

125. Serhan CN, Chiang N, Dalli J. The resolution code of acute inflammation : Novel pro-resolving lipid mediators in resolution. Semin Immunol [Internet]. 2015;27(3):200–15. Available from: http://dx.doi.org/10.1016/j.smim.2015.03.004

126. Fang X, Abbott J, Cheng L, Jennifer K, Lee JW, Levy BD, et al. Human Mesenchymal Stem (Stromal) Cells Promote the Resolution of Acute Lung Injury in Part through Lipoxin A 4. thw J Immunol. 2015;195:875–81.

127. Levy BD, Clish CB, Schmidt B, Gronert K, Serhan CN, Lts L. Lipid mediator class switching during acute inflammation : signals in resolution. Nat Immunol. 2001;2(7).

128. Bijlsma JWJ, Berenbaum F, Lafeber FPJG. Arthritis 1 Osteoarthritis : an update with relevance for clinical practice. Lancet. 2011;377:2115–26.

129. Weber AE. Biological strategies for osteoarthritis : from early diagnosis to treatment. 2021;335–44.

130. Singh A, Ansari K, Quraishi M, Lgaz H. Effect of Electron Donating Functional Groups on Corrosion Inhibition of J55 Steel in a Sweet Corrosive Environment : Experimental , Density Functional Theory , and Molecular Dynamic Simulation. Materials (Basel). 2019;12(17).

131. Cui N, Hu M, Khalil R. Biochemical and Biological Attributes of Matrix Metalloproteinases. Vol. 147, Progress in Molecular Biology and Translational Science. 2017. 1–73 p.

132. Bottini M, Magrini A, Fadeel B, Rosato N. Tackling chondrocyte hypertrophy with multifunctional nanoparticles. 2016;(October 2015):560–4.

133. Platas J, Guillén MI, Dolores M, Gomar F, Mirabet V, Alcaraz MJ. Conditioned Media from Adipose-Tissue-Derived Mesenchymal Stem Cells Downregulate Degradative Mediators Induced by Interleukin-1 β in Osteoarthritic Chondrocytes. 2013;2013.

134. Niada S, Giannasi C, Gomarasca M, Stanco D, Casati S, Brini AT. Adipose-derived stromal cell secretome reduces TNFα-induced hypertrophy and catabolic markers in primary human articular chondrocytes. Stem Cell Res [Internet]. 2019;38(March):101463. Available from: https://doi.org/10.1016/j.scr.2019.101463

135. Amin AR AS. The role of nitric oxide in articular cartilage breakdown in osteoarthritis. Curr Opin Rheumatol. 1998;10:263–8.

136. Ahmad N, Ansari MY. Role of iNOS in osteoarthritis : Pathological and therapeutic aspects Role of iNOS in osteoarthritis : Pathological and therapeutic aspects. 2020;(December).

137. Amin AR, Patel IR, Abramson SB, Cartilage O. Superinduction of cyclooxygenase-2 activity in human osteoarthritis-affected cartilage . Influence of nitric oxide . Find the latest version : Superinduction of Cyclooxygenase-2 Activity in Human. 1997;99(6):1231–7.

138. Scher JU, Pillinger MH, Abramson SB. Nitric oxide synthases and osteoarthritis. Curr Rheumatol Rep. 2007;9(1):9–15.

139. Loef M, Schoones JW, Kloppenburg M, Ioan-Facsinay A. Fatty acids and osteoarthritis: different types, different effects. Jt Bone Spine [Internet]. 2019;86(4):451–8. Available from: http://dx.doi.org/10.1016/j.jbspin.2018.07.005

140. Scanzello CR, Plaas A, Crow MK. Innate immune system activation in osteoarthritis : is osteoarthritis a chronic wound ? Curr Opin Rheumatol. 2008;

141. Baker KR, Matthan NR, Lichtenstein AH, Niu J, Guermazi A, Roemer F, et al. Association of plasma n-6 and n-3 polyunsaturated fatty acids with synovitis in the knee : the MOST study. Osteoarthr Cartil [Internet]. 2012;20(5):382–7. Available

from: http://dx.doi.org/10.1016/j.joca.2012.01.021

142. Zainal Z, Longman AJ, Hurst S, Duggan K, Caterson B, Hughes CE, et al. Relative efficacies of omega-3 polyunsaturated fatty acids in reducing expression of key proteins in a model system for studying osteoarthritis. Osteoarthr Cartil [Internet]. 2009;17(7):896–905. Available from: http://dx.doi.org/10.1016/j.joca.2008.12.009

143. Wang Z, Guo AI, Ma L, Yu H, Zhang L, Meng HAI, et al. Docosahexenoic acid treatment ameliorates cartilage degeneration via a p38 MAPK-dependent mechanism. Int J Mol Med. 2016;(19):1542–50.

144. Brouwers H, Hegedus J Von, Kloppenburg M, Ioan-facsinay A. Lipid mediators of in fl ammation in rheumatoid arthritis and osteoarthritis. Best Pract Res Clin Rheumatol. 2016;29(2015):741–55.

145. Hardy MM, Seibert K, Manning PT, Currie MG, Woerner BM, Edwards D, et al. Cyclooxygenase 2 – Dependent Prostaglandin E 2 Modulates Cartilage Proteoglycan Degradation in Human Osteoarthritis Explants. ARTHRITIS Rheum. 2002;46(7):1789–803.

146. Shimpo H, Sakay T, Kondo S, Mishima S, Yoda M, Hiraiwa H, et al. Regulation of prostaglandin E 2 synthesis in cells derived from chondrocytes of patients with osteoarthritis. J Orthop Sci. 2009;14:611–7.

147. Benabdoune H, Qin ER, Julio S. The role of resolvin D1 in the regulation of inflammatory and catabolic mediators in osteoarthritis. Inflamm Res. 2016;65(8):635–45.

148. Schuelert N, McDougall JJ. Cannabinoid-mediated antinocicep- tion is enhanced in rat osteoarthritic knees. Arthritis Rheum. 2008;58:145– 153.

149. Schuelert N, Zhang C, Mogg AJ, Broad LM, Hepburn DL, Nisen- baum, E.S., Johnson MP, et al. Paradoxical effects of the cannabinoid CB2 receptor agonist GW405833 on rat osteoarthritic knee joint pain. Osteoarthr Cartil. 18:1536–1543.

150. Richardson D, Pearson RG, Kurian N, Latif ML, Garle MJ, Barrett DA, et al. Characterisation of the cannabinoid receptor system in synovial tissue and fluid in

patients with osteoarthritis and rheumatoid arthritis. Arthritis Res Ther. 2008;(10):R43.

151. Burston JJ, Mapp PI, Sarmad S, Barrett DA, Niphakis MJ, Cravatt BF, et al. Robust anti-nociceptive effects of monoacylglycerol lipase inhibition in a model of osteoarthritis pain Tables of Links. 2016;

152. McAlindon TE, Bannuru RR, Sullivan MC, Arden NK, Berenbaum F, Bierma-Zeinstra SM, et al. OARSI guidelines for the non-surgical management of knee osteoarthritis. Osteoarthr Cartil [Internet]. 2014;22(3):363–88. Available from: http://dx.doi.org/10.1016/j.joca.2014.01.003

153. Huebner K, Frank RM, Getgood A. Ortho-Biologics for Osteoarthritis. Clin Sports Med. 2019;38(1):123–41.

154. Sherman B, Chahla J, Glowney J, Frank R. The Role of Orthobiologics in the Management of Osteoarthritis and Focal Cartilage Defects. Orthopedics. 2019;42(2):66–73.

155. Lopa S, Colombini A, Moretti M, de Girolamo L. Injective mesenchymal stem cell-based treatments for knee osteoarthritis: from mechanisms of action to current clinical evidences. Knee Surgery, Sport Traumatol Arthrosc [Internet]. 2019;27(6):2003–20. Available from: http://dx.doi.org/10.1007/s00167-018-5118-9

156. Demoor M, Ollitrault D, Gomez-leduc T, Bouyoucef M, Hervieu M, Fabre H, et al. Cartilage tissue engineering : Molecular control of chondrocyte differentiation for proper cartilage matrix reconstruction ☆. Biochim Biophys Acta [Internet]. 2014;1840(8):2414–40. Available from: http://dx.doi.org/10.1016/j.bbagen.2014.02.030

157. Maumus M, Manferdini C, Toupet K, Peyrafitte JA, Ferreira R, Facchini A, et al. Adipose mesenchymal stem cells protect chondrocytes from degeneration associated with osteoarthritis. Stem Cell Res [Internet]. 2013;11(2):834–44. Available from: http://dx.doi.org/10.1016/j.scr.2013.05.008

158. Manferdini C, Maumus M, Gabusi E, Piacentini A, Filardo G, Peyrafitte J, et al.

Adipose-Derived Mesenchymal Stem Cells Exert Antiinflammatory Effects on Chondrocytes and Synoviocytes From Osteoarthritis Patients Through Prostaglandin E 2. 2013;65(5):1271–81.

159. Lee KBL, Hui JHP, Song IC, Ardany L, Lee EH. Injectable Mesenchymal Stem Cell Therapy for Large Cartilage Defects-A Porcine Model. Stem Cells. 2007;25(11):2964–71.

160. Xie X, Wang Y, Zhao C, Guo S, Liu S, Jia W, et al. Comparative evaluation of MSCs from bone marrow and adipose tissue seeded in PRP-derived scaffold for cartilage regeneration. Biomaterials [Internet]. 2012;33(29):7008–18. Available from: http://dx.doi.org/10.1016/j.biomaterials.2012.06.058

161. Brini AT, Amodeo G, Ferreira LM, Milani A, Niada S, Moschetti G, et al. Therapeutic effect of human adipose-derived stem cells and their secretome in experimental diabetic pain. Sci Rep [Internet]. 2017;(February):1–15. Available from: http://dx.doi.org/10.1038/s41598-017-09487-5

162. Kay AG, Long G, Tyler G, Stefan A, Broadfoot SJ, Piccinini AM, et al. Mesenchymal Stem Cell-Conditioned Medium Reduces Disease Severity and Immune Responses in Inflammatory Arthritis. Sci Rep [Internet]. 2017;7(1):1–11. Available from: http://dx.doi.org/10.1038/s41598-017-18144-w

163. Kuljanin M, Elgamal RM, Bell GI, Xenocostas A, Lajoie GA, Hess DA. Human Multipotent Stromal Cell Secreted Effectors Accelerate Islet Regeneration. Stem Cells. 2019;37(4):516–28.

164. Squillaro T, Peluso G, Galderisi U. Clinical trials with mesenchymal stem cells: An update. Cell Transplant. 2016;25(5):829–48.

165. Gentile P, Casella D, Palma E, Calabrese C. Engineered Fat Graft Enhanced with Adipose-Derived Stromal Vascular Fraction Cells for Regenerative Medicine: Clinical, Histological and Instrumental Evaluation in Breast Reconstruction. J Clin Med. 2019;8(4):504.

166. Giannasi C, Niada S, Magagnotti C, Ragni E, Andolfo A, Brini AT. Comparison of two ASC-derived therapeutics in an in vitro OA model : secretome versus

extracellular vesicles. 2020;5:1–15.

167. Amodeo G, Niada S, Moschetti G, Franchi S, Savadori P, Brini A, et al. Human adipose mesenchymal stem cell secretome relieves pain and neuroinflammation independently of the route of administration in the MIA murine model of osteoarthritis. submitted to Brain Behavior and Immunity (under review).

168. PHINNEY D, PITTENGER M. Concise Review : MSC-Derived Exosomes for Cell-Free Therapy. Stem Cells. 2017;35:851–8.

169. Bruno S, Grange C, Collino F, Deregibus MC, Cantaluppi V, Biancone L, et al. Microvesicles Derived from Mesenchymal Stem Cells Enhance Survival in a Lethal Model of Acute Kidney Injury. PLoS One. 2012;7(3).

170. Ratajczak MZ. The emerging role of microvesicles in cellular therapies for organ / tissue regeneration. Nephrol Dial Transpl. 2011;26:1453–6.

171. Haraszti RA, Didiot MC, Sapp E, Leszyk J, Shaffer SA, Rockwell HE, et al. High-resolution proteomic and lipidomic analysis of exosomes and microvesicles from different cell sources. J Extracell Vesicles. 2016;5(1).

172. Llorente A, Skotland T, Sylvänne T, Kauhanen D, Róg T, Or A, et al. Biochimica et Biophysica Acta Molecular lipidomics of exosomes released by PC-3 prostate cancer cells. Biochim Biophys Acta. 2013;1831:1302–9.

173. XIANG C, YANG K, LIANG Z, WAN Y, CHENG Y, MA D, et al. Sphingosine-1-phosphate mediates the therapeutic effects of bone marrow mesenchymal stem cell-derived microvesicles on articular cartilage defect. Transl Res [Internet]. 2017;193:42–53. Available from: https://doi.org/10.1016/j.trsl.2017.12.003

174. Ottria R, Casati S, Ciuffreda P. Optimized synthesis and characterization of N-acylethanolamines and O-acylethanolamines , important family of lipid-signalling molecules. Chem Phys Lipids [Internet]. 2012;165(7):705–11. Available from: http://dx.doi.org/10.1016/j.chemphyslip.2012.06.010

175. Ottria R, Casati S, Ciuffreda P. 1H,13C and15N NMR assignments for N- and O-acylethanolamines, important family of naturally occurring bioactive lipid mediators.

Magn Reson Chem. 2012;50(12):Pages 823-828.

176. Giannasi C, Niada S, Farronato D, Lombardi G, Manfredi B, Farronato G, et al. Nitrogen containing bisphosphonates impair the release of bone homeostasis mediators and matrix production by human primary pre-osteoblasts. Int J Med Sci. 2019;16(1):23–32.

177. Niada S, Giannasi C, Gualerzi A, Banfi G, Brini AT. Differential proteomic analysis predicts appropriate applications for the secretome of adipose-derived mesenchymal stem/stromal cells and dermal fibroblasts. Stem Cells Int. 2018;2018.

178. Théry C, Clayton A, Amigorena S, Raposo and G. Isolation and Characterization of Exosomes from Cell Culture Supernatants. Curr Protoc Cell Biol. 2006;30:3.22:3.22.1–3.22.29.

179. Gualerzi A, Niada S, Giannasi C, Picciolini S, Morasso C, Vanna R, et al. Raman spectroscopy uncovers biochemical tissue-related features of extracellular vesicles from mesenchymal stromal cells. Sci Rep [Internet]. 2017;7(1):1–11. Available from: http://dx.doi.org/10.1038/s41598-017-10448-1

180. Guidance for Industry Bioanalytical Method Validation [Internet]. 2018. Available from: https://www.fda.gov/downloads/drugs/guidances/ucm070107.Pdf

181. van de Merbel NC. Quantitative determination of endogenous compounds in biological samples using chromatographic techniques. Trends Anal Chem [Internet]. 2008;27(10):924–33. Available from: http://dx.doi.org/10.1016/j.trac.2008.09.002

182. Marcel Jakob, Olivier Démarteau, Dirk Schäfer, Michael Stumm, Michael Heberer IM. Enzymatic digestion of adult human articular cartilage yields a small fraction of the total available cells. Connect Tissue Res. 2003;44((3-4)):173–80.

183. Laganà, Matteo; Arrigoni, Chiara; Lopa, Silvia; Sansone, Valerio; Zagra, Luigi; Moretti, Matteo; Raimondi MT. Characterization of articular chondrocytes isolated from 211 osteoarthritic patients. Cell Tissue Bank. 2014;15(1):59–66.

184. Caron M, Emans P, Coolsen M, Voss L, Surtel D, Cremers A, et al. Redifferentiation of dedifferentiated human articular Chondrocytes: comparison of 2D and 3D

cultures. Osteoarthr Cart. 2012;20(10):1170–8.

185. Goldrin M. Human chondrocyte cultures as models of cartilage-specific gene regulation. Methods Mol Med. 2005;107:69–95.

186. Westacott C, Barakat A, Wood L, Perry M, Neison P, Bisbinas I, et al. Tumor necrosis factor alpha can contribute to focal loss of cartilage in osteoarthritis. Osteoarthr Cart. 2000;8(3):213–21.

187. Ottria R, Ravelli A, Gigli F, Ciuffreda P. Simultaneous ultra-high performance liquid chromathograpy-electrospray ionization-quadrupole-time of flight mass spectrometry quantification of endogenous anandamide and related N -acylethanolamides in bio-matrices. J Chromatogr B [Internet]. 2014;958:83–9. Available from: http://dx.doi.org/10.1016/j.jchromb.2014.03.019

188. Liakh I, Pakiet A, Sledzinski T, Mika A. Modern Methods of Sample Preparation for the Analysis of Oxylipins in Biological Samples. Molecules. 2019;1:1–38.

189. Marchioni C, Donizeti I, Souza D, Ricardo V, Junior A. Analytica Chimica Acta Recent advances in LC-MS / MS methods to determine endocannabinoids in biological samples : Application in neurodegenerative diseases. 2018;1044.

190. Folch J, Lees M, Sloane Stanley G. A simple method for the isolation and purification of total lipides from animal tissues. J Biol Chem. 1987;55(5):999–1033.

191. Balvers MGJ, Wortelboer HM, Witkamp RF, Verhoeckx KCM. Liquid chromatography-tandem mass spectrometry analysis of free and esterified fatty acid N-acyl ethanolamines in plasma and blood cells. Anal Biochem [Internet]. 2013;434(2):275–83. Available from: http://dx.doi.org/10.1016/j.ab.2012.11.008

192. Gachet MS, Rhyn P, Bosch OG, Quednow BB, Gertsch J. A quantitiative LC-MS/MS method for the measurement of arachidonic acid, prostanoids, endocannabinoids, N-acylethanolamines and steroids in human plasma. J Chromatogr B Anal Technol Biomed Life Sci [Internet]. 2015;976–977:6–18. Available from: http://dx.doi.org/10.1016/j.jchromb.2014.11.001

193. Gouveia-Figueira S, Nording ML. Validation of a tandem mass spectrometry method

using combined extraction of 37 oxylipins and 14 endocannabinoid-related compounds including prostamides from biological matrices. Prostaglandins Other Lipid Mediat. 2015;121:110–21.

194. Stenson W. Measurement of prostaglandins and other eicosanoids. Curr Protoc Immunol. 2001;7(7):33.

195. Pautke C, Schieker M, Tischer T, Kolk A, Neth P, Mutschler W, et al. Characterization of osteosarcoma cell lines MG-63, Saos-2 and U-2 OS in comparison to human osteoblasts. Anticancer Res. 2004;24(6):3743–8.

196. Hong ES, Burkett SS, Morrow J, Lizardo MM, Osborne T, Li SQ, et al. Characterization of the metastatic phenotype of a panel of established osteosarcoma cells. Oncotarget. 2015;6(30):29469–81.

197. Ichim TE, Heeron PO, Kesari S. Fibroblasts as a practical alternative to mesenchymal stem cells. J Transl Med [Internet]. 2018;1–9. Available from: https://doi.org/10.1186/s12967-018-1536-1

198. Nilforoushzadeh MA, Reza H, Ashtiani A, Jaffary F, Jahangiri F, Nikkhah N, et al. Dermal Fibroblast Cells : Biology and Function in Skin Regeneration. 2017;4(2).

199. Fitzsimmons REB, Mazurek MS, Soos A, Simmons CA. Review Article Mesenchymal Stromal / Stem Cells in Regenerative Medicine and Tissue Engineering. 2018;2018.

200. Giannasi C, Niada S, Morte E Della, Casati S, Orioli M, Gualerzi A, et al. Towards Secretome Standardization : Identifying Key Ingredients of MSC-Derived Therapeutic Cocktail. 2021;2021.

201. Tang Y, Huang Y, Zheng LEI, Qin S, Xu X, An T. Comparison of isolation methods of exosomes and exosomal RNA from cell culture medium and serum. 2017;834–44.

202. Takov K, Yellon DM, Davidson SM, Takov K, Yellon DM, Comparison SMD. Comparison of small extracellular vesicles isolated from plasma by ultracentrifugation or size- exclusion chromatography : yield , purity and functional potential. J Extracell Vesicles [Internet]. 2019;8(1). Available from:

https://doi.org/10.1080/20013078.2018.1560809

203. Chu D, Nguyen T, Phuong T, Le N, Tien B, Tran DK. Adipose Tissue Stem Cells for Therapy : An Update on the Progress of Isolation , Culture , Storage , and Clinical Application. 2019;

204. D'Arrigo D, Roffi A, Cucchiarini M, Moretti M, Candrian C, Filardo G. Secretome and Extracellular Vesicles as New Biological Therapies for Knee Osteoarthritis: A Systematic Review. J Clin Med. 2019;8(11):1867.

205. Mancuso P, Raman S, Glynn A, Barry F, Murphy JM. Mesenchymal Stem Cell Therapy for Osteoarthritis : The Critical Role of the Cell Secretome. 2019;7(January):1–9.

206. Vergauwen G, Dhond B, Deun J Van, Smedt E De, Berx G, Timmerm E, et al. Confounding factors of ultrafiltration and protein analysis in extracellular vesicle research. 2017;1–12.

207. Witkamp R. Fatty acids, endocannabinoids and inflammation. Eur J Pharmacol. 2016;785:96–107.

208. De Jesús ML, Hostalot C, Garibi JM, Sallés J, Meana JJ, Callado LF. Opposite changes in cannabinoid CB1 and CB2 receptor expression in human gliomas. Neurochem Int. 2010;56(6–7):829–33.

209. Rubio-araiz A, Arévalo-martín Á, Gómez-torres O, Navarro-galve B, García-ovejero D, Suetterlin P, et al. Molecular and Cellular Neuroscience The endocannabinoid system modulates a transient TNF pathway that induces neural stem cell proliferation. 2008;38:374–80.

210. Lou Z, Chen C, He Q, Zhao C, Xiao B. Targeting CB 2 receptor as a neuroinflammatory modulator in experimental autoimmune encephalomyelitis. Mol Immunol [Internet]. 2011;49(3):453–61. Available from: http://dx.doi.org/10.1016/j.molimm.2011.09.016

211. Lou Z, Zhao C, Xiao B. Immunoregulation of Experimental Autoimmune Encephalomyelitis by the Selective CB1 Receptor Antagonist. 2012;95:84–95.

212. Jean-Gilles L, Braitch M, Latif ML, Aram J, Fahey AJ, Edwards LJ, et al. Effects of pro-inflammatory cytokines on cannabinoid CB 1 and CB 2 receptors in immune cells. 2015;2:63–74.

213. López AJS. Regulation of cannabinoid receptor gene expression and endocannabinoid levels in lymphocyte subsets by interferon- β : a longitudinal study in multiple sclerosis patients. 2014;119–27.

214. Gabrielsson L, Gouveia-Figueira S, Haggstrom J, Alhouayek M, Fowler C. The anti-inflammatory compound palmitoylethanolamide inhibits prostaglandin and hydroxyeicosatetraenoic acid production by a macrophage cell line. 2017;1–13.

215. Tchetina E V, Battista JA Di, Zukor DJ, Antoniou J, Poole AR. Research article Prostaglandin PGE 2 at very low concentrations suppresses collagen cleavage in cultured human osteoarthritic articular cartilage : this involves a decrease in expression of proinflammatory genes , collagenases and COL10A1 , a gene linked to chondrocyte hypertrophy. 2007;9(4):1–9.

216. Li X, Ellman M, Muddasani P, Wang JH, Cs-szabo G, Wijnen AJ Van, et al. Prostaglandin E 2 and Its Cognate EP Receptors Control Human Adult Articular Cartilage Homeostasis and Are Linked to the Pathophysiology of Osteoarthritis. 2009;60(2):513–23.

217. Attur M, Al-mussawir HE, Patel J, Dave M, Palmer G, Pillinger MH, et al. Prostaglandin E 2 Exerts Catabolic Effects in Osteoarthritis Cartilage: Evidence for Signaling via the EP4 Receptor. 2021;

218. Roman-Blas J, Jimenez M. NF-kB as a potential therapeutic target in osteoarthritis and rheumatoid arthritis. 2006;

219. Esposito G, Capoccia E, Turco F, Palumbo I, Lu J, Steardo A, et al. Palmitoylethanolamide improves colon in fl amm ation through an enteric glia / toll like receptor 4-dependent PPAR- α activation. 2014;1300–12.

220. Agostino GD, La G, Russo R, Sasso O, Iacono A, Esposito E, et al. Central administration of palmitoylethanolamide reduces hyperalgesia in mice via inhibition of NF- κ B nuclear signalling in dorsal root ganglia. Eur J Pharmacol [Internet].

2009;613(1–3):54–9. Available from: http://dx.doi.org/10.1016/j.ejphar.2009.04.022

221. Romano A, Romano A, Friuli M, Coco L Del, Longo S, Vergara D, et al. Chronic Oleoylethanolamide Treatment Decreases Hepatic Triacylglycerol Level in Rat Liver by a PPAR γ / SREBP-Mediated Suppression of Fatty Acid and Triacylglycerol Synthesis. 2021;(January).

222. Mendes AF, Carvalho AP, Caramona MM, Lopes MC. Role of nitric oxide in the activation of NF- k B , AP-1 and NOS II expression in articular chondrocytes. 2002;51:369–75.

223. Abramson SB. Osteoarthritis and nitric oxide. 2008;

224. Leonidou A, Lepetsos P, Mintzas M, Kenanidis E, Macheras G, Tzetis M, et al. Inducible nitric oxide synthase as a target for osteoarthritis treatment. Expert Opin Ther Targets. 2018;22(4):299-318.

225. D RMCP, D PFGP, Abramson SBMD. Nitric oxide sustains nuclear factor kappaB activation in cytokine-stimulated chondrocytes. 2004;552–8.

226. Jimi E, Aoki K, Saito H, Acquisto FD, May MJ, Nakamura I, et al. Selective inhibition of NF- κ B blocks osteoclastogenesis and prevents inflammatory bone destruction in vivo. 2004;10(6):617–24.

List of figures and tables

Figures

Fig 8. Box and whisker plots referred to EC and NAE levels in EV (ng per 106 cells) and CM (ng/ml per 106) cells from BMSC, ASC and DF

Fig 9. Box and whisker plots referred to PUFA and PGE2 levels in EV (ng per 106 cells) and CM (ng/ml per 106) from BMSC, ASC and DF

Fig 10. Quantification of CB1 (a) and CB2 (b) expression in untreated, TNFα and TNFα+ASC-CM stimulated CH at day 3 analyzed by Western blot. Data (n=7 independent experiments) were normalized on GAPDH and expressed as relative values (CTR=1). (c-d) Representative Western Blots of CB1 (c) and CB2 (d) expression by TNFα-stimulated and ASC-CM-treated CH. GAPDH was used as internal control and CB1 or CB2 densitometric evaluation was normalized on it.

Fig 11. Modulation of PGE2 (a) and COX2 (b) by 2AG (1pg/ml) and PEA (0.5pg/ml). (a) PGE2 release, analyzed by UHPLC-MS/MS in CH culture medium (n=8 independent experiments) 3 days after treatments. (b) Quantification of the COX2 expression in TNFα-stimulated and 2AG or PEA-treated CH at day 3 analyzed by Western blot. Data (n=4 independent experiments) were normalized on GAPDH and expressed as relative values (CTR=1). (c) Representative Western Blots of COX2 expression by TNFα-stimulated and 2AG- or PEA-treated CH. GAPDH was used as internal control and COX2 densitometric evaluation was normalized on it.

Fig 12. Quantification of NO by 2AG (1pg/ml), PEA (0.5pg/ml) and ASC-CM treatments NO production, analyzed in CH culture medium (n=4 independent experiments) at day 3, is expressed as [nitrite] μM. Data were expressed as relative values (CTR=1)

Fig 13. Quantification of AA, EPA and DHA in untreated and 2AG, PEA, ASC-CM treated CH cell media (absence of TNFα) at day 3 analyzed by UHPLC-MS/MS analysis. Data (n=5 independent experiments) were expressed in ng/ml

Fig 14. Quantification of AA, EPA and DHA in TNFα-stimulated CH cell media at day 3 analyzed by UHPLC-MS/MS analysis. Data (n=9 independent experiments) were expressed in ng/ml

Fig 15. Quantification of lipids in untreated and 2AG, PEA, ASC-CM treated CH cell media (absence of TNFα) at day 3 analyzed by UHPLC-MS/MS analysis. Data (n=5 independent experiments) were expressed in ng/ml

Fig 16. Quantification of lipids in CH cell media at day 3 analyzed by UHPLC-MS/MS analysis. Data (n=7 independent experiments) were expressed in ng/ml

Tables

Appendix

Supplementary Figures

F1. Quantification of MMP13 and MMP3 expression in TNFα-stimulated and 2AG or PEA-treated CH at day 3 analyzed by Western blot. Data (n=4 independent experiments) were normalized on GAPDH and expressed as relative values (CTR=1) (pag.51)

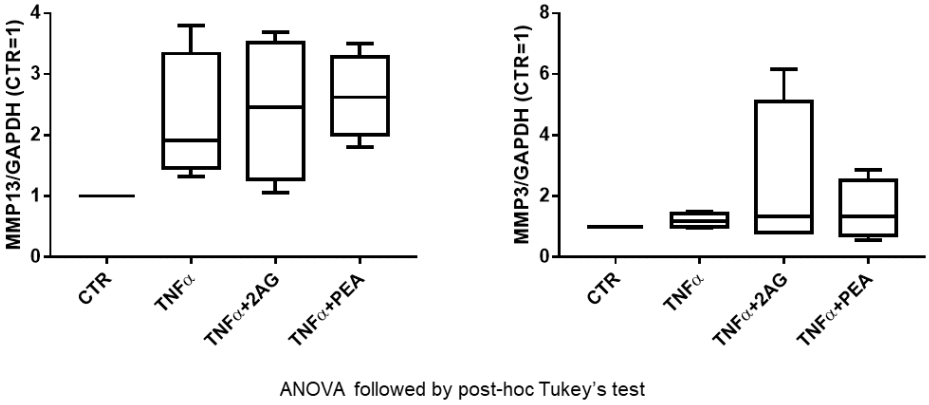

F2. Quantification of AA, EPA and DHA expression in TNFα-stimulated and 2AG or PEA-treated CH cell media at day 3 analyzed by UHPLC-MS/MS analysis. Data (n=9 independent experiments) were expressed in ng/ml (pag.52)

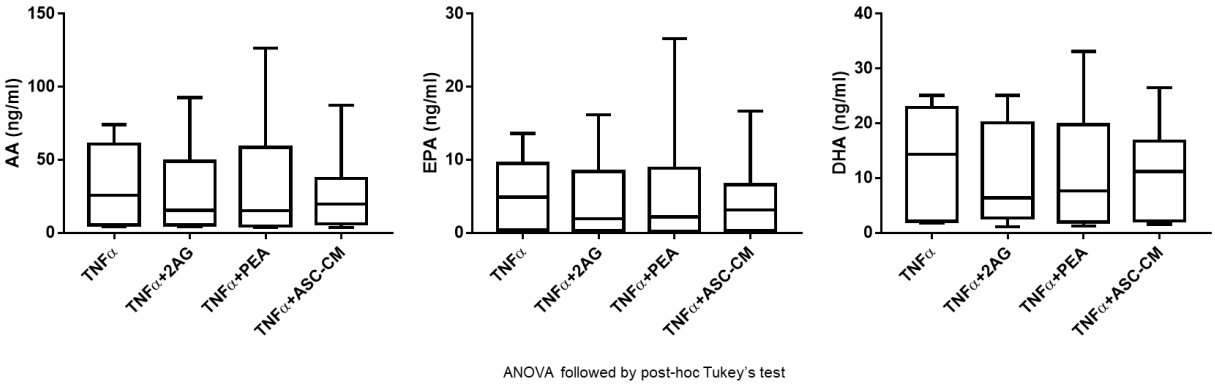

F3. Quantification of AA, EPA and DHA expression in untreated, TNFα-stimulated and 2AG- PEA- or ASC-CM treated CH cell lysates at day 3 analyzed by UHPLC-MS/MS analysis. Data (n=6 independent experiments) were expressed in ng/μg proteins (pag.52)

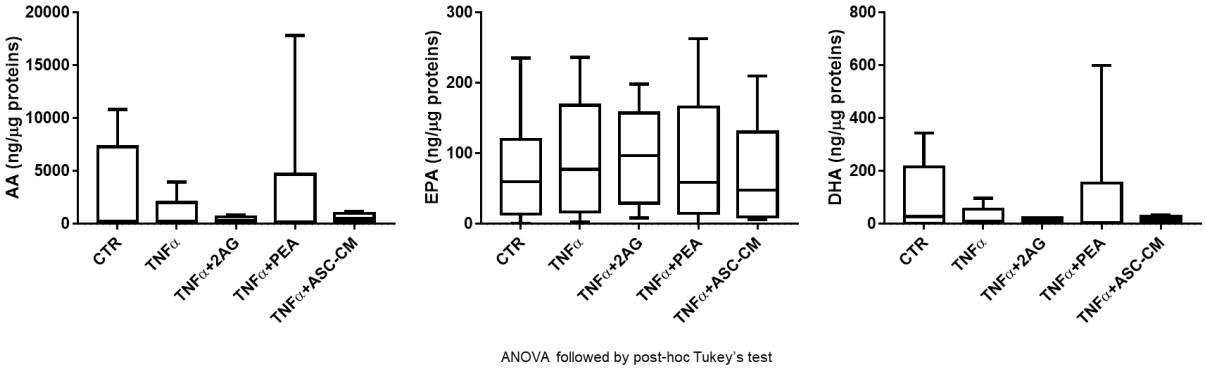

F4 Quantification of lipids detected in untreated, TNFα-stimulated and 2AG- PEA-or ASC-CM treated CH cell lysates at day 3 analyzed by UHPLC-MS/MS analysis. Data (n=6 independent experiments) were expressed in ng/µg proteins (pag.54)

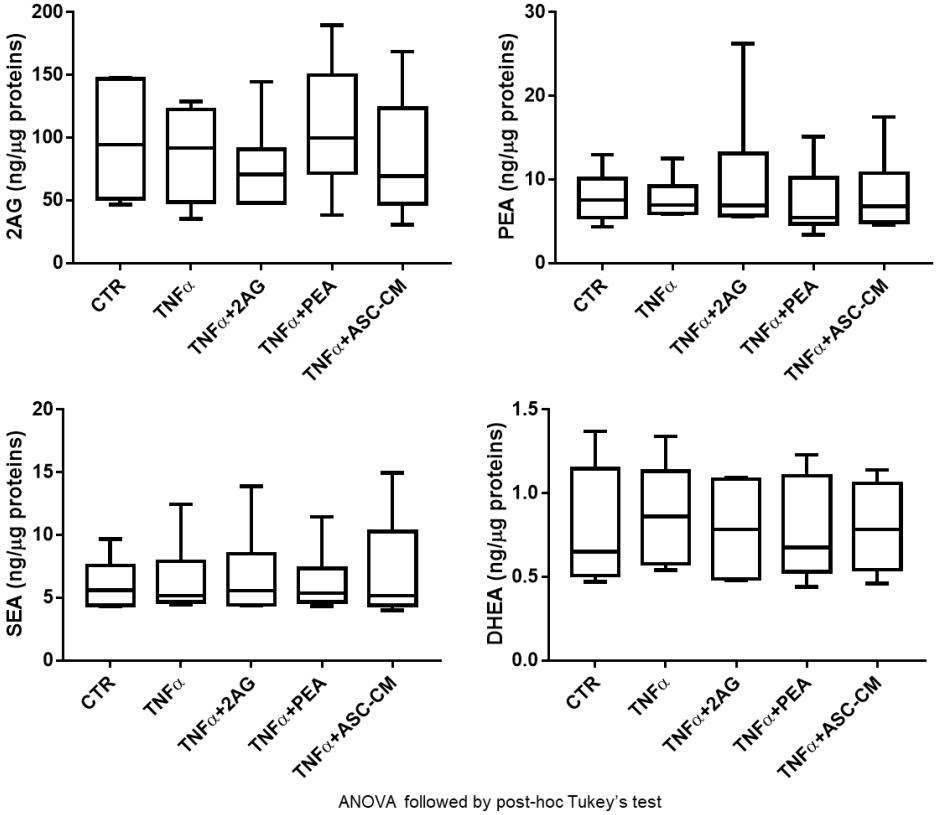

Supplementary Tables

S1. Precision and accuracy parameters for PUFA/eicosanoids group (pag.41)

Compound	Measured amount (ng/mL)	CV (%)	BIAS (%)
AA	1 5 25	14.9 9.00 1.08	10.8 8.32 0.88
EPA	1 5 25	2.76 2.54 0.08	5.20 2.08 1.05
DHA	1 5 25	7.81 3.49 3.43	9.52 6.96 3.84
TXB_2	0.1 0.5 2.5	8.84 4.23 10.6	14.1 11.5 12.6
PGE_2	0.1 0.5 2.5	12.4 4.58 0.45	10.1 4.49 0.90
PGD_2	0.1 0.5 2.5	5.23 2.22 2.99	6.98 2.31 3.19
$PGF_{2\alpha}$	0.1 0.5 2.5	5.06 1.78 1.54	10.9 1.56 1.65
6αKeto-$PGF_{1\alpha}$	0.1 0.5 2.5	3.66 7.61 1.38	10.8 7.25 1.13
LTB_4	0.1 0.5 2.5	6.16 10.1 9.79	10.5 9.36 9.30
5(S)-HETE	0.1 0.5 2.5	2.30 11.1 4.76	1.91 13.7 9.72
15(S)-HETE	0.1 0.5 2.5	10.2 10.0 13.4	13.5 14.1 11.9
14.15-EET	0.1 0.5 2.5	3.23 14.5 3.15	13.6 12.0 3.67

S2. Precision and accuracy parameters for EC/NAE group (pag.41)

Compound	Measured amount (ng/mL)	CV (%)	BIAS (%)
AEA	0.1	7.64	12.5
	0.5	6.38	12.0
	2.5	0.03	2.82
2AG	0.1	4.65	7.38
	0.5	1.82	1.70
	2.5	8.01	11.3
2AGE	0.1	13.3	13.5
	0.5	11.7	10.6
	2.5	0.71	0.58
LNEA	0.1	14.3	11.0
	0.5	13.4	10.1
	2.5	1.23	1.59
LEA	0.1	13.4	11.1
	0.5	10.5	7.88
	2.5	3.72	2.88
PEA	0.1	1.24	14.0
	0.5	11.1	14.6
	2.5	9.13	10.2
OEA	0.1	3.89	9.49
	0.5	5.44	5.38
	2.5	4.68	4.64
SEA	0.1	10.9	12.7
	0.5	4.31	3.40
	2.5	9.15	8.54
DHEA	0.1	14.9	14.3
	0.5	0.85	0.85
	2.5	1.28	3.74
EPEA	0.1	7.66	14.3
	0.5	13.5	10.4
	2.5	6.73	3.04
ADA	0.1	14.1	12.2
	0.5	3.18	5.09
	2.5	8.19	9.37
ODA	0.1	15.4	11.0
	0.5	4.28	0.39
	2.5	9.90	11.3
ASer	0.1	14.4	12.5
	0.5	14.1	11.1
	2.5	0.86	2.58
AGly	0.1	8.24	14.3

	0.5	13.3	14.4
	2.5	2.50	4.41
OGly	0.1	7.44	13.7
	0.5	8.30	14.3
	2.5	5.89	12.6
PalGly	0.1	11.1	14.3
	0.5	1.75	8.99
	2.5	2.82	10.0
AGABA	0.1	7.00	5.10
	0.5	8.50	12.1
	2.5	0.08	0.06
A5HT	0.1	13.1	14.7
	0.5	11.3	13.5
	2.5	7.66	6.58
O5HT	0.1	8.66	6.38
	0.5	5.83	14.0
	2.5	0.81	1.87
Pal5HT	0.1	8.56	10.5
	0.5	6.62	14.1
	2.5	2.98	4.23

S3. Extraction recovery and matrix effect of PUFA/eicosanoids groups in human serum and urine (pag.42)

Compound	Measured amount (ng/mL)	Matrix	Recovery (%)	Matrix effect (%)
EPA-d5	1	Serum	63.6	+13.99
		Urine	73.1	+10.01
	5	Serum	79.3	+3.23
		Urine	65.6	+10.39
	25	Serum	62.4	+7.24
		Urine	93.0	+28.79
TXB_2-d4	0.1	Serum	89.1	+68.0
		Urine	110	+54.2
	0.5	Serum	113	+49.5
		Urine	101	+49.4
	2.5	Serum	98.2	+52.2
		Urine	103	+66.0
$PGF_{2\alpha}$-d4	0.1	Serum	86.8	-14.9
		Urine	110	-10.3
	0.5	Serum	101	-2.04
		Urine	113	-10.8
	2.5	Serum	78.9	-9.01
		Urine	108	-6.32
LTB_4-d4	0.1	Serum	110	+12.1
		Urine	114	+4.81
	0.5	Serum	98.18	-5.93
		Urine	102	-14.1
	2.5	Serum	110	-7.17
		Urine	112	-10.5

S4. Extraction recovery and matrix effect of EC/NAE group in human serum and urine (pag.42)

Compound	Measured amount (ng/mL)	Matrix	Recovery (%)	Matrix effect (%)
AEA-d8	0.1	Serum	93.4	-14.6
		Urine	67.6	-5.56
	0.5	Serum	85.7	-13.3
		Urine	67.7	-8.99
	2.5	Serum	85.2	-14.4
		Urine	79.6	-1.72
PEA-d5	0.1	Serum	88.5	-66.5
		Urine	89.8	-8.25
	0.5	Serum	102.6	-59.3
		Urine	80.7	-4.74
	2.5	Serum	88.8	-52.5
		Urine	87.7	+3.24
OEA-d2	0.1	Serum	104	-57.1
		Urine	89.2	-5.65
	0.5	Serum	69.1	-63.7
		Urine	77.8	+8.60
	2.5	Serum	84.8	-75.0
		Urine	91.0	+4.83
SEA-d4	0.1	Serum	76.0	-17.8
		Urine	95.7	-7.20
	0.5	Serum	79.4	-19.9
		Urine	78.0	+7.92
	2.5	Serum	66.2	-10.6
		Urine	82.9	+7.74
EPEA-d4	0.1	Serum	93.4	+2.86
		Urine	87.9	-6.86
	0.5	Serum	98.1	-1.73
		Urine	73.3	+7.96
	2.5	Serum	93.5	+0.63
		Urine	92.9	+3.92
ADA-d8	0.1	Serum	82.0	-9.77
		Urine	92.6	-11.9
	0.5	Serum	69.8	-12.5
		Urine	60.7	-6.50
	2.5	Serum	74.5	-6.23
		Urine	96.8	-13.4
ASer-d8	0.1	Serum	10.8	-17.2
		Urine	92.2	+6.73
	0.5	Serum	85.2	-9.2
		Urine	85.4	-1.55

	2.5	Serum	75.8	-11.3
		Urine	90.8	+6.23
AGly-d8	0.1	Serum	98.9	-63.8
		Urine	74.1	-13.1
	0.5	Serum	89.5	-51.3
		Urine	80.9	-10.0
	2.5	Serum	92.8	-46.5
		Urine	98.2	-1.92
O5HT-d17	0.1	Serum	92.6	-12.7
		Urine	100	+5.23
	0.5	Serum	74.6	+3.22
		Urine	63.5	+10.9
	2.5	Serum	89.3	-14.2
		Urine	77.2	+13-3

S5. Stability of QC samples after exposure to 4 °C and – 20°C for 24h (pag.43)

Compound	Concentration (ng/mL)	Condition	Mean deviation (%) from Day 0
AEA	0.1	4 °C -20 °C	+8.13 +4.88
	0.5	4 °C -20 °C	-2.14 -1.58
	2.5	4 °C -20 °C	+4.39 +6.15
2AG	0.1	4 °C -20 °C	+0.61 -1.19
	0.5	4 °C -20 °C	+9.66 -9.72
	2.5	4 °C -20 °C	+7.31 +8.19
2AGE	0.1	4 °C -20 °C	+3.93 -3.51
	0.5	4 °C -20 °C	-4.92 -2.45
	2.5	4 °C -20 °C	+7.19 -2.62
LNEA	0.1	4 °C -20 °C	+4.49 -8.64
	0.5	4 °C -20 °C	-0.72 -2.26
	2.5	4 °C -20 °C	+2.33 +6.96
LEA	0.1	4 °C -20 °C	-0.69 0.51
	0.5	4 °C -20 °C	-1.54 -4.56
	2.5	4 °C -20 °C	+1.08 +6.68
PEA	0.1	4 °C -20 °C	-14.6 -13.1
	0.5	4 °C -20 °C	-10.3 -6.46
	2.5	4 °C -20 °C	+13.58 +13.70
OEA	0.1	4 °C -20 °C	+11.4 +7.48
	0.5	4 °C -20 °C	-2.47 -13.4

	2.5	4 °C -20 °C	+7.71 +12.13
SEA	0.1	4 °C -20 °C	-14.6 -11.2
	0.5	4 °C -20 °C	-1.19 3.45
	2.5	4 °C -20 °C	+11.1 +4.17
DHEA	0.1	4 °C -20 °C	+7.81 -8.40
	0.5	4 °C -20 °C	-5.57 +10.2
	2.5	4 °C -20 °C	-3.32 +2.39
EPEA	0.1	4 °C -20 °C	+11.5 -3.54
	0.5	4 °C -20 °C	+2.94 +2.19
	2.5	4 °C -20 °C	+8.91 +6.74
ADA	0.1	4 °C -20 °C	+8.54 +11.0
	0.5	4 °C -20 °C	+3.93 +2.35
	2.5	4 °C -20 °C	-2.38 -4.35
ODA	0.1	4 °C -20 °C	-10.8 -4.62
	0.5	4 °C -20 °C	-11.7 +6.59
	2.5	4 °C -20 °C	-13.7 -6.88
ASer	0.1	4 °C -20 °C	+10.6 +1.30
	0.5	4 °C -20 °C	+9.47 +1.15
	2.5	4 °C -20 °C	+10.0 +5.96
AGly	0.1	4 °C -20 °C	+9.10 -9.79
	0.5	4 °C -20 °C	-5.60 -8.91

	2.5	4 °C -20 °C	+11.2 +12.3
OGly	0.1	4 °C -20 °C	-1.22 -9.72
	0.5	4 °C -20 °C	-10.0 -3.31
	2.5	4 °C -20 °C	+7.04 +14.3
PalGly	0.1	4 °C -20 °C	-8.38 -5.24
	0.5	4 °C -20 °C	-4.38 +2.86
	2.5	4 °C -20 °C	+11.8 +7.55
AGABA	0.1	4 °C -20 °C	+3.57 +3.27
	0.5	4 °C -20 °C	+5.31 -3.66
	2.5	4 °C -20 °C	+1.28 +4.24
A5HT	0.1	4 °C -20 °C	-7.66 -0.90
	0.5	4 °C -20 °C	-7.98 -2.25
	2.5	4 °C -20 °C	+2.91 +7.10
O5HT	0.1	4 °C -20 °C	-9.15 -5.78
	0.5	4 °C -20 °C	-1.55 +1.16
	2.5	4 °C -20 °C	+8.48 +6.07
Pal5HT	0.1	4 °C -20 °C	-8.84 -9.01
	0.5	4 °C -20 °C	+1.14 -3.66
	2.5	4 °C -20 °C	+6.28 +3.27
AA	1	4 °C -20 °C	-6.75 -1.78
	5	4 °C -20 °C	-7.81 -6.85

	25	4 °C -20 °C	-9.51 -13.1
EPA	0.1	4 °C -20 °C	-2.72 -7.61
	0.5	4 °C -20 °C	-1.94 -13.9
	2.5	4 °C -20 °C	-1.50 -12.2
DHA	1	4 °C -20 °C	-13.8 -9.79
	5	4 °C -20 °C	+3.91 +11.4
	25	4 °C -20 °C	-3.98 +0.34
TXB_2	0.1	4 °C -20 °C	-10.3 -6.47
	0.5	4 °C -20 °C	+10.6 +10.5
	2.5	4 °C -20 °C	+4.41 +9.15
PGE_2	0.1	4 °C -20 °C	+0.60 +8.74
	0.5	4 °C -20 °C	-8.17 -11.4
	2.5	4 °C -20 °C	-4.13 -6.51
PGD_2	0.1	4 °C -20 °C	+7.03 +50.3
	0.5	4 °C -20 °C	-2.27 +33.1
	2.5	4 °C -20 °C	-4.83 +25.9
$PGF_{2\alpha}$	0.1	4 °C -20 °C	-10.9 +0.89
	0.5	4 °C -20 °C	-5.60 -11.4
	2.5	4 °C -20 °C	-14.6 -1.00
6αKeto-$PGF_{1\alpha}$	0.1	4 °C -20 °C	-8.90 -5.74
	0.5	4 °C -20 °C	-14.8 -12.8

	2.5	4 °C -20 °C	-11.6 -9.43
LTB_4	0.1	4 °C -20 °C	-13.5 -10.3
	0.5	4 °C -20 °C	-5.91 -7.06
	2.5	4 °C -20 °C	-14.8 -14.2
5(S)-HETE	0.1	4 °C -20 °C	-7.6 -9.1
	0.5	4 °C -20 °C	-13.3 -33.3
	2.5	4 °C -20 °C	-14.4 -11.2
15(S)-HETE	0.1	4 °C -20 °C	-14.9 -42.8
	0.5	4 °C -20 °C	-14.3 -36.5
	2.5	4 °C -20 °C	-13.7 -11.1
14,15-EET	0.1	4 °C -20 °C	-14.1 -37.1
	0.5	4 °C -20 °C	-6.95 -23.9
	2.5	4 °C -20 °C	-10.0 -4.08

Publications related to the project

Stem Cell Research 38 (2019) 101463

Contents lists available at ScienceDirect

Stem Cell Research

journal homepage: www.elsevier.com/locate/scr

Short report

Adipose-derived stromal cell secretome reduces TNFα-induced hypertrophy and catabolic markers in primary human articular chondrocytes

Stefania Niada[a,*,1], Chiara Giannasi[a,1], Marta Gomarasca[a], Deborah Stanco[b], Sara Casati[c], Anna Teresa Brini[a,c]

[a] Laboratory of Biotechnological Applications, IRCCS Istituto Ortopedico Galeazzi, Italy
[b] Department of Mechanical and Aerospace Engineering, Politecnico di Torino, Turin, Italy
[c] Department of Biomedical, Surgical and Dental Sciences, University of Milan, Italy

ARTICLE INFO

Keywords:
Adipose-derived stromal cells
Secretome
Chondrocytes
Hypertrophy
MMPs
TIMPs

ABSTRACT

Recent clinical trials show the efficacy of Adipose-derived Stromal Cells (ASCs) in contrasting the osteoarthritis scenario. Since it is quite accepted that ASCs act predominantly through a paracrine mechanism, their secretome may represent a valid therapeutic substitute. The aim of this study was to investigate the effects of ASC conditioned medium (ASC-CM) on TNFα-stimulated human primary articular chondrocytes (CHs).

CHs were treated with 10 ng/ml TNFα and/or ASC-CM (1:5 recipient:donor cell ratio). ASC-CM treatment blunted TNFα-induced hypertrophy, reducing the levels of Osteocalcin (−37%), Collagen X (−18%) and MMP-13 activity (−61%). In addition, it decreased MMP-3 activity by 59%. We showed that the reduction of MMP activity correlates to the abundance of TIMPs (Tissue Inhibitors of MMPs) in ASC secretome (with TIMP-1 exceeding 200 ng/ml and TIMP-2/3 in the ng/ml range) rather than to a direct down-modulation of the expression and/or release of these proteases. In addition, ASC secretome contains high levels of other cartilage protecting factors, i.e. OPG and DKK-1.

ASC-CM comprises cartilage-protecting factors and exerts anti-hypertrophic and anti-catabolic effects on TNFα-stimulated CHs in vitro. Our results support a future use of this cell-derived but cell-free product as a therapeutic approach in the management of osteoarthritis.

1. Introduction

Osteoarthritis (OA) is a common age-related condition affecting millions of people worldwide. It is a multifactorial disease whose pathogenesis involves multiple causes, processes and tissues (Martel-Pelletier et al., 2016). This pathology is characterized by the destruction of articular cartilage associated with subchondral bone erosion and inflammation. Cartilage damage seems to be one of the earliest disease-causing events (Berenbaum, 2013). In OA, articular chondrocytes (CHs) undergo a phenotypic change: from quiescent and stable they engage a hypertrophic differentiation, characterized by increased cell proliferation and altered expression and activity of matrix-degrading enzymes (matrix metalloproteinases, MMPs) (Singh et al., 2018). The hypertrophic shift of CHs starts with the abnormal modulation of several signaling molecules and transcription factors that leads to the overexpression of Collagen X and distinct MMPs, such as MMP-1, MMP-9 and MMP-13. Among these enzymes, the latter is considered the main marker of hypertrophy (Singh et al., 2018). In animal models, the down-modulation of hypertrophy-inducing factors enhances the resistance to OA development, suggesting the arrest of chondrocyte hypertrophy as a valid therapeutic approach (Bottini et al., 2016). In addition, several in vitro models of hypertrophic chondrocytes have been developed treating cells with IL-1β or TNFα, the two major players in OA physiopathology (Cecil et al., 2009; Platas et al., 2013). Up to now, most treatments against OA are not curative. Cartilage regeneration does not occur spontaneously and the most common surgical approaches to circumvent the loss of cartilage, e.g. microfracture, subchondral drilling or autologous cartilage implantation, often lead to the formation of low-quality fibrocartilage. In the last years, the use of Mesenchymal Stromal Cells (MSCs) has emerged as a promising tool (Lopa et al., 2018). Its efficacy in contrasting cartilage damage has been shown in vitro (Manferdini et al., 2013; Maumus et al., 2013) and in

* Corresponding author at: IRCCS Istituto Ortopedico Galeazzi, Laboratory of Biotechnological Applications, Via R. Galeazzi 4, Milan, CAP 20161, Italy.
E-mail addresses: stefania.niada@grupposandonato.it (S. Niada), chiara.giannasi@grupposandonato.it (C. Giannasi), marta.gomarasca@grupposandonato.it (M. Gomarasca), sara.casati@unimi.it (S. Casati), anna.brini@unimi.it (A.T. Brini).
[1] Equal contribution

https://doi.org/10.1016/j.scr.2019.101463
Received 25 March 2019; Received in revised form 7 May 2019; Accepted 13 May 2019
Available online 15 May 2019

vivo (Lee et al., 2007; Xie et al., 2012). Moreover, > 50 clinical trials have been investigating the safety, feasibility and efficacy of MSC intra-articular injection (clinicaltrials.gov). Since nowadays it is widely recognized that MSC therapeutic action largely depends on paracrine mechanisms, the scientific interest has shifted to their secretome, namely the conditioned medium (CM). MSC-CM has been successfully tested in several preclinical models (e.g. Brini et al., 2017; Kay et al., 2017; Kuljanin et al., 2019), suggesting its promising potential in future clinical applications. Here, we have investigated the anti-hypertrophic and anti-catabolic action of Adipose-derived Stromal Cell conditioned medium (ASC-CM) on an in vitro model of TNFα-stimulated primary human articular chondrocytes.

2. Methods

2.1. Human primary cells

Human ASCs were isolated from the adipose tissue of 8 healthy donors (2 males and 6 females; 46 ± 16 y/o) undergoing aesthetic or prosthetic surgery at IRCCS Galeazzi Orthopaedic Institute, following previously described protocols (Niada et al., 2016). Human CHs were isolated from the articular cartilage of the femoral heads collected from 18 patients (11 males and 7 females; 62 ± 11 y/o) undergoing total hip replacement surgery at the same Clinical Institute (additional information in supplementary methods). All waste tissues were collected following the procedure PQ 7.5.125, version 4, dated 22.01.2015, approved by IRCCS Istituto Ortopedico Galeazzi. Written informed consent was obtained from all the patients.

2.2. Concentrated conditioned media

Conditioned media were collected from about 90–95% confluent ASCs cultured for 72 h in starving conditions (i.e. without FBS) and concentrated through Amicon Ultra-15 Centrifugal Filter Devices with 3 kDa cut-off (Merck Millipore)(Brini et al., 2017; Niada et al., 2018). The product was concentrated about 40–50 folds becoming handy for in vitro treatments (final volume of 50-60 µl~10^6 ASCs).

2.3. Cell viability

CHs were stimulated with 10 ng/ml TNFα and/or ASC-CM (added at a 1:5 recipient to donor cell ratio). Cell viability was assessed by Alamar Blue assay (Thermo Fisher Scientific) (Giannasi et al., 2018) before the first treatment and after 3, 5 and 7 days. After 4 h incubation with Alamar Blue (1:10 dilution), emitted fluorescence was measured using Wallac Victor II plate reader (Perkin Elmer).

2.4. Analyses of gene and protein expression

CHs were seeded at the density of 8×10^3 cells/cm^2 in complete medium with 1% FBS and treated with 10 ng/ml TNFα and/or ASC-CM (1:5 recipient to donor cell ratio). 24, 48 and 72 h later, cells were lysed, and total RNA was extracted with RNaeasy kit (Qiagen). cDNA was synthesized using the High Capacity Reverse-Transcription Kit (Thermo Fisher Scientific). The expression levels of the target genes and of the housekeeping gene *TBP* were quantified by RT-qPCR using TaqMan technology (MMP3: hs00968305_m1; MMP13: hs00233992_m1; TBP: hs00427600_m1). The real-time PCR was conducted on a StepOne Plus Applied Biosystem apparatus (Life Technologies). Data were analysed with the $2^{-\Delta\Delta Ct}$ method.

MMP-3, MMP-13 and Collagen X protein expression was assessed after 1 or 3 days of treatment using western blotting, as described in supplementary methods.

2.5. Luminex multiplex assay

CH culture supernatants were prepared as described in supplementary methods. The analyses were conducted using MILLIPLEX MAP Human Bone Panel (HBNMAG-51 K, Millipore), Human MMP Panel 1 and 2 (HMMP1MAG-55 K and HMMP2MAG-55 K), and Human TIMP Magnetic Luminex Performance Assay (LKTM003, R&D Systems). Technical duplicates were analysed for each condition (25-50 µl/sample) and read through Bio-Plex Multiplex System (Bio-Rad) following standard procedures. Data analysis was performed with MAGPIX xPONENT 4.2 software (Luminex Corporation).

2.6. MMP-3 and MMP-13 activity assay

72-h culture supernatants were analysed to assess the activity of MMP-3 and MMP-13 with SensoLyte 520 Generic MMP Assay Kit (AnaSpec) following the manufacturer's instructions. Pro-MMP activation was achieved after incubating samples with 1 mM 4-aminophenylmercuric acetate (APMA) at 37 °C for 4 h (MMP-3) or 40 min (MMP-13). Fluorescence (490 nm excitation λ, 520 nm emission λ) was read with Wallac Victor II plate reader (Perkin Elmer).

2.7. Statistical analysis

Data are expressed as mean ± standard deviation (SD) of at least 3 independent experiments. Statistical analysis was performed by one-way or two-way ANOVA using Prism 5 software (GraphPad Software Inc). Differences were considered significant at $p \leq .05$.

3. Results

ASC-CM exerted specific effects on OA-related factors, blunting the increase of hypertrophic markers induced by TNFα stimulation. Collagen X expression and Osteocalcin (OC) release were reduced by 18% (day 1) and 37% (day 3) (Fig. 1C and D, Supplementary Fig. 1 A), while MMP-13 activity was lowered by 61% (Fig. 1F). In addition, ASC-CM halved the activity of MMP-3, another OA-related cartilage-degrading enzyme (Fig. 1E). These were most likely specific effects. Indeed, ASC-CM did not induce any alteration in chondrocyte viability and proliferation (Fig. 1A and B), not even when TNFα significantly increased these parameters (+27% and + 31% at day 5 and 7, respectively). Since in the OA context the reduction in MMP-3 and MMP-13 activity represents a promising goal, we explored its possible causes. Initially, we investigated MMP expression and release. At an early time point (24 h after treatments), ASC-CM reduced the expression of *MMP-3* (−49%) and, by a lower extent, *MMP-13* (−31%) in TNFα-treated CHs (Fig. 2A and B). The down-modulation of *MMP-3* was maintained up to day 3 (−38%, data not shown), while *MMP-13* one was lost at later time points (data not shown). Surprisingly, ASC-CM treatment stimulated both the intracellular (Fig. 2C) and the extracellular (Fig. 2E) levels of MMP-3. The intracellular expression was increased in both untreated (+81%) and TNFα-treated CHs (+39%) (Fig. 2C and Supplementary Fig. 1 B) and a similar induction was revealed extracellularly (+245% versus control CHs and + 33% compared to TNFα-treated cells) (Fig. 2E). On the other hand, ASC-CM caused a mild reduction of MMP-13 expression (−12%, Fig. 2D and Supplementary Fig. 1 B) in TNFα-stimulated CHs, in full accordance with its lower release (−20%, Fig. 2F). Taken together these evidences cannot explain the blunting effect of ASC-CM on TNFα-induced MMP activity. Since MMP activities are physiologically modulated by their endogenous inhibitors, we analysed the levels of TIMPs in CH supernatants after 3 days of TNFα stimulation and/or ASC-CM administration. Following CM treatment, TIMP levels were significantly increased in respect to both control and TNFα-stimulated cells (Fig. 3). TIMP-1 was the more abundant (> 200 ng/ml), followed by TIMP-2 (around 80 ng/ml), TIMP-3 (around 5 ng/ml) and the less represented TIMP-4 (Fig. 3A-D

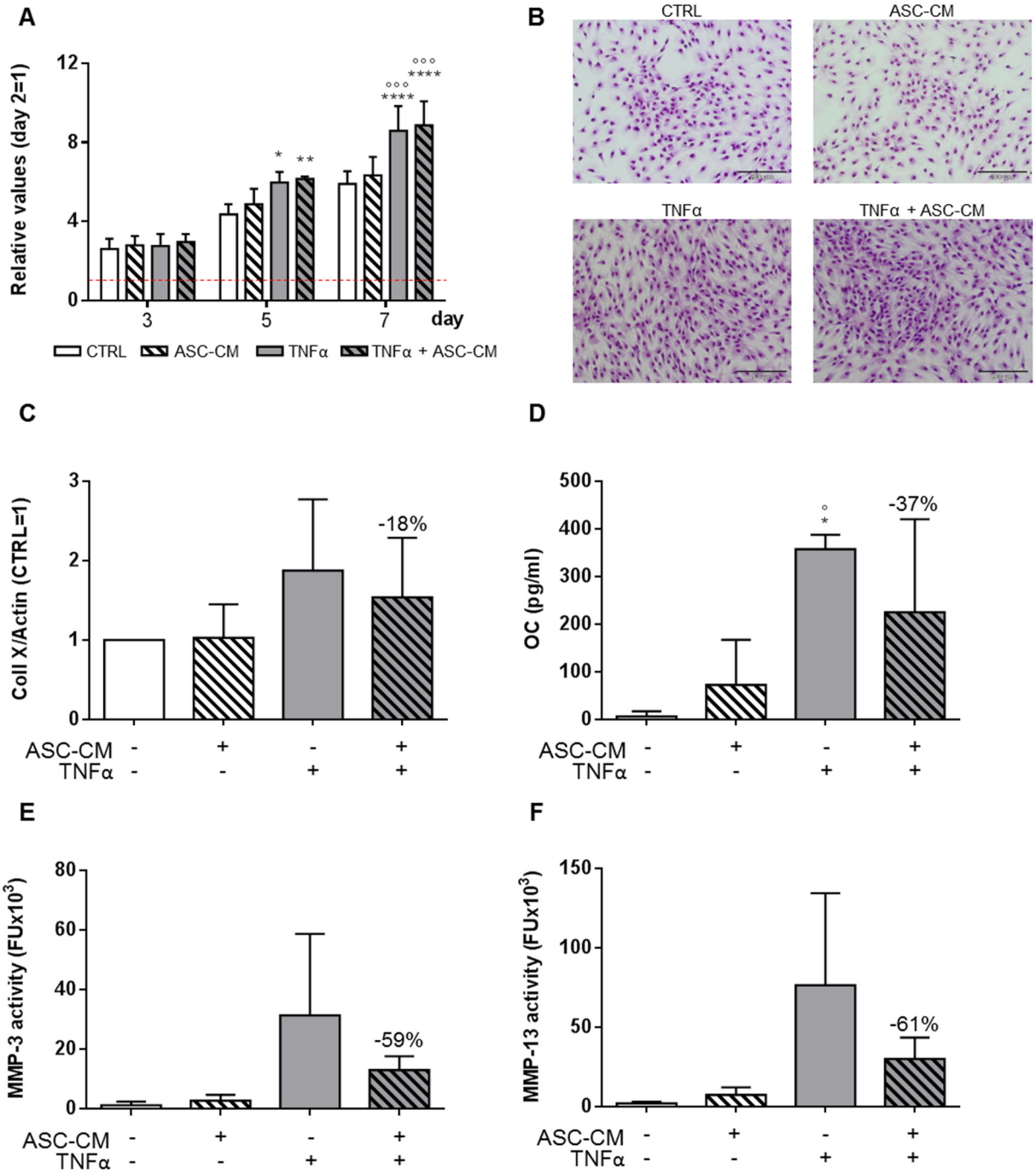

Fig. 1. Reduction of hypertrophic markers and MMP activity by ASC-CM treatment in TNFα-stimulated articular chondrocytes. (A) Cell metabolic activity measured by Alamar Blue assay. Data are shown as mean ± SD ($n = 3$) of relative values calculated as ratios on day 2 (red dashed line). Two-way ANOVA was performed, and significance vs CTRL is shown as $^{*}p < .05$, $^{**}p < .01$ and $^{****}p < .0001$, vs CM as $^{\circ\circ\circ}p < .001$. (B) Cell confluency at the final time point (day 7) displayed by Diff Quick staining (100× magnification; scale bar: 200 μm). (C) Collagen X expression at day 1 by Western Blot. Data ($n = 4$) were normalized on β-Actin and expressed as relative values (CTRL = 1). (D) Osteocalcin (OC) levels in CH culture media (day 3) measured by Luminex Multiplex Assay ($n = 9$ CHs, 3 pools). (*E*-F) Activity of MMP-3 and MMP-13 in chondrocyte culture medium ($n = 10$ CHs, 3 pools and 1 single population) expressed as fluorescence units (FU). Data were analysed by one-way ANOVA followed by Tukey's multiple comparison test. Significance vs CTRL is shown as $^{*}p < .05$, vs CM as $^{\circ}p < .05$.

respectively). Similar levels were already measured after 24 h of treatments (data not shown). This, together with the analysis of the naïve treating medium (Table 1), indicates that the high levels of TIMPs depend on their abundance in ASC secretome rather than to an increased production by treated CHs.

In conclusion, our data suggest that the reduction of MMP activity in TNFα-stimulated-CHs can be ascribed to the presence of TIMPs in ASC secretome rather than to its direct modulation of MMP gene and protein levels. Similar speculations can be made considering other MMPs whose secretion was enhanced by TNFα, such as MMP-1 (reduced by 31% following ASC-CM administration), MMP-9 (−52%) and MMP-10 (−16%) (Supplementary Fig. 2).

Moreover, the analysis of the naïve treating medium revealed the presence of two other factors involved in cartilage protection, namely OPG and DKK-1 (Table 1). MMP-1, MMP-3 and MMP-10 were also detected, even though their activity was probably inactivated by TIMPs

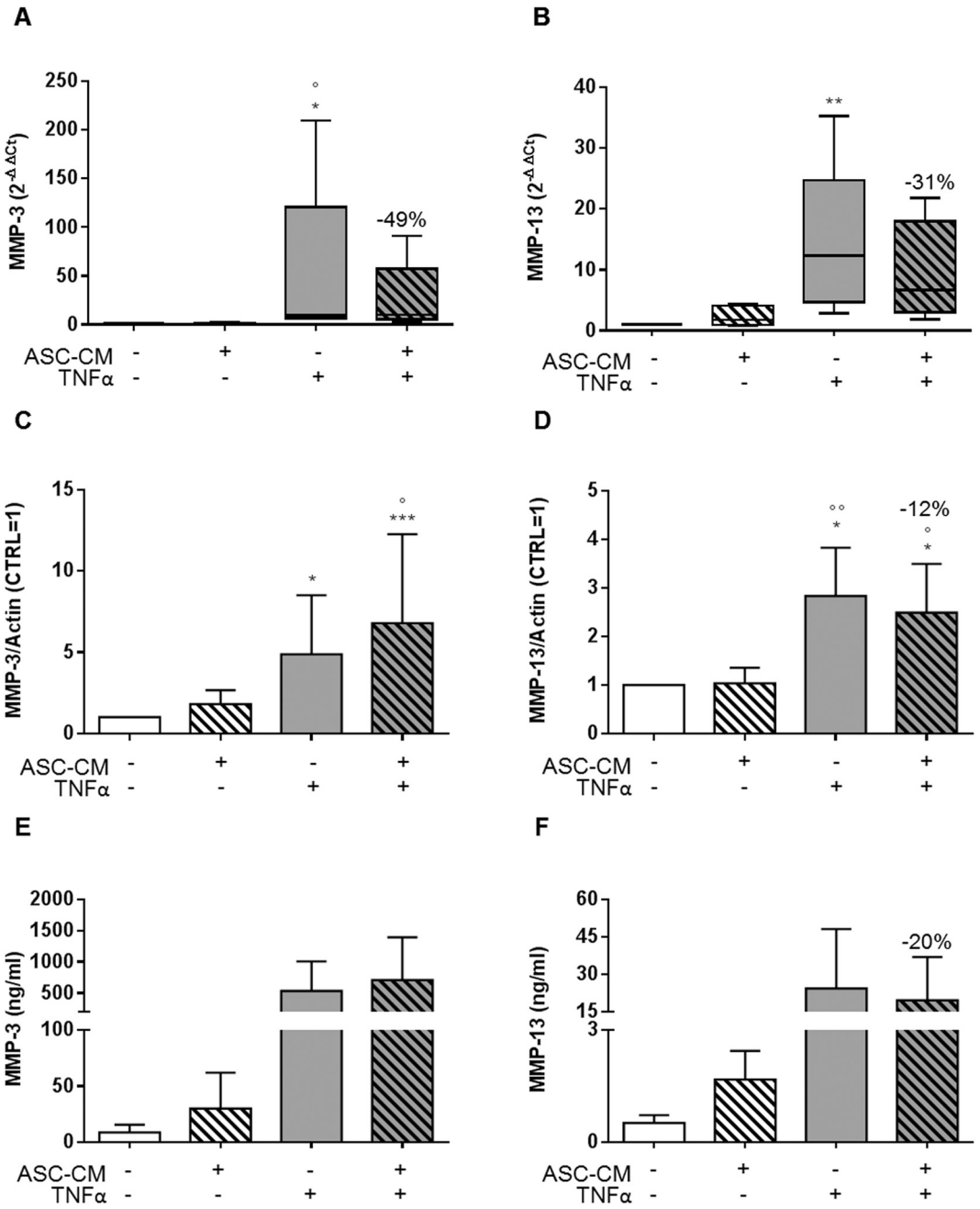

Fig. 2. Gene, protein expression and extracellular levels of MMP-3 and MMP-13 by ASC-CM-treated and/or TNFα-stimulated chondrocytes. (A-B) MMP-3 (A) and MMP-13 (B) mRNA expression at day 1 measured by real-time PCR. Data are expressed as $2^{-\Delta\Delta Ct}$ (TBP was used as housekeeping gene). Data were analysed by Friedman's test followed by Dunn's test. (C-D) MMP-3 (C) and MMP-13 (D) protein expression measured at day 3 by Western Blot. Data ($n = 7$) were normalized on β-Actin, expressed as relative values (CTRL = 1) and analysed using one-way ANOVA followed by Tukey's test. (E-F) MMP-3 (E) and MMP-13 (F) levels measured by Luminex Multiplex Assay (n = 9 CHs, 3 pools). Significance vs CTRL is shown as *p < .05 and ***p < .001, vs CM as °p < .05.

(e.g. MMP-3 in Fig. 1E).

4. Discussion

The complex nature of osteoarthritis might demand a multifactorial treatment. Adipose-derived Stromal Cell secretome is a mixture of soluble (proteins, lipids and nucleic acids) and vesicular elements, representing the entire regenerative milieu of its cell source. However, in the OA context, despite the chondroprotective action of ASCs has been described in vitro (Manferdini et al., 2013; Maumus et al., 2013; Tofino-Vian et al., 2018), in vivo (Choi et al., 2018; Desando et al., 2013) and in clinical trials (Lopa et al., 2018), there is no consensus yet on the efficacy of cell secretome (Manferdini et al., 2015; Platas et al., 2013). The studies of Platas (Platas et al., 2013), Manferdini (Manferdini et al., 2015) and Tofino-Vian (Tofino-Vian et al., 2018) suggest that ASC-CM action depends on the "activated" status of recipient. Our data confirm this hypothesis, as in our hands ASC-CM acts on TNFα-stimulated articular chondrocytes only. Moreover, the reduction of OA-related factors did not correlate with a decrease in cell metabolism nor proliferation, providing further evidence of the specificity of ASC-CM effects. One of the most promising results is the blunting of the TNFα-mediated hypertrophic shift. The reduction in MMP-13 activity is particularly interesting. Indeed, in vivo evidences on MMP-13-deficient or -depleted mice demonstrate that the action of this hypertrophy-

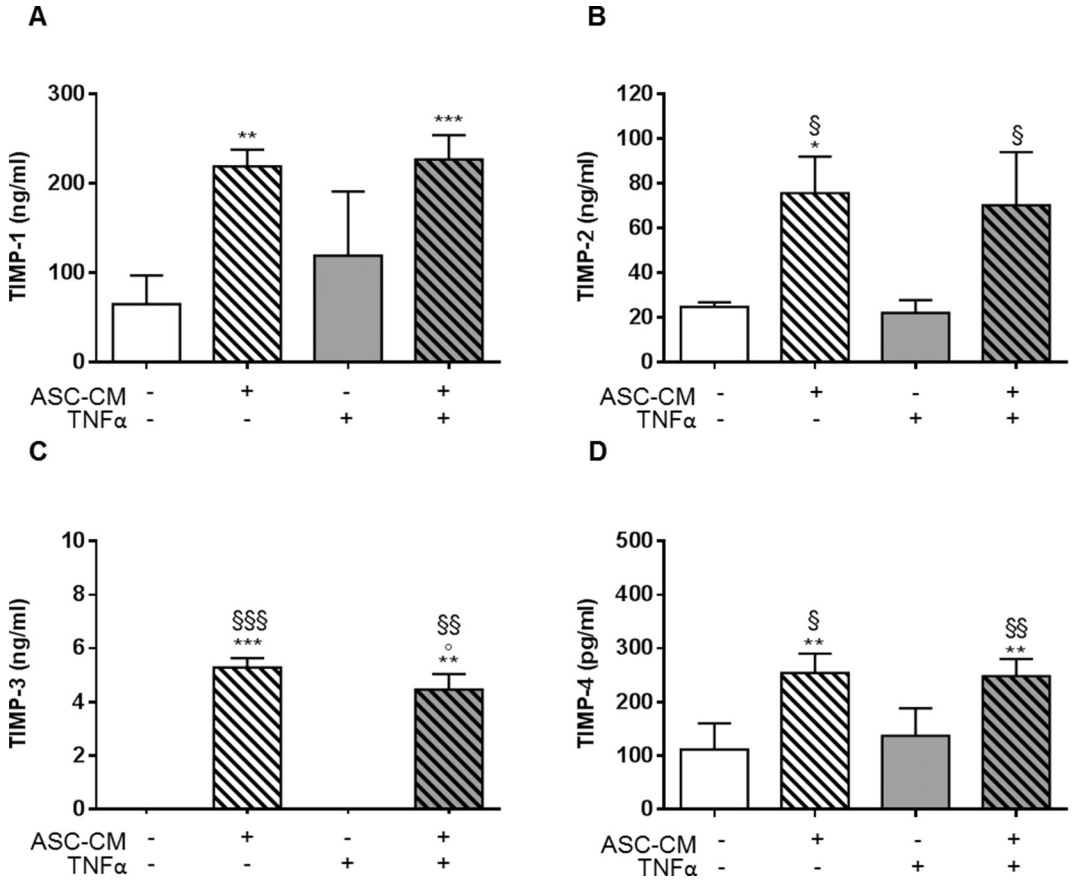

Fig. 3. TIMP levels in ASC-CM-treated and/or TNFα-stimulated chondrocyte culture media. (A-D) TIMP-1 (A), TIMP-2 (B), TIMP-3 (C) and TIMP-4 (D) levels measured by Luminex Multiplex Assay (n = 10 CHs, 3 pools and 1 single population). Data were analysed by one-way ANOVA followed by Tukey's multiple comparison test. Significance vs CTRL is shown as *p < .05, **p < .01 and *** < 0.001, vs CM as °p < .05 and vs TNFα as § p < .05, §§ p < .01 and §§§ p < .001.

Table 1
Concentrations of factors in the treating medium containing ASC-CM. Protein levels were measured by Luminex Multiplex Assay.

	[] of factors in the treating medium containing ASC-CM (pg/ml)
TIMP-1	2.6×10^5
TIMP-2	2.7×10^4
TIMP-3	3.8×10^3
TIMP-4	166
OC	nd
OPG	$1.1–1.9 \times 10^3$
DKK-1	$1.8–2.1 \times 10^3$
MMP-1	$2.1–2.6 \times 10^3$
MMP-3	$1.9–2.1 \times 10^3$
MMP-9	nd
MMP-10	17.7–20.3
MMP-12	0–56
MMP-13	nd

associated metalloprotease plays a key role in cartilage erosion during OA onset (Little et al., 2009; Wang et al., 2013). Here, we show that the ASC-CM-mediated reduction of MMP-13 activity, as well as MMP-3 one, depends only partially by the modulation of their expression. Indeed, the downmodulation of *MMP-3* and *MMP-13* transcription, the latter fully in agreement with what observed by Tofino-Vian (Tofino-Vian et al., 2018), was evident until day 1 only. When we investigated MMP-13 mRNA levels at subsequent time points (48 and 72 h,-data not shown-), no clear-cut regulation emerged. A possible explanation is that the effectors of *MMP-13* downmodulation could be active only in a short time period. As example, several miRNAs are among the major players involved in MMP-13 inhibition (Li et al., 2017). In this perspective, the short-lasting effect of CM could be ascribed to miRNA limited half-life, usually considered < 24 h. Regardless mRNA, also intracellular and secreted MMP-13 levels were decreased to a minor extent compared to the enzymatic activity. Moreover, the influence of ASC secretome on MMP-3 protein expression is not consistent with what observed at mRNA level. Even though this discrepancy was not expected, a lack of correlation between MMP mRNA and protein levels has been described before (Lichtinghagen et al., 2002). We hypothesize that CM reduces both MMP-3 mRNA transcription and its degradation rate, favouring the translation of MMP-3 and increasing the protein levels. These aspects might demand further investigations. However, in our setting, the robust inhibition of MMP-3 and MMP-13 activity is mainly due to the presence of active TIMPs. Besides MMP-3 and MMP-13, ASC-CM reduced also the activity of the collagenase MMP-1, the metallopeptidase MMP-12 and MMP-9/10, both Aggrecan-degrading enzymes (preliminary data not shown). The presence of these inhibitors in the secretome of MSCs is particularly interesting considering the relevance of developing clinical grade MMP inhibitors (Liu and Khalil, 2017). Of note, TIMPs in ASC secretome did not alter the physiologic MMP activity but buffered the TNFα-induced one. In the OA context, it is noteworthy that TIMPs are known to inhibit other metalloproteinases, namely ADAM-10 (a disintegrin and metalloproteinase-10), ADAM-12, ADAMTS-4 (a disintegrin and metalloproteinase with thrombospondin motif) and ADAMTS-5 (Liu and Khalil, 2017; Yang et al., 2017). Moreover, TIMP-1 has been implicated in the reduction of angiogenesis mediated by MSC secretome (Zanotti et al., 2016). Consequently, ASC-CM could also play a role in re-establishing the anti-angiogenic environment of a healthy cartilage.

Besides TIMPs, other cartilage-protecting factors, namely OPG and DKK-1, were detected in ASC-CM (Table 1). OPG is known to prevent cartilage degradation by inhibiting proteoglycan loss and chondrocyte apoptosis (Feng et al., 2015; Kadri et al., 2008) while DKK-1 acts mainly by preserving CH phenotype, counteracting hypertrophy (Zhong et al., 2016) and inhibiting the expression of catabolic factors (Oh et al., 2012). Of note, we have recently shown that DKK-1 is one of the 34 proteins more abundantly secreted by ASCs compared with dermal fibroblast (Niada et al., 2018).

In the last few years, the first in vivo evidences of the beneficial effect of MSC-secretome administration in pre-clinical OA models have been produced (Cosenza et al., 2017; Khatab et al., 2018; Tao et al., 2017; Toh et al., 2017; Wang et al., 2017; Zhang et al., 2018; Zhu et al., 2017). Even though many of these experimental plans rely on the administration of the purified vesicular component, Khatab et al. showed the effects of the whole secretome (Khatab et al., 2018) on pain reduction and arrest of cartilage damage in a murine collagenase OA model. The rationale of their choice relies on the lack of current knowledge on which component plays a major role. We chose to use a cell product containing both freely dissolved factors and vesicular components (Supplementary Fig. 3) for the same reason. Moreover, in the OA context, the use of selected CM subcomponents may lead to a diminished efficacy of the treatment. In fact, many factors released by ASCs that can be therapeutically exploited are both conveyed in vesicles and released as soluble mediators. TIMPs have been described both in the whole secretome (Niada et al., 2018)(Egashira et al., 2012; Kono et al., 2014; Maffioli et al., 2017) and in the vesicular elements (exosomes or microvesicles) (Haraszti et al., 2016). Similarly, DKK-1, HGF, recognized as a mediator of ASC anti-fibrotic effect (Maumus et al., 2013), and Prostaglandin E2, an immunosuppressive factor acting also on chondrocyte hypertrophic shift (Li et al., 2004; Manferdini et al., 2013), have been identified both in whole ASC-CM (Manferdini et al., 2013; Maumus et al., 2013) and in vesicles (vesiclepedia (Pathan et al., 2019)). Therefore, the use of secretome fractions would subtract effectors at the additional cost of increasing manipulations. This is particularly risky, also considering how different isolation methods can alter EV content (Gualerzi et al., 2019).

In conclusion, ASC-CM might constitute a novel tool to counteract OA development. It inhibits the aberrant activity of MMPs and blunts the hypertrophic changes induced by the inflammatory cytokine TNFα (Graphical Abstract). This complete cell product can be easily obtained, prepared in advance and stored. Therefore it constitutes a ready-to-use product. Both the soluble factors and the extracellular vesicles released by ASCs may be responsible of CM beneficial action, including its well-known anti-inflammatory properties. Further investigations should aim at disclosing all the components of the secretome that are involved in its therapeutic role in the perspective of a future clinical setting.

Supplementary data to this article can be found online at https://doi.org/10.1016/j.scr.2019.101463.

Disclosure of potential conflicts of interest

The authors declare that they have no competing interests.

Acknowledgements

This research was funded by the Italian Ministry of Health (Ricerca Corrente L2033 and L1027 of IRCCS Istituto Ortopedico Galeazzi) and by the Department of Biomedical, Surgical and Dental Sciences (Università degli Studi di Milano, fund RV_RIC_AT16RWEIBN_02, RV_LIB16ABRIN_M). The authors would like to thank Davide Molinaro for his contribute to the manuscript.

References

Berenbaum, F., 2013. Osteoarthritis as an inflammatory disease (osteoarthritis is not osteoarthrosis!). Osteoarthr. Cartil. 21, 16–21.
Bottini, M., Magrini, A., Fadeel, B., Rosato, N., 2016. Tackling chondrocyte hypertrophy with multifunctional nanoparticles. Gene Ther. 23, 560–564 England.
Brini, A.T., Amodeo, G., Ferreira, L.M., et al., 2017. Therapeutic effect of human adipose-derived stem cells and their secretome in experimental diabetic pain. Sci. Rep. 7, 9904.
Cecil, D.L., Appleton, C.T., Polewski, M.D., et al., 2009. The pattern recognition receptor CD36 is a chondrocyte hypertrophy marker associated with suppression of catabolic responses and promotion of repair responses to inflammatory stimuli. J. Immunol. 182, 5024–5031.
Choi, S., Kim, J.H., Ha, J., et al., 2018. Intra-articular injection of alginate-micro-encapsulated adipose tissue-derived Mesenchymal stem cells for the treatment of osteoarthritis in rabbits. Stem Cells Int. 2018, 2791632.
Cosenza, S., Ruiz, M., Toupet, K., Jorgensen, C., Noel, D., 2017. Mesenchymal stem cells derived exosomes and microparticles protect cartilage and bone from degradation in osteoarthritis. Sci. Rep. 7, 16214.
Desando, G., Cavallo, C., Sartoni, F., et al., 2013. Intra-articular delivery of adipose derived stromal cells attenuates osteoarthritis progression in an experimental rabbit model. Arthritis. Res. Ther. 15, R22.
Egashira, Y., Sugitani, S., Suzuki, Y., et al., 2012. The conditioned medium of murine and human adipose-derived stem cells exerts neuroprotective effects against experimental stroke model. Brain Res. 1461, 87–95.
Feng, Z.Y., He, Z.N., Zhang, B., et al., 2015. Adenovirus-mediated osteoprotegerin ameliorates cartilage destruction by inhibiting proteoglycan loss and chondrocyte apoptosis in rats with collagen-induced arthritis. Cell Tissue Res. 362, 187–199.
Giannasi, C., Pagni, G., Polenghi, C., et al., 2018. Impact of dental implant surface modifications on adhesion and proliferation of primary human gingival keratinocytes and progenitor cells. Int J Periodontics Restorative Dent 38, 127–135.
Gualerzi, A., Kooijmans, S.A.A., Niada, S., et al., 2019. Raman spectroscopy as a quick tool to assess purity of extracellular vesicle preparations and predict their functionality. J. Extracell. Vesicles 8, 1568780.
Haraszti, R.A., Didiot, M.C., Sapp, E., et al., 2016. High-resolution proteomic and lipidomic analysis of exosomes and microvesicles from different cell sources. J. Extracell. Vesicles 5, 32570.
Kadri, A., Ea, H.K., Bazille, C., Hannouche, D., Liote, F., Cohen-Solal, M.E., 2008. Osteoprotegerin inhibits cartilage degradation through an effect on trabecular bone in murine experimental osteoarthritis. Arthritis Rheum. 58, 2379–2386.
Kay, A.G., Long, G., Tyler, G., et al., 2017. Mesenchymal stem cell-conditioned medium reduces disease severity and immune responses in inflammatory arthritis. Sci. Rep. 7, 18019.
Khatab, S., van Osch, G.J., Kops, N., et al., 2018. Mesenchymal stem cell secretome reduces pain and prevents cartilage damage in a murine osteoarthritis model. Eur. Cell. Mater 36, 218–230.
Kono, T.M., Sims, E.K., Moss, D.R., et al., 2014. Human adipose-derived stromal/stem cells protect against STZ-induced hyperglycemia: analysis of hASC-derived paracrine effectors. Stem Cells 32, 1831–1842.
Kuljanin, M., Elgamal, R.M., Bell, G.I., Xenocostas, A., Lajoie, G.A., Hess, D.A., 2019. Human multipotent stromal cell secreted effectors accelerate islet regeneration. Stem Cells 37 (4), 516–528.
Lee, K.B., Hui, J.H., Song, I.C., Ardany, L., Lee, E.H., 2007. Injectable mesenchymal stem cell therapy for large cartilage defects–a porcine model. Stem Cells 25, 2964–2971.
Li, T.F., Zuscik, M.J., Ionescu, A.M., et al., 2004. PGE2 inhibits chondrocyte differentiation through PKA and PKC signaling. Exp. Cell Res. 300, 159–169.
Li, H., Wang, D., Yuan, Y., Min, J., 2017. New insights on the MMP-13 regulatory network in the pathogenesis of early osteoarthritis. Arthritis. Res. Ther. 19, 248.
Lichtinghagen, R., Musholt, P.B., Lein, M., et al., 2002. Different mRNA and protein expression of matrix metalloproteinases 2 and 9 and tissue inhibitor of metalloproteinases 1 in benign and malignant prostate tissue. Eur. Urol. 42, 398–406.
Little, C.B., Barai, A., Burkhardt, D., et al., 2009. Matrix metalloproteinase 13-deficient mice are resistant to osteoarthritic cartilage erosion but not chondrocyte hypertrophy or osteophyte development. Arthritis Rheum. 60, 3723–3733.
Liu, J., Khalil, R.A., 2017. Matrix metalloproteinase inhibitors as investigational and therapeutic tools in unrestrained tissue Remodeling and pathological disorders. Prog. Mol. Biol. Transl. Sci. 148, 355–420.
Lopa, S., Colombini, A., Moretti, M., de Girolamo, L., 2018. Injective mesenchymal stem cell-based treatments for knee osteoarthritis: from mechanisms of action to current clinical evidences. Knee Surg. Sports Traumatol. Arthrosc. 148. https://doi.org/10.1007/s00167-018-5118-9.
Maffioli, E., Nonnis, S., Angioni, R., et al., 2017. Proteomic analysis of the secretome of human bone marrow-derived mesenchymal stem cells primed by pro-inflammatory cytokines. J. Proteome 166, 115–126.
Manferdini, C., Maumus, M., Gabusi, E., et al., 2013. Adipose-derived mesenchymal stem cells exert antiinflammatory effects on chondrocytes and synoviocytes from osteoarthritis patients through prostaglandin E2. Arthritis Rheum. 65, 1271–1281.
Manferdini, C., Maumus, M., Gabusi, E., et al., 2015. Lack of anti-inflammatory and anti-catabolic effects on basal inflamed osteoarthritic chondrocytes or synoviocytes by adipose stem cell-conditioned medium. Osteoarthr. Cartil. 23, 2045–2057.
Martel-Pelletier, J., Barr, A.J., Cicuttini, F.M., et al., 2016. Osteoarthritis. Nat. Rev. Dis. Primers 2, 16072.
Maumus, M., Manferdini, C., Toupet, K., et al., 2013. Adipose mesenchymal stem cells protect chondrocytes from degeneration associated with osteoarthritis. Stem Cell Res. 11, 834–844.
Niada, S., Giannasi, C., Ferreira, L.M., Milani, A., Arrigoni, E., Brini, A.T., 2016. 17beta-estradiol differently affects osteogenic differentiation of mesenchymal stem/stromal cells from adipose tissue and bone marrow. Differentiation 92, 291–297.
Niada, S., Giannasi, C., Gualerzi, A., Banfi, G., Brini, A.T., 2018. Differential proteomic

analysis predicts appropriate applications for the Secretome of adipose-derived Mesenchymal stem/stromal cells and dermal fibroblasts. Stem Cells Int. 2018, 7309031.
Oh, H., Chun, C.H., Chun, J.S., 2012. Dkk-1 expression in chondrocytes inhibits experimental osteoarthritic cartilage destruction in mice. Arthritis Rheum. 64, 2568–2578.
Pathan, M., Fonseka, P., Chitti, S.V., et al., 2019. Vesiclepedia 2019: a compendium of RNA, proteins, lipids and metabolites in extracellular vesicles. Nucleic Acids Res. 47, D516–D519.
Platas, J., Guillen, M.I., del Caz, M.D., Gomar, F., Mirabet, V., Alcaraz, M.J., 2013. Conditioned media from adipose-tissue-derived mesenchymal stem cells down-regulate degradative mediators induced by interleukin-1beta in osteoarthritic chondrocytes. Mediat. Inflamm. 2013, 357014.
Singh, P., Marcu, K.B., Goldring, M.B., Otero, M., 2018. Phenotypic instability of chondrocytes in osteoarthritis: on a path to hypertrophy. Ann. N. Y. Acad. Sci. 1442 (1), 17–34.
Tao, S.C., Yuan, T., Zhang, Y.L., Yin, W.J., Guo, S.C., Zhang, C.Q., 2017. Exosomes derived from miR-140-5p-overexpressing human synovial mesenchymal stem cells enhance cartilage tissue regeneration and prevent osteoarthritis of the knee in a rat model. Theranostics 7, 180–195.
Tofino-Vian, M., Guillen, M.I., Perez Del Caz, M.D., Silvestre, A., Alcaraz, M.J., 2018. Microvesicles from human adipose tissue-derived Mesenchymal stem cells as a new protective strategy in osteoarthritic chondrocytes. Cell. Physiol. Biochem. 47, 11–25.
Toh, W.S., Lai, R.C., Hui, J.H.P., Lim, S.K., 2017. MSC exosome as a cell-free MSC therapy for cartilage regeneration: implications for osteoarthritis treatment. Semin. Cell Dev. Biol. 67, 56–64.
Wang, M., Sampson, E.R., Jin, H., et al., 2013. MMP13 is a critical target gene during the progression of osteoarthritis. Arthritis. Res. Ther. 15, R5.
Wang, Y., Yu, D., Liu, Z., et al., 2017. Exosomes from embryonic mesenchymal stem cells alleviate osteoarthritis through balancing synthesis and degradation of cartilage extracellular matrix. Stem Cell Res Ther 8, 189.
Xie, X., Wang, Y., Zhao, C., et al., 2012. Comparative evaluation of MSCs from bone marrow and adipose tissue seeded in PRP-derived scaffold for cartilage regeneration. Biomaterials 33, 7008–7018.
Yang, C.Y., Chanalaris, A., Troeberg, L., 2017. ADAMTS and ADAM metalloproteinases in osteoarthritis - looking beyond the 'usual suspects'. Osteoarthr. Cartil. 25, 1000–1009.
Zanotti, L., Angioni, R., Cali, B., et al., 2016. Mouse mesenchymal stem cells inhibit high endothelial cell activation and lymphocyte homing to lymph nodes by releasing TIMP-1. Leukemia 30, 1143–1154.
Zhang, S., Chuah, S.J., Lai, R.C., et al., 2018. MSC exosomes mediate cartilage repair by enhancing proliferation, attenuating apoptosis and modulating immune reactivity. Biomaterials 156, 16–27.
Zhong, L., Huang, X., Rodrigues, E.D., et al., 2016. Endogenous DKK1 and FRZB regulate Chondrogenesis and hypertrophy in three-dimensional cultures of human chondrocytes and human Mesenchymal stem cells. Stem Cells Dev. 25, 1808–1817.
Zhu, Y., Wang, Y., Zhao, B., et al., 2017. Comparison of exosomes secreted by induced pluripotent stem cell-derived mesenchymal stem cells and synovial membrane-derived mesenchymal stem cells for the treatment of osteoarthritis. Stem Cell Res Ther 8, 64.

biomolecules

MDPI

Article

Quantitative Lipidomic Analysis of Osteosarcoma Cell-Derived Products by UHPLC-MS/MS

Sara Casati [1,*,†], Chiara Giannasi [2], Mauro Minoli [1], Stefania Niada [2], Alessandro Ravelli [1], Ilaria Angeli [1], Veronica Mergenthaler [1], Roberta Ottria [3], Pierangela Ciuffreda [3], Marica Orioli [1] and Anna T. Brini [1,2]

1 Dipartimento di Scienze Biomediche, Chirurgiche ed Odontoiatriche, Università degli studi di Milano, 20133 Milan, Italy; mauro.minoli@unimi.it (M.M.); alessandro.ravelli@unimi.it (A.R.); ilaria.angeli@unimi.it (I.A.); veronica.mergenthaler@gmail.com (V.M.); marica.orioli@unimi.it (M.O.); anna.brini@unimi.it (A.T.B.)

2 IRCCS Istituto Ortopedico Galeazzi, 20161 Milan, Italy; chiara.giannasi@grupposandonato.it (C.G.); stefania.niada@grupposandonato.it (S.N.)

3 Dipartimento di Scienze Biomediche e Cliniche "L.Sacco", Università degli studi di Milano, 20157 Milan, Italy; roberta.ottria@unimi.it (R.O.); pierangela.ciuffreda@unimi.it (P.C.)

* Correspondence: sara.casati@unimi.it

† PhD Student in Experimental Medicine, Università degli studi di Milano, 20129 Milan, Italy.

Received: 23 July 2020; Accepted: 6 September 2020; Published: 9 September 2020

Abstract: Changes in lipid metabolism are involved in several pathological conditions, such as cancer. Among lipids, eicosanoids are potent inflammatory mediators, synthesized from polyunsaturated fatty acids (PUFAs), which coexist with other lipid-derived ones, including endocannabinoids (ECs) and *N*-acylethanolamides (NAEs). In this work, a bioanalytical assay for 12 PUFAs/eicosanoids and 20 ECs/NAEs in cell culture medium and human biofluids was validated over a linear range of 0.1–2.5 ng/mL. A fast pretreatment method consisting of protein precipitation with acetonitrile followed by a double step liquid–liquid extraction was developed. The final extracts were injected onto a Kinetex ultra-high-performance liquid chromatography (UHPLC) XB-C18 column with a gradient elution of 0.1% formic acid in water and methanol/acetonitrile (5:1; *v*/*v*) mobile phase. Chromatographic separation was followed by detection with a triple-quadrupole mass spectrometer operating both in positive and negative ion-mode. A full validation was carried out in a small amount of cell culture medium and then applied to osteosarcoma cell-derived products. To the best of our knowledge, this is the first lipid profiling of bone tumor cell lines (SaOS-2 and MG-63) and their secretome. Our method was also partially validated in other biological matrices, such as serum and urine, ensuring its broad applicability as a powerful tool for lipidomic translational research.

Keywords: polyunsaturated fatty acids (PUFAs); eicosanoids; endocannabinoids; *N*-acylethanolamides; lipidomics; mass spectrometry; osteosarcoma

1. Introduction

1.1. Bioactive Lipids

Bioactive lipids comprise a variety of molecules, whose biosynthesis and activity are responsible for several cell functions, including cell membrane integrity, energy storage, and lipid signaling, by exchanges within and outside the cell [1,2]. The biosynthesis of many lipids depends on the presence of their precursors, and changes in lipid metabolism are involved both in physiological processes and in pathological conditions, such as inflammation, immune system diseases, and cancer [1–5]. Moreover, lipid moieties are necessary for the generation of lipid messengers, such as arachidonic

acid (AA)-derived eicosanoids, endocannabinoids (ECs), and long-chain fatty acid derivatives such as *N*-acylethanolamides (NAEs), which modulate important cellular processes, such as proliferation, apoptosis, and inflammation. Among these, eicosanoids are potent lipid inflammatory mediators, synthesized from polyunsaturated fatty acids (PUFAs) via cyclooxygenase (COX), lipoxygenase (LOX), and cytochrome P450. Prostaglandins, the first identified eicosanoids, are synthesized from AA by both COX-1 and 2. Cyclooxygenase-1 is constitutively expressed in almost all tissues, whereas COX-2 expression is mainly correlated to acute inflammation [6]. Prostaglandins (PGs) are pro-inflammatory molecules that promote the early stages of acute inflammation and are also implicated in the initiation and propagation of cancer [1,7]. Another component of the eicosanoids family is thromboxane, responsible for platelet aggregation and vascular smooth muscle contraction [8]. Alternatively, free AA may be metabolized by LOXs yielding leukotrienes, lipoxins, hepoxilins, and hydroxyeicosatetraenoic acids [9–11]. Moreover, PUFAs and eicosanoids exist in a dynamic balance with other different lipid-derived mediators, including ECs and NAEs [12,13]. Endocannabinoids are a family of lipid mediators obtained from long-chain PUFAs linked to amides, esters, or ethers able to modulate physiological responses through interaction with the endogenous cannabinoid system (ECS) [14]. The ECS is composed of lipid-derived ECs, their G-protein-coupled receptors (CB1 and CB2), and the enzymes responsible for their synthesis, transport, and metabolism [15]. The most common ECs, *N*-arachidonoylethanolamine (AEA) [16] and 2-arachidonoylglycerol (2AG) [17,18], are two AA-derivatives belonging to the large families of *N*-acylethanolamines and 2-monoacylglycerols, respectively. Since AEA and 2AG are both derivatives of AA, there is an intimate interrelationship between the EC and eicosanoid signaling systems. Other ECs have been identified, including *O*-arachidonoylethanolamine and *N*-arachidonoyldopamine (ADA), which are derived from non-oxidative metabolism of arachidonic acid [14]. Endogenous lipoamino acid analogs of AEA, including glycine (AGly), alanine, and serine (ASer) have been identified in mammals [19]. Moreover, ethanolamides and amino acids derivatives of long-chain saturated or polyunsaturated fatty acids, such as *N*-palmitoylethanolamide (PEA) and *N*-oleylethanolamide (OEA), belonging to the NAEs family, have been demonstrated to interact with the ECS components, leading to entourage effects [20,21]. Endogenous cannabinoid system ligands mediate most of the biological effects through their interactions with CB1 and CB2 receptors expressed in the central nervous system and on immune and peripheral cells [22]. Nevertheless, the ECs and NAEs interact not only with CB receptors but also with the deorphanized GPR55 receptors, transient receptor potential vanilloid 1 channel, and peroxisome proliferator-activated nuclear receptors that modulate anti-inflammatory and analgesic effects [23]. The deregulation of the ECs activity and the consequent alteration of the levels of the endogenous ECs and NAEs in different biological fluids have been associated to various pathological conditions [24,25], such as inflammation and pain perception [26]. It is clear that an altered qualitative or quantitative lipid profile, including PUFAs, eicosanoids, ECs, and NAEs, might be associated to pathological conditions and contribute to the outcome and progression of different pathologies. Therefore, a thorough understanding of the mechanisms underlying the action of PUFAs/eicosanoids and ECs/NAEs in bio-matrices requires a sensitive analytical method for an accurate identification and quantification of these molecules.

1.2. Lipid Analysis Features

Lipid analysis is challenging because of the very low concentrations in biological fluids and tissues (picograms to nanograms per milliliter or milligram), in vitro metabolism, and autoxidation. For the extraction of PUFAs/eicosanoids and ECs/NAEs from bio-matrices, an optimized solvent combination is necessary to cover the whole polarity and pKa ranges of these metabolites, including the polar prostaglandins and the less polar PUFAs. Several protocols for the extraction and the subsequent analysis of ECs and NAEs, mainly AEA and 2AG, or PUFAs and eicosanoids in various bio-matrices have been published [27–29]. The majority of liquid–liquid extraction (LLE) protocols according to Bligh and Dyer or Folch [30,31], are limited by the distribution of analytes in both water and chloroform

layers. However, application of ternary solvent combinations including polar as well as nonpolar solvents seems to be a way to overcome these problems [28,29,32]. Moreover, the last step in sample preparation is often manual desalting by solid-phase extraction (SPE) [33,34]. Special requirements for lipid analysis in bio-matrices also include the preliminary deproteinization and pre-/post-extraction at reproducible temperature conditions. Finally, the limited amount of sample available from in vitro and preclinical studies should be taken into consideration since it may not be possible to perform multiple analyses.

1.3. Aim of the Work

In this case, we proposed a double LLE step from a single sample in different mixtures of organic solvents to cover a broad polarity range. The aim of the present work was to develop and validate fast and sensitive quantitative ultra-high-performance liquid chromatography-tandem mass spectrometry (UHPLC-MS/MS) methods using a simple LLE protocol for a simultaneous investigation of PUFAs, eicosanoids, and ECs and NAEs from small amounts of different bio-matrices. This new method, besides allowing a deep and quantitative lipid profiling of the four major lipid signaling families, has been validated in a wide range of different biological matrices, such as cell lysates, extracellular vesicles (EVs), conditioned medium (CM), urine, and serum. The validation of the method in very small amounts of these matrices ensures its applicability to a large number of different studies, leading to a powerful tool for lipidomic translational research.

1.4. Osteosarcoma-Derived Lipids

There is increasing evidence that the majority of ECS ligands exert significant effects on tumor cell growth, motility, spread, and metastasis rate [35–38]. In particular, in this work, we assess the lipid quantitative profile in osteosarcoma (OS)-derived samples. It has been demonstrated that the ECS influence bone cell activity and bone remodeling in physiological and pathological conditions such as cancer [39,40]. The most frequent primary cancers affecting skeletal system are osteosarcoma (OS) and chondrosarcoma [41]. In particular, OS is the most common malignant tumor of bone in children and young adults, exhibiting high invasion and metastasis rate [42]. It is well known that cancer cells may communicate via the release of soluble factors or EVs that are enriched not only in protein and nucleic acids but also in lipids. Several studies show a direct connection between tumor progression and inflammatory status [43,44]. Therefore, elucidating the lipidomic profile, in OS cells, OS-derived EVs, and secretome, might improve our understanding about OS biology. The OS-derived samples (cell lysates, CM, and EVs) were collected from Saos-2 and MG-63 cell lines, and a partial elucidation of their lipid composition was obtained. These results represent the first step in the challenging final aim of investigating the role of lipid signaling molecules in the crosstalk between OS and the surrounding microenvironment.

2. Material and Methods

2.1. Chemicals

Ultrapure water, acetonitrile, dichloromethane, isopropanol, methanol, ethyl acetate, n-exane, and hydrochloride acid were of analytical grade and purchased from Carlo Erba (Milan, Italy). Formic acid (98–100%) was purchased from Sigma–Aldrich (Milan, Italy). The reference materials *N*-arachidonoylethanolamide (AEA), *N*-linolenoylethanolamide (LNEA), *N*-linoleoylethanolamide (LEA), *N*-oleoylethanolamide (OEA), *N*-palmitoylethanolammide (PEA), *N*-stearoylethanolamide (SEA), and *N*-stearoylethanolamide-d4 (SEA-d4) were synthesized and completely characterized in our laboratories, as previously described [45,46]. The reference materials *N*-docosahexaenoylethanolamide (DHEA), *N*-eicosapentaenoylethanolamide (EPEA), *N*-arachidonoyldopamine (ADA), *N*-oleoyldopamine (ODA), *N*-arachidonoylglycine (AGly), *N*-oleoylglycine (OGly), *N*-palmitoylglicine (PalGly), *N*-arachidonoylserine (ASer), *N*-arachidonoylserotonine (A5HT), *N*-oleoylserotonine (O5HT),

N-palmitoylserotonine (Pal5HT), 2-arachidonoylglycerylether (2AGE), 2-arachidonoyglycerol (2AG), *N*-arachidonoyl-3-hydroxy-γ-aminobutyric acid (AGABA), arachidonoyl acid (AA), eicosapentaenoyl acid (EPA), docosahexaenoic acid (DHA), thromboxane-B_2 (TXB_2), prostaglandin-$F_{2\alpha}$ ($PGF_{2\alpha}$), 6α-keto-prostaglandin-F1α (6α-keto-$PGF_{1\alpha}$), prostaglandin-E_2 (PGE_2), prostaglandin-D_2 (PGD_2), leukotriene-B4 (LTB_4), 5-hydroxyeicosatetraenoic acid (5(*S*)-HETE), 15-hydroxyeicosatetraenoic acid (15(*S*)-HETE), and (±)14(15)-epoxyeicosatrienoic acid (14,15-EET), and internal standards *N*-arachidonoylethanolamide-d8 (AEA-d8), *N*-oleoylethanolamide-d2 (OEA-d2), *N*-palmitoylethanolammide-d5 (PEA-d5), *N*-eicosapentaenoylethanolamide-d4 (EPEA-d4), *N*-arachidonoyldopamine-d8 (ADA-d8), *N*-arachidonoylglycine-d8 (AGly-d8), *N*-arachidonoylserine-d8 (ASer-d8), *N*-oleoylserotonine-d17 (O5HT-d17), eicosapentaenoyl acid-d5 (EPA-d5), thromboxane-B_2-d4 (TXB_2-d4), prostaglandin-$F_{2\alpha}$-d4 ($PGF_{2\alpha}$-d4), and leukotriene-B_4-d4 (LTB_4-d4) were purchased from Cayman Chemical (Ann Arbor, MI, USA).

2.2. Cell Cultures

The Saos-2 and MG-63 cell lines (ATCC, Rockville, MD, USA) were plated in tissue culture vessels (Corning, New York, NY, USA) at a density of 5×10^3 cells/cm^2 in complete culture medium [47]: Dulbecco's Modified Eagle Medium (DMEM, Euroclone, Milan, Italy) supplemented with 10% fetal bovine serum (Euroclone), penicillin 50 U/mL, 50 μg/mL streptomycin (Sigma Aldrich, Milan, Italy), and 2 mM L-glutamine (L-Glu, Euroclone). Cultures were maintained at 37 °C in a humidified atmosphere, containing 5% CO_2. After 48 h culture, non-adherent cells were removed, and the medium replaced. At 70–80% confluence, the cells were detached with 0.5% trypsin/0.2% ethylenediaminetetraacetic acid (EDTA, Sigma Aldrich) and expanded.

2.3. Sample Collection

2.3.1. Cell Samples

Once at 80–90% confluence, cells were washed twice with phosphate buffered saline (PBS, composed of NaCl 137 mM, KCl 2.7 mM, $Na_2HPO_4 \times 2H_2O$ 8.1 mM, KH_2PO_4 1.7 mM-pH 7.4) and kept for 1 h in starving medium (SM) (phenol red-free DMEM supplemented with 2 mM L-glutamine, 50 U/mL penicillin, 50 μg/mL streptomycin without fetal bovine serum) for additional washing. Medium was replaced by fresh SM and cells were starved for 72 h.

Concentrated Conditioned Media (CM)

Conditioned media were collected from approximately 6×10^6 cells in starving conditions, centrifuged for 15 min at 2500× *g*, at 4 °C to remove debris and large apoptotic bodies, and concentrated through Amicon Ultra-15 Centrifugal Filter Devices with 3 kDa cut-off (Merck Millipore, Milan, Italy) for 90 min at 4000× *g*, 4 °C [48]. The final product was concentrated about 40–50 folds. The purified solution was analyzed for protein-anchored lipids or lipids enclosed in macromolecular components.

Extracellular Vesicles (EVs)

Extracellular vesicles were isolated from cell-conditioned medium using differential centrifugation, as previously described [49,50]. In brief, after 72 h of starvation, the conditioned medium from approximately 15×10^6 cells was centrifuged for 15 min at 2500× *g*, 4 °C, and then ultra-centrifuged for 70 min at 100,000× *g* (L7–65; Rotor 55.2 Ti; Beckman Coulter, Brea, CA, USA) at 4 °C. Pellet was resuspended in sterile PBS and ultra-centrifuged again under the same conditions. The resulting EV pellet was kept at −20 °C for mass spectrometry analysis.

Cells Pellets

After 72 h of starvation, cells were harvested with 0.5% trypsin/0.2% EDTA and centrifuged for 4 min at 350× *g*. Cell pellets (approximately 1×10^6 cells) obtained by this first centrifugation were washed twice with sterile PBS and stored at −20 °C until use.

2.3.2. Serum and Urine Samples

Control human serum samples used for purification and extraction studies and for validation experiments were obtained from healthy volunteers, which gave informed consent to offer their biological samples for research intent. Blood samples were collected in Vacuette® 6 mL non-gel serum separator tubes and aliquots of 1–2 mL serum were stored at −20 °C. Human urine specimens, obtained from volunteer colleagues, were collected after a circadian cycle and aliquots of 1–2 mL were stored at −20 °C until analysis.

2.4. Standard Solutions, Calibrators, and Quality Control (QC) Samples

Stock solutions of reference materials and internal standards (ISs) were prepared at the final concentration of 10 µg/mL by appropriate dilution with acetonitrile (ACN) under a stream of nitrogen. All solutions were stored in the dark at −20 °C. Working solutions were prepared in ACN from stock solutions and used for the preparation of calibration curves and quality QC samples at 100 ng/mL, except for AA, DHA, EPA, and EPA-d5 (1 µg/mL).

2.4.1. Cell Samples

Calibration standards (CS) containing 0, 0.1, 0.25, 0.5, 1.25, 2.5, and 5 ng/mL for all compounds, 0, 1, 2.5, 5, 12.5, and 25 ng/mL for AA, DHA, and EPA, 1 ng/mL for ISs, and 10 ng/mL for EPA-d5 were prepared daily for each analytical batch by adding suitable amounts of working solutions to 500 µL of SM. Quality control samples were prepared in SM at three different concentration levels (low, intermediate, and high).

2.4.2. Serum and Urine Samples

Calibrators and QC samples were prepared by adding ISs at the same concentration levels (see Section 2.4.1) to 500 µL of PBS, serum, and urine. Pooled serum and urine CS and QC used for validation experiments were prepared combining 20 and five different samples, respectively.

2.5. Sample Preparation

Extracellular vesicles and cell pellets, stored at −20 °C, were resuspended in 500 µL of SM and strongly vortexed three times for 1 min. Prior to extraction, 10 µL ISs and 1 mL of ice-cold ACN were added to 500 µL CM (as well as for serum and urine), EVs, and cell suspensions, and centrifuged for 10 min at 350× *g* at 4 °C. The clear supernatant was then transferred into glass test tubes and extracted with 4 mL of dichloromethane/isopropanol (8:2; *v*/*v*). After centrifugation at 350 g for 10 min, the organic layer was separated and dried under a stream of nitrogen. The dried residue was reconstituted with 60 µL methanol and a 3 µL aliquot was injected into the UHPLC-MS/MS system for ECs and NAEs analysis. The remaining aqueous solution was used for PUFAs and eicosanoids extraction, by adding 500 µL hydrochloride acid (HCl, 0.125 N) and 4 mL ethyl acetate/*n*-hexane (9:1; *v*/*v*). The organic phase was dried, and the residue was reconstituted with 60 µL ACN. A 30 µL aliquot of methanol obtained from the neutral extraction and a 30 µL aliquot from acid extraction were merged and transferred into an autosampler vial. A 10 µL aliquot was injected into the UHPLC/MS-MS system for PUFAs and eicosanoids determination (Figure 1).

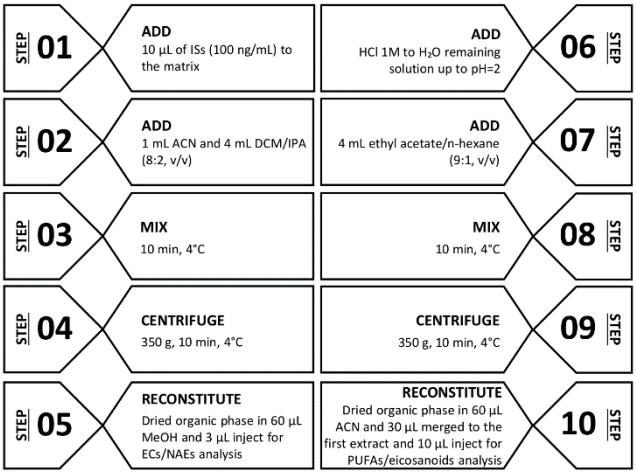

Figure 1. Diagram of the LLE procedure for ECs/NAEs (step 1–5) and PUFAs/eicosanoids (step 6–10). Abbreviations: internal standards (ISs), acetonitrile (ACN), dichloromethane/isopropanol (DCM/IPA), methanol (MeOH), endocannabinoids (ECs), *N*-acylethanolamides (NAEs), polyunsaturated fatty acids (PUFAs).

2.6. Equipment

Analyses were performed on a 1290 Infinity UHPLC system (Agilent Technologies, Palo Alto, CA, USA) coupled to a Q Trap 5500 triple quadrupole linear ion trap mass spectrometer (Sciex, Darmstadt, Germany), equipped with an electrospray (ESI) source. Compounds were separated on a Kinetex UHPLC XB-C18 column (100 × 2.1 mm i.d, 2.6 p.s.) (Phenomenex, Torrance, CA, USA) using 0.1% formic acid in water (mobile phase A) and methanol/acetonitrile (5:1; *v*/*v*) (mobile phase B). For ECs and NAEs analysis, solvent A and B were 75% and 25% at 1.00 min, respectively. Solvent B was increased to 70% from 1.00 to 1.50 min, then increased to 85% from 1.50 to 6.00 min, and to 100% from 6.00 to 7.00, held at 100% from 7.00 to 9.00 min, and then decreased back to 25% from 9.00 to 9.20 min and held at 25% from 9.20 to 11.0 min for re-equilibration. For PUFAs and eicosanoids analysis, solvent A and B were 75% and 25% at 1.00 min, respectively. Solvent B was increased to 40% from 1.00 to 3.00 min, then ncreased to 95% from 3.00 to 5.50 min and to 100% from 5.50 to 7.00, held at 100% from 7.00 to 8.00 min, and then decreased back to 25% from 8.00 to 8.20 min and held at 25% from 8.20 to 10.0 min for re-equilibration. The flow rate was 0.60 mL/min and the column thermostatic oven was kept at 40 °C. The working conditions and parameters of the MS were optimized by direct infusion (flow rate 7 µL/min) of a standard mix solution (100 ng/mL) as follows: the ion source was ESI-operated in positive mode for the ECs/NAEs and in negative mode for PUFAs/eicosanoids analysis, resolution of Q1 and Q3 was 0.7 ± 0.1 amu (atomic mass unit), the curtain gas, ion gas 1, and ion source gas 2 were set at 25, 45, and 40 psi (pound per square inch) respectively, the source temperature was 550 °C, the ionization voltage was 5500 eV (positive mode) and −4500 eV (negative mode), the entrance potential was 10 eV, and dwell time was fixed 70 ms for each multiple reaction monitoring (MRM) transition. The MRM conditions and parameters including ion transitions, de-clustering potential (DP), and relative collision energy (CE) are provided in Table 1. In detail, the following product ions were applied:

- AEA, LNEA, LEA, PEA, OEA, SEA → *m*/*z* 62 relative to the protonated ethanolamine moiety.
- 2AG → *m*/*z* 287 relative to glycerol neutral loss.
- ODA, ADA → *m*/*z* 154 relative to the protonated dopamine moiety.
- A5HT, O5HT, Pal5HT → *m*/*z* 160 relative to the protonated dehydroxy-5HT moiety.
- ASer → *m*/*z* 106 relative to the protonated serine moiety.
- AGly, OGly, PalGly → *m*/*z* 76 relative to the protonated glycine moiety.

Table 1. Multiple reaction monitoring (MRM) parameters: precursor and product ion transitions (quantifier underlined) for all the analytes and internal standards (ISs), de-clustering potential (DP), and collision energy (CE).

Compound	Precursor Ion (*m*/*z*)	Product Ions (*m*/*z*)	DP (eV)	CE (eV)
AA (20:4)	303.1	59.1	−45	−42
		259.6	−45	−20
EPA (20:5)	301.4	59.1	−55	−42
		203.1	−55	−20
DHA (22:6)	327.3	283.3	−80	−10
		59.1	−80	−35
TXB_2	369	177	−50	−22
		195	−50	−20
PGE_2	351.5	315	−50	−25
		271.1	−50	−25
PGD_2	351.5	271	−50	−30
		189	−50	−30
$PGF_{2\alpha}$	353	291	−50	−35
		193	−50	−35
6αKeto-$PGF_{1\alpha}$	369.5	245	−50	−35
		163	−50	−35
LTB_4	335	273	−45	−23
		195	−45	−23
5(S)-HETE	319.5	115	−50	−18
		301.1	−50	−18
15(S)-HETE	319.5	219	−50	−15
		301.2	−50	−15
14,15-EET	319.,5	219.1	−50	−22
		301	−50	−40
AEA	348	62	76	42
		133	76	33
2AG	379.4	287.3	76	18
		203	76	25
LNEA	322.3	62.2	85	35
		81.2	85	35
LEA	324.3	62.2	85	35
		109	85	32
PEA	300.1	62	98	19
		283	98	36
OEA	326.3	62.2	85	35
		309	85	21
SEA	328.3	62.2	85	35
		311.1	85	22

Table 1. *Cont.*

Compound	Precursor Ion (*m*/*z*)	Product Ions (*m*/*z*)	DP (eV)	CE (eV)
DHEA	372.3	62	85	18
		67	85	36
AGly	362.3	287	85	18
		76	85	18
ADA	440.5	137	95	34
		154	95	23
2AGE	365.3	273	85	10
		121	85	20
ODA	418.3	137	85	24
		154	85	35
EPEA	346.3	62	85	35
		135	85	35
ASer	392.5	106	85	35
		137.3	85	33
OGly	340.5	76	85	35
		265	85	35
PalGly	314.5	76	85	35
		239	85	20
AGABA	406.5	287.4	85	24
		84.1	85	55
A5HT	463.3	160.4	85	35
		132.2	85	35
O5HT	441.7	160.4	85	35
		132.2	85	35
Pal5HT	415.7	160.4	130	47
		132.2	130	47
TXB_2-d4	373	199	−50	−22
		173	−50	−22
PGF_{2a}-d4	357	295	−50	−35
		197	−50	−35
LTB_4-d4	339	197	−45	−23
		277	−45	−23
EPA-d5	306.3	59.1	−50	−35
		208.1	−50	−18
AEA-d8	356.3	62	76	35
		70	76	35
SEA-d4	332.3	66.2	85	35
		62	85	18
EPEA-d4	350.3	66	85	35
		135	85	35

Table 1. *Cont.*

Compound	Precursor Ion (*m*/*z*)	Product Ions (*m*/*z*)	DP (eV)	CE (eV)
OEA-d2	328.3	62	85	35
		311	85	35
PEA-d5	305.1	62	85	35
		288	85	35
ADA-d8	448.5	137	85	35
		154	85	35
AGly-d8	370.6	76	85	20
		84	85	20
ASer-d8	400.6	106	85	35
		70	85	35
O5HT-d17	458.7	160.4	130	47
		132.2	130	47

Abbreviations: arachidonoyl acid (AA), eicosapentaenoyl acid (EPA), docosahexaenoic acid (DHA), thromboxane-B2 (TXB2), prostaglandin-F2α (PGF2α), 6α-keto-prostaglandin-F1α (6α-keto-PGF1α), prostaglandin-E2 (PGE2), prostaglandin-D2 (PGD2), leukotriene-B4 (LTB4), 5-hydroxyeicosatetraenoic acid (5(*S*)-HETE), 15-hydroxyeicosatetraenoic acid (15(*S*)-HETE), (±)14(15)-epoxyeicosatrienoic acid (14,15-EET), arachidonoylethanolamide (AEA), *N*-linolenoylethanolamide (LNEA), *N*-linoleoylethanolamide (LEA), *N*-oleoylethanolamide (OEA), *N*-palmitoylethanolammide (PEA), *N*-stearoylethanolamide (SEA), *N*-docosahexaenoylethanolamide (DHEA), *N*-eicosapentaenoylethanolamide (EPEA), *N*-arachidonoyldopamine (ADA), *N*-oleoyldopamine (ODA), *N*-arachidonoylglycine (AGly), *N*-oleoylglycine (OGly), *N*-palmitoylglicine (PalGly), *N*-arachidonoylserine (ASer), N-arachidonoylserotonine (A5HT), N-oleoylserotonine (O5HT), *N*-palmitoylserotonine (Pal5HT), 2-arachidonoylglycerylether (2AGE), 2-arachidonoyglycerol (2AG), *N*-arachidonoyl-3-hydroxy-γ-aminobutyric acid (AGABA), eicosapentaenoyl acid-d5 (EPA-d5), thromboxane-B2-d4 (TXB2-d4), prostaglandin-F2α-d4 (PGF2α-d4), and leukotriene-B4-d4 (LTB4-d4), *N*-arachidonoylethanolamide-d8 (AEA-d8), *N*-oleoylethanolamide-d2 (OEA-d2), *N*-palmitoylethanolammide-d5 (PEA-d5), *N*-stearoylethanolamide-d4 (SEA-d4), *N*-eicosapentaenoylethanolamide-d4 (EPEA-d4), *N*-arachidonoyldopamine-d8 (ADA-d8), *N*-arachidonoylglycine-d8 (AGly-d8), *N*-arachidonoylserine-d8 (ASer-d8), *N*-oleoylserotonine-d17 (O5HT-d17).

2.7. Data Evaluation

Data acquisition and processing were performed using Analyst®1.6.2 and MultiQuant®2.1.1 software (Sciex, Darmstadt, Germany), respectively. Calculations for validation assessment, which includes linearity, precision, accuracy, sensibility, recovery, and stability, were performed using Microsoft Office Excel 2013.

2.8. Validation Procedure

Assay validation was carried out in accordance with the recommendations endorsed by Food and Drugs Administration (FDA) guidelines referring to drugs and non-endogenous compounds [51], and specific issues for endogenous compounds [52] were addressed. A full validation was performed in the analyte-free SM and the following parameters were assessed: linearity, precision and accuracy, sensitivity in terms of limits of detection (LODs) and limits of quantitation (LOQs), specificity, recovery, matrix effect, and stability. Additionally, the described method was partially validated in serum and urine. Surrogate analyte-free matrix (i.e., water and/or appropriate buffer) are usually used for the preparation of CS and QC in the method validation of endogenous compounds to overcome the lack of analyte-free matrix [52]. For this reason, to avoid the interference of endogenous analytes, linearity, slope, recovery, and the influence of matrix effect were obtained by spiking serum and urine with ISs at the same concentration levels (see Section 2.4.2), whereas LOD and LOQ evaluation was achieved on PBS.

2.8.1. Calibration Range and Linearity

Calibration standards (n = 6) were obtained by spiking analyte-free SM with appropriate amounts of working solutions in the range 0.1–2.5 and 0.5–25 ng/mL (EPA, AA, and DHA), as described at Section 2.4. A linear model was used to describe the relation between analyte concentration and instrument response (analyte peak area/internal standard peak area). Linearity was considered satisfactory for each curve if $R^2 \geq 0.990$. Additionally, to evaluate linearity and slope, CS were also prepared in the analyte-free PBS, as well as in urine and serum, by spiking ISs at the same concentration levels.

2.8.2. Sensitivity and Specificity

Reagents and consumables were extracted, following the procedures described before, and analyzed in triplicate to evaluate and exclude interferences and false-positive responses derived from sample preparation. The specificity of the method and matrix-to-matrix reproducibility was evaluated by analyzing SM in triplicate from different lots number (n = 3). Sensitivity was expressed in terms of LOD and LOQ as 3.3 and 10 times respectively, the ratio between the standard deviation of the response and the slope of the calibration curve. LOD and LOQ were calculated on calibration curves prepared in the analyte-free SM for cell samples' quantification. Additionally, LOD and LOQ were also tested in the analyte-free PBS in order to quantify serum and urine samples.

2.8.3. Precision and Accuracy

Precision and accuracy of the method were determined through the analysis of six independent replicates of QC materials extracted from the analyte-free SM at three concentration levels (low, intermediate, and high). Precision was denoted by percent coefficient of variation (CV%), while the accuracy was expressed as bias (BIAS%), the percent deviation of the mean determined concentration from the accepted reference value. The accuracy and precision were required to be ≤15% CV (Supplementary Tables S1 and S2).

2.8.4. Recovery and Matrix Effects

Extraction recovery (%) was measured by comparing the peak area of the analyte-free SM (n = 3) fortified with standards at three concentration levels prior to and after extraction. Peak areas of pre- and post-extraction samples were used for calculations, considering as 100% recovery, the analytes area in post-extraction spiked samples. The matrix effects (%) were determined by comparing the analytes peak area in PBS and in the analyte-free SM, fortified in the low, intermediate, and high concentration range after extraction. Concerning the extraction recovery evaluation in human and serum and urine, which are matrices endogenously containing all the analytes, we spiked them with ISs before and after LLE. The matrix effect was assessed by comparing the peak area of ISs spiked in eluate from serum and urine to those in PBS. As for SM, the extraction recovery and matrix effect were evaluated at the three concentration levels.

2.8.5. Stability Studies

Lipids' stability was assessed in QC samples at low, intermediate, and high concentrations, by analyzing them the initial day (T0) as well as 24 h later at 4 and –20 °C. The response factor at each concentration was compared to the original vial at T0, and a mean deviation % below 15% from day 0 was considered acceptable.

2.9. Application to Real Samples

The proposed method was applied to Saos-2- and MG-63-derived CM, EVs, and cell lysates in order to identify and quantify lipids belonging to PUFAs/eicosanoids and ECs/NAEs groups, as described at Section 2.3. Each sample was injected into UHPLC-MS/MS three times (n = 3 analytical replicates).

3. Results and Discussion

3.1. Sample Extraction

Different protocols for the purification and several combinations of solvents over the expected polarity range were examined for the extraction of the considered analytes; however, the highest lipids count was detected through a double-step extraction preparation with dichloromethane/isopropanol (8:2; *v*/*v*) and ethyl acetate/n-hexane (9:1; *v*/*v*), respectively. On the basis of the analytes' lipophilicity, a LLE procedure was developed with water-immiscible solvents in order to isolate both PUFAs/eicosanoids and ECs/NAEs. Despite the fact that in several studies SPE has provided concentrated and free interfering matrix components' extracts [27,33,53,54], this extraction procedure is money- and time-consuming (because of the different steps). Contrarily, LLE is easier, and its shorter extraction time, as opposed to the most commonly used SPE procedures, could be an advantage for studies that involve a huge number of samples. LLEs commonly used to isolate lipids from biological samples require the use of toxic organic solvents. In our applied extraction protocol, a simple and fast pretreatment method consisting of protein exclusion with can, followed by a first extraction with dichloromethane/isopropanol (8:2; *v*/*v*) and a second one with ethyl acetate/n-hexane (9:1; *v*/*v*), both less toxic than other solvents (i.e., toluene, chloroform or tert-methyl-butyl ether), was used. In general, the combination of two or more sample preparation techniques, such as protein precipitation and LLE, improves method selectivity [29,53,54]. Additionally, the second extraction is preceded by a pH adjustment step, which is fundamental since some eicosanoids present a lower pKa value than ECs. In detail, acidification with HCl improves the extraction of the less polar eicosanoids HETEs and EETs. A lower pH leads to a reduced protein binding and the protonation of carboxylate anions, which both allow improved extraction by the organic solvent. Otherwise, greater acidification may lead to eicosanoid alteration [55], and therefore, an extremely low pH should be avoided. The optimized solvent mixture combined with the pH adjustment, which allows the decreased protein binding and the enhanced extraction of the non-ionized forms, was necessary to cover the whole polarity range of these numerous metabolites. Moreover, the two sequential extraction steps from a single sample also allowed the analysis when limited amounts of samples were available.

3.2. Instrumental Parameters

Mass spectrometry parameters were optimized by infusing a standard mix solution containing PUFAs, eicosanoids, ECs, and NAEs at a concentration of 100 ng/mL in methanol, and by acquiring both in the positive and negative ionization mode. Positive ionization mode provided better signal responses for the ECs/NAEs group, whereas for the analysis of PUFAs and eicosanoids, a negative polarization was used. The source/gas parameters were optimized to obtain the highest ion abundance of the peaks. CE and DP were varied from 0 to ±60 eV and 0 to ±150 eV respectively, in order to obtain the best response for the product ions used for quantitative MRM analysis. Precursors and product ions, CE and DP, shown in Table 1, were selected for analytes' quantification. Several reversed phase columns, mobile phases, and elution gradients have been assessed in order to improve the responses of the target compounds belonging to EC/NAE and PUFA/eicosanoid classes and to reduce the time of the analysis. Two different elution gradients performed on a Kinetex UHPLC XB-C18 column using 0.1% formic acid in water and methanol/acetonitrile (5:1; *v*/*v*), characterized by a total runtime of 11.0 min each comprising cleaning and reconditioning of the column, exhibited the best analytes' sensitivity and peak shape. These instrumental conditions allowed the consequential analysis of the two classes of interest using both the same elution column and mobile phases.

3.3. Method Validation

Methods specificity was achieved by means of the selection of a precursor ion followed by detection and quantification of product ions. All the reagents and consumables used for the methods set-up and development have been shown not to interfere with the detection or quantification of the analytes. False-positive response or co-eluting components were not detected in analyzed bio-matrices.

3.3.1. Calibration Range and Linearity

Standard calibration curves (n = 6) were obtained by fortifying 500 µL aliquots of analyte-free SM with standard solutions, as described at Section 2.4.1. The calibration curves showed excellent linearity ($R^2 > 0.991$) over the following concentration ranges: 0.1–2.5 ng/mL for all the compounds and 1–25 ng/mL for AA, EPA, and DHA. Different calibration ranges for the eicosanoids AA, EPA, and DHA have been chosen in relation to expected higher concentrations in real samples. The R^2 values relative to PUFAs/eicosanoids and ECs/NAEs are reported in Tables 2 and 3, respectively. Linearity was also maintained in all matrices assessed. Calibration curves prepared spiking ISs at the same concentration levels in PBS and in human serum and urine (see Section 2.4.2) were found to be parallel (standard deviation of correlation coefficients <0.0001). For this reason, calibration lines obtained from CS spiked in PBS may be used for PUFAs, eicosanoids, ECs, and NAEs quantification. Specificity tests, performed on all reagents and disposable materials used, have shown no interference with the determination of both PUFAs/eicosanoids and ECs/NAEs by UHPLC-MS/MS. LOD and LOQ values, obtained for the two lipid groups both in the analyte-free SM and PBS, are listed in Tables 2 and 3.

Table 2. Calibration parameters for PUFAs/eicosanoids group.

Compound	R^2	Analytical Range (ng/mL)	LOD (SM) (ng/mL)	LOQ (SM) (ng/mL)	LOD (PBS) (ng/mL)	LOQ (PBS) (ng/mL)
AA (20:4)	1.000	1–25	0.259	0.864	0.014	0.046
EPA (20:5)	1.000	1–25	0.039	0.132	0.007	0.024
DHA (22:6)	0.999	1–25	0.013	0.042	0.022	0.073
TXB_2	0.991	0.1–2.5	0.021	0.070	0.022	0.073
PGE_2	1.000	0.1–2.5	0.018	0.061	0.010	0.035
PGD_2	0.999	0.1–2.5	0.008	0.028	0.031	0.103
$PGF_{2\alpha}$	1.000	0.1–2.5	0.008	0.028	0.018	0.059
6aKeto-$PGF_{1\alpha}$	1.000	0.1–2.5	0.006	0.020	0.014	0.048
LTB_4	0.999	0.1–2.5	0.011	0.037	0.033	0.110
5(S)-HETE	0.998	0.1–2.5	0.031	0.100	0.016	0.053
15(S)-HETE	0.999	0.1–2.5	0.012	0.041	0.021	0.070
14,15-EET	0.999	0.1–2.5	0.002	0.006	0.027	0.090

Abbreviations: arachidonoyl acid (AA), eicosapentaenoyl acid (EPA), docosahexaenoic acid (DHA), thromboxane-B2 (TXB2), prostaglandin-F2α (PGF2α), 6α-keto-prostaglandin-F1α (6α-keto-PGF1α), prostaglandin-E2 (PGE2), prostaglandin-D2 (PGD2), leukotriene-B4 (LTB4), 5-hydroxyeicosatetraenoic acid (5(*S*)-HETE), 15-hydroxyeicosatetraenoic acid (15(*S*)-HETE), (±)14(15)-epoxyeicosatrienoic acid (14,15-EET).

Table 3. Calibration parameters for ECs/NAEs group.

Compound	R^2	Analytical Range (ng/mL)	LOD (SM) (ng/mL)	LOQ (SM) (ng/mL)	LOD (PBS) (ng/mL)	LOQ (PBS) (ng/mL)
AEA	0.9960	0.1–2.5	0.013	0.045	0.027	0.088
2AG	0.9918	0.1–2.5	0.004	0.015	0.027	0.089
2AGE	0.9986	0.1–2.5	0.008	0.026	0.015	0.049
LNEA	0.9965	0.1–2.5	0.033	0.109	0.019	0.064
LEA	0.9916	0.1–2.5	0.030	0.100	0.028	0.094
PEA	0.9954	0.1–2.5	0.030	0.101	0.027	0.090
OEA	0.9998	0.1–2.5	0.020	0.076	0.025	0.084
SEA	0.9999	0.1–2.5	0.005	0.018	0.013	0.045
DHEA	0.9964	0.1–2.5	0.020	0.081	0.028	0.092
EPEA	0.9982	0.1–2.5	0.010	0.033	0.005	0.017
ADA	0.9980	0.1–2.5	0.018	0.059	0.029	0.099
ODA	0.9998	0.1–2.5	0.031	0.106	0.029	0.099
ASer	0.9959	0.1–2.5	0.019	0.064	0.023	0.081
AGly	0.9998	0.1–2.5	0.030	0.101	0.029	0.099
OGly	0.9985	0.1–2.5	0.028	0.094	0.035	0.100
PalGly	0.9999	0.1–2.5	0.006	0.019	0.026	0.099
AGABA	0.9988	0.1–2.5	0.021	0.084	0.017	0.057
A5HT	0.9982	0.1–2.5	0.008	0.028	0.007	0.024
O5HT	0.9942	0.1–2.5	0.002	0.073	0.013	0.043
Pal5HT	0.9980	0.1–2.5	0.007	0.023	0.012	0.042

Abbreviations: arachidonoylethanolamide (AEA), *N*-linolenoylethanolamide (LNEA), *N*-linoleoylethanolamide (LEA), *N*-oleoylethanolamide (OEA), N-palmitoylethanolammide (PEA), *N*-stearoylethanolamide (SEA), *N*-docosahexaenoylethanolamide (DHEA), *N*-eicosapentaenoylethanolamide (EPEA), *N*-arachidonoyldopamine (ADA), *N*-oleoyldopamine (ODA), *N*-arachidonoylglycine (AGly), *N*-oleoylglycine (OGly), *N*-palmitoylglicine (PalGly), *N*-arachidonoylserine (ASer), *N*-arachidonoylserotonine (A5HT), *N*-oleoylserotonine (O5HT), *N*-palmitoylserotonine (Pal5HT), 2-arachidonoylglycerylether (2AGE), 2-arachidonoyglycerol (2AG), *N*-arachidonoyl-3-hydroxy-γ-aminobutyric acid (AGABA).

3.3.2. Precision and Accuracy

Regarding precision and accuracy, the method showed good performance in terms of both repeatability and reproducibility, showing CV values below 15%. The same results were obtained for accuracy studies (BIAS < 15%). Precision and accuracy levels for all the analytes belonging to PUFAs/eicosanoids and ECs/NAEs groups were within acceptable limits, as reported in the Supplementary Tables S1 and S2, respectively. A representative chromatogram of a SM sample spiked at the intermediate concentration level for PUFAs/eicosanoids and ECs/NAEs groups is reported in Figures 2 and 3, respectively.

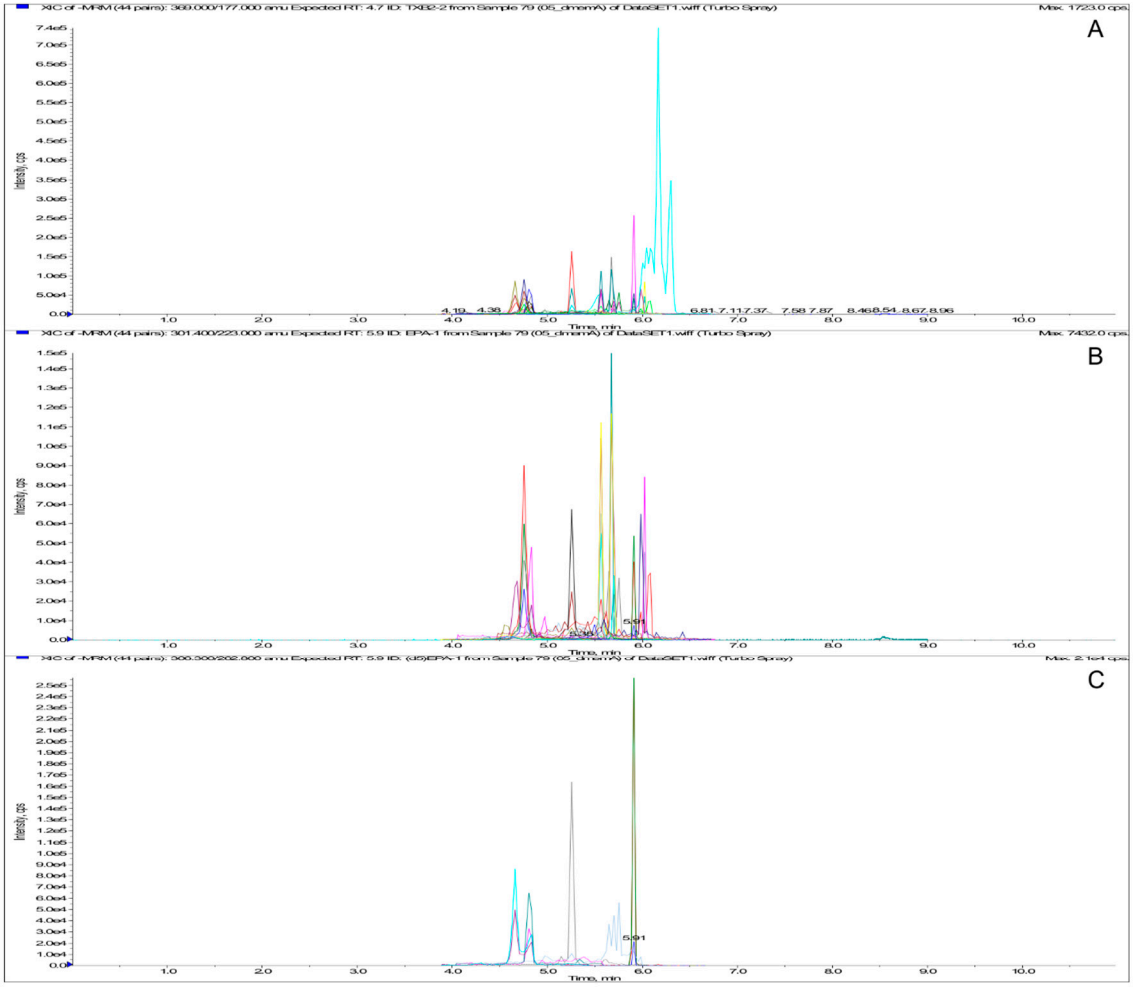

Figure 2. MRM chromatogram of PUFAs/eicosanoids extract. From the top: Total ion Current (**A**), standard extraction (0.5 and 5 ng/mL for AA, EPA, and DHA) (**B**), and ISs extraction (**C**).

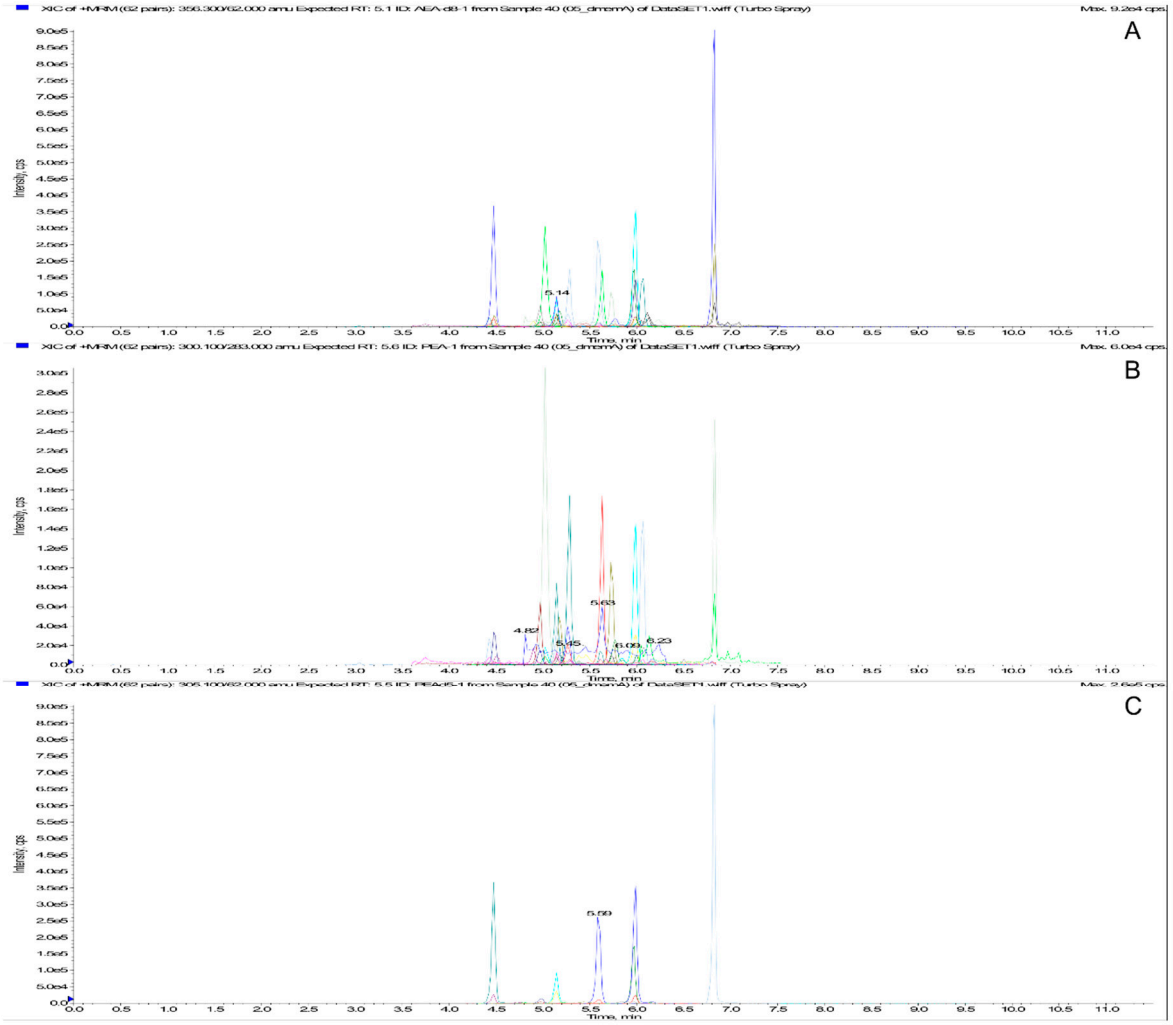

Figure 3. MRM chromatogram of ECs/NAEs extract. From the top: Total ion Current (**A**), standard extraction (0.5 ng/mL) (**B**), and ISs extraction (**C**).

3.3.3. Extraction Recovery and Matrix Effect

The mean extraction recovery in analyte-free SM was satisfactory, being over 41% for all the compounds belonging to the PUFAs/eicosanoids class (Figure 4A) and 52% for the ECs/NAEs class (Figure 4B), except for the basic compounds A5HT, O5HT, and Pal5HT. According to their chemical-physical properties, the 5HT-derivatives are protonated at neutral pH and the passage from aqueous solution to organic solvent is less-favored. Matrix effects ranged from ±20% for both lipids groups, except for PGF2α, 5(S)-HETE, and O5HT (Figure 4C,D). To avoid the interference of serum and urine endogenous analytes on the evaluation of recovery and matrix effect, the peak area of ISs spiked in these eluates was compared to those in the extract and PBS, respectively. Results for PUFAs/eicosanoids and ECs/NAEs are shown in the Supplementary Tables S3 and S4, respectively. All results were within the acceptance criteria, except for the PEA-d5, OEA-d2, and AGly-d8 matrix effect in human serum, whose percentage mean was 59% ± 8%, and TXB_2-d4 in both serum and urine, which was 56% ± 7%.

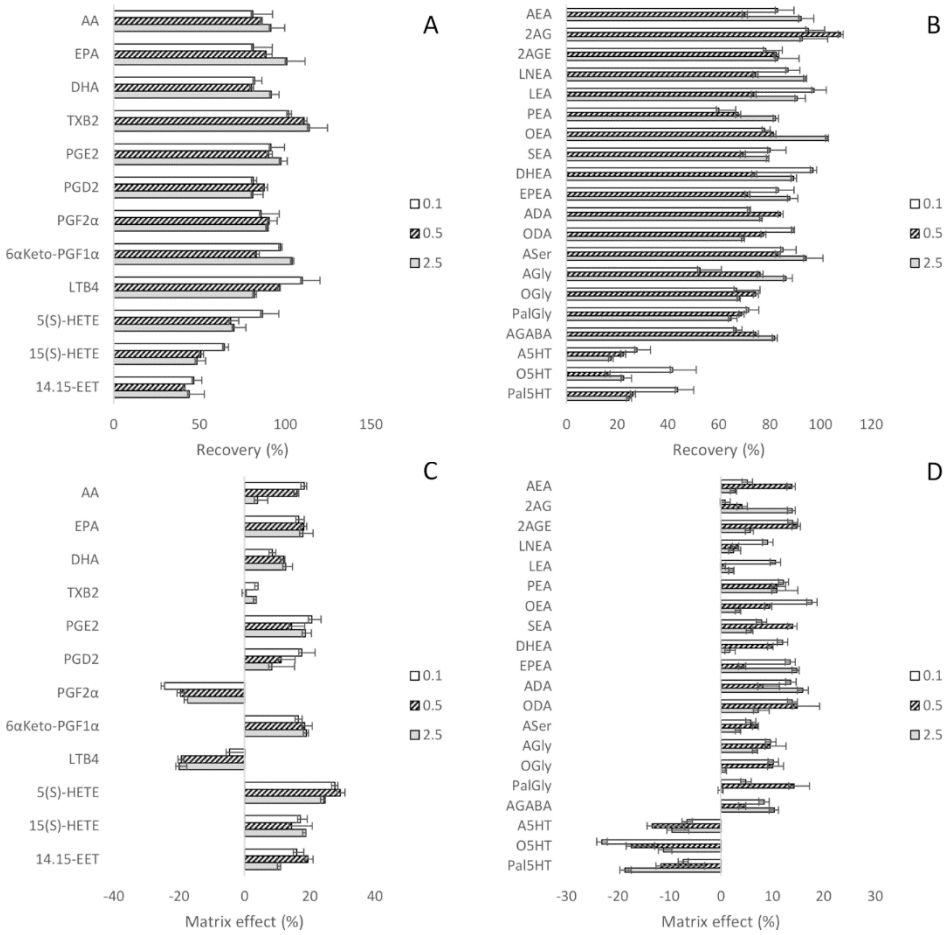

Figure 4. Extraction recovery and matrix effect of PUFAs/eicosanoids (**A**,**C**, respectively) and ECs/NAEs (**B**,**D**, respectively).

3.3.4. Stability Studies

The analytes' concentration in QC samples was not altered when kept at 4 and –20 °C for 24 h, except for PGD_2, 5(S)-HETE,15(S)-HETE, and 14,15-EET, especially at –20 °C (Supplementary Table S5). The response factor did not show unacceptable differences compared with the first determination (mean deviation % from day 0 < 15%).

3.4. Application to Real Samples

The bioanalytical assay was applied to osteosarcoma cell (Saos-2 and MG-63) lysates, EVs, and CM, as described at Section 2.3. By analyzing the CM, only protein-anchored lipids or lipids enclosed in macromolecular components were detectable. The filtered solution, accounting for the free lipid portion, will be analyzed in the near future. Quantitative data regarding the PUFAs/eicosanoids and ECs/NAEs in the six samples are presented in Figures 5 and 6, respectively. Five PUFAs and eicosanoids (AA, EPA, DHA, 5(S)-HETE, and 14,15-EET) and seven ECs/NAEs (2AG, LEA, OEA, SEA, DHEA, PEA, and PalGly) were quantified (>LOQs). PUFAs (AA, DHA, and EPA) (Figure 5A–C) and AA-derived metabolites 5(*S*)-HETE, 14,15-EET, and 2AG (Figure 5A,D,E) were more expressed in Saos-derived samples than in MG-63-derived ones. Surprisingly, almost no PUFA/eicosanoid was detectable in MG-63 samples, except for a small amount of DHA only measured in the cell lysate (Figure 5B). Among ECs, PalGly is the only compound belonging to N-acylglycines, which was found only in Saos-2-derived EVs (Figure 6C). Only three ECs/NAEs (2AG, LEA, and SEA) were quantified in all six analyzed samples (Figure 6C,D,G). LEA, PEA, OEA, and SEA (Figure 6D–G) were found more abundant in MG-63-derived samples, with PEA detectable only in EVs (Figure 6E). Interestingly, 2AG and DHEA

(Figure 6A,B) were more abundant and/or quantified only in Saos-2-derived samples, as well as their related compounds AA and DHA, respectively (Figure 5A,B). Several studies have focused on the differences in growth, gene expression, and immunohistochemical profiles of OS cell lines [56,57], revealing that they possess peculiar characteristics. In particular, Saos-2 cells exhibit a more mature osteoblastic phenotype with a stronger alkaline phosphatase activity and a greater expression of osteoblastic markers (osteocalcin, bone sialoprotein, decorin, and procollagen-I) than MG-63. The latter present both mature and immature osteoblastic features, with only a small subpopulation expressing the typical osteoblastic markers. Here, we provide evidence of several differences in the bioactive lipid profile between these two bone tumor cell lines and their derivatives (both whole secretome and isolated EVs). In this perspective, a recent work by Roy et al. [58] investigated the lipid profile of two OS cell lines (the nonmetastatic HOS (human osteosarcoma) and the metastatic 143B cells). The authors reported interesting differences in the expression of lipids involved in the metastatic process between the two OS cell lines and in tumorigenesis in comparison to normal feline osteoblasts (FOB).

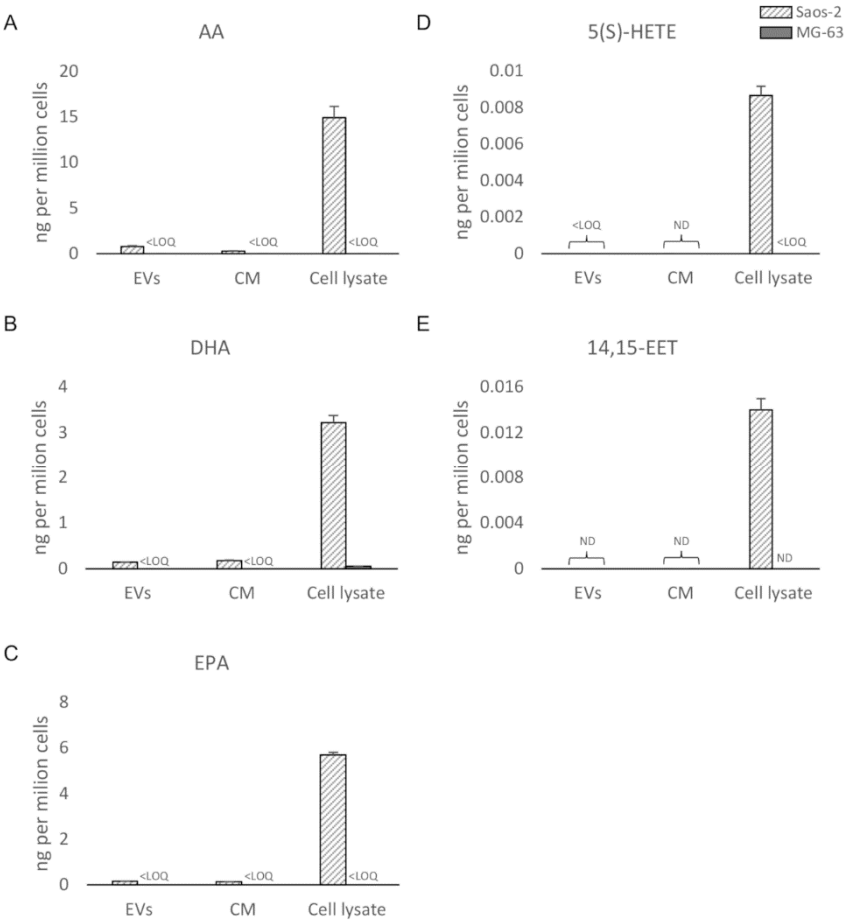

Figure 5. UHPLC-MS/MS quantitation (ND = not detectable; LOQ = limit of quantitation) in EVs, CM, and cell lysate from Saos-2 and MG-63 cell lines of (**A**) arachidonoyl acid (AA); (**B**) Docosahexaenoic acid (DHA); (**C**) eicosapentaenoyl acid (EPA); (**D**) 5-hydroxyeicosatetraenoic acid (5(*S*)-HETE; (**E**) (±)14(15)-epoxyeicosatrienoic acid (14,15-EET).

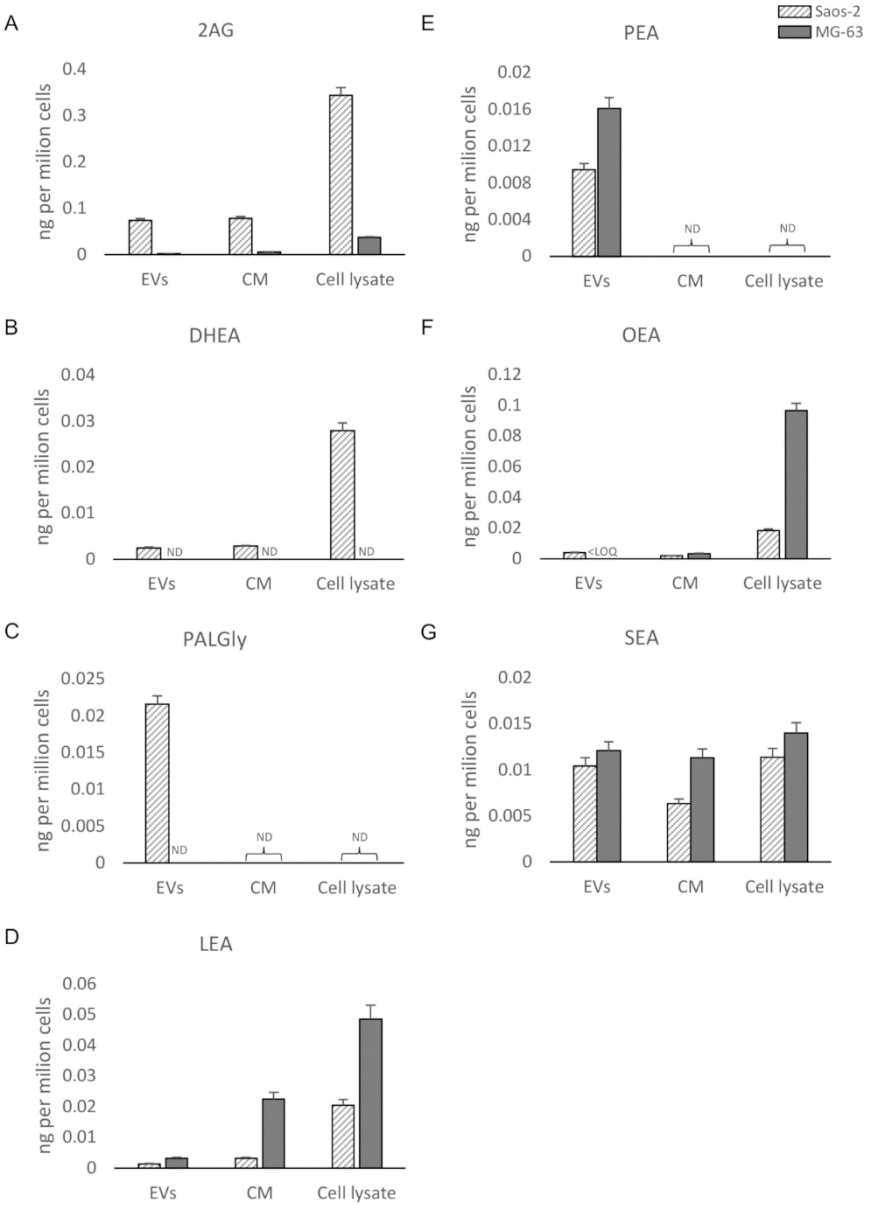

Figure 6. UHPLC-MS/MS quantitation (ND = not detectable; LOQ = limit of quantitation) in EVs, CM, and cell lysate from Saos-2 and MG-63 cell lines of (**A**) 2-arachidonoylglycerol (2AG); (**B**) *N*-docosahexaenoylethanolamide (DHEA); (**C**) *N*-palmitoylglicine (PalGly); (**D**) *N*-linoleoylethanolamide (LEA); (**E**) *N*-palmitoylethanolammide (PEA); (**F**) *N*-oleoylethanolamide (OEA); (**G**) *N*-stearoylethanolamide (SEA).

4. Conclusions

In this work, a bioanalytical assay for 12 PUFAs/eicosanoids and 20 ECs/NAEs in culture medium, human serum, and urine was developed and validated over a linear range of 0.1–2.5 or 1–25 ng/mL (AA, EPA, and DHA). The method was fully validated in cell culture medium and partially in urine and serum. Our double-step LLE protocol was found to be suitable for the simultaneous investigation of PUFA, eicosanoid, ECs, and NAEs content by UHPLC–MS/MS in small amounts of bio-matrices. The protocol allows simultaneous and reproducible analyses of a broad range of chemically different bioactive lipids by a pH adjustment. The proposed protocol for cell lysates, EVs, and CM can be easily adapted to other liquid and/or solid bio-matrices. With the LLE technique, we have achieved a shorter extraction time, if compared to the most common SPE procedure, and this represent a clear advantage for studies that involve a huge number of samples; moreover, the two sequential extraction steps from

a single sample also allow the analysis when limited amounts of samples are available. However, the limitations of the protocol may be the great manual effort and the lack of automation. In more detail, the validated method applied to OS cell lysates, EVs, and CM allowed the quantification of five eicosanoids and seven ECs/NAEs (>LOQs). Eicosanoids and ECs/NAEs are biologically active lipid mediators that play a critical role in different pathological processes, and little is still known about their release in secretome/EVs from OS cell lines. In this work, we investigated the lipid content of Saos-2, MG-63, and their derivatives, providing evidence of a different lipid profile and secretion between the two OS cell lines. This method could be harnessed to investigate other components of OS microenvironment, relevant for the cellular crosstalk among bone tumor cells, normal osteoblasts, and mesenchymal stem/stromal cells, which is actually investigated in our laboratory by a proteomic approach. Moreover, an all-encompassing profiling of the lipids expressed and secreted by OS cells in comparison to normal osteoblasts would provide an insight in the mechanisms of bone tumor development and eventually suggest potential therapeutic targets and/or new biomarkers for the diagnosis and monitoring of this pathology. These data could lay the basis to better elucidate the biological role played by lipid mediators in a pathological context, which will be investigated in the future by in vitro studies.

Supplementary Materials: The following are available online at http://www.mdpi.com/2218-273X/10/9/1302/s1. Table S1: Precision and accuracy parameters for PUFAs/eicosanoids group, Table S2: Precision and accuracy parameters for ECs/NAEs group, Table S3: Extraction recovery and matrix effect of PUFAs/eicosanoids groups in human serum and urine, Table S4: Extraction recovery and matrix effect of ECs/NAEs groups in human serum and urine, Table S5: Stability of QC samples after exposure to 4 °C and – 20°C for 24 h.

Author Contributions: Conceptualization, S.C., C.G., S.N., A.T.B.; methodology, S.C., I.A., M.M., A.R.; software, S.C., M.M.; validation: S.C., M.M., V.M.; formal analysis, S.C., V.M.; resources, M.O., A.T.B., P.C.; data curation, S.C., V.M., C.G.; writing—original draft preparation, S.C.; writing—review, S.C., C.G., S.N., R.O., M.O., A.T.B.; project administration, A.T.B., M.O.; funding acquisition, A.T.B., M.O. All authors have read and agreed to the published version of the manuscript.

Funding: This work was partially supported by the Italian Ministry of Health (RC L1038 of IRCCS Istituto Ortopedico Galeazzi), and the Department of Biomedical, Surgical and Dental Sciences (University of Milan, grant # G44I19000700001).

Acknowledgments: The authors would like to thank Giovanni Lombardi for providing the MG-63 cell line.

Conflicts of Interest: The authors declare that they have no conflict of interest.

References

1. Wang, D.; Dubois, R.N. Eicosanoids and cancer. *Nat. Rev. Cancer* **2010**, *10*, 181–193. [CrossRef] [PubMed]
2. Krishnamoorthy, S.; Honn, K.V. Eicosanoids and other lipid mediators and the tumor hypoxic microenvironment. *Cancer Metastasis Rev.* **2011**, *30*, 613–618. [CrossRef] [PubMed]
3. Rossi, F.; Tortora, C.; Punzo, F.; Bellini, G.; Argenziano, M.; di Paola, A.; Torella, M.; Perrotta, S. The Endocannabinoid/Endovanilloid System in Bone: From Osteoporosis to Osteosarcoma. *Int. J. Mol. Sci.* **2019**, *20*, 1919. [CrossRef] [PubMed]
4. Yan, G.; Li, L.; Zhu, B.; Li, Y. Lipidome in colorectal cancer. *Oncotarget* **2016**, *7*, 33429–33439. [CrossRef]
5. Sulciner, M.L.; Gartung, A.; Gilligan, M.M.; Serhan, C.N.; Panigrahy, D. Targeting lipid mediators in cancer biology. *Cancer Metastasis Rev.* **2018**, *37*, 557–572. [CrossRef]
6. Crofford, L. COX-1 and COX-2 tissue expression: Implications and predictions. *J. Rheumatol. Suppl.* **1997**, *49*, 9.
7. Wang, D.; Dubois, R.N. Prostaglandins and cancer. *Gut* **2006**, *55*, 115–122. [CrossRef]
8. Wang, T.; Falardeau, P.; Powell, W.S. Synthesis of prostaglandins and thromboxane B 2 by cholesterol-fed rabbits. *Arterioscler. Thromb.* **1991**, *11*, 501–508. [CrossRef]
9. Serhan, C.N.; Chiang, N.; Van Dyke, T.E. Resolving inflammation: Dual anti-inflammatory and pro-resolution lipid mediators. *Nat. Rev. Immunol.* **2008**, *8*, 349–361. [CrossRef]
10. Murphy, R.C.; Gijón, M.A. Biosynthesis and metabolism of leukotrienes. *Biochem. J.* **2007**, *405*, 379–395. [CrossRef]
11. Spector, A.A. Arachidonic acid cytochrome P450 epoxygenase pathway. *J. Lipid Res.* **2009**, *50*. [CrossRef] [PubMed]

12. Rouzer, C.A.; Marnett, L.J. Endocannabinoid Oxygenation by Cyclooxygenases, Lipoxygenases, and Cytochromes P450: Cross-Talk between the Eicosanoid and Endocannabinoid Signaling Pathways. *Chem. Rev.* **2011**, *111*, 5899–5921. [CrossRef] [PubMed]
13. Witkamp, R. Fatty acids, endocannabinoids and inflammation. *Eur. J. Pharmacol.* **2016**, *785*, 96–107. [CrossRef] [PubMed]
14. Pertwee, R.G.; Howlett, A.C.; Abood, M.E.; Alexander, S.P.H.; Di Marzo, V.; Elphick, M.R.; Greasley, P.J.; Hansen, H.S.; Kunos, G. Cannabinoid Receptors and Their Ligands: Beyond CB 1 and CB 2. *Pharmacol. Rev.* **2010**, *62*, 588–631. [CrossRef]
15. Di Marzo, V.; Bifulco, M.; De Petrocellis, L. The endocannabinoid system and its therapeutic exploitation. *Nat. Rev. Drug Discov.* **2004**, *3*, 771–784. [CrossRef] [PubMed]
16. Devane, W.A.; Hanuš, L.; Breuer, A.; Pertwee, R.G.; Stevenson, L.A.; Griffin, G.; Gibson, D.; Mandelbaum, A.; Etinger, A.; Mechoulam, R. Isolation and structure of a brain constituent that binds to the cannabinoid receptor. *Science* **1992**, *258*, 1946–1949. [CrossRef]
17. Mechoulam, R.; Ben-Shabat, S.; Hanus, L.; Ligumsky, M.; Kaminski, N.E.; Schatz, A.R.; Gopher, A.; Almog, S.; Martin, B.R.; Compton, D.R.; et al. Identification of an endogenous 2-monoglyceride, present in canine gut, that binds to cannabinoid receptors. *Biochem. Pharmacol.* **1995**, *50*, 83–90. [CrossRef]
18. Sugiura, T.; Kondo, S.; Sukagawa, A.; Nakane, S.; Shinoda, A.; Itoh, K.; Yamashita, A.; Waku, K. 2-arachidonoylglycerol: A possible endogenous cannabinoid receptor ligand in brain. *Biochem. Biophys. Res. Commun.* **1995**, *215*, 89–97. [CrossRef]
19. Burstein, S. The elmiric acids: Biologically active anandamide analogs. *Neuropharmacology* **2008**, *55*, 1259–1264. [CrossRef]
20. Chu, C.J.; Huang, S.M.; De Petrocellis, L.; Bisogno, T.; Ewing, S.A.; Miller, J.D.; Zipkin, R.E.; Daddario, N.; Appendino, G.; Di Marzo, V.; et al. *N*-Oleoyldopamine, a Novel Endogenous Capsaicin-like Lipid That Produces Hyperalgesia. *J. Biol. Chem.* **2003**, *278*, 13633–13639. [CrossRef]
21. Smith, M.; Wilson, R.; O'Brien, S.; Tufarelli, C.; Anderson, S.I.; O'Sullivan, S.E. The effects of the endocannabinoids anandamide and 2-arachidonoylglycerol on human osteoblast proliferation and differentiation. *PLoS ONE* **2015**, *10*, e0136546. [CrossRef] [PubMed]
22. De Jesús, M.L.; Hostalot, C.; Garibi, J.M.; Sallés, J.; Meana, J.J.; Callado, L.F. Opposite changes in cannabinoid CB1 and CB2 receptor expression in human gliomas. *Neurochem. Int.* **2010**, *56*, 829–833. [CrossRef] [PubMed]
23. Pertwee, R.G.; Howlett, A.C.; Abood, M.E.; Alexander, S.P.H.; Di Marzo, V.; Elphick, M.R.; Greasley, P.J.; Hansen, H.S.; Kunos, G.; Mackie, K.; et al. International Union of Basic and Clinical Pharmacology LXXIX. Cannabinoid Receptors and Their Ligands: Beyond CB 1 and CB 2. *Pharmacol. Rev.* **2010**, *4*, 588–631. [CrossRef] [PubMed]
24. Ding, J.; Luo, X.; Yao, Y.; Xiao, H.; Guo, M. Investigation of changes in endocannabinoids and N-acylethanolamides in biofluids, and their correlations with female infertility. *J. Chromatogr. A* **2017**, *1509*, 16–25. [CrossRef]
25. Vago, R.; Ravelli, A.; Bettiga, A.; Casati, S.; Lavorgna, G.; Benigni, F.; Salonia, A.; Montorsi, F.; Orioli, M.; Ciu, P.; et al. Urine Endocannabinoids as Novel Non-Invasive Biomarkers for Bladder Cancer at Early Stage. *Cancers* **2020**, *12*, 870. [CrossRef]
26. Ottria, R.; Cappelletti, L.; Ravelli, A.; Mariotti, M.; Gigli, F.; Romagnoli, S.; Ciuffreda, P.; Banfi, G.; Drago, L. Plasma endocannabinoid behaviour in total knee and hip arthroplasty. *J. Biol. Regul. Homeost. Agents* **2016**, *30*, 1147–1152.
27. Ottria, R.; Ravelli, A.; Gigli, F.; Ciuffreda, P. Simultaneous ultra-high performance liquid chromathograpy-electrospray ionization-quadrupole-time of flight mass spectrometry quantification of endogenous anandamide and related N -acylethanolamides in bio-matrices. *J. Chromatogr. B* **2014**, *958*, 83–89. [CrossRef]
28. Liakh, I.; Pakiet, A.; Sledzinski, T.; Mika, A. Modern Methods of Sample Preparation for the Analysis of Oxylipins in Biological Samples. *Molecules* **2019**, *24*, 1639. [CrossRef]
29. Marchioni, C.; Donizeti, I.; Souza, D.; Ricardo, V.; Junior, A. Recent advances in LC-MS/MS methods to determine endocannabinoids in biological samples: Application in neurodegenerative diseases. *Anal. Chim. Acta* **2018**, *1044*. [CrossRef]
30. Bligh, E.G.; Dyer, W.J. A rapid method of total lipid extraction and purification. *Can. J. Psychiatry* **1979**, *24*, 422. [CrossRef]

31. Folch, J.; Lees, M.; Sloane Stanley, G. A simple method for the isolation and purification of total lipides from animal tissues. *J. Biol. Chem.* **1987**, *55*, 999–1033.
32. Breil, C.; Abert Vian, M.; Zemb, T.; Kunz, W.; Chemat, F. "Bligh and Dyer" and Folch methods for solid–liquid–liquid extraction of lipids from microorganisms. Comprehension of solvatation mechanisms and towards substitution with alternative solvents. *Int. J. Mol. Sci.* **2017**, *18*, 708. [CrossRef] [PubMed]
33. Gouveia-Figueira, S.; Nording, M.L. Validation of a tandem mass spectrometry method using combined extraction of 37 oxylipins and 14 endocannabinoid-related compounds including prostamides from biological matrices. *Prostaglandins Other Lipid Mediat.* **2015**, *121*, 110–121. [CrossRef] [PubMed]
34. Masoodi, M.; Mir, A.A.; Petasis, N.A.; Serhan, C.N.; Nicolaou, A. Simultaneous lipidomic analysis of three families of bioactive lipid mediators leukotrienes, resolvins, protectins and related hydroxy-fatty acids by liquid chromatography/electrospray ionisation tandem mass spectrometry. *Rapid Commun. Mass Spectrom.* **2008**, *22*, 75–83. [CrossRef]
35. Fowler, C.J.; Fowler, C.J. Monoacylglycerol lipase—A target for drug development? *Br. J. Pharmacol.* **2012**, *166*, 1568–1585. [CrossRef]
36. Pertwee, R.G.; Ross, R.A. Cannabinoid receptors and their ligands. *Prostaglandins Leukot. Essent. Fat. Acids* **2002**, *66*, 101–121. [CrossRef]
37. Di Marzo, V. Targeting the endocannabinoid system: To enhance or reduce? *Nat. Rev. Drug Discov.* **2008**, *7*, 438–455. [CrossRef]
38. Moreno, E.; Cavic, M.; Krivokuca, A.; Casadó, V. The Endocannabinoid System as a Target in Cancer Diseases: Are We There Yet? *Front. Pharmacol.* **2019**, *10*. [CrossRef]
39. Idris, A.I.; Sophocleous, A.; Landao-Bassonga, E.; Van't Hof, R.J.; Ralston, S.H. Regulation of bone mass, osteoclast function, and ovariectomy-induced bone loss by the type 2 cannabinoid receptor. *Endocrinology* **2008**, *149*, 5619–5626. [CrossRef]
40. Munro, S.; Thomas, K.; Abu-Shaar, M. Molecular characterization of a peripheral receptor for cannabinoids. *Nature* **1993**, *365*, 61–65. [CrossRef]
41. Bovée, J.V.M.G.; Hogendoorn, P.C.W.; Wunder, J.S.; Alman, B.A. Cartilage tumours and bone development: Molecular pathology and possible therapeutic targets. *Nat. Rev. Cancer* **2010**, *10*, 481–488. [CrossRef]
42. Zamborsky, R.; Kokavec, M.; Harsanyi, S.; Danisovic, L. Identification of Prognostic and Predictive Osteosarcoma Biomarkers. *Med. Sci.* **2019**, *7*, 28. [CrossRef]
43. Roy, J.; Watson, J.E.; Hong, I.S.; Fan, T.M.; Das, A. Antitumorigenic Properties of Omega-3 Endocannabinoid Epoxides. *J. Med. Chem.* **2018**, *61*, 5569–5579. [CrossRef]
44. Carnovali, M.; Ottria, R.; Pasqualetti, S.; Banfi, G.; Ciuffreda, P.; Mariotti, M. Effects of bioactive fatty acid amide derivatives in zebrafish scale model of bone metabolism and disease. *Pharmacol. Res.* **2016**, *104*, 1–8. [CrossRef]
45. Ottria, R.; Casati, S.; Ciuffreda, P. Optimized synthesis and characterization of N-acylethanolamines and O-acylethanolamines, important family of lipid-signalling molecules. *Chem. Phys. Lipids* **2012**, *165*, 705–711. [CrossRef]
46. Ottria, R.; Casati, S.; Ciuffreda, P. 1H,13C and15N NMR assignments for N- and O-acylethanolamines, important family of naturally occurring bioactive lipid mediators. *Magn. Reson. Chem.* **2012**, *50*, 823–828. [CrossRef]
47. Giannasi, C.; Niada, S.; Farronato, D.; Lombardi, G.; Manfredi, B.; Farronato, G.; Brini, A.T. Nitrogen containing bisphosphonates impair the release of bone homeostasis mediators and matrix production by human primary pre-osteoblasts. *Int. J. Med. Sci.* **2019**, *16*, 23–32. [CrossRef]
48. Niada, S.; Giannasi, C.; Gomarasca, M.; Stanco, D.; Casati, S.; Brini, A.T. Adipose-derived stromal cell secretome reduces TNFα-induced hypertrophy and catabolic markers in primary human articular chondrocytes. *Stem Cell Res.* **2019**, *38*, 101463. [CrossRef]
49. Théry, C.; Clayton, A.; Amigorena, S.; Raposo, G. Isolation and Characterization of Exosomes from Cell Culture Supernatants. *Curr. Protoc. Cell Biol.* **2006**. [CrossRef]
50. Gualerzi, A.; Niada, S.; Giannasi, C.; Picciolini, S.; Morasso, C.; Vanna, R.; Rossella, V.; Masserini, M.; Bedoni, M.; Ciceri, F.; et al. Raman spectroscopy uncovers biochemical tissue-related features of extracellular vesicles from mesenchymal stromal cells. *Sci. Rep.* **2017**, *7*, 1–11. [CrossRef]
51. Guidance for Industry Bioanalytical Method Validation. Available online: https://www.fda.gov/downloads/drugs/guidances/ucm070107.Pdf (accessed on 6 April 2020).

52. Van de Merbel, N.C. Quantitative determination of endogenous compounds in biological samples using chromatographic techniques. *Trends Anal. Chem.* **2008**, *27*, 924–933. [CrossRef]
53. Balvers, M.G.J.; Wortelboer, H.M.; Witkamp, R.F.; Verhoeckx, K.C.M. Liquid chromatography-tandem mass spectrometry analysis of free and esterified fatty acid N-acyl ethanolamines in plasma and blood cells. *Anal. Biochem.* **2013**, *434*, 275–283. [CrossRef]
54. Gachet, M.S.; Rhyn, P.; Bosch, O.G.; Quednow, B.B.; Gertsch, J. A quantitiative LC-MS/MS method for the measurement of arachidonic acid, prostanoids, endocannabinoids, N-acylethanolamines and steroids in human plasma. *J. Chromatogr. B Anal. Technol. Biomed. Life Sci.* **2015**, *976–977*, 6–18. [CrossRef]
55. Stenson, W. Measurement of prostaglandins and other eicosanoids. *Curr. Protoc. Immunol.* **2001**, *7*, 33. [CrossRef]
56. Pautke, C.; Schieker, M.; Tischer, T.; Kolk, A.; Neth, P.; Mutschler, W.; Milz, S. Characterization of osteosarcoma cell lines MG-63, Saos-2 and U-2 OS in comparison to human osteoblasts. *Anticancer Res.* **2004**, *24*, 3743–3748.
57. Hong, E.S.; Burkett, S.S.; Morrow, J.; Lizardo, M.M.; Osborne, T.; Li, S.Q.; Luu, H.H.; Meltzer, P.; Khanna, C. Characterization of the metastatic phenotype of a panel of established osteosarcoma cells. *Oncotarget* **2015**, *6*, 29469–29481. [CrossRef]
58. Roy, J.; Dibaeinia, P.; Fan, T.M.; Sinha, S.; Das, A. Global analysis of osteosarcoma lipidomes reveal altered lipid profiles in metastatic versus nonmetastatic cells. *J. Lipid Res.* **2019**, *60*, 375–387. [CrossRef]

International Journal of
Molecular Sciences

MDPI

Review

Bioactive Lipids in MSCs Biology: State of the Art and Role in Inflammation

Sara Casati [1,*], Chiara Giannasi [1,2], Stefania Niada [2], Roberta F. Bergamaschi [1], Marica Orioli [1] and Anna T. Brini [1,2]

[1] Dipartimento di Scienze Biomediche, Chirurgiche ed Odontoiatriche, Università degli Studi di Milano, 20133 Milan, Italy; chiara.giannasi@unimi.it (C.G.); roberta.bergamaschi@unimi.it (R.F.B.); marica.orioli@unimi.it (M.O.); anna.brini@unimi.it (A.T.B.)
[2] IRCCS Istituto Ortopedico Galeazzi, 20161 Milan, Italy; stefania.niada@grupposandonato.it
* Correspondence: sara.casati@unimi.it

Abstract: Lipidomics is a lipid-targeted metabolomics approach that aims to the comprehensive analysis of lipids in biological systems in order to highlight the specific functions of lipid species in health and disease. Lipids play pivotal roles as they are major structural components of the cellular membranes and energy storage molecules but also, as most recently shown, they act as functional and regulatory components of intra- and intercellular signaling. Herein, emphasis is given to the recently highlighted roles of specific bioactive lipids species, as polyunsaturated fatty acids (PUFA)-derived mediators (generally known as eicosanoids), endocannabinoids (eCBs), and lysophospholipids (LPLs), and their involvement in the mesenchymal stem cells (MSCs)-related inflammatory scenario. Indeed, MSCs are a heterogenous population of multipotent cells that have attracted much attention for their potential in regulating inflammation, immunomodulatory capabilities, and reparative roles. The lipidomics of the inflammatory disease osteoarthritis (OA) and the influence of MSCs-derived lipids have also been addressed.

Keywords: bioactive lipids; lipidomics; mesenchymal stem cells; inflammation; osteoarthritis

Citation: Casati, S.; Giannasi, C.; Niada, S.; Bergamaschi, R.F.; Orioli, M.; Brini, A.T. Bioactive Lipids in MSCs Biology: State of the Art and Role in Inflammation. *Int. J. Mol. Sci.* **2021**, *22*, 1481. https://doi.org/10.3390/ijms22031481

Academic Editor: Gabriella Calviello
Received: 15 January 2021
Accepted: 29 January 2021
Published: 2 February 2021

1. Introduction: Lipidomics and Lipids Mediated Inflammation in Mesenchymal Stem Cells

1.1. Lipidomics

The lipidome is defined as the complete set of lipids present within a cell, a tissue, or an organism [1,2]. In the last decades, it has become clear that the lipidome, as well as the transcriptome and the proteome, is in a dynamic balance and it can be affected by physio-pathological conditions, stimuli, and changes in diet [3,4]. Lipidomics is a relatively new "-omics" that characterizes, identifies, and quantifies the lipidome and its metabolic pathways and other networks that are involved within different biological mechanisms [5]. With analytical approaches, such as thin-layer chromatography (TLC) and gas chromatography (GC), lipidomics was able to develop new diagnostic tools and therapeutic strategies [6]; but it was with the advent of the next-generation mass spectrometry (MS) that there have been significant advances in the field of lipidomics [7–11]. In a typical lipidomic workflow, lipids are extracted from the biological matrices using organic solvents and analyzed by direct infusion into a mass spectrometer (technique known as "shotgun" lipidomics), or separated by liquid (LC) or gas chromatography (GC), prior to detection by MS. These two approaches are complementary, since the "shotgun" method allows a larger lipid profiling by simultaneous identification of several classes of lipids, meanwhile LC or GC/MS enable a more targeted analysis with the detection of structurally similar lipids belonging to a single class [12–14]. In both methods, the quantification is performed using a ratio against internal standard(s), which is routinely added for sample normalization and matrix effect influence correction. Internal standard structures and physicochemical

properties are representative of the endogenous lipid species of interest and are added at the earliest possible step during sample preparation. For shotgun lipidomics, a semi-quantification is generally possible by using exogenous lipids representative of the main lipid classes of interest; whereas for targeted lipidomics, labeled lipids (i.e., deuterated internal standards) should be included for absolute quantification. In the last few years, the aforementioned advanced analytical techniques have led to multiple improvements in lipidomics, particularly in the extraction methods and bioinformatics. These enhancements have allowed important goals, such as the identification of several lipid-based biomarkers, useful as diagnostic tools [5,10]. However, the number of lipidomics studies in the field of mesenchymal stem cells (MSCs) remains rather limited, especially when compared to the numerous investigations about their transcriptome and proteome. Thus, the objective of the current review was to focus on recently highlighted roles of specific bioactive lipid species and their involvement in the MSCs-related inflammatory scenario.

1.2. Involvement of MSC in Inflammatory Processes

MSCs are non-hematopoietic multipotent progenitor cells with the ability to differentiate into different mesodermal lineages including osteocytes, chondrocytes, and adipocytes [15,16]. The three criteria adopted by the International Society for Cellular Therapy to define and identify MSCs are: (1) MSCs must be adherent to plastic under standard culture conditions; (2) their phenotypes must present the expression of CD105, CD73, and CD90 and lack the expression of the hematopoietic cell surface markers CD45, CD34, CD14 or CD11b, CD79α, or CD19 and HLA-DR; (3) they must be able to differentiate under stimulation in vitro into osteoblasts, adipocytes, and chondroblasts [17,18]. MSCs are currently being studied in many preclinical and clinical applications. In particular, they have attracted the scientific interest for their ability to regulate inflammatory processes and promote tissue repair due to their multi-lineage differentiation potential, pro-angiogenic characteristics, and immune-modulatory properties [19–21]. Recently, MSC-based treatment has been proposed as a suitable therapeutic approach for the severe acute respiratory infection caused by the corona virus SARS-CoV-2. In the COVID-19 scenario, where the immune system produces large amounts of inflammatory factors, the MSC therapy can prevent the storm release of cytokines by the immune system and promote endogenous repair through their immunomodulatory, anti-inflammatory, and reparative properties [22,23].

Furthermore, the therapeutic potential of MSCs, largely mediated by paracrine signaling [24], is currently under investigation for several degenerative, autoimmune, and inflammatory disorders, as well as the exact mechanisms underlying their effect [21]. Nevertheless, it is very likely that either a direct cell-cell contact and/or the secretion of soluble factors, including bioactive lipids, and/or extracellular vesicles (EVs) are needed [24–26].

Generally, MSCs can modulate both innate and adaptive immune responses in vitro and in vivo due to their ability to inhibit T-cell proliferation and dendritic cell maturation, recruit regulatory T-cells, and modulate B-cell functions [21,27,28]. Expanded for the first time from human bone marrow (BM), MSCs can also be collected and cultured from several sources including adipose tissue, skeletal muscle, or umbilical cord blood and expanded ex vivo for clinical use [29,30]. Compared to BMs, adipose-derived stem cells (ASCs) have an easier and faster growth in culture, age with a lower rate, maintain the mesenchymal pluripotency and stem cell phenotype even after a high number of passages in culture, and show a great proliferative rate with a consequent relatively high yield (about 2500 fold higher than BM) [15,16,31,32]. Moreover, ASCs have shown a great potential of differentiation into several cellular lineages and a good stability throughout long-term cultures; they are characterized by immunomodulatory properties making them immunosuppressive [30]. Moreover, their secretome presents a mix of cytokines, extracellular matrix molecules and proteases, lipid mediators, hormones, and growth factors that are also involved in the angiogenesis process with a great utility and applicability in wound healing and tissue regeneration [15,33–35]. In addition to BMSCs and ASCs, skeletal muscle-derived stem cells (MDSCs) have been used in clinical trials for the regener-

ation and repair of injured tissues, because of their high proliferation rate and their ability to secrete trophic factors promoting endogenous tissues repair [36]; moreover, MDSCs harvesting consists in micro-biopsies obtained as small skin punctures under local anesthesia [37,38]. Although they exhibit slow-growing adherent behavior after isolation, MDSCs are characterized by a long-term self-renewal, and an easy differentiation into osteoblasts, adipocytes, and chondrocytes in vitro [37].

1.3. Functional Role of Endogenous Bioactive Lipids in Inflammation

Endogenous bioactive lipids cover a pivotal role in very important biological phenomena, such as inflammation, immune regulation, and maintenance of homeostasis [39,40]. Indeed, defects in their metabolism and unbalanced biosynthesis are involved in the pathogenesis and clinical course of chronic inflammation diseases [39,40]. Based on their biosynthesis, bioactive lipids can be grouped into different families (Table 1): polyunsaturated fatty acids (PUFA)-derived mediators (generally known as eicosanoids), endocannabinoids (eCBs), and lysophospholipids (LPLs) [41]. Bioactive lipids derived from PUFA can be further divided into two subgroups: one is represented by ω6 arachidonic acid (AA, 20:4 ω6)-derived lipid mediators, including prostaglandins (PGs), leukotrienes (LTs), thromboxanes (TXs), and lipoxins (LXs); the other includes ω3-PUFA-derived lipid mediators, such as the eicosapentaenoic acid (EPA, 20:5 ω3) and the docosahexaenoic acid (DHA, 22:6 ω3), i.e., E-series and D-series resolvins (Rvs), protectins (PDs), and maresins (MaRs), collectively termed "specialized pro-resolving mediators" (SPMs). Except for LXs, ω6-PUFA-derived lipids are pro-inflammatory, in contrast with ω3-PUFA-derived lipids, which act as anti-inflammatory. In detail, SPMs stimulate key cellular events, by acting as agonists, stopping further neutrophil influx and the activation of non-phlogistic responses by macrophages and, therefore, leading to the resolution of the inflammation. ECBs and eCB-like compounds originate from ω6- and ω3-PUFA metabolism, but also from saturated and monounsaturated fatty acids (SFA and MUFA), such as palmitic (16:0), stearic (18:0), or oleic acids (18:1 n9). Nowadays, pro- and anti-inflammatory properties exerted by eCBs and eCB-like compounds are issues of intense research [42,43]. Finally, membrane-derived bioactive lipids derived from LPLs can be divided into lysoglycerophospholipids (LGPLs) and lysosphingophospholipids (LSLs), based on the presence of glycerol or sphingosine (S) as backbone of their structures. LPLs exert pleiotropic effects such as inflammation, vesicular trafficking, endocytosis, apoptosis, cell migration, and cell-stress responses [44]. In this review, we will outline the biological activities and metabolisms of the major bioactive lipids identified as essential regulators in the complex scenario of inflammation and as players in the immunoregulation exerted by MSCs.

Table 1. Composition, functions, and classes or examples of the different categories of bioactive lipids.

Categories	Composition	Function	Classes or Examples
Polyunsaturated fatty acids	Carboxylic acid + hydrocarbon chain; synthesized by chain elongation of an acetyl-CoA with malonyl-CoA	Cell signaling; building blocks to complex lipids	AA, EPA, DHA
Endocannabinoids and related compounds	Ethanolamide or other head groups + FAs	Cell signaling	AEA, 2AG
Lysophospholipids	Polar head group + glycerol or sphingosine backbone	Membrane and lipoprotein composition, cell signaling	LGPLs, LSLs

2. Lipids as Signaling Mediators in Inflammation

2.1. Eicosanoids

The group of eicosanoids represents the widest family of bioactive lipids and includes several molecules characterized by the long carbon chain ω6 AA or ω3 EPA and DHA as

common precursors. ω6 AA, released from membrane phospholipids firstly via phospholipase A2 and secondarily by phospholipase C, is the substrate for three different enzymes leading to the generation of pleiotropic and heterogenous compounds: (1) cyclooxygenases 1 and 2 (COX-1/2) drive the synthesis of PGs (PGD_2, PGE_2, PGI_2, and $PGF_{2\alpha}$), prostacyclins, and TXs [45,46], also known as prostanoids; (2) 5-, 12- and 15-lypooxygenases (5/12/15-LOX) synthetize LTs [47,48], lipoxins (LXs) [49] and hydroxyeicosatetraenoids (HETEs) [50]; (3) P450 epoxygenase generates also HETEs, and epoxyeicosatrienoids (ETEs) [50]. ω3 PUFAs-derived bioactive products are Rvs, PDs, and MaRs. Rvs derive from either EPA or DHA and can be further divided into E-series or D-series, respectively. DHA acts also as a precursor for the biosynthesis of PDs and MaRs (Figure 1). The ω6 eicosanoids play an essential active role in the inflammatory response, such as leukocyte chemotaxis and activation, fever, pain [40], and are usually associated to acute inflammatory processes and chronic inflammation. Indeed, PGs seem to promote inflammation through several mechanisms such as increasing the release of the pro-inflammatory cytokines [51–53], enhancing the expression of pro-inflammatory genes, promoting innate immunity response [54], recruiting leukocytes and activating two distinct T helper subsets, TH1 and TH17 [55,56]. LTs generally recruit neutrophils, macrophages, eosinophils, and TH17 lymphocytes, and are responsible for the induction of edema. Vasoconstriction and vasodilatation are promoted instead by TXs and prostacyclins, respectively [57]. On the other hand, the ω3 family seems to have a beneficial impact on inflammation, by acting via different mechanisms, for example by working as substrate competitors able to inhibit the conversion of AA into pro-inflammatory eicosanoids or serving as an alternative substrate to produce less potent LTs, PGs, and TGs. In animal models, Rvs and PDs shorten the resolution of inflammation for certain diseases [41,58,59] and can also increase animal survival [60,61]. Two of the major Rvs, RvD1 and RvD2, have shown in vivo anti-inflammatory and pro-resolution properties, by blocking the neutrophil infiltration in many disorders, such as obesity and pathologies affecting the vascular [62], renal and dermal systems, and also in processes as wound healing, fibrosis, and pain [60]. Moreover, ω3 PUFA-derived mediators that have been found within the inflammatory exudate (RvE1 and PD1) show great anti-inflammatory and pro-resolving actions both in vitro and in vivo [51,63]. However, the resolution of inflammation is also mediated by other metabolites of AA [64]. Indeed, PGJ (15-deoxy-delta-13,14-PGJ_2), the bioconversion product of PGD_2, increases during the resolution phase and acts as a brake on inflammation by inducing apoptosis of inflammatory cells [65]. The concentration of the lipoxygenase product LXA_4 (lipoxin A_4) is also increased during the resolution phase and acts as a stop signal for the acute response [66]. Finally, AA-derived EETs present anti-inflammatory properties through the suppression of nuclear factor kappa-light-chain-enhancer of activated B cells (NF-kB) activation and govern vasorelaxation and fibrinolysis [67].

2.2. Endocannabinoids (eCBs) and Endocannabinoid-Like Compounds

eCBs are endogenous lipid compounds that can bind G-protein coupled cannabinoid receptors (CB1 and CB2) in the same way as tetrahydrocannabinol (THC), the major psychoactive component of *Cannabis sativa*. The plant *Cannabis sativa* and its preparations, marijuana and hashish, are being used for many years for recreational and medical purposes [68] because of the pleasurable effects triggered by THC, modulated by the other major, non-psychoactive phytocannabinoid, called cannabidiol (CBD). Both components possess other important medical properties, such as anti-inflammatory, analgesic, anti-emetic (THC), and anxiolytic (CBD). [69]. Thanks to the studies performed on cannabis plants and their peculiar chemical components, researchers were able to discover one of the most intriguing and pleiotropic endogenous signaling systems, the endocannabinoid system (eCBS). eCBs, CB receptors, and the biochemical entities that produce and degrade these lipids, are involved in most aspects of the mammalian physiology and pathology [70]. The compound arachidonoylethanolamide (AEA) [71], the first isolated ethanolamide of AA, represents a partial agonist of CB receptors, while 2- arachidonoylglicerol (2-AG) (another derivative

of AA) [72,73], is a full agonist (Figure 1). Both compounds AEA and 2-AG belong to the group of PUFA AA-related lipid mediators, and as CB receptor ligands, they stimulate a variety of bioactivities, including analgesia, catalepsy, hypolocomotion, and hypothermia [68]. Moreover, AEA exhibits anti-inflammatory properties [74], whereas 2-AG shows both pro- and anti-inflammatory characteristics [75,76]. Thus, dysfunctions leading to changes in concentration levels, metabolism, and receptors of eCBs could be related to alterations in homeostasis and to the progression of chronic inflammatory status [77]. Moreover, two metabolically active ω3 fatty acid ethanolamides, N-eicosapentaenoylethanolamine (EPEA) and N-docosahexaenoylethanolamine (DHEA) [78,79], have been proposed as additional CB receptor agonists [80]. These ω3 eCBs were found to possess anti-inflammatory properties in macrophages [81] and adipocytes [82]. In addition to CB1 and CB2 receptors, pharmacological studies suggest the presence also of different receptors that can mediate the cannabinoids effects. Indeed, besides AEA, other ethanolamides coming from various long-chain fatty acids were discovered, and collectively known as N-acylethanolamines (NAEs). Ethanolamides of SFA and MUFA such as palmitic, stearic, and oleic acids, which are more abundant than AEA in mammals, show no activity for CB receptors, but act on other receptors, like the nuclear receptor peroxisome proliferator-activated receptor-α (PPARα), leading to the trigger of biological events including anti-inflammation and appetite suppression [83,84]. In detail, the PPARα-mediated actions of N-palmitoylethanolamide (PEA) include anti-inflammatory, analgesic, anti-epileptic, and neuroprotective properties [85,86]. Moreover, PEA could also activate the orphan G protein-coupled receptor GPCR55 [87], one of the discussed candidates as CB3 receptor, even though this agonist activity has not been fully elucidated yet. Another saturated NAE, N-stearoylethanolamide (SEA), was reported to act as an anti-inflammatory/immunomodulatory agent and cell growth controller, through still unknown targets [88–90]. Finally, a variety of eCB-related compounds, containing fatty acid chains conjugated with different polar heads, have been discovered as a result of advancements of the analytical techniques [91,92]. Within the novel group of lipids generally referred as lipoamino acids, N-arachidonoylglycine (NAGly), the most important member, possesses anti-inflammatory effects by targeting the G-protein coupled receptor GPCR18 [93,94], vasorelaxant properties [95] and seems to be involved in cell migration [96], and inhibition of the fatty acid amide hydrolase (FAAH) [97], the AEA inactivating enzyme. Moreover, NAgly might have either a physiological role in the resolution of acute inflammatory response and become a potential therapeutic candidate for the resolution of chronic inflammation, by increasing the production of PGJ and LXA_4, reducing the migration of inflammatory cells into areas of acute inflammation and inducing the death of inflammatory cells [93].

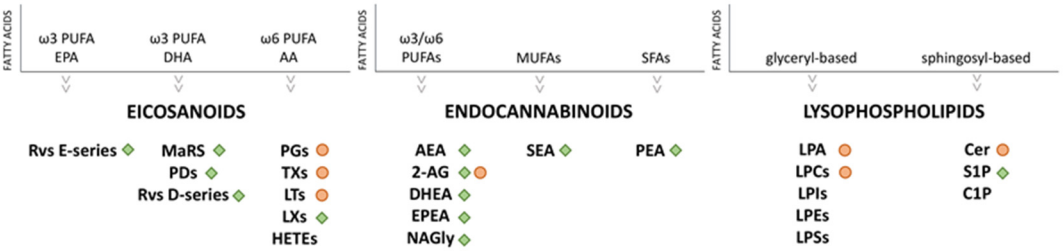

Figure 1. Lipids involved in inflammation. The green squares indicate lipids with anti-inflammatory properties and the orange dots indicate lipids with pro-inflammatory properties. Abbreviations. PUFAs: polyunsaturated fatty acids; MUFAs: monounsaturated fatty acids; SFAs: saturated fatty acids; EPA: eicosapentaenoic acid; DHA: docosahexaenoic acid; AA: arachidonic acid; Rvs E-series: resolvins E-series; Rvs D-series: resolvins D-series; MaRS: maresines; PDs: protectins; PGs: prostaglandins; TXs: thromboxanes; LTs: leukotrienes; LXs: Lipoxins; HETEs: hydroxyeicosatetraenoids; AEA: anandamide; 2-AG: 2-arachidonoilglycerol; DHEA: N-docosahexaenoylethanolamine; EPEA: N-eicosapentaenoylethanolamine; NAGly: N-arachidonoylglycine; SEA: stearoylethanolamide; PEA: N-palmitoylethanolamide; LPCs: lysophosphatidylcholines; LPA: lysophoshatidic acid; LPIs: lysophosphatidylinositols; LPEs: lysophosphatidylethanolamines; LPSs: lysophosphatidylserines; Cer: ceramide; S1P: sphingosine 1-phosphate; C1P: ceramide-1-phosphate.

2.3. Lysophospholipids (LPLs)

LPLs are bioactive signaling lipids consisting of *O*-acyl chain, generated from phospholipase-mediated hydrolyzation of membrane glycerophospholipids (GPLs) and sphingolipids (SLs). Consequently, LPLs are classified into two main categories: glyceryl-based LPLs (including LPA) and sphingosyl-based (including S1P) with a glycerol or a sphingosine backbone, respectively [98,99] (Figure 1). Several LPLs compounds are asymmetrically distributed in the plasma membrane and are characterized by a polar head group (ethanolamine, choline, inositol, serine) and a hydrophobic tail of carbon chain. LPLs act as signaling mediators by binding seven-transmembrane domain G-protein coupled receptors (GPCRs). The two major bioactive LPLs are the well-characterized lysophosphatidic acid (LPA) and sphingosine-1-phosphate (S1P) and they play important roles in various physio-pathological processes, including inflammation. LPA, a byproduct of lysophosphaditylcholine (LPC) and lysophosphatidilinositol (LPI), is a signaling mediator involved in cell renewal, immune response, and inflammatory cascade [100,101]. LPA can be synthetized both intracellularly and extracellularly by different enzymes and via different pathways, such as autotaxin/ectonucleotide pyrophosphatase phosphodiesterase 2 (ENNP2) and/or phospholipases A1 and A2, whereas its degradation is mediated by lipid phosphate phosphatases 1–3 [102]. Currently, six LPA receptors (LPA 1–6) are known [102]. Recently, LPA is reported to be rapidly formed during the resolution phase of the inflammation and, successively, to be recruited via the common pro-resolving formyl peptide receptor 2 (FPR2, also known as ALX), which is expressed on T cells and their subsets [103]. On the other hand, SLs, such as ceramides and sphingosines, participate in different stages of inflammation as well, by controlling intracellular trafficking and signaling, cell proliferation, adhesion, vascularization, survival, and apoptosis [104,105]. In particular, the phosphate forms of sphingolipids, ceramide-1-phosphate (C1P) and S1P [106], are notably associated to inflammatory responses. S1P is synthesized by the intracellular phosphorylation of sphingosine via sphingosine kinases 1 and 2 (SK1 and SK2) and degraded by S1P lyase or ceramide synthases. It is involved in the resolution phase (together with C1P) since apoptotic cells present at the inflammation sites attract pro-resolving macrophages via S1P receptor 1 [107] and, additionally, it can act either on COX-2 or NF-kB, whereas C1P acts on phospholipase A2 [102].

3. Bioactive Lipids in MSCs

3.1. Lipid Metabolism in MSCs Maintenance and Differentiation

Lipid metabolism plays a pivotal role in stem cells physiopathology [108–110]. However, at the moment the number of studies about the lipidome of MSCs is limited, and mainly focused on variations in lipid composition during stem cell proliferation and differentiation [111–130] (Figure 2).

Recently, profiles of glycerophopholipids (GPLs) present in human BMSCs were assessed from young and old donors and across passages during in vitro culture [111–113]. In particular, since the clinical use of MSCs demands sequential ex vivo expansion, the determination of GPL profiles through the different steps of the in vitro culture represents a crucial and relevant advancement. In general, long-term culturing could contribute to the decrease of the proliferation and the differentiation potential, shorten the telomers, and accumulate ω6 PUFAs with signaling roles, consequently promoting inflammation [114,115]. It is well established that membrane GPLs provide precursors for signaling lipids that modulate cellular functions, and small changes in their compositions can lead to significant biological consequences. Kilpinen et al. studied the effect of the donor's age and cell doublings on the profile of GPLs of human BMSCs, demonstrating that an extensive expansion modulates membrane GPLs, by increasing total phosphatidylinositol (PI) and lysophospatidylcholine (LPC). Specifically, the effect was more pronounced when BMSCs were isolated from young donors. Moreover, changes in membrane FAs profile during expansion and senescence of BMSCs was highlighted: the ω6 AA content increased, while ω3 PUFAs (especially DHA) decreased during long-term cultivation, leading to an impair-

ment of the immunological functionality [111]. In addition, in the later steps of the process, an increment of the fraction of individual SFA was noticed [111]. A significant modification of membrane FAs composition of MSCs derived from human fetal membranes (FM-MSCs), occurring during in vitro culture, was assessed by Chatgilialoglu et al. [112]. In detail, fresh uncultured FM-MSCs showed variability in their membrane FAs composition, likely due to the genetic diversity and different lifestyle of the donors. This study also reveals that cultured cells have lower proportions of PUFAs than freshly isolated cells showing a great drop in ω6 FAs, counterbalanced by a marked increase in MUFA and ω3 FAs. These data are in contrast with Kilpinen et al. [111]. More recently, a lipidomics profiling analysis during BMSCs culturing passages by Lu et al. investigates the metabolic alteration of various lipid species in the senescence process [113]. They applied an untargeted lipidomics approach based on liquid chromatography coupled to mass spectrometry (HPLC-MS), which allowed the reduction of the complexity of the matrix and the enhancement of the sensitivity, factors that represent an improvement relative to the previously described shotgun-based methods. The majority of GPLs, as well as SLs, were found to significantly increase across the culturing passages, whereas the PA, PIs, and phosphatidylserines (PSs) levels were lower in aged cells. These findings were largely coherent with previous described studies, except for PI species, which were found to be increased during all the passages [111]. Nevertheless, the reduced amount of PIs is inconsistent with the relative transcriptomics analysis, which showed an increase in the enzymes expression with consequential conversion of PA into PIs suggesting an enhanced PIs biosynthesis activity. Moreover, research on the functional FAs has largely supported regulatory roles for PGs in MSCs proliferation. In particular, PGE_2 increases human umbilical cord blood-derived MSCs (UCMSCs) proliferation through β-catenin-mediated c-Myc and vascular endothelial growth factor expression via exchange protein directly activated by cAMP (Epac1)/Ras-related protein 1 (Rap1)/Akt and PKA cooperation [116], and through interaction of profilin-1 (Pfn-1) and filamentous-actin (F-actin) via EP2 receptor-dependent β-arrestin-1/JNK signaling pathways [117]. On the contrary, the investigation of PGE_2 and prostaglandin D2 (PGD_2) effects on MSCs proliferation and osteogenic differentiation suggests that both their receptors are highly expressed in these cells and both prostaglandins seem to have a negative impact [118]. In detail, PGE_2 firstly enhances the MSCs growth-rate, while longer stimulation leads to a growth-inhibitory effect. Contrarily, PGD_2 inhibits MSCs growth regardless of the duration of the exposure. Moreover, their inhibitory effect on calcium deposition also suggests a negative impact on MSCs osteogenic differentiation [118]. Moreover, TXs class has been investigated for its effect on MSCs proliferation, suggesting the role of TXA_2 as potent modulator of ASCs migration and proliferation through ERK and p38 MAPK signaling mechanisms [119]. In addition, TXA_2 appears to induce ASCs differentiation into smooth-muscle-like cells [119,120]. Concerning eCBS, Rossi et al. [121] described a gradual decrease during subculture in AEA and 2-AG levels secreted by human BMSCs starting from passage 1 (AEA: 5 pmol/mg protein and 2-AG: 11 pmol/mg protein 2-AG) and this finding was also confirmed by Kose et al. [122]. ASCs secrete AEA and 2-AG at 3.5 and 7.3 pmol/mg protein, respectively, at early passages [123]. In addition, 2-AG and CB1/CB2 stimulation recruits BMSCs, most probably via an indirect activation of CB2 receptors [124].

During MSCs differentiation, eCBS variation was also highlighted and the expression of CB1 and CB2 is considerably lower in undifferentiated cells and it increases during osteogenic [125,126] and adipogenic commitment [125]. Furthermore, the activation of CB2 signaling plays an important role in promoting the osteogenic differentiation of BMSCs in vitro, with an increase of alkaline phosphatase activity (ALP), an induction of the expression of specific osteogenic genes including Runx2, Osterix, IBSP, SPP1, OCN, COL1a1, and an enhanced deposition of calcium in the extracellular matrix [126]. This result indicates a key role of CB2 receptor in BMSCs differentiation towards osteoblasts, suggesting also that MSCs might produce endogenous cannabinoids able to reinforce their osteogenic differentiation as well. Moreover, the knockdown of CB2 receptor in BMSCs by small interference RNA (siRNA) inhibits ALP activity and mineralization [126]. Most recently the osteogenic

differentiation induced by CB2 signaling activation has been shown to involve autophagy induction and sequestosome 1/p62-mediated Nuclear Factor Erythroid 2Related Factor 2 deactivation [127]. Whereas, the implication of eCBs in BMSCs physiology related to their adipocyte differentiation was validated looking at the increased expression of CB1, transient receptor potential vanilloid type 1 (TRPV1) and PPARγ during adipogenesis [128]. Moreover, the effects of AEA, N-arachidonoydopamine (NADA), and 2-AG were evaluated suggesting a promotion of adipocyte differentiation by AEA and an inhibition by NADA. No changes were observed with 2-AG at non-cytotoxic concentrations. Furthermore, CB1 may stimulate protein expression, such as adiponectin during adipogenesis [125,129], since it is enriched in mature adipocytes compared to other cell types [129]. Moreover, based on the effect of AEA, CB1 expression seems to be correlated to the increment of FAAH and COX-2 during adipogenic differentiation [130].

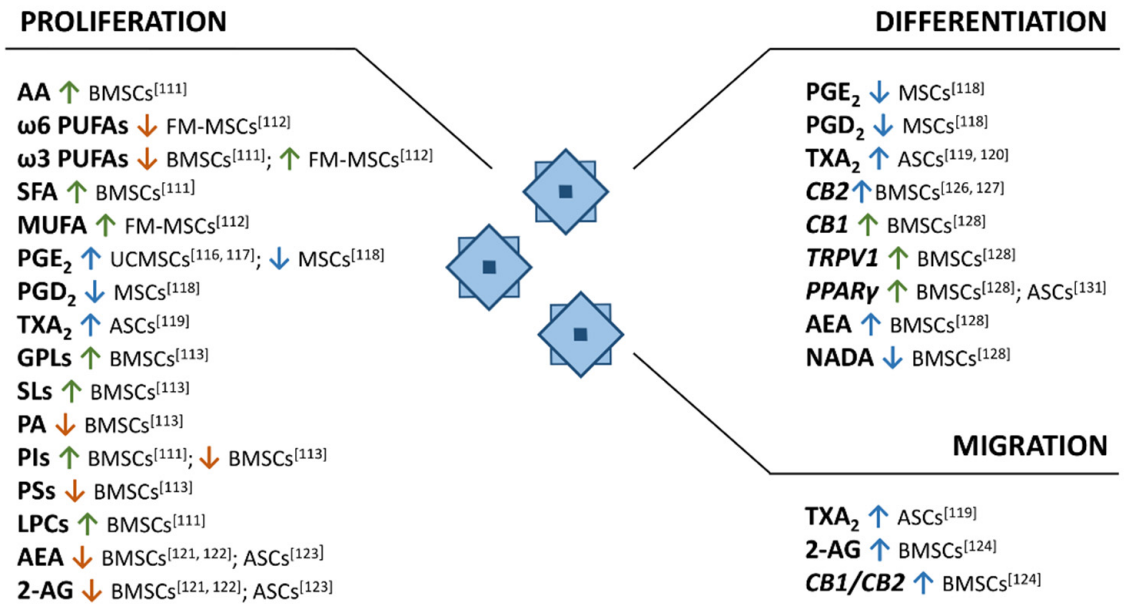

Figure 2. Lipids and their receptors involved in MSCs proliferation, differentiation and migration. The green and orange arrows indicate an increment and a decrease of lipids or their receptors, respectively; whereas blue arrows indicate their action on MSCs. Abbreviations. AA: arachidonic acid; PUFAs: polyunsaturated fatty acids; SFAs: saturated fatty acids; MUFAs: monounsaturated fatty acids; PGE_2: prostaglandin E_2; PGD_2: prostaglandin D_2; TXA_2: thromboxane A_2; GPLs: glycerophospholipids; SLs: sphingolipids; PA: phoshatidic acid; PIs: phosphatidylinositols; PSs: phosphatidylserines; LPCs: lysophosphatidylcholines; AEA: anandamide; 2-AG: 2-arachidonoilglycerol; CB2: cannabinoid receptor 2; CB1: cannabinoid receptor 1; TRPV1: transient receptor potential vanilloid type 1; PPARγ: peroxisome proliferator-activated receptor-γ; NADA: N-arachidonoydopamine; BMSCs: bone marrow-derived stem cells; FM-MSCs: fetal membrane-derived stem cells; UCMSCs: umbilical cord blood-derived stem cells; ASCs: adipose-derived stem cells.

In addition, Pagano et al. found out that ASCs exposed to the synthetic cannabinoid WIN55,212–2 increase the glucose uptake, the calcium influx, and the expression of the adipogenesis regulator PPAR-γ; contrarily, these effects are inhibited by the specific CB1-antagonist Rimonabant [131]. Finally, Silva et al. has analyzed the lipidome of rabbit ASCs and MDSCs and their adipogenic and osteogenic differentiation identifying 1687 lipid species [132]. These animal MSCs have shown different lipid profiles as well as changes in lipid composition after adipogenic and osteogenic differentiation. Moreover, the N-acyl-phosphatidylethanolamine (PE) and phosphatidylcholine (PC) expression levels suggest lipid similarities in cells differentiated from different stem cell sources [132]. In conclusion, PUFAs and their bioactive derivatives affect both the proliferation and differentiation of several MSCs and consequently modulate their immunological interaction with other cells. In this perspective, lipid profiling can represent a valuable tool also in the screening of

MSC populations prior to their use in both experimental and clinical settings. Indeed, the possibility of evaluating selected lipid classes or MSC entire lipidome can rapidly provide a screenshot of their differentiative status and growth rate, thus, allowing to harness MSC potential at its best for the diverse applications.

3.2. Pro and Anti-Inflammatory Properties of MSC-Derived Lipids

MSCs present anti-inflammatory properties and are being used with great success as treatment for inflammatory and autoimmune diseases. They have been shown to migrate towards injured tissues affected by inflammatory events, led by several growth factors, cytokines, and chemokines [133]. Being physiologically recruited at the damaged site, MSCs are often submitted to a strong, pro-inflammatory environment. It is well known that the PGE_2 secretion is increased upon incubation with the tumor necrosis factor alpha (TNF-α) and the interferon gamma (IFN-γ) [28]. To better understand the involvement of the lipidome in the MSCs anti-inflammatory properties and underlying its mechanisms of action, Campos et al. [134] have performed a wide range lipidomic analysis of MSCs under pro-inflammatory conditions induced by the presence of 10 ng/mL TNF-α and 500 U/mL IFN-γ. This study has evidenced a change in MSCs PL profile under the pro-inflammatory stimulus: indeed, higher levels of molecular PC species with longer FA acyl chains and lower levels of molecular PC species with shorter FA acyl chains were assessed. Moreover, the expressions of the specific PE(40:6), PS(36:1), LPC(18:0), and SM(34:0) were enhanced, while PE(O-38:6) and PS(40:4) expressions decreased simultaneously. The increase of LPC (18:0) has already been correlated with anti-inflammatory properties by others [135,136]. These differences were identified only in specific GPL subspecies, suggesting that each GPL subspecies could play a role in MSCs immunological functions. Moreover, the characteristics of the lipidome of the untreated MSCs described by Campos et al. were consistent with previous results [111], with the exception of the presence of sphingomyelins [134], which have not been previously identified. As formerly described, some derivatives of SLs, such as S1P, are bioactive and mediate essential cell functions [137].

Concerning the MSCs lipid secretion, PGE_2 was widely investigated given its key role in the immunosuppressive activity of MSCs [28]. Masoodi and colleagues [138] have analyzed the release of PGs by human heart-derived MSCs by HPLC-MS/MS, finding the presence of PGE_1, PGE_2, PGE_3, 6-keto $PGF_{1\alpha}$, $PGF_{2\alpha}$, and PGJ_2 in the conditioned medium. Although PGE_2 has been linked to the immunosuppressive effects of MSCs since their inhibitors production attenuate MSC-mediated immunomodulation [28], PGs are best known for their ability to mediate vasodilatation that allows immune cells to invade inflamed tissue. Indeed, recent evidence suggests also that PGE_2 may have an immunostimulatory role by facilitating Th1 differentiation and expanding the Th17 T-cells population [55]. Since prostaglandins have a short half-life, they act as paracrine and autocrine factors in the local environment. MSCs themselves also express receptors for prostaglandins: EP1, EP2, EP4, FP, and IP. The effects triggered by the stimulation of these receptors on MSCs are still unknown. However, the profile of PGs highlighted in MSCs is superimposable with that of their receptors (prostaglandins type E and F, and prostacyclin). Thus, the dual and controversial immunomodulatory properties of MSCs can depend on the local environment, where IFN-γ and TNF-α play a pivotal role in promoting immunosuppressive function of MSCs [139,140].

In the presence of PGE_2, also a higher expression of EP3, which is involved in the stimulation of angiogenesis, was obtained in MSCs suggesting a possible correlation with the early phases of inflammation [118].

Recent studies have evidenced the roles of LXs as regulators of the resolution phase of inflammation [61] and of Rvs as players in the immunoregulation of MSCs [141]. Fang et al. have demonstrated the MSCs ability of promoting the resolution of acute lung injuries in mice through the secretion of lipoxin A_4 (LXA_4), the first identified anti-inflammatory and pro-resolving lipid mediator [142], signaling via the G protein coupled ALX/FPR2 receptors [141].

3.3. Effect of Exogenous Supplements of PUFAs on MSCs

The ω3 fatty acids EPA and DHA, which are found mainly in marine oils, have long been thought to have anti-inflammatory properties, whereby they compete with AA, by reducing pro-inflammatory eicosanoids [143]. The molecular mechanism through which this occurs is still unclear, and there are no evidences about beneficial effects of ω3 EPA and DHA for human health as well as their role as potential treatments for human diseases. In most mammalian cell types, different exogenous supplements of PUFAs are incorporated into plasma membrane GPL and then metabolized by phospholipases in order to produce various lipid mediators. Thus, the biochemical homeostasis of lipid profile in mammalian membranes must be perturbed not only by physio-pathological inputs, but also by external lipid uptake (i.e., dietary fats). A recent study performed on human BMSCs has demonstrated the increase of the secretion of the pro-inflammatory PGE_2 after AA supplements intake. However, this possible harmful effect can be attenuated by the chain elongation on the less active precursor, ω6 22:4. The ω3 PUFAs precursor, the alfa-linolenic acid (18:3), shows a slight reduction of its GPL AA content, while the EPA (20:5) and DHA (22:6) acid supplements efficiently displace the AA, creating several pools of GPL species substrates that allow attenuation of inflammatory signaling [144].

3.4. MSCs as an Alternative Treatment of Inflammatory Diseases: The Example of Osteoarthritis

Osteoarthritis (OA) is a heterogeneous chronic joint disease characterized by the processes of degradation, repair, and inflammation that occur in the connective tissue, the vulnerable layer of joints, synovium, and subchondral bone [145]. From a molecular point of view, the catabolic and anabolic activities are unbalanced, and the major injury response occurs at the joint cartilage level. Recently, findings regarding the involvement of lipids in OA development and progression indicate a possible involvement of ω3 PUFAs and their anti-inflammatory SPMs derivatives [146]. The most studied bioactive lipids, PGs and LTs, have been detected in plasma and synovial fluid of OA patients showing pro-inflammatory and catabolic effects on fibroblasts, osteoblasts and cartilage [147]. Moreover, the PGE_2 and AA-derived oxylipin 15-HETE levels were related to knee OA [148], suggesting a possible role in the disease progression. Because of the similarities between OA course and chronic wound accompanied by cell death, inflammation, and pain [149] and since ω3 PUFAs/SPMs have been shown to target all these processes, it is conceivable that these lipids could be effective therapeutic agents for OA. In the context of this disease, few studies have investigated the FAs presence in OA affecting patients and their relationship to clinical symptoms. These studies indicated that increases of ω3 FAs levels could be associated with a reduced cartilage loss while the increase of the increase of ω6 FAs levels with enhanced synovitis [150]. All studies performed with ω3 PUFAs suggest that the beneficial effects consist primarily in an improvement in symptoms and pain, whereas little effects are observed on structural progression of the OA disease. However, previous studies have reported that ω3 PUFAs can counteract the pro-inflammatory and catabolic actions of interleukin-1a (IL-1a) on cartilage in vitro [151]. These results were consistent with a more recent study in which the authors have shown the involvement of DHA in the downregulation of MMP-13 through a P38 mitogen activated protein kinases (p38-MAPK)-mediated mechanism [152] both in vitro and in vivo in a rat model of OA. Apart from direct effects of ω3 PUFAs on OA, it is conceivable that ω3-derived oxylipins could be generated in vitro (i.e., by chondrocytes) and these could mediate the observed effects. Another study confirmed the presence of pro-inflammatory lipid mediators, such as PGE_2, in OA synovial fluid, as well as oxylipins derived from ω3 and ω6 PUFA such as 15-HETE (derived from AA), 17-HDHA (derived from DHA), and 18-HEPE (derived from EPA). When the pro-inflammatory response occurs in the cartilage, some types of prostanoid enzymes, such as COX, will be produced and released in excessive amounts. COX activation will increase the production of MMP, inhibit the expression of PGE_2 and collagen genes and will stimulate the apoptosis process. Studies conducted by Hardy et al. [153] and Shimpo et al. [154] have analyzed the role of PGE_2 in chondro-

cytes. The pro-inflammatory cytokine IL-1β stimulates the production of PGE_2 in large quantities, and this could induce the degradation process of OA. At the molecular level, IL-1β will increase the expression of the COX-2 gene and the microsomal prostaglandin E synthase-1 at mRNA and protein levels. Therefore, an increase in PGE_2 production is related to mPGES-1 and COX-2 derivatives from osteoarthritis chondrocytes stimulated by IL-1β. Another recent study has shown the beneficial effects of resolvin D1 on OA chondrocytes. RvD1 belongs to the family of D-series Rvs, which includes RvD2–RvD6 and share the common precursor 17-HDHA. In one study, RvD1 was found to inhibit the IL-1β-mediated upregulation of COX-2, PGE_2, MMP13, and nitric oxide and to prevent chemically induced apoptosis in human osteoarthritis chondrocytes [155]. These effects are mediated by the downregulation of the nuclear factor NF-kB, p38-MAPK, and c-Jun N-terminal kinases activation, as well as inactivation of caspase9 and upregulation of Bcl-2 and Akt. Despite the high concentrations of RvD1 used in this study (mM range), these data indicate for the first time the potency of an SPM to counteract deleterious processes in OA chondrocytes. MSCs have been demonstrated to be effective in the treatments of different tissue injuries and, in particular, they have been considered as a promising alternative cell source for cartilage repair [156]. However, recent studies have suggested that the beneficial effects of MSCs on injured tissues could be attributed to the activation of a protective mechanism and the stimulation of endogenous regeneration rather than to their differentiation potential [157]. MSC-secreted bioactive molecules and/or EVs may act as paracrine or endocrine mediators that directly activate target cells or neighboring cells to secrete functionally active agents. Indeed, we recently demonstrated the therapeutic potential of ASCs secretome and EVs both in vitro on TNFα-stimulated articular chondrocytes [158,159], and in vivo in a mouse model of OA [160], providing evidences of MSC mediated anti-inflammatory and immunomodulatory action. Consistently, the influence of MSCs towards PGE_2 gene expression was studied in the pathogenesis of OA. One study showed that MSCs could significantly ($p < 0.05$) reduce PGE_2 expression in OA synoviocytes after 24 and 48 h co-culture compared to control cells [161]. Moreover, several researches disclosed that MSC-derived EVs stimulate tissue regeneration [162], and EVs have generally important functions in cell communication and regulation. EVs are home to the inflammatory site and transfer proteins/peptides, mRNA, microRNA, lipids, or organelles with reparative and anti-inflammatory properties [161,163]. Lipids are essential components of the EVs membranes, and it is well known that specific lipids are enriched in EVs compared to their parent cells. For example, it has been shown a 2–3 times enrichment from cells to EVs for cholesterol, GPLs, and PSs [164,165]. On the contrarily, EVs generally contained less PCs than their parent cells. At the moment, the physiological importance of the asymmetric lipids distribution between EVs and parent cells is still largely unknown. Compared to the original BMSCs, Xiang et al. found out that MSC-EVs were highly enriched in the cell proliferation and migration mediator S1P by the involvement of sphingosine kinase 1 (SK1) [166]. In detail, human chondrocytes were co-cultured with MSC-EVs showing enhanced proliferation and decreased apoptosis induced by IL-1β, known as one of the main inflammatory mediators for arthritis. The highlighted MSC-EVs therapeutic effect occurs in part through the S1P/S1P receptor 1 (S1PR1) signaling pathway activation. So, also this study suggests the implication of lipids and their related pathways (i.e., S1P/S1PR1) into the clinical application of MSC-EVs to the treatment of articular cartilage defect. Future lipidomic research, aimed at characterizing the lipid mediators of the crosstalk among MSCs and other articular cell types (e.g., chondrocytes, synoviocytes, or osteoblasts), would likely uncover additional inflammatory pathways associated with OA, with interesting repercussions in the clinical management of this pathology.

4. Conclusions

In the last few years, lipidomics has gathered the interest of the scientific community because of the recently confirmed role of lipids in several biochemical aspects as first actors. In detail, lipids are recognized as key players in cells membrane and signaling

processes, such as inflammation and immunomodulation. Furthermore, cell lipidome changes according to different cell phases and microenvironment features. Therefore, by analyzing differences in profiles of specific lipid species, it is possible to obtain insights regarding lipids interference in cell signaling and other cellular mechanisms. Lipidomics has proved being successful in identifying viable and functional cell cultures, which could guarantee efficient and safe MSCs application. Despite the limited availability of data regarding MSC lipidomics, the pleiotropic biological actions of different lipid families indicate them as promising candidates for future therapeutic interventions.

Author Contributions: Conceptualization, S.C., C.G., A.T.B.; investigation, S.C.; data curation, S.C.; writing—original draft preparation, S.C.; writing—review and editing, S.C., C.G., R.F.B., S.N., M.O., A.T.B.; visualization, S.C., C.G., S.N.; supervision, M.O., A.T.B. All authors have read and agreed to the published version of the manuscript.

Funding: This research received no external funding.

Data Availability Statement: No new data were created or analyzed in this study. Data sharing is not applicable to this article.

Acknowledgments: The authors acknowledge support from the University of Milan through the APC initiative.

Conflicts of Interest: The authors declare that they have no conflict of interest.

Abbreviations

2-AG 2-arachidonoilglycerol; AA arachidonic acid; AEA anandamide; ALP alkaline phosphatase activity; ASCs adipose-derived stem cells; BM bone marrow; BMSCs bone marrow-derived stem cells; C1P ceramide 1-phosphate; CB cannabinoid receptors; CBD cannabidiol; COL1a1 collagen type I α 1; COVID-19 coronavirus disease 2019; COX cyclooxygenases; DHA docosahexaenoic acid; DHEA N-docosahexaenoylethanolamine; eCB endocannabinoids; EETs epoxyeicosatrienoic acids; EPA eicosapentaenoic acid; EPEA N-eicosapentaenoylethanolamine; ETEs epoxyeicosatrienoids; EVs extracellular vesicles; FAs fatty acids; FM-MSC fetal membrane-derived stem cells; GC gas chromatography; GPCR G protein-coupled receptor; GPLs glycerophospholipids; GPLs glycerophospholipids; HETEs hydroxyeicosatetraenoic acids; HPLC-MS liquid chromatography coupled to mass spectrometry; IBSP integrin-binding sialoprotein; IFN-γ interferon gamma; LC liquid chromatography; LGPLs lysoglycerophospholipids; LOX lipoxygenases; LPA lysophosphatidic acid; LPCs lysophosphatidylcholines; LPEs lysophosphatidylethanolamines; LPIs lysophosphatidylinositols; LPLs lysophospholipids; LPSs lysophosphatidylserines; LSLs lysosphingophospholipids; LTs leukotrienes; LXs lipoxins; MaRs maresins; MDSCs skeletal muscle-derived stem cells; MS mass spectrometry; MSCs mesenchymal stem cells; MUFAs monounsaturated fatty acids; NADA N-arachidonoyldopine; NAEs N-acylethanolamines; NAGly N-arachidonoylglycine; OA osteoarthritis; OCN osteocalcin; OSX osterix; PA phoshatidic acid; PDs protectins; PEA N-palmitoylethanolamide; PGs prostaglandins; PIs phosphatidylinositols; PPARα receptor peroxisome proliferator-activated receptor-α; PSs phosphatidylserines; PUFAs; polyunsaturated fatty acids; RUNX2 runt-related transcription factor 2; Rvs resolvins; S1P sphingosine 1-phosphate; SEA N-stearoylethanolamide; SFAs saturated fatty acids; SK sphingosine kinases; SLs sphingolipids; SPMs specialized pro-resolving mediators; SPP1 secreted phosphoprotein 1; THC delta9-tetrahydrocannabinol; TLC thin-layer chromatography; TNF-α tumor necrosis factor alpha; TRPV1 transient receptor potential vanilloid type 1; TXs thromboxanes; UCMSCs umbilical cord blood-derived MSCs; ω-3 PUFAs omega-3 polyunsaturated fatty acids; ω-6 PUFAs omega-3 polyunsaturated fatty acids.

References

1. Fahy, E.; Subramaniam, S.; Murphy, R.C.; Nishijima, M.; Raetz, C.R.H.; Shimizu, T.; Spener, F.; Van Meer, G.; Wakelam, M.J.O.; Dennis, E.A. Update of the LIPID MAPS comprehensive classification system for lipids. *J. Lipid Res.* **2009**, *50*, S9–S14. [CrossRef]
2. Fahy, E.; Cotter, D.; Sud, M.; Subramaniam, S. Lipid classification, structures and tools. *Biochim. Biophys. Acta (BBA) Mol. Cell Biol. Lipids* **2011**, *1811*, 637–647. [CrossRef]
3. García-Cañaveras, J.C.; Peris-Díaz, M.D.; Alcoriza-Balaguer, M.I.; Cerdán-Calero, M.; Donato, M.T.; Lahoz, A. A lipidomic cell-based assay for studying drug-induced phospholipidosis and steatosis. *Electrophoresis* **2017**, *38*, 2331–2340. [CrossRef]
4. Lydic, T.; Goo, Y.-H. Lipidomics unveils the complexity of the lipidome in metabolic diseases. *Clin. Transl. Med.* **2018**, *7*, 4. [CrossRef]
5. Sethi, S.; Brietzke, E. Recent advances in lipidomics: Analytical and clinical perspectives. *Prostaglandins Other Lipid Mediat.* **2017**, *128–129*, 8–16. [CrossRef]
6. Nguyen, V.L.; Haber, P.; Seth, D. Applications and Challenges for the Use of Phosphatidylethanol Testing in Liver Disease Patients (Mini Review). *Alcohol. Clin. Exp. Res.* **2018**, *42*, 238–243. [CrossRef]
7. German, J.B.; Gillies, L.A.; Smilowitz, J.T.; Zivkovic, A.M.; Watkins, S.M. Lipidomics and lipid profiling in metabolomics. *Curr. Opin. Lipidol.* **2007**, *18*, 66–71.
8. Wenk, M.R. The emerging field of lipidomics. *Nat. Rev. Drug Discov.* **2005**, *4*, 594–610. [CrossRef]
9. Wenk, M.R. Lipidomics: New Tools and Applications. *Cell* **2010**, *143*, 888–895. [CrossRef]
10. Schwudke, D.; Shevchenko, A.; Hoffmann, N.; Ahrends, R. Lipidomics informatics for life-science. *J. Biotechnol.* **2017**, *261*, 131–136. [CrossRef]
11. Shevchenko, A.; Simons, K. Lipidomics: Coming to grips with lipid diversity. *Nat. Rev. Mol. Cell Biol.* **2010**, *11*, 593–598. [CrossRef]
12. Li, L.; Han, J.; Wang, Z.; Liu, J.; Wei, J.; Xiong, S.; Zhao, Z. Mass Spectrometry Methodology in Lipid Analysis. *Int. J. Mol. Sci.* **2014**, *15*, 10492–10507. [CrossRef]
13. Yang, K.; Han, X. Lipidomics: Techniques, Applications, and Outcomes Related to Biomedical Sciences. *Trends Biochem. Sci.* **2016**, *41*, 954–969. [CrossRef]
14. Casati, S.; Giannasi, C.; Minoli, M.; Niada, S.; Ravelli, A.; Angeli, I.; Mergenthaler, V.; Ottria, R.; Ciu, P.; Orioli, M.; et al. Quantitative Lipidomic Analysis of Osteosarcoma Cell-Derived Products by UHPLC-MS/MS. *Biomolecules* **2020**, *10*, 1302. [CrossRef]
15. Locke, M.; Windsor, J.; Dunbar, P.R. Human adipose-derived stem cells: Isolation, characterization and applications in surgery. *ANZ J. Surg.* **2009**, *79*, 235–244. [CrossRef]
16. Strem, B.M.; Hicok, K.C.; Zhu, M.; Wulur, I.; Alfonso, Z.; Schreiber, R.E.; Fraser, J.K.; Hedrick, M.H. Multipotential differentiation of adipose tissue-derived stem cells. *Keio J. Med.* **2005**, *54*, 132–141. [CrossRef]
17. Dominici, M.; Le Blanc, K.; Mueller, I.; Slaper-Cortenbach, I.; Marini, F.; Krause, D.; Deans, R.; Keating, A.; Prockop, D.; Horwitz, E. Minimal criteria for defining multipotent mesenchymal stromal cells. The International Society for Cellular Therapy position statement. *Cytotherapy* **2006**, *8*, 315–317. [CrossRef]
18. Horwitz, E.M.; Le Blanc, K.; Dominici, M.; Mueller, I.; Slaper-Cortenbach, I.; Marini, F.C.; Deans, R.J.; Krause, D.S.; Keating, A. Clarification of the nomenclature for MSC: The International Society for Cellular Therapy position statement. *Cytotherapy* **2005**, *7*, 393–395. [CrossRef]
19. Glassberg, M.K.; Minkiewicz, J.; Toonkel, R.L.; Simonet, E.S.; Rubio, G.A.; DiFede, D.; Shafazand, S.; Khan, A.; Pujol, M.V.; LaRussa, V.F.; et al. Allogeneic Human Mesenchymal Stem Cells in Patients with Idiopathic Pulmonary Fibrosis via Intravenous Delivery (AETHER): A Phase I Safety Clinical Trial. *Chest* **2017**, *151*, 971–981. [CrossRef]
20. Lindsay, J.O.; Allez, M.; Clark, M.; Labopin, M.; Ricart, E.; Rogler, G.; Rovira, M.; Satsangi, J.; Farge, D.; Hawkey, C.J.; et al. Autologous stem-cell transplantation in treatment-refractory Crohn's disease: An analysis of pooled data from the ASTIC trial. *Lancet Gastroenterol. Hepatol.* **2017**, *2*, 399–406. [CrossRef]
21. Shi, Y.; Wang, Y.; Li, Q.; Liu, K.; Hou, J.; Shao, C.; Wang, Y. Immunoregulatory mechanisms of mesenchymal stem and stromal cells in inflammatory diseases. *Nat. Rev. Nephrol.* **2018**, *14*, 493–507. [CrossRef] [PubMed]
22. Mehta, P.; McAuley, D.F.; Brown, M.; Sanchez, E.; Tattersall, R.S.; Manson, J.J. COVID-19: Consider cytokine storm syndromes and immunosuppression. *Lancet* **2020**, *395*, 1033–1034. [CrossRef]
23. Golchin, A.; Seyedjafari, E.; Ardeshirylajimi, A. Mesenchymal Stem Cell Therapy for COVID-19: Present or Future. *Stem Cell Rev. Rep.* **2020**, *16*, 427–433. [CrossRef] [PubMed]
24. Gowen, A.; Shahjin, F.; Chand, S.; Odegaard, K.E.; Yelamanchili, S.V. Mesenchymal Stem Cell-Derived Extracellular Vesicles: Challenges in Clinical Applications. *Front. Cell Dev. Biol.* **2020**, *8*, 149. [CrossRef] [PubMed]
25. Sagini, K.; Costanzi, E.; Emiliani, C.; Buratta, S.; Urbanelli, L. Extracellular Vesicles as Conveyors of Membrane-Derived Bioactive Lipids in Immune System. *Int. J. Mol. Sci.* **2018**, *19*, 1227. [CrossRef]
26. Harrell, C.R.; Fellabaum, C.; Jovicic, N.; Djonov, V.; Arsenijevic, N.; Volarevic, V. Molecular Mechanisms Responsible for Therapeutic Potential of Mesenchymal Stem Cell-Derived Secretome. *Cells* **2019**, *8*, 467. [CrossRef]
27. English, K. Mechanisms of mesenchymal stromal cell immunomodulation. *Immunol. Cell Biol.* **2013**, *91*, 19–26. [CrossRef]
28. Aggarwal, S.; Pittenger, M.F. Human mesenchymal stem cells modulate allogeneic immune cell responses. *Blood* **2005**, *105*, 1815–1822. [CrossRef]

29. Bernardo, M.E.; Locatelli, F.; Fibbe, W.E. Mesenchymal Stromal Cells. *Ann. N. Y. Acad. Sci.* **2009**, *1176*, 101–117. [CrossRef]
30. Bernardo, M.E.; Cometa, A.M.; Pagliara, D.; Vinti, L.; Rossi, F.; Cristantielli, R.; Palumbo, G.; Locatelli, F. Ex vivo expansion of mesenchymal stromal cells. *Best Pract. Res. Clin. Haematol.* **2011**, *24*, 73–81. [CrossRef]
31. Mushahary, D.; Spittler, A.; Kasper, C.; Weber, V.; Charwat, V. Isolation, cultivation, and characterization of human mesenchymal stem cells. *Cytom. Part A* **2018**, *93*, 19–31. [CrossRef]
32. Baer, P.C.; Geiger, H. Adipose-Derived Mesenchymal Stromal/Stem Cells: Tissue Localization, Characterization, and Heterogeneity. *Stem Cells Int.* **2012**, *2012*, 1–11. [CrossRef]
33. Bertozzi, N.; Simonacci, F.; Grieco, M.P.; Grignaffini, E.; Raposio, E. The biological and clinical basis for the use of adipose-derived stem cells in the field of wound healing. *Ann. Med. Surg.* **2017**, *20*, 41–48. [CrossRef]
34. Kokai, L.E.; Marra, K.; Rubin, J.P. Adipose stem cells: Biology and clinical applications for tissue repair and regeneration. *Transl. Res.* **2014**, *163*, 399–408. [CrossRef]
35. Muhammad, G.; Xu, J.; Bulte, J.; Jablonska, A.; Walczak, P.; Janowski, M. Transplanted adipose-derived stem cells can be short-lived yet accelerate healing of acid-burn skin wounds: A multimodal imaging study. *Sci. Rep.* **2017**, *7*, 1–11. [CrossRef]
36. Pavyde, E.; Maciulaitis, R.; Mauricas, M.; Sudzius, G.; Didziokiene, E.I.; Laurinavicius, A.; Sutkeviciene, N.; Stankevicius, E.; Maciulaitis, J.; Usas, A. Skeletal Muscle-Derived Stem/Progenitor Cells: A Potential Strategy for the Treatment of Acute Kidney Injury. *Stem Cells Int.* **2016**, *2016*. [CrossRef]
37. Jankowski, R.J.; Deasy, B.M.; Huard, J. Muscle-derived stem cells. *Gene Ther.* **2002**, *9*, 642–647. [CrossRef]
38. Ceusters, J.; Lejeune, J.P.J.; Sandersen, C.C.; Niesten, A.; Lagneaux, L.; Serteyn, D.D. From skeletal muscle to stem cells: An innovative and minimally-invasive process for multiple species. *Sci. Rep.* **2017**, *7*, 1–9. [CrossRef]
39. Shimizu, T. Lipid Mediators in Health and Disease: Enzymes and Receptors as Therapeutic Targets for the Regulation of Immunity and Inflammation. *Annu. Rev. Pharmacol. Toxicol.* **2009**, *49*, 123–150. [CrossRef]
40. Leuti, A.; Fazio, D.; Fava, M.; Piccoli, A.; Oddi, S.; Maccarrone, M. Bioactive lipids, inflammation and chronic diseases. *Adv. Drug Deliv. Rev.* **2020**, *159*, 133–169. [CrossRef]
41. Chiurchiù, V.; Leuti, A.; Maccarrone, M. Bioactive Lipids and Chronic Inflammation: Managing the Fire Within. *Front. Immunol.* **2018**, *9*, 38. [CrossRef]
42. Chiurchiù, V.; Battistini, L.; Maccarrone, M. Endocannabinoid signalling in innate and adaptive immunity. *Immunology* **2015**, *144*, 352–364. [CrossRef]
43. Chiurchiù, V.; Maccarrone, M. Bioactive lipids as modulators of immunity, inflammation and emotions. *Curr. Opin. Pharmacol.* **2016**, *29*, 54–62. [CrossRef]
44. Maceyka, M.; Spiegel, S. Sphingolipid metabolites in inflammatory disease. *Nat. Cell Biol.* **2014**, *510*, 58–67. [CrossRef]
45. Smith, W.L.; DeWitt, D.L.; Garavito, R.M. Cyclooxygenases: Structural, Cellular, and Molecular Biology. *Annu. Rev. Biochem.* **2000**, *69*, 145–182. [CrossRef]
46. Stitham, J.; Midgett, C.R.; Martin, K.A.; Hwa, J. Prostacyclin: An Inflammatory Paradox. *Front. Pharmacol.* **2011**, *2*, 24. [CrossRef]
47. Mandal, A.K.; Jones, P.B.; Bair, A.M.; Christmas, P.; Miller, D.; Yamin, T.-T.D.; Wisniewski, D.; Menke, J.; Evans, J.F.; Hyman, B.T.; et al. The nuclear membrane organization of leukotriene synthesis. *Proc. Natl. Acad. Sci. USA* **2008**, *105*, 20434–20439. [CrossRef]
48. Murphy, R.; Gijón, M.A. Biosynthesis and metabolism of leukotrienes. *Biochem. J.* **2007**, *405*, 379–395. [CrossRef]
49. Serhan, C.N. Pro-resolving lipid mediators are leads for resolution physiology. *Nature* **2014**, *510*, 92–101. [CrossRef]
50. Dennis, E.A.; Norris, P.C. Eicosanoid storm in infection and inflammation. *Nat. Rev. Immunol.* **2015**, *15*, 511–523. [CrossRef]
51. Aoki, T.; Narumiya, S. Prostaglandins and chronic inflammation. *Trends Pharmacol. Sci.* **2012**, *33*, 304–311. [CrossRef]
52. Narumiya, S.; Furuyashiki, T. Fever, inflammation, pain and beyond: Prostanoid receptor research during these 25 years. *FASEB J.* **2010**, *25*, 813–818. [CrossRef]
53. Honda, T.; Segi-Nishida, E.; Miyachi, Y.; Narumiya, S. Prostacyclin-IP signaling and prostaglandin E2-EP2/EP4 signaling both mediate joint inflammation in mouse collagen-induced arthritis. *J. Exp. Med.* **2006**, *203*, 325–335. [CrossRef]
54. Hirata, T.; Narumiya, S. *Chapter Five—Prostanoids as Regulators of Innate and Adaptive Immunity*; Elsevier: Amsterdam, The Netherlands, 2012; Volume 116.
55. Yao, C.; Sakata, D.; Esaki, Y.; Li, Y.; Matsuoka, T.; Kuroiwa, K.; Sugimoto, Y.; Narumiya, S. Prostaglandin E2–EP4 signaling promotes immune inflammation through TH1 cell differentiation and TH17 cell expansion. *Nat. Med.* **2009**, *15*, 633–640. [CrossRef]
56. Chen, Q.; Muramoto, K.; Masaaki, N.; Ding, Y.; Yang, H.; Mackey, M.F.; Li, W.; Inoue, Y.; Ackermann, K.; Shirota, H.; et al. A novel antagonist of the prostaglandin E2 EP4 receptor inhibits Th1 differentiation and Th17 expansion and is orally active in arthritis models. *Br. J. Pharmacol.* **2010**, *160*, 292–310. [CrossRef]
57. Gilroy, D.W.; Bishop-Bailey, D. Lipid mediators in immune regulation and resolution. *Br. J. Pharmacol.* **2019**, *176*, 1009–1023. [CrossRef]
58. Chiurchiù, V.; Leuti, A.; Dalli, J.; Jacobsson, A.; Battistini, L.; Maccarrone, M.; Serhan, C.N. Proresolving lipid mediators resolvin D1, resolvin D2, and maresin 1 are critical in modulating T cell responses. *Sci. Transl. Med.* **2016**, *8*, 353ra111. [CrossRef]
59. Schwab, J.M.; Chiang, N.; Arita, M.; Serhan, C.N. Resolvin E1 and protectin D1 activate inflammation-resolution programmes. *Nat. Cell Biol.* **2007**, *447*, 869–874. [CrossRef]
60. Serhan, C.N.; Chiang, N. Resolution phase lipid mediators of inflammation: Agonists of resolution. *Curr. Opin. Pharmacol.* **2013**, *13*, 632–640. [CrossRef]

61. Serhan, C.N.; Chiang, N.; Dalli, J. The resolution code of acute inflammation: Novel pro-resolving lipid mediators in resolution. *Semin. Immunol.* **2015**, *27*, 200–215. [CrossRef]
62. Miyahara, T.; Runge, S.; Chatterjee, A.; Chen, M.; Mottola, G.; Fitzgerald, J.M.; Serhan, C.N.; Conte, M.S. D-series resolvin attenuates vascular smooth muscle cell activation and neointimal hyperplasia following vascular injury. *FASEB J.* **2013**, *27*, 2220–2232. [CrossRef]
63. Basil, M.C.; Levy, B.D. Specialized pro-resolving mediators: Endogenous regulators of infection and inflammation. *Nat. Rev. Immunol.* **2016**, *16*, 51–67. [CrossRef]
64. Stables, M.J.; Gilroy, D.W. Old and new generation lipid mediators in acute inflammation and resolution. *Prog. Lipid Res.* **2011**, *50*, 35–51. [CrossRef]
65. Herlong, J.; Scott, T. Positioning prostanoids of the D and J series in the immunopathogenic scheme. *Immunol. Lett.* **2006**, *102*, 121–131. [CrossRef]
66. Bannenberga, G.; Serhanb, C.N. Specialized Pro-Resolving Lipid Mediators in the Inflammatory Response: An Update. *Biochim. Biophys. Acta (BBA)* **2010**, *1801*, 1260–1273. [CrossRef]
67. Spector, A.A.; Fang, X.; Snyder, G.D.; Weintraub, N.L. Epoxyeicosatrienoic acids (EETs): Metabolism and biochemical function. *Prog. Lipid Res.* **2004**, *43*, 55–90. [CrossRef]
68. Ligresti, A.; De Petrocellis, L.; Di Marzo, V. From Phytocannabinoids to Cannabinoid Receptors and Endocannabinoids: Pleiotropic Physiological and Pathological Roles Through Complex Pharmacology. *Physiol. Rev.* **2016**, *96*, 1593–1659. [CrossRef]
69. Pertwee, R.G. Cannabidiol as a potential medicine. In *Cannabinoids as Therapeutics*; Birkhäuser: Basel, Switzerland, 2005. [CrossRef]
70. Di Marzo, V. Targeting the endocannabinoid system: To enhance or reduce? *Nat. Rev. Drug Discov.* **2008**, *7*, 438–455. [CrossRef]
71. Devane, W.A.; Hanus, L.; Breuer, A.; Pertwee, R.G.; Stevenson, L.A.; Griffin, G.; Gibson, D.; Mandelbaum, A.; Etinger, A.; Mechoulam, R. Isolation and structure of a brain constituent that binds to the cannabinoid receptor. *Science* **1992**, *258*, 1946–1949. [CrossRef]
72. Sugiura, T.; Kondo, S.; Sukagawa, A.; Nakane, S.; Shinoda, A.; Itoh, K.; Yamashita, A.; Waku, K. 2-Arachidonoylgylcerol: A Possible Endogenous Cannabinoid Receptor Ligand in Brain. *Biochem. Biophys. Res. Commun.* **1995**, *215*, 89–97. [CrossRef]
73. Mechoulam, R.; Ben-Shabat, S.; Hanus, L.; Ligumsky, M.; Kaminski, N.E.; Schatz, A.R.; Gopher, A.; Almog, S.; Martin, B.R.; Compton, D.R.; et al. Identification of an endogenous 2-monoglyceride, present in canine gut, that binds to cannabinoid receptors. *Biochem. Pharmacol.* **1995**, *50*, 83–90. [CrossRef]
74. Ribeiro, A.; Pontis, S.; Mengatto, L.; Armirotti, A.; Chiurchiù, V.; Capurro, V.; Fiasella, A.; Nuzzi, A.; Romeo, E.; Moreno-Sanz, G.; et al. A Potent Systemically Active *N*-Acylethanolamine Acid Amidase Inhibitor that Suppresses Inflammation and Human Macrophage Activation. *ACS Chem. Biol.* **2015**, *10*, 1838–1846. [CrossRef]
75. Maestroni, G.J.M. The endogenous cannabinoid 2-arachidonoyl glycerol as in vivo chemoattractant for dendritic cells and adjuvant for Th1 response to a soluble protein. *FASEB J.* **2004**, *18*, 1914–1916. [CrossRef]
76. Gallily, R.; Breuer, A.; Mechoulam, R. 2-Arachidonylglycerol, an endogenous cannabinoid, inhibits tumor necrosis factor-α production in murine macrophages, and in mice. *Eur. J. Pharmacol.* **2000**, *406*, R5–R7. [CrossRef]
77. Barrie, N.; Manolios, N. The endocannabinoid system in pain and inflammation: Its relevance to rheumatic disease. *Eur. J. Rheumatol.* **2017**, *4*, 210–218. [CrossRef]
78. Artmann, A.; Petersen, G.; Hellgren, L.I.; Boberg, J.; Skonberg, C.; Nellemann, C.L.; Hansen, S.H.; Hansen, H.S. Influence of dietary fatty acids on endocannabinoid and *N*-acylethanolamine levels in rat brain, liver and small intestine. *Biochim. Biophys. Acta (BBA) Mol. Cell Biol. Lipids* **2008**, *1781*, 200–212. [CrossRef]
79. Lucanic, M.; Held, J.M.; Vantipalli, M.C.; Klang, I.M.; Graham, J.B.; Gibson, B.W.; Lithgow, G.J.; Gill, M.S. *N*-acylethanolamine signalling mediates the effect of diet on lifespan in Caenorhabditis elegans. *Nat. Cell Biol.* **2011**, *473*, 226–229. [CrossRef]
80. Brown, I.; Cascio, M.G.; Wahle, K.W.; Smoum, R.; Mechoulam, R.; Ross, R.A.; Pertwee, R.G.; Heys, S.D. Cannabinoid receptor-dependent and -independent anti-proliferative effects of omega-3 ethanolamides in androgen receptor-positive and -negative prostate cancer cell lines. *Carcinogenesis* **2010**, *31*, 1584–1591. [CrossRef]
81. Meijerink, J.; Plastina, P.; Vincken, J.-P.; Poland, M.; Attya, M.; Balvers, M.G.J.; Gruppen, H.; Gabriele, B.; Witkamp, R.F. The ethanolamide metabolite of DHA, docosahexaenoylethanolamine, shows immunomodulating effects in mouse peritoneal and RAW264.7 macrophages: Evidence for a new link between fish oil and inflammation. *Br. J. Nutr.* **2011**, *105*, 1798–1807. [CrossRef]
82. Piomelli, D. More surprises lying ahead. The endocannabinoids keep us guessing. *Neuropharmacology* **2014**, *76*, 228–234. [CrossRef]
83. Payahoo, L.; Khajebishak, Y.; Ostadrahimi, A. Oleoylethanolamide: A novel pharmaceutical agent in the management of obesity-an updated review. *J. Cell. Physiol.* **2019**, *234*, 7893–7902. [CrossRef]
84. TuTunchi, H.; Saghafi-Asl, M.; Ostadrahimi, A. A systematic review of the effects of oleoylethanolamide, a high-affinity endogenous ligand of PPAR-α, on the management and prevention of obesity. *Clin. Exp. Pharmacol. Physiol.* **2020**, *47*, 543–552. [CrossRef] [PubMed]
85. Raso, G.M.; Russo, R.; Calignano, A.; Meli, R. Palmitoylethanolamide in CNS health and disease. *Pharmacol. Res.* **2014**, *86*, 32–41. [CrossRef] [PubMed]
86. Petrosino, S.; Di Marzo, V. The pharmacology of palmitoylethanolamide and first data on the therapeutic efficacy of some of its new formulations. *Br. J. Pharmacol.* **2017**, *174*, 1349–1365. [CrossRef] [PubMed]

87. Ryberg, E.; Larsson, N.; Sjögren, S.; Hjorth, S.; Hermansson, N.-O.; Leonova, J.; Elebring, T.; Nilsson, K.; Drmota, T.; Greasley, P.J. The orphan receptor GPR55 is a novel cannabinoid receptor. *Br. J. Pharmacol.* **2007**, *152*, 1092–1101. [CrossRef]
88. Hansen, H.S. Palmitoylethanolamide and other anandamide congeners. Proposed role in the diseased brain. *Exp. Neurol.* **2010**, *224*, 48–55. [CrossRef]
89. Maccarrone, M.; Cartoni, A.; Parolaro, D.; Margonelli, A.; Massi, P.; Bari, M.; Battista, N.; Finazzi-Agrò, A. Cannabimimetic activity, binding, and degradation of stearoylethanolamide within the mouse central nervous system. *Mol. Cell. Neurosci.* **2002**, *21*, 126–140. [CrossRef]
90. Carbonare, M.D.; Del Giudice, E.; Stecca, A.; Colavito, D.; Fabris, M.; D'Arrigo, A.; Bernardini, D.; Dam, M.; León, A. A Saturated *N*-Acylethanolamine Other than *N*-Palmitoyl Ethanolamine with Anti-inflammatory Properties: A Neglected Story. *J. Neuroendocr.* **2008**, *20*, 26–34. [CrossRef]
91. Balvers, M.G.J.; Verhoeckx, K.C.; Witkamp, R.F. Development and validation of a quantitative method for the determination of 12 endocannabinoids and related compounds in human plasma using liquid chromatography–tandem mass spectrometry. *J. Chromatogr. B* **2009**, *877*, 1583–1590. [CrossRef]
92. Han, B.; Wright, R.; Kirchhoff, A.M.; Chester, J.A.; Cooper, B.R.; Davisson, V.J.; Barker, E.L. Quantitative LC–MS/MS analysis of arachidonoyl amino acids in mouse brain with treatment of FAAH inhibitor. *Anal. Biochem.* **2013**, *432*, 74–81. [CrossRef]
93. Burstein, S.; McQuain, C.A.; Ross, A.H.; Salmonsen, R.A.; Zurier, R.E. Resolution of inflammation by N-arachidonoylglycine. *J. Cell. Biochem.* **2011**, *112*, 3227–3233. [CrossRef] [PubMed]
94. Burstein, S.; Adams, J.K.; Bradshaw, H.B.; Fraioli, C.; Rossetti, R.G.; Salmonsen, R.A.; Shaw, J.W.; Walker, J.M.; Zipkin, R.E.; Zurier, R.B. Potential anti-inflammatory actions of the elmiric (lipoamino) acids. *Bioorg. Med. Chem.* **2007**, *15*, 3345–3355. [CrossRef] [PubMed]
95. Parmar, N.; Ho, W.S.V. *N*-arachidonoyl glycine, an endogenous lipid that acts as a vasorelaxant via nitric oxide and large conductance calcium-activated potassium channels. *Br. J. Pharmacol.* **2010**, *160*, 594–603. [CrossRef] [PubMed]
96. McHugh, D.; Hu, S.S.-J.; Rimmerman, N.; Juknat, A.; Vogel, Z.; Walker, J.M.; Bradshaw, H. *N*-arachidonoyl glycine, an abundant endogenous lipid, potently drives directed cellular migration through GPR18, the putative abnormal cannabidiol receptor. *BMC Neurosci.* **2010**, *11*, 44. [CrossRef]
97. Cascio, M.G.; Minassi, A.; Ligresti, A.; Appendino, G.; Burstein, S.; Di Marzo, V. A structure-activity relationship study on N-arachidonoyl-amino acids as possible endogenous inhibitors of fatty acid amide hydrolase. *Biochem. Biophys. Res. Commun.* **2004**, *314*, 192–196. [CrossRef]
98. Goetzl, E.J.; Graeler, M.; Huang, M.-C.; Shankar, G. Lysophospholipid Growth Factors and Their G Protein-Coupled Receptors in Immunity, Coronary Artery Disease, and Cancer. *Sci. World J.* **2002**, *2*, 324–338. [CrossRef]
99. Huang, M.-C.; Graeler, M.; Shankar, G.; Spencer, J.; Goetzl, E.J. Lysophospholipid mediators of immunity and neoplasia. *Biochim. Biophys. Acta (BBA) Mol. Cell Biol. Lipids* **2002**, *1582*, 161–167. [CrossRef]
100. Makide, K.; Kitamura, H.; Sato, Y.; Okutani, M.; Aoki, J. Emerging lysophospholipid mediators, lysophosphatidylserine, lysophosphatidylthreonine, lysophosphatidylethanolamine and lysophosphatidylglycerol. *Prostaglandins Other Lipid Mediat.* **2009**, *89*, 135–139. [CrossRef]
101. Sevastou, I.; Kaffe, E.; Mouratis, M.; Aidinis, V. Lysoglycerophospholipids in chronic inflammatory disorders: The PLA2/LPC and ATX/LPA axes. *Biochim. Biophys. Acta (BBA) Mol. Cell Biol. Lipids* **2013**, *1831*, 42–60. [CrossRef]
102. Gault, C.R.; Obeid, L.M.; Hannun, Y.A. An Overview of Sphingolipid Metabolism: From Synthesis to Breakdown. In *Sphingolipids as Signaling and Regulatory Molecules*; Springer: New York, NY, USA, 2010. [CrossRef]
103. McArthur, S.; Gobbetti, T.; Kusters, D.H.M.; Reutelingsperger, C.P.; Flower, R.J.; Perretti, M. Definition of a Novel Pathway Centered on Lysophosphatidic Acid to Recruit Monocytes during the Resolution Phase of Tissue Inflammation. *J. Immunol.* **2015**, *195*, 1139–1151. [CrossRef]
104. El Alwani, M.; Wu, B.X.; Obeid, L.M.; Hannun, Y.A. Bioactive sphingolipids in the modulation of the inflammatory response. *Pharmacol. Ther.* **2006**, *112*, 171–183. [CrossRef]
105. Gomez-Muñoz, A.; Presa, N.; Gomez-Larrauri, A.; Rivera, I.-G.; Trueba, M.; Ordoñez, M. Control of inflammatory responses by ceramide, sphingosine 1-phosphate and ceramide 1-phosphate. *Prog. Lipid Res.* **2016**, *61*, 51–62. [CrossRef]
106. Bartke, N.; Hannun, Y.A. Bioactive sphingolipids: Metabolism and function. *J. Lipid Res.* **2009**, *50*, S91–S96. [CrossRef]
107. Weichand, B.; Weis, N.; Weigert, A.; Grossmann, N.; Levkau, B.; Brüne, B. Apoptotic cells enhance sphingosine-1-phosphate receptor 1 dependent macrophage migration. *Eur. J. Immunol.* **2013**, *43*, 3306–3313. [CrossRef]
108. Yanes, O.; Clark, J.; Wong, D.M.; Patti, G.J.; Sánchez-Ruiz, A.; Benton, H.P.; Trauger, S.A.; Desponts, C.; Ding, S.; Siuzdak, G. Metabolic oxidation regulates embryonic stem cell differentiation. *Nat. Chem. Biol.* **2010**, *6*, 411–417. [CrossRef]
109. Knobloch, M.; Braun, S.M.G.; Zurkirchen, L.; Von Schoultz, C.; Zamboni, N.; Araúzo-Bravo, M.J.; Kovacs, W.J.; Karalay, Ö.; Suter, U.; Machado, R.A.C.; et al. Metabolic control of adult neural stem cell activity by Fasn-dependent lipogenesis. *Nat. Cell Biol.* **2013**, *493*, 226–230. [CrossRef]
110. Clémot, M.; Demarco, R.S.; Jones, D.L. Lipid Mediated Regulation of Adult Stem Cell Behavior. *Front. Cell Dev. Biol.* **2020**, *8*, 115. [CrossRef]
111. Kilpinen, L.; Tigistu-Sahle, F.; Oja, S.; Greco, D.; Parmar, A.; Saavalainen, P.; Nikkilä, J.; Korhonen, M.; Lehenkari, P.; Käkelä, R.; et al. Aging bone marrow mesenchymal stromal cells have altered membrane glycerophospholipid composition and functionality. *J. Lipid Res.* **2013**, *54*, 622–635. [CrossRef]

112. Chatgilialoglu, A.; Rossi, M.; Alviano, F.; Poggi, P.; Zannini, C.; Marchionni, C.; Ricci, F.; Tazzari, P.L.; Taglioli, V.; Calder, P.C.; et al. Restored in vivo-like membrane lipidomics positively influence in vitro features of cultured mesenchymal stromal/stem cells derived from human placenta. *Stem Cell Res. Ther.* **2017**, *8*, 1–11. [CrossRef]
113. Lu, X.; Chen, Y.; Wang, H.; Bai, Y.; Zhao, J.; Zhang, X.; Liang, L.; Chen, Y.; Ye, C.; Li, Y.; et al. Integrated Lipidomics and Transcriptomics Characterization upon Aging-Related Changes of Lipid Species and Pathways in Human Bone Marrow Mesenchymal Stem Cells. *J. Proteome Res.* **2019**, *18*, 2065–2077. [CrossRef]
114. Wagner, W.; Horn, P.; Castoldi, M.; Diehlmann, A.; Bork, S.; Saffrich, R.; Benes, V.; Blake, J.; Pfister, S.; Eckstein, V.; et al. Replicative Senescence of Mesenchymal Stem Cells: A Continuous and Organized Process. *PLoS ONE* **2008**, *3*, e2213. [CrossRef]
115. Gharibi, B.; Hughes, F.J. Effects of Medium Supplements on Proliferation, Differentiation Potential, and In Vitro Expansion of Mesenchymal Stem Cells. *Stem Cells Transl. Med.* **2012**, *1*, 771–782. [CrossRef] [PubMed]
116. Jang, M.W.; Yun, S.P.; Park, J.H.; Ryu, J.M.; Lee, J.H.; Han, H.J. Cooperation of Epac1/Rap1/Akt and PKA in prostaglandin E2-induced proliferation of human umbilical cord blood derived mesenchymal stem cells: Involvement of c-Myc and VEGF expression. *J. Cell. Physiol.* **2012**, *227*, 3756–3767. [CrossRef] [PubMed]
117. Yun, S.P.; Ryu, J.M.; Jang, M.W.; Han, H.J. Interaction of profilin-1 and F-actin via a β-arrestin-1/JNK signaling pathway involved in prostaglandin E2-induced human mesenchymal stem cells migration and proliferation. *J. Cell. Physiol.* **2010**, *226*, 559–571. [CrossRef] [PubMed]
118. Ern, C.; Frasheri, I.; Berger, T.; Kirchner, H.; Heym, R.; Hickel, R.; Folwaczny, M. Effects of prostaglandin E2 and D2 on cell proliferation and osteogenic capacity of human mesenchymal stem cells. *Prostaglandins Leukot. Essent. Fat. Acids* **2019**, *151*, 1–7. [CrossRef]
119. Yun, D.H.; Song, H.Y.; Lee, M.J.; Kim, M.R.; Kim, M.Y.; Lee, J.S.; Kim, J.H. Thromboxane A2modulates migration, proliferation, and differentiation of adipose tissue-derived mesenchymal stem cells. *Exp. Mol. Med.* **2009**, *41*, 17–24. [CrossRef]
120. Kim, M.R.; Jeon, E.S.; Kim, Y.M.; Lee, J.S.; Kim, J.H. Thromboxane A2Induces Differentiation of Human Mesenchymal Stem Cells to Smooth Muscle-Like Cells. *Stem Cells* **2009**, *27*, 191–199. [CrossRef]
121. Rossi, F.; Bernardo, M.E.; Bellini, G.; Luongo, L.; Conforti, A.; Manzo, I.; Guida, F.; Cristino, L.; Imperatore, R.; Petrosino, S.; et al. The Cannabinoid Receptor Type 2 as Mediator of Mesenchymal Stromal Cell Immunosuppressive Properties. *PLoS ONE* **2013**, *8*, e80022. [CrossRef]
122. Köse, S.; Aerts-Kaya, F.S.F.; Köprü, Ç.Z.; Nemutlu, E.; Kuşkonmaz, B.; Karaosmanoğlu, B.; Taşkıran, E.Z.; Altun, B.; Çetinkaya, D.U.; Korkusuz, P. Human bone marrow mesenchymal stem cells secrete endocannabinoids that stimulate in vitro hematopoietic stem cell migration effectively comparable to beta-adrenergic stimulation. *Exp. Hematol.* **2018**, *57*, 30–41.e1. [CrossRef]
123. Ivanov, I.; Borchert, P.; Hinz, B. A simple method for simultaneous determination of *N*-arachidonoylethanolamine, N-oleoylethanolamine, *N*-palmitoylethanolamine and 2-arachidonoylglycerol in human cells. *Anal. Bioanal. Chem.* **2014**, *407*, 1781–1787. [CrossRef] [PubMed]
124. Scutt, A.; Williamson, E.M. Cannabinoids Stimulate Fibroblastic Colony Formation by Bone Marrow Cells Indirectly via CB2 Receptors. *Calcif. Tissue Int.* **2007**, *80*, 50–59. [CrossRef]
125. Galve-Roperh, I.; Chiurchiù, V.; Díaz-Alonso, J.; Bari, M.; Guzmán, M.; Maccarrone, M. Cannabinoid receptor signaling in progenitor/stem cell proliferation and differentiation. *Prog. Lipid Res.* **2013**, *52*, 633–650. [CrossRef]
126. Sun, Y.-X.; Xu, A.-H.; Yang, Y.; Zhang, J.-X.; Yu, A.-W. Activation of Cannabinoid Receptor 2 Enhances Osteogenic Differentiation of Bone Marrow Derived Mesenchymal Stem Cells. *BioMed Res. Int.* **2015**, *2015*, 1–8. [CrossRef]
127. Xu, A.; Yang, Y.; Shao, Y.; Wu, M.; Sun, Y. Activation of cannabinoid receptor type 2-induced osteogenic differentiation involves autophagy induction and p62-mediated Nrf2 deactivation. *Cell Commun. Signal.* **2020**, *18*, 9–11. [CrossRef]
128. Ahn, S.; Yi, S.; Seo, W.J.; Lee, M.J.; Song, Y.K.; Baek, S.Y.; Yu, J.; Hong, S.H.; Lee, J.; Shin, D.W.; et al. A Cannabinoid Receptor Agonist *N*-Arachidonoyl Dopamine Inhibits Adipocyte Differentiation in Human Mesenchymal Stem Cells. *Biomol. Ther.* **2015**, *23*, 218–224. [CrossRef]
129. Bellocchio, L.; Cervino, C.; Vicennati, V.; Pasquali, R.; Pagotto, U. Cannabinoid Type 1 Receptor: Another Arrow in the Adipocytes' Bow. *J. Neuroendocr.* **2008**, *20*, 130–138. [CrossRef]
130. Karaliota, S.; Siafaka-Kapadai, A.; Gontinou, C.; Psarra, K.; Mavri-Vavayanni, M. Anandamide Increases the Differentiation of Rat Adipocytes and Causes PPARγ and CB1 Receptor Upregulation. *Obesity* **2009**, *17*, 1830–1838. [CrossRef]
131. Pagano, C.; Pilon, C.; Calcagno, A.; Urbanet, R.; Rossato, M.; Milan, G.; Bianchi, K.; Rizzuto, R.; Bernante, P.; Federspil, G.; et al. The Endogenous Cannabinoid System Stimulates Glucose Uptake in Human Fat Cells via Phosphatidylinositol 3-Kinase and Calcium-Dependent Mechanisms. *J. Clin. Endocrinol. Metab.* **2007**, *92*, 4810–4819. [CrossRef]
132. Da Silva, C.G.; Barretto, L.S.D.S.; Turco, E.G.L.; Santos, A.D.L.; Lessio, C.; Júnior, H.A.M.; De Almeida, F.G. Lipidomics of mesenchymal stem cell differentiation. *Chem. Phys. Lipids* **2020**, *232*, 232. [CrossRef]
133. Griffin, M.; Elliman, S.; Cahill, E.; English, K.; Ceredig, R.; Ritter, T. Concise Review: Adult Mesenchymal Stromal Cell Therapy for Inflammatory Diseases: How Well Are We Joining the Dots? *Stem Cells Regen. Med.* **2013**, *31*, 2033–2041. [CrossRef]
134. Campos, A.M.; Maciel, E.; Moreira, A.S.P.; Sousa, B.; Melo, T.; Domingues, P.; Curado, L.; Antunes, B.; Domingues, M.D.R.; Dos Santos, F. Lipidomics of Mesenchymal Stromal Cells: Understanding the Adaptation of Phospholipid Profile in Response to Pro-Inflammatory Cytokines. *J. Cell. Physiol.* **2016**, *231*, 1024–1032. [CrossRef]

135. Cunningham, T.J.; Yao, L.; Lucena, A. Product inhibition of secreted phospholipase A2 may explain lysophosphatidylcholines' unexpected therapeutic properties. *J. Inflamm.* **2008**, *5*, 1–10. [CrossRef]
136. Chen, G.; Li, J.; Qiang, X.; Czura, C.J.; Ochani, M.; Ochani, K.; Ulloa, L.; Yang, H.; Tracey, K.J.; Wang, P.; et al. Suppression of HMGB1 release by stearoyl lysophosphatidylcholine:an additional mechanism for its therapeutic effects in experimental sepsis. *J. Lipid Res.* **2005**, *46*, 623–627. [CrossRef]
137. Olivera, A.; Rivera, J. Sphingolipids and the Balancing of Immune Cell Function: Lessons from the Mast Cell. *J. Immunol.* **2005**, *174*, 1153–1158. [CrossRef]
138. Masoodi, M.; Nicolaou, A. Lipidomic analysis of twenty-seven prostanoids and isoprostanes by liquid chromatography/electrospray tandem mass spectrometry. *Rapid Commun. Mass Spectrom.* **2006**, *20*, 3023–3029. [CrossRef]
139. English, K.; Barry, F.P.; Field-Corbett, C.P.; Mahon, B.P. IFN-γ and TNF-α differentially regulate immunomodulation by murine mesenchymal stem cells. *Immunol. Lett.* **2007**, *110*, 91–100. [CrossRef]
140. Renner, P.; Eggenhofer, E.; Rosenauer, A.; Popp, F.; Steinmann, J.; Slowik, P.; Geissler, E.; Piso, P.; Schlitt, H.; Dahlke, M. Mesenchymal Stem Cells Require a Sufficient, Ongoing Immune Response to Exert Their Immunosuppressive Function. *Transplant. Proc.* **2009**, *41*, 2607–2611. [CrossRef]
141. Fang, X.; Abbott, J.; Cheng, L.; Colby, J.K.; Lee, J.W.; Levy, B.D.; Matthay, M.A. Human Mesenchymal Stem (Stromal) Cells Promote the Resolution of Acute Lung Injury in Part through Lipoxin A_4. *J. Immunol.* **2015**, *195*, 875–881. [CrossRef]
142. Levy, B.D.; Clish, C.B.; Schmidt, B.A.; Gronert, K.; Serhan, C.N. Lipid mediator class switching during acute inflammation: Signals in resolution. *Nat. Immunol.* **2001**, *2*, 612–619. [CrossRef]
143. Lands, W. *Fish, Omega-3 and Human Health*, 2nd ed.; AOCS Publishing: New York, NY, USA, 2005; ISBN 1893997812.
144. Tigistu-Sahle, F.; Lampinen, M.; Kilpinen, L.; Holopainen, M.; Lehenkari, P.; Laitinen, S.; Käkelä, R. Metabolism and phospholipid assembly of polyunsaturated fatty acids in human bone marrow mesenchymal stromal cells. *J. Lipid Res.* **2017**, *58*, 92–110. [CrossRef]
145. Bijlsma, J.W.J.; Berenbaum, F.; Lafeber, F.P.J.G. Osteoarthritis: An update with relevance for clinical practice. *Lancet* **2011**, *377*, 2115–2126. [CrossRef]
146. Loef, M.; Schoones, J.W.; Kloppenburg, M.; Ioan-Facsinay, A. Fatty acids and osteoarthritis: Different types, different effects. *Jt. Bone Spine* **2019**, *86*, 451–458. [CrossRef]
147. Brouwers, H.; Von Hegedus, J.; Toes, R.E.M.; Kloppenburg, M.; Ioan-Facsinay, A. Lipid mediators of inflammation in rheumatoid arthritis and osteoarthritis. *Best Pract. Res. Clin. Rheumatol.* **2015**, *29*, 741–755. [CrossRef]
148. Barnes, I.; Krasnokutsky, S.; Statnikov, A.; Samuels, J.; Li, Z.; Friese, O.; Le Graverand-Gastineau, M.-P.H.; Rybak, L.; Kraus, V.B.; Jordan, J.M.; et al. Low-Grade Inflammation in Symptomatic Knee Osteoarthritis: Prognostic Value of Inflammatory Plasma Lipids and Peripheral Blood Leukocyte Biomarkers. *Arthritis Rheumatol.* **2015**, *67*, 2905–2915. [CrossRef]
149. Scanzello, C.R.; Plaas, A.; Crow, M.K. Innate immune system activation in osteoarthritis: Is osteoarthritis a chronic wound? *Curr. Opin. Rheumatol.* **2008**, *20*, 565–572. [CrossRef]
150. Baker, K.R.; Matthan, N.R.; Lichtenstein, A.; Niu, J.; Guermazi, A.; Roemer, F.; Grainger, A.; Nevitt, M.; Clancy, M.; Lewis, C.E.; et al. Association of plasma n-6 and n-3 polyunsaturated fatty acids with synovitis in the knee: The MOST study. *Osteoarthr. Cartil.* **2012**, *20*, 382–387. [CrossRef]
151. Zainal, Z.; Longman, A.J.; Hurst, S.; Duggan, K.; Caterson, B.; Hughes, C.E.; Harwood, J.L. Relative efficacies of omega-3 polyunsaturated fatty acids in reducing expression of key proteins in a model system for studying osteoarthritis. *Osteoarthr. Cartil.* **2009**, *17*, 896–905. [CrossRef]
152. Wang, Z.; Guo, A.; Ma, L.; Yu, H.; Zhang, L.; Meng, H.; Cui, Y.; Yu, F.; Yang, B. Docosahexenoic acid treatment ameliorates cartilage degeneration via a p38 MAPK-dependent mechanism. *Int. J. Mol. Med.* **2016**, *37*, 1542–1550. [CrossRef]
153. Hardy, M.M.; Seibert, K.; Manning, P.T.; Currie, M.G.; Woerner, B.M.; Edwards, D.; Koki, A.; Tripp, C.S. Cyclooxygenase 2-dependent prostaglandin E2 modulates cartilage proteoglycan degradation in human osteoarthritis explants. *Arthritis Rheum.* **2002**, *46*, 1789–1803. [CrossRef]
154. Shimpo, H.; Sakai, T.; Kondo, S.; Mishima, S.; Yoda, M.; Hiraiwa, H.; Ishiguro, N. Regulation of prostaglandin E2 synthesis in cells derived from chondrocytes of patients with osteoarthritis. *J. Orthop. Sci.* **2009**, *14*, 611–617. [CrossRef]
155. Benabdoun, H.A.; Rondon, E.-P.; Shi, Q.; Fernandes, J.; Ranger, P.; Fahmi, H.; Benderdour, M. The role of resolvin D1 in the regulation of inflammatory and catabolic mediators in osteoarthritis. *Inflamm. Res.* **2016**, *65*, 635–645. [CrossRef]
156. Demoor, M.; Ollitrault, D.; Gomez-Leduc, T.; Bouyoucef, M.; Hervieu, M.; Fabre, H.; Lafont, J.; Denoix, J.-M.; Audigié, F.; Mallein-Gerin, F.; et al. Cartilage tissue engineering: Molecular control of chondrocyte differentiation for proper cartilage matrix reconstruction. *Biochim. Biophys. Acta (BBA) Gen. Subj.* **2014**, *1840*, 2414–2440. [CrossRef]
157. Baraniak, P.R.; McDevitt, T.C. Stem cell paracrine actions and tissue regeneration. *Regen. Med.* **2010**, *5*, 121–143. [CrossRef]
158. Niada, S.; Giannasi, C.; Gomarasca, M.; Stanco, D.; Casati, S.; Brini, A.T. Adipose-derived stromal cell secretome reduces TNFα-induced hypertrophy and catabolic markers in primary human articular chondrocytes. *Stem Cell Res.* **2019**, *38*, 101463. [CrossRef]
159. Giannasi, C.; Niada, S.; Magagnotti, C.; Ragni, E.; Andolfo, A.; Brini, A.T. Comparison of two ASC-derived therapeutics in an in vitro OA model: Secretome versus extracellular vesicles. *Stem Cell Res. Ther.* **2020**, *11*, 1–15. [CrossRef]

160. Amodeo, G.; Niada, S.; Moschetti, G.; Franchi, S.; Savadori, P.; Brini, A.; Sacerdote, P. Human adipose mesenchymal stem cell secretome relieves pain and neuroinflammation independently of the route of administration in the MIA murine model of osteoarthritis. *Brain Behav. Immun.*. Under review.
161. Bruno, S.; Grange, C.; Collino, F.; Deregibus, M.C.; Cantaluppi, V.; Biancone, L.; Tetta, C.; Camussi, G. Microvesicles Derived from Mesenchymal Stem Cells Enhance Survival in a Lethal Model of Acute Kidney Injury. *PLoS ONE* **2012**, *7*, e33115. [CrossRef]
162. Phinney, D.G.; Pittenger, M.F. Concise Review: MSC-Derived Exosomes for Cell-Free Therapy. *Stem Cells* **2017**, *35*, 851–858. [CrossRef]
163. Ratajczak, M.Z. The emerging role of microvesicles in cellular therapies for organ/tissue regeneration. *Nephrol. Dial. Transplant.* **2011**, *26*, 1453–1456. [CrossRef]
164. Haraszti, R.A.; Didiot, M.-C.; Sapp, E.; Leszyk, J.; Shaffer, S.A.; Rockwell, H.E.; Gao, F.; Narain, N.R.; DiFiglia, M.; Kiebish, M.A.; et al. High-resolution proteomic and lipidomic analysis of exosomes and microvesicles from different cell sources. *J. Extracell. Vesicles* **2016**, *5*, 32570. [CrossRef]
165. Llorente, A.; Skotland, T.; Sylvänne, T.; Kauhanen, D.; Róg, T.; Orłowski, A.; Vattulainen, I.; Ekroos, K.; Sandvig, K. Molecular lipidomics of exosomes released by PC-3 prostate cancer cells. *Biochim. Biophys. Acta (BBA) Mol. Cell Biol. Lipids* **2013**, *1831*, 1302–1309. [CrossRef]
166. Xiang, C.; Yang, K.; Liang, Z.; Wan, Y.; Cheng, Y.; Ma, N.; Zhang, H.; Hou, W.; Fu, P. Sphingosine-1-phosphate mediates the therapeutic effects of bone marrow mesenchymal stem cell-derived microvesicles on articular cartilage defect. *Transl. Res.* **2018**, *193*, 42–53. [CrossRef]

Hindawi
Stem Cells International
Volume 2021, Article ID 3086122, 13 pages
https://doi.org/10.1155/2021/3086122

Research Article

Towards Secretome Standardization: Identifying Key Ingredients of MSC-Derived Therapeutic Cocktail

Chiara Giannasi,[1,2] **Stefania Niada**,[2] **Elena Della Morte**,[2] **Sara Casati**,[1] **Marica Orioli**,[1] **Alice Gualerzi**,[3] **and Anna Teresa Brini**[1,2]

[1]*Department of Biomedical, Surgical and Dental Sciences, Università degli Studi di Milano, Milan, Italy*
[2]*IRCCS Istituto Ortopedico Galeazzi, Laboratorio di Applicazioni Biotecnologiche, Milan, Italy*
[3]*IRCCS Fondazione Don Carlo Gnocchi ONLUS, Milano, Italy*

Correspondence should be addressed to Chiara Giannasi; chiara.giannasi@unimi.it

Received 1 June 2021; Revised 2 August 2021; Accepted 7 August 2021; Published 26 August 2021

Academic Editor: Vasilis Paspaliaris

The therapeutic potential of the conditioned medium (CM) derived from MSCs (mesenchymal stem/stromal cells) in disparate medical fields, from immunology to orthopedics, has been widely suggested by *in vitro* and *in vivo* evidences. Prior to MSC-CM use in clinical applications, appropriate quality controls are needed in order to assess its reproducibility. Here, we evaluated different CM characteristics, including general features and precise protein and lipid concentrations, in 3 representative samples from adipose-derived MSCs (ASCs). In details, we first investigated the size and distribution of the contained extracellular vesicles (EVs), lipid bilayer-delimited particles whose pivotal role in intercellular communication has been extensively demonstrated. Then, we acquired Raman signatures, providing an overlook of ASC-CM composition in terms of proteins, lipids, and nucleic acids. At last, we analyzed a panel of 200 molecules including chemokines, cytokines, receptors, and inflammatory and growth factors and searched for 32 lipids involved in cell signalling and inflammation. All ASC-CM contained a homogeneous and relevant number of EVs ($1.0 \times 10^9 \pm 1.1 \times 10^8$ particles per million donor ASCs) with a mean size of 190 ± 5.2 nm, suggesting the appropriateness of the method for EV retaining and concentration. Furthermore, also Raman spectra confirmed a high homogeneity among samples, allowing the visualization of specific peaks for nucleic acids, proteins, and lipids. An in depth investigation that focused on 200 proteins involved in relevant biological pathways revealed the presence in all specimens of 104 factors. Of these, 26 analytes presented a high degree of uniformity, suggesting that the samples were particularly homogenous for a quarter of the quantified molecules. At last, lipidomic analysis allowed the quantification of 7 lipids and indicated prostaglandin-E2 and N-stearoylethanolamide as the most homogenous factors. In this study, we assessed that ASC-CM samples obtained with a standardized protocol present stable features spanning from Raman fingerprint to specific marker concentrations. In conclusion, we identified key ingredients that may be involved in ASC-CM therapeutic action and whose consistent levels may represent a promising quality control in the pipeline of its preparation for clinical applications.

1. Introduction

Over the years, the transplantation of autologous or allogeneic stem cells, either naïve, differently primed, or genetically manipulated, has paved the way to the successful clinical management of several diseases whose pharmacological need was previously unmet. In particular, mesenchymal stem/stromal cells (MSCs), thanks to their regenerative and immunomodulatory potential [1, 2], have gained popularity as cell therapy in disparate clinical scenarios, from immunological diseases [3] to orthopedic conditions [4] and central nervous system injuries and disorders (e.g., traumatic brain injury, Parkinson's disease, and ischemic stroke) [5]. Besides the overall promising results, MSC transplantation (as well as cell-based therapy in general) entails evident drawbacks, such as ethical controversies, concerns linked to ex vivo

expansion and high manufacturing costs. Starting from 2006 with the work of Gnecchi et al. [6], a growing body of evidence identifies paracrine signalling as the main effector of MSC therapeutic action, overturning the initial hypothesis that acknowledged cell engraftment, differentiation, and replacement as the main actors. Consequently, in 2010, Professor Caplan, the father of MSCs who firstly characterized and named them, proposed the new terminology of medicine signalling cells to highlight their secretory nature [7]. The term secretome, coined at the beginning of 2000's by Tjalsma and colleagues [8], defines the plethora of factors of different natures (lipids, nucleic acids, and proteins) secreted by a cell, both freely dissolved and conveyed into extracellular vesicles (EVs). The paradigm shift on MSC mode of action promoted cell secretome, intended both as an entire formula and as selected fractions (i.e., soluble and vesicular subcomponents), to a novel class of biological therapeutics. Indeed, the last few years witnessed the entrance of MSC secretome to several clinical trials, mostly in the regenerative medicine field, retracing the path of the clinical application of donor cells [9]. A critical search through ClinicalTrials.gov database, performed at the end of April 2021 using alternatively the keywords "secretome," "conditioned medium," or "extracellular vesicles" and the filter "interventional" as study type, lists a total of 14 studies based on MSC-secretome administration. Interestingly, most of these protocols relied on the use of CM ($n = 11$ versus $n = 3$ studies using EVs) derived from allogeneic MSCs ($n = 8$ versus $n = 1$ study specifically following an autologous setting). Thus far, only 3 of these studies are completed (NCT04315025, NCT03676400, and NCT04134676), but unluckily, there are no available results yet. Nevertheless, this picture allows us extrapolating some general considerations on the state of the art of MSC-based cell-free therapies:

(i) To date, the clinical use of complete secretome, accounting for both soluble and vesicular fractions, seems more easily applicable than isolated EVs. However, at the moment, EV potential in diagnostics remains pivotal, as confirmed by the high number of clinical trials relying on their use in this field

(ii) Allogeneic settings are widely implemented, confirming the lack of immunogenicity and allowing to minimize interdonor variability and to avoid the need of performing additional procedures on patients for cell harvesting, thus excluding also donor site morbidity

(iii) Donor MSCs are harvested from both neonatal (mostly umbilical cord) and adult (e.g., adipose tissue and bone marrow) tissue sources

(iv) As for MSC-based cell therapy, the nature of the targeted pathologies is extremely various (among others, COVID-19 pneumonia, chronic wounds, alopecia, and osteoarthritis)

It is worth noting that up to now, the regulatory framework for the clinical use of cell secretome, or its subproducts, has not been clearly stated by any national nor international agency such as the FDA or the EMA. In the light of a successful translation to the clinics, there are still many technical issues to be addressed, mainly concerning the mode of action, scalability, standardization, and characterization.

In recent years, our research focused on the investigation of the conditioned medium (CM) from adipose tissue-derived MSCs (ASCs) in terms of biochemical composition [10–13] and therapeutic action, both *in vitro* [14, 15] and *in vivo* [16, 17]. Most of these studies provided the comparison between ASC-CM, consisting of both soluble factors and vesicle-conveyed ones, and ultracentrifuge-isolated EVs. Here, we decided to focus selectively on complete secretome. The present work takes a step forward in the perspective of ASC-CM characterization by quantifying a wide panel of molecules (cytokines, chemokines, receptors, growth and inflammatory factors, and bioactive lipids) in 3 different samples, in order to define some quality control criteria in the light of its future translation into clinics as an innovative cell-free therapeutic.

2. Materials and Methods

2.1. Cell Cultures. ASCs were isolated from the subcutaneous adipose tissue of 3 nonobese (BMI < 30) donors (1 male and 2 females, 54.7 ± 2.3 years old) who underwent total hip replacement surgery ($n = 2$) or liposuction ($n = 1$). All tissues were collected at IRCCS Istituto Ortopedico Galeazzi upon Institutional Review Board approval. Every donor provided a written informed consent. Adipose tissue samples were shredded with a sterile scalpel, digested for 30 min with 0.75 mg/ml type I collagenase (Worthington Biochemical Corporation, Lakewood, NJ, USA), and filtered with a 100 μm cell strainer (Corning Incorporated, Corning, NY, USA). ASCs were grown in a culture medium composed by high-glucose DMEM (Sigma-Aldrich, St. Louis, MO, USA), 10% fetal bovine serum (FBS, Euroclone, Pero, Italy), 2 mM L-glutamine, 50 U/ml penicillin, and 50 μg/ml streptomycin (Sigma-Aldrich, St. Louis, MO, USA) at 37°C, 5% CO_2.

2.2. CM Production. ASCs from V to VII passage at 90% of confluence were incubated in starving conditions (without FBS) for 72 h. No signals of cell suffering were ever recorded during the period. The medium was then collected and centrifuged at 2500 g for 15 min at 4°C with the purpose of eliminating cell debris, dead cells, and large apoptotic bodies. The supernatants were then concentrated about 60 times by centrifuging at 4000 g for 90 min at 4°C in Amicon Ultra-15 Centrifugal Filter Devices with 3 kDa molecular weight cut-off (Merck Millipore, Burlington, MA, USA). This procedure allows the retention of the vesicular component of cell secretome, as previously demonstrated in [12, 13, 15]. The safety and efficacy of the final product obtained through this procedure have been already tested both *in vitro* [14, 15] and *in vivo* [16, 17].

2.3. Nanoparticle Tracking Analysis (NTA). ASC-CM samples were appropriately diluted in 0.22 μm triple-filtered PBS and analyzed by NanoSight NS3000 (Malvern

Panalytical, Salisbury, UK). Three videos, each one lasting 1 min, have been recorded for every sample. All measurements respected the quality criteria of 20-120 particles/-frame, concentration of $10^6 - 4 \times 10^9$ particles/ml, and number of valid tracks > 20%. After capture, the videos have been analyzed by the in-build NanoSight Software NTA.

2.4. Protein Array. Undiluted ASC-CM samples were analyzed by RayBiotech facility (RayBiotech, Norcross, GA, USA). The concentration (pg/ml) of 200 analytes of different natures (cytokines, chemokines, receptors, and inflammatory and growth factors) was investigated using the Quantibody® Human Cytokine Array 4000 Kit, a combination of Human Cytokine Array Q4, Human Chemokine Array Q1, Human Receptor Array Q1, Human Inflammation Array Q3, and Human Growth Factor Array Q1 (https://www.raybiotech.com/quantibody-human-cytokine-array-4000/). Obtained values were normalized on donor cell number (pg/10^6 ASCs).

2.5. Raman Spectroscopy. ASC-CM samples were diluted in sterile saline solution and analyzed with the Raman microspectroscope (LabRAM Aramis, Horiba Jobin Yvon S.A.S., Lille, France) equipped with a 532 nm laser following a previously reported protocol [10, 13]. CM samples were deposited on a calcium fluoride slide and air-dried, and then, measurements were performed in the spectral ranges 600-1800 and 2600-3200 cm^{-1}. At least 15 spectra per sample were acquired and processed (baseline correction, unit vector normalization, and postacquisition calibration) taking advantage of the integrated software LabSpec 6 (Horiba Jobin Yvon S.A.S., Lille, France).

2.6. Targeted UHPLC-MS/MS-Based Lipidomics. Polyunsaturated fatty acids, eicosanoids, endocannabinoids, and N-acylethanolamides were quantified on a QTRAP 5500 triple quadrupole linear ion trap mass spectrometer (Sciex, Darmstadt, Germany) coupled with an Agilent 1200 Infinity pump ultrahigh-pressure liquid chromatography (UHPLC) system (Agilent Technologies, Palo Alto, CA, USA) using the UHPLC-MS/MS methods previously reported [18]. Briefly, undiluted ASC-CM samples (approximately 200 μl/sample) were spiked with deuterated internal standards and 1 ml of cold acetonitrile was added for protein precipitation. After centrifugation, the supernatants were extracted with a 4 ml of dichloromethane/isopropanol (8 : 2; *v*/*v*) and centrifuged again. The organic layer was separated, dried, and reconstituted in 60 μl methanol. 3 μl aliquot was analyzed for endocannabinoids and N-acylethanolamides. The remaining solution was added with 500 μl hydrochloride acid (0.125 N) and 4 ml ethyl acetate/n-hexane (9 : 1; *v*/*v*). The organic phase was dried, and the residue was reconstituted in 60 μl acetonitrile. 30 μl aliquot of methanol obtained from the neutral extraction and 30 μl aliquot from acid extraction were merged, and 10 μl was analyzed for polyunsaturated fatty acids and eicosanoid determination. Data acquisition and processing were performed using Analyst®1.6.2 and MultiQuant®2.1.1 software (Sciex, Darmstadt, Germany), respectively.

2.7. Validation of Selected Proteins and Lipids. The validation of selected proteins was performed on 5 additional ASC-CM samples (deriving from cells harvested from 2 female and 3 male donors, mean age = 54.6 ± 22.3 years old). The Human Magnetic Luminex Screening Assay Rk4yTGNI (R&D Systems, Minneapolis, MN, USA) was customized to contain 5 molecules: MCP-4, PDGF-AA, TNF RI, DKK-1, and RAGE. Duplicates of each ASC-CM (50 μl/sample) were tested, undiluted, and read through Bio-Plex Multiplex System (Bio-Rad, Milan, Italy) following standard procedures. Data analysis was performed with MAGPIX xPONENT 4.2 software (Luminex Corporation, Austin, TX, USA). The validation of SEA and PGE2 levels was performed through the UHPLC-MS/MS methods previously described on the CM derived from 5 additional ASC populations (all female donors, mean age = 49.0 ± 11.1 years old).

2.8. Data Analysis and Statistics. Statistics was performed with GraphPad Prism 7 software (GraphPad Software, La Jolla, CA, USA) and Excel. p values < 0.05 were considered statistically significant. NTA data were analyzed by the Kruskal-Wallis test to evaluate interdonor variability. For the Raman spectra, descriptive and multivariate statistical analyses were performed with Origin2021 (OriginLab, Northampton, MA, USA). Principal component analysis (PCA) was performed to reduce the dimensionality of Raman spectral datasets and to highlight differences between the spectra, with the resulting principal components (PC) representing these spectral differences with increasing percentage of variance. For protein array data, D'Agostino and Pearson omnibus normality test was used to determine whether the samples come from a Gaussian distribution. None of the datasets passed the normality test and correlation (Spearman r), and linear regression analyses were then performed accordingly. Coefficient of variation (CV, also known as relative standard deviation or RSD) was calculated as the ratio of the standard deviation to the mean. A CV < 33% was set as threshold. PCA and clustering were performed by ClustVis (https://biit.cs.ut.ee/clustvis). Process/pathway analysis was performed by STRING (https://string-db.org/) following default settings.

3. Results

CM samples were obtained, as previously described, from the culture medium harvested from confluent ASCs cultured for 3 days in serum-free conditions and concentrated by centrifugal filter devices of about 60 times. Since EVs represent a fundamental component of cell secretome, the first step of CM characterization focused on particle analysis. NTA revealed a similar size distribution between all the samples (Figures 1(a)–1(c)), with a mean EV size of 190 ± 5.2 nm (Figure 1(d)). Mode values (Figure 1(e)) further confirmed the homogeneity between preparations, indicating that the dimensions of the most frequently occurring particle populations ranged from 110 to 150 nm. All samples counted a relevant number of EVs, with an average of $1.0 \times 10^9 \pm 1.1 \times 10^8$ particles per million donor ASCs (Figure 1(f)), confirming the appropriateness of our protocol

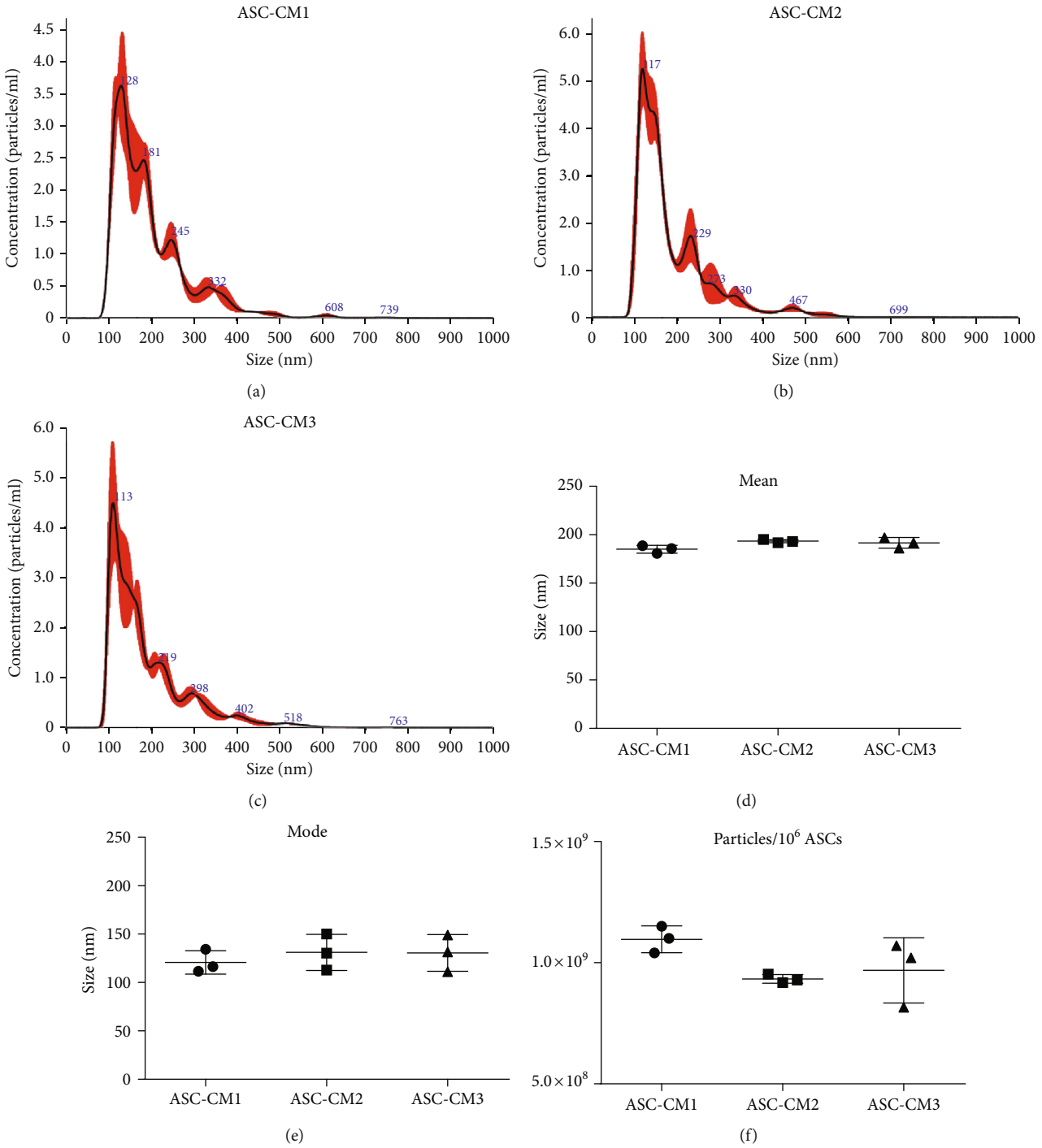

Figure 1: Dimensional characterization and quantification of ASC-CM extracellular vesicles. (a–c) Representative images of NTA referred to ASC-CM1 (a), ASC-CM2 (b), and ASC-CM3 (c). (d–f) Size distribution (d, e) and vesicular yield (f) deriving from 3 NTA measurements/sample. Data are shown as the mean ± SD.

in retaining the vesicular component of cell secretome. No significant difference was observed in any parameter (non-parametric Kruskal-Wallis test, $p > 0.05$).

CM samples were then characterized by Raman spectroscopy, a vibrational spectroscopy method that was already proved to be effective in characterizing the soluble and the vesicular components of MSC secretome, verifying the purity and reproducibility of cell-free preparations [10, 13]. The obtained average spectra (Figure 2(a)) provide detailed biochemical information about the considered samples, with the Raman fingerprint accounting for proteins (amide I 1.650 cm^{-1}), lipids (2700–3200 cm^{-1}), and nucleic acids (720–820 cm^{-1}), in agreement with previously reported data [13]. In particular, CM spectra showed a good signal-to-noise ratio and a good reproducibility, as assessed by the reported standard deviation (gray shaded areas in

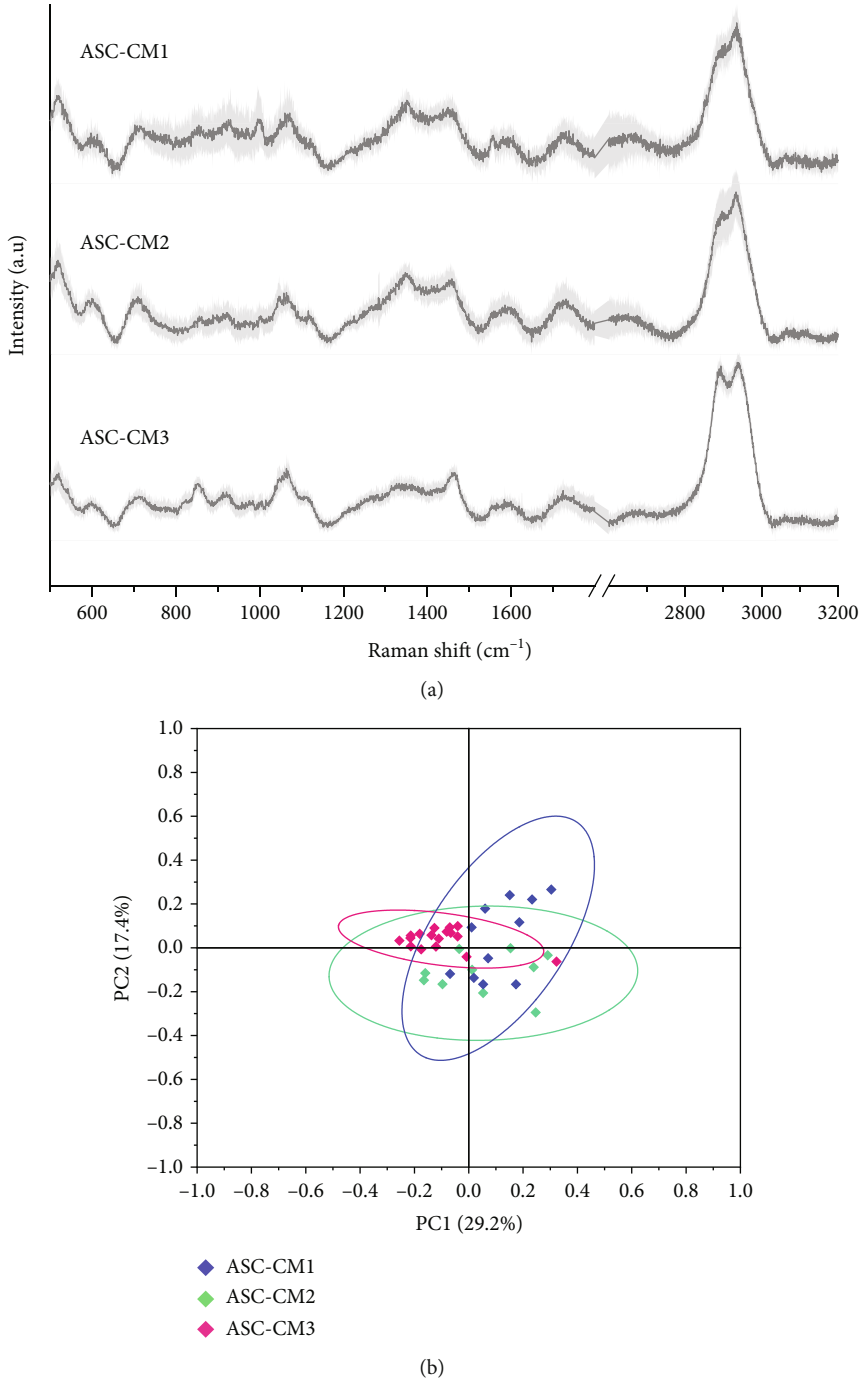

Figure 2: Raman spectroscopy analysis of ASC-CM samples. (a) Average Raman spectra obtained with 532 nm laser line on air-dried drops of ASC-CM samples. Gray shaded areas represent ±1 standard deviation. (b) Scatter plot of the PC1 and PC2 scores obtained for the 3 considered samples after multivariate statistical analysis (PCA). Ellipses represent the 95% confidence intervals calculated for each sample.

Figure 2(a)). The similarities in the chemical composition of the samples were further verified by multivariate statistical analysis: the PC1 and PC2 scores obtained for the three considered samples showed substantial overlap in the reported scatter plot (Figure 2(b)).

In order to identify and quantify putative key factors involved in ASC-CM therapeutic action, we analyzed a panel of 200 chemokines, cytokines, receptors, and inflammatory and growth factors (40 molecules/category). 104 proteins were reliably quantified in all the samples (19 chemokines, 14 cytokines, 24 receptors, and 37 inflammatory and 10 growth factors), while 44 molecules were always undetectable (5 chemokines, 10 cytokines, 7 receptors, and 1 inflammatory and 21 growth factors) (Supplementary Tables 1 and 2). PCA on the 104 quantified factors unveiled a similar heterogeneity across the 3 samples (Figure 3(a)). The heat map further confirmed the lack of major differences among the specimens (Figure 3(b)). Correlation analysis, performed

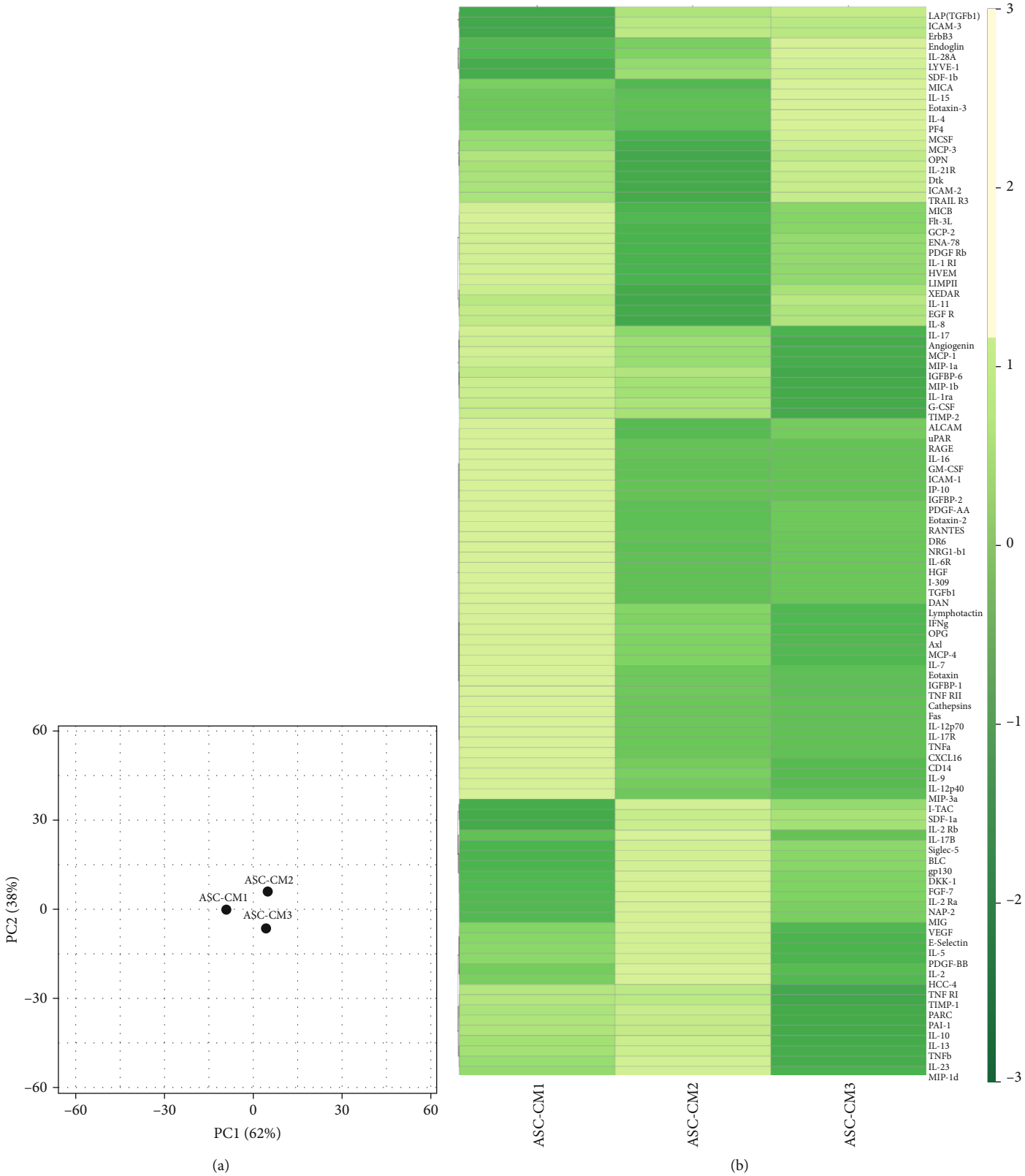

Figure 3: Continued.

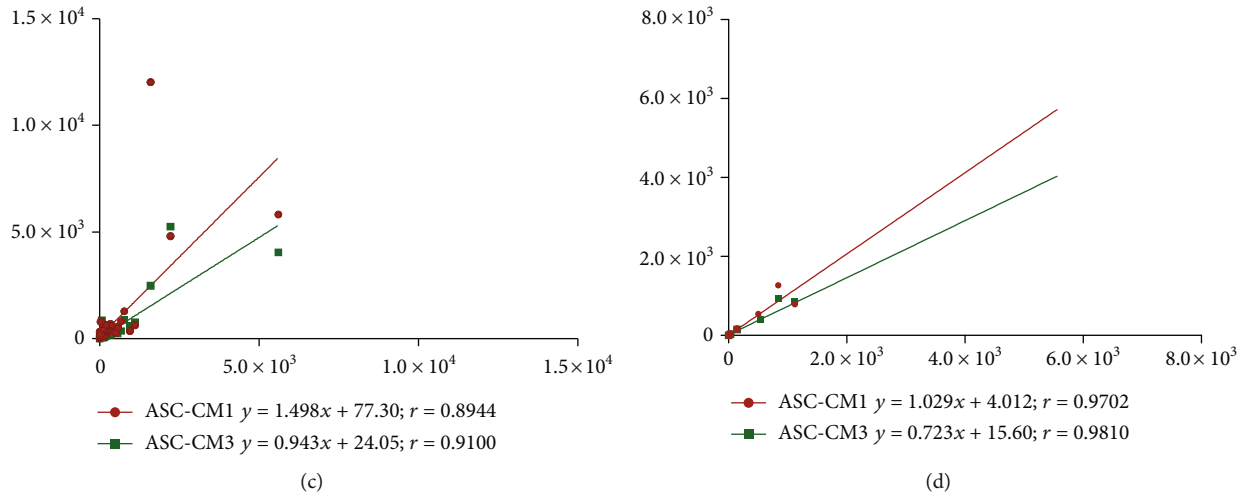

FIGURE 3: Clustering and correlation analysis of the 104 factors quantified in all ASC-CM samples. For the analyses, the levels of each analyte (pg/ml) were normalized on donor cell number and expressed as pg/10^6 ASCs. (a) PCA plot and (b) heat map visualization of the protein levels in ASC-CM1, ASC-CM2, and ASC-CM3. (c, d) Correlation analysis of all the 104 factors (c) and of the 26 molecules (d) having a coefficient of variation below 33% (CV < 33%). For each graph, the equation of the regression lines is reported, together with Spearman r values.

both on the entire datasets (Figure 3(c)) and on 26 selected factors with a coefficient of variation (CV) lower than 33% (Figure 3(d) and Figure 4(a)), showed a strong relationship between the quantitative variables among samples. Indeed, the slope of the regression lines always tended to 1 (Figures 3(c) and 3(d)). Moreover, Spearman r always resulted higher than 0.8, confirming a highly significant direct correlation between specimens (Figures 3(c) and 3(d), nonparametric Spearman correlation, $p < 0.0001$).

Since we aim at suggesting standards for CM quality control, further analyses focused on selected analytes particularly homogeneous across the samples. In details, around 25% ($n = 26$) of the quantified factors presented a CV < 33%, indicating a high degree of uniformity in all CM (Figure 4(a), Supplementary Table 3). Of note, 15 of these were inflammatory factors (Supplementary Table 3). STRING analysis underlined strict interconnections between these factors (Figure 4(b)). As expected, a strong enrichment in proteins involved in immune system regulation emerged by pathway analysis (Supplementary Table 4). In particular, the top 15 pathways ranked by FDR (Figure 4(c)) list proteins involved in cytokine-cytokine interaction (cytokine-cytokine receptor interaction/Jak-STAT signalling pathway) and T cell regulation (T cell receptor signalling pathway/Th1 and Th2 cell differentiation).

Besides proteins, lipids might also exert important roles in immune regulation. For this reason, in our CM samples, we analyzed a panel of endocannabinoids and eicosanoids known to be involved in inflammation. Seven lipid molecules, i.e., arachidonoyl acid (AA), eicosapentaenoyl acid (EPA), docosahexaenoic acid (DHA), prostaglandin-E2 (PGE2), prostaglandin-F2α (PGF2α), N-palmitoylethanolamide (PEA), and N-stearoylethanolamide (SEA) (Supplementary Table 5), were reliably quantified by UHPLC-MS/MS analysis in all ASC-CM samples. Except for 2-arachidonoylglycerol (2AG), quantified in 2 out of 3 samples, the other 24 lipids were always undetectable or unquantifiable (<LODs or LOQs). A coefficient of variation lower than 33% was found for SEA and PGE2 molecules (Figures 5(a) and 5(b), Supplementary Table 5), indicating a good degree of uniformity in the 3 CM. It is interesting to point out that, in CM, bioactive lipid by-products are more homogenous than precursors. This could suggest that mainly the firsts are released in a controlled fashion. Indeed, analyzing the pellets of the donor cells and also the precursors DHA, AA, and EPA presents strongly similar concentrations at intracellular level (Supplementary Table 6).

Since quantifying specific analytes could become a good quality control step for ASC-CM, we analyzed the concentration of a subset of factors in larger validation cohorts ($n = 5$ ASC-CM for both protein and lipid validation). Regarding proteins, our results confirmed both the presence and the homogeneity of the selected factors in all the analyzed samples (Figure 6(a)). Of note, while the mean concentrations of RAGE (18.5 ± 9.3 pg/10^6 ASCs), TNF RI (368.4 ± 78.3 pg/10^6 ASCs), and MCP-4 (19.5 ± 11.6 pg/10^6 ASCs) nicely fit the ones observed in the original set (Figure 4(a)), the detected values for PDGF-AA (3.7 ± 2.9 pg/10^6 ASCs) and DKK-1 (2524.9 ± 734.6 pg/10^6 ASCs) are, respectively, lower and higher than expected. This discrepancy can be attributed to the implementation of distinct immunological techniques that therefore may have a different sensibility and specificity and may rely on the use of antibodies raised against disparate regions of the analytes. Conversely, lipid validation was performed through the same UHPLC-MS/MS methods used to test the original set. As shown in Figure 6(b), SEA (128.2 ± 98.8 pg/10^6 ASCs) and PGE2 (50.8 ± 38.6 pg/10^6 ASCs) were quantified in the entire ASC-CM lipid validation cohort within a concentration range that strongly overlaps what was previously observed (Figure 5(a)).

	pg/10^6ASCs		
	Mean	SD	CV (RSD)
IL-13	0,2	0,0	3%
IFNg	8,0	0,3	4%
MIP-1b (CCL4)	13,7	0,8	6%
RAGE (MOK)	34,5	2,7	8%
PDGF-AA	152,6	12,1	8%
IL-4	0,3	0,0	12%
BLC (CXCL13)	0,1	0,0	13%
IL-5	6,0	1,0	17%
TNF RI (TNFRSF1A)	515,3	88,8	17%
SDF-1a (CXCL12)	10,5	1,9	18%
IGFBP-6	5155,6	972,2	19%
IL-17	0,2	0,0	21%
ALCAM	261,6	59,5	23%
IL-16	0,8	0,2	23%
G-CSF (CSF3)	2,5	0,6	24%
TNFa	7,7	1,8	24%
IL-2	0,5	0,1	24%
GM-CSF (CSF2)	6,6	1,6	25%
TNFb (LTA)	165,7	42,1	25%
LYVE-1	0,3	0,1	27%
uPAR (PLAUR)	980,3	267,6	27%
MCSF (CSF1)	9,9	2,9	30%
IL-2 Ra	13,4	4,0	30%
DKK-1	839,1	251,7	30%
Fas	79,1	25,3	32%
MCP-4 (CCL13)	8,5	2,7	32%

(a)

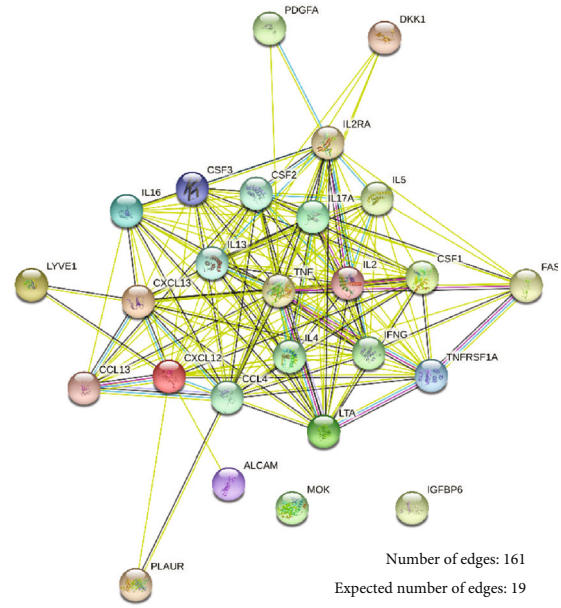

(b)

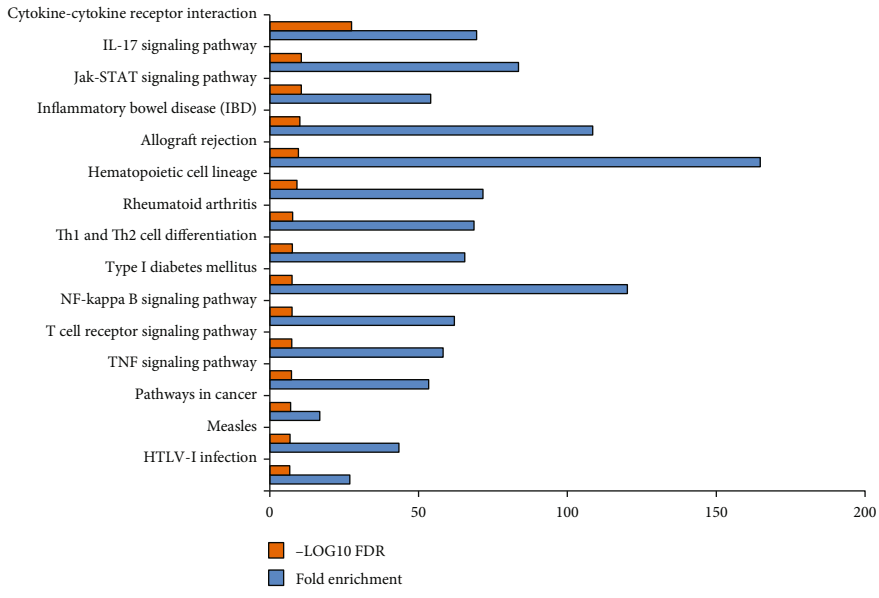

(c)

Figure 4: Protein interactions and functional prediction of the 26 most homogeneous factors quantified in ASC-CM samples. (a) List of the 26 selected factors having a coefficient of variation below 33% (CV < 33%) and (b) corresponding protein-protein interactions uncovered by STRING analysis. (c) Top 15 KEGG pathways associated with the 26 proteins selected based on false discovery rate (FDR) p value ($-\log_{10}$ FDR p values are reported as orange bars). Fold enrichment was calculated as follows: Fold enrichment = (observed protein count/number of most homogeneous factors)/(background gene count/total gene number) and is reported as blue bars.

	pg/10^6 ASCs		
	Mean	SD	CV (RSD)
SEA	157,6	39,4	25%
PGE2	54,1	15,4	28%

(a)

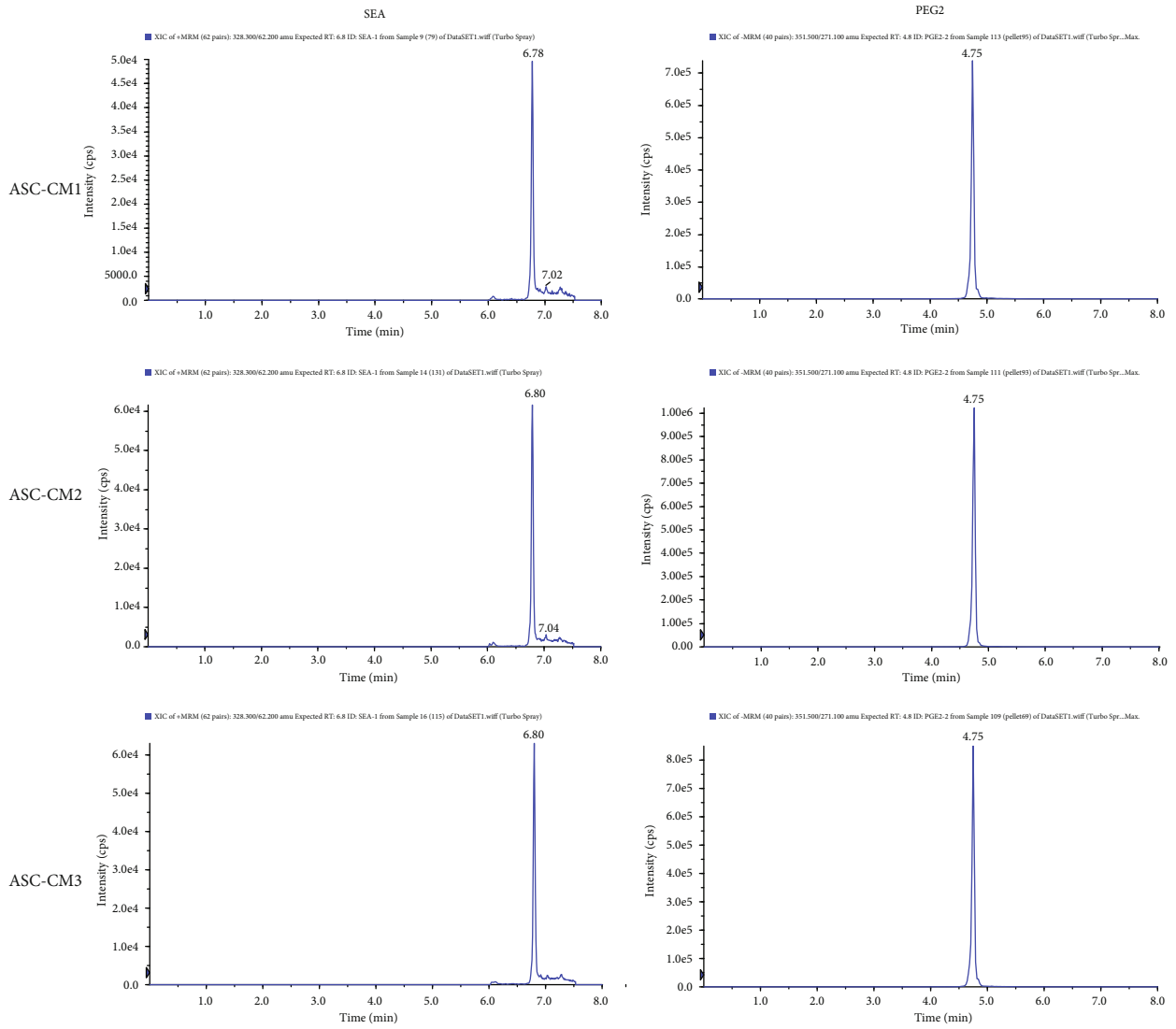

(b)

Figure 5: Lipid levels in ASC-CM samples. (a) Concentration of SEA and PGE2 in ASC-CM and (b) corresponding multiple reaction monitoring (MRM) chromatograms.

4. Discussion

The secretome from mesenchymal stem/stromal cells represents a mixture of biologically active ingredients whose individual role is still unknown. Nevertheless, their synergistic action in producing a clear therapeutic effect supports the rationale for investigating its clinical potential. This study is aimed at defining key elements of ASC secretome produced according to our protocol, which contemplates the culture of 90% confluent cells for 72 hours under serum deprivation and the following concentration of the conditioned medium through 3 kDa molecular weight cut off filters. Other groups currently implement a similar procedure [19, 20], although in literature, there are plenty of alternatives [21]. Therefore, according to the aphorism "the process is the product," any change in the manufacturing process will undoubtedly affect the final product. Moreover, it should be pointed out that ASC-CM thus produced retains a

	pg/10^6 ASCs				
	ASC-CM PV1	ASC-CM PV2	ASC-CM PV3	ASC-CM PV4	ASC-CM PV5
RAGE (MOK)	29,1	21,4	12,3	23,7	5,9
PDGF-AA	1,7	6,3	7,5	1,7	1,4
TNF RI (TNFRSF1A)	356,6	347,4	443,0	441,0	254,1
DKK-1	3593,3	2871,1	2415,0	2004,0	1741,2
MCP-4 (CCL13)	16,3	39,9	13,2	16,9	11,2

(a)

	pg/10^6 ASCs				
	ASC-CM LV1	ASC-CM LV2	ASC-CM LV3	ASC-CM LV4	ASC-CM LV5
SEA	97,8	85,7	116,1	298,3	43,2
PGE2	44,9	34,8	45,9	115,6	12,8

(b)

Figure 6: Validation of selected proteins and lipids. (a) Levels of 5 selected proteins (RAGE, PDGF-AA, TNF RI, DKK-1, and MCP-4) quantified in an ASC-CM protein validation (PV) cohort ($n = 5$). (b) SEA and PGE2 levels confirmed in an ASC-CM lipid validation (LV) cohort ($n = 5$). The levels of each analyte (pg/ml) were normalized on donor cell number and expressed as pg/10^6 ASCs.

substantial number of EVs and indeed previous evidences demonstrated a vesicular yield even higher than the one obtained by ultracentrifugation [13, 15].

Here, we focused on key parameters that could be exploited either as general quality controls, such as vesicular component and Raman signature, or as specific markers, such as the quantification of selected proteins and lipids. A summary of the production process and the proposed quality controls is indicated in Figure 7. For the sake of completeness, even though nucleic acids such as miRNAs were not investigated in the current study, their role has been largely discussed by others (e.g., [22]) making them interesting candidates for additional or alternative quality control checks.

Given the biological relevance of EVs, their determination in CM was the first analysis performed in this study. EVs were abundant in all samples. Their number and size distribution were homogeneous and coherent with previous findings [13, 15]. Of note, the filtration protocol allows the retaining and concentration of the vesicular component with a process that is faster, easier, and less demanding than the gold-standard procedure (i.e., ultracentrifugation) [15]. Since EVs are strategic shuttles for biologicals, we suggest their quantification in CM preparations as a general quality control. Together with EV quantification, also Raman spectroscopy can provide a comprehensive picture of CM composition. It reveals the presence of macromolecules and points out differences and similarities across the samples, as reported here and in a previous study [13].

Differently, the investigation and quantification of selected factors could be adapted according to specific downstream applications.

The broad range analysis on 200 proteins playing pivotal roles in a variety of biological processes highlighted the presence of 26 highly conserved molecules in the 3 ASC-CM. Among these, we chose to validate 5 analytes, each belonging to a different panel: the chemokine MCP-4 (CV = 32%), the cytokine DKK-1 (CV = 30%), the receptor RAGE (CV = 8%), the inflammatory mediator TNF RI (CV = 8%), and the growth factor PDGF-AA (CV = 17%). For all these analytes, a high homogeneity among ASC-CM samples was confirmed. Given our promising *in vitro* [14, 15] and *in vivo* [17] results on the therapeutic action of ASC-CM in counteracting osteoarthritis (OA), herein, we focused our attention on the potential role of each molecule in this frame.

Monocyte chemoattractant protein 4 (MCP-4, also known as CCL13) is a member of the CC chemokine family that displays, besides a strong chemotaxis towards immune cells, a variety of immunomodulatory functions, spanning from induction of cytokine release to antimicrobial activity [23]. Interestingly, MCP-4 can undergo proteolytic cleavage by matrix metalloproteinases (MMPs), resulting in biologically active peptides that exert opposite actions on chemotaxis and inflammation [24]. This aspect is particularly intriguing since the aberrant MMP activity represents one of the milestones of OA progression [25]. In this perspective, ASC-CM therapeutic potential may rely also on the possibility of harnessing the anti-inflammatory properties of MCP-4 metabolites generated in situ by MMPs.

DKK-1 (Dickkopf-1) is a chondroprotective factor, acting as inhibitor of the Wnt/β-catenin signalling pathway. A massive activation of this pathway is involved in diseases like OA [26], where the conditional accumulation of β-catenin affects chondrocytes inducing a hypertrophic phenotype together with the overexpression of MMPs [27]. Interestingly, recent *in vitro* evidences described positive changes in the expression of β-catenin by subchondral osteoblasts following the administration of DKK-1 [28]. Consequently, its abundance in ASC-CM may represent a promising cue in counteracting OA progression.

The receptor for advanced glycation end products (RAGE) appeared remarkably homogenous in ASC-CM

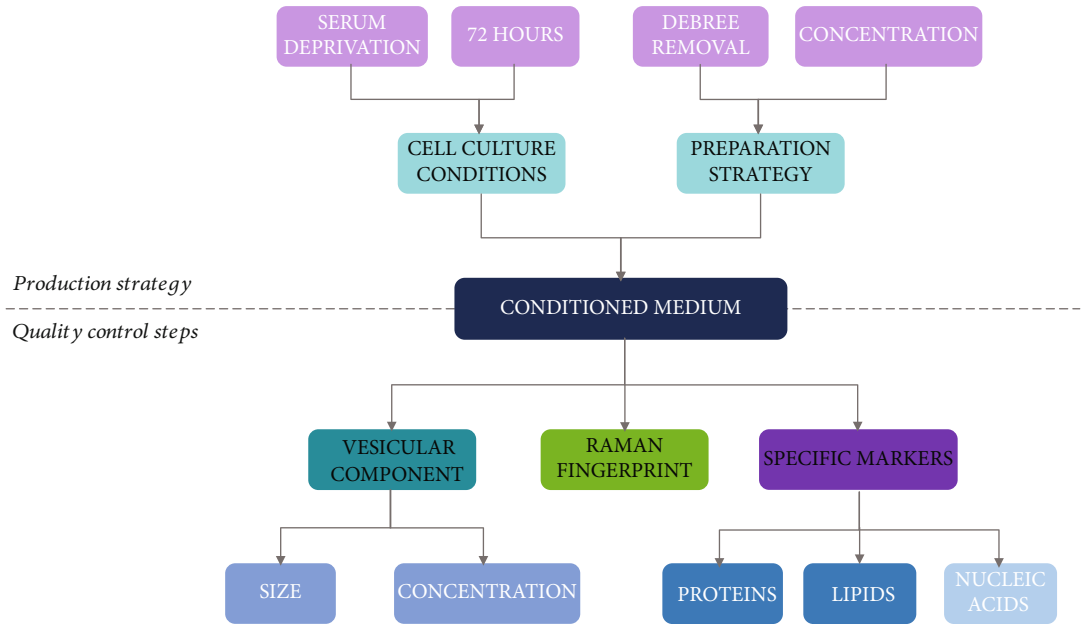

Figure 7: Scheme of our strategy for ASC-CM production together with the proposed quality control steps discussed in the text.

samples. Physiologically and pathologically, this is a transmembrane receptor whose activation by ligand interaction triggers intracellular signalling leading to increased release of reactive oxygen species and proinflammatory cytokines [29]. The presence of RAGE in ASC-CM cannot induce such a response so it might act as a decoy receptor. This could be exploited for the treatment of pathologies presenting a reduction of soluble RAGE (sRAGE, the "conventional" RAGE decoy receptor), together with an increase of its ligands. In OA, a reduction of sRAGE is associated with an increase in AGE levels in the synovial fluid [29, 30]. In this context, we hypothesize that ASC-CM injection in a limited space such as the synovial environment could mitigate the pathological sRAGE/AGE unbalance.

A similar consideration can fit for TFN RI (TNFRSF1A). This receptor is usually involved in the transduction of various inflammatory/stress stimuli by the activation of NF-κB and the consequent transcription of specific genes leading to the production of proinflammatory and catabolic factors [31]. Again, the molecule present in ASC-CM medium cannot trigger these intracellular events while it could compete with cellular receptor. This could be of particular relevance in the treatment of pathologies associated with a relevant increase in TNF, such as rheumatoid arthritis [32], Crohn's disease [33], and OA [34]. In the latter, ASC-CM intra-articular administration could be particularly beneficial since the increase in TNF in the synovial fluid, synovial membrane, cartilage, and subchondral bone is also associated with an increased TNFRI in synovial fibroblasts, further amplifying the noxious signalling [34].

Platelet-derived growth factors (PDGFs) are key players in bone metabolism, and, in particular, PDGF-AA is involved in the crosstalk between subchondral bone and articular cartilage during OA onset [35]. Moreover, recent evidences suggest that PDGF-AA promotes remyelination and increases tissue repair in a rat model of spinal cord injury, overall improving the locomotor functional recovery [36].

Since recently, the involvement of lipids in physiological and pathological processes has been widely demonstrated; in our opinion, their analysis holds paramount importance. With the advent of the next-generation mass spectrometry (MS), significant advances occurred in the field of lipidomics. Our UHPLC-MS/MS method [18] is aimed at profiling a high number of bioactive lipids belonging to structurally similar classes, including polyunsaturated fatty acids, eicosanoids, endocannabinoids, and N-acylethanolamides. Since it is conceivable that these lipids released by ASCs may play a role in inflammatory processes, we performed an absolute quantification of 32 molecules thanks to the high sensitivity and specificity of triple quadrupole mass spectrometry and the use of labeled lipids. Among quantified lipids, SEA and PGE2 showed a relevant uniformity that was therefore validated in a larger ASC-CM cohort. SEA is an endogenous lipid belonging to the N-acylethanolamides family that acts as an anti-inflammatory/immunomodulatory agent through the downregulation of several proinflammatory cytokines [37]. Conversely, PGE2 exerts a well-known inflammatory action. Nevertheless, in the OA context, it can exert either anabolic or catabolic effects on chondrocytes and synoviocytes depending on its concentration [38–40]. Evidence suggests also that PGE2 may have an immune stimulatory role by facilitating Th1 differentiation and expanding Th17 T cells [37].

5. Conclusions

In conclusion, in this work, we identified key ingredients of ASC secretome that may be involved in its therapeutic action and whose stable levels among different ASC-CM

batches may represent promising quality control criteria. Indeed, these indications may be relevant for a rapid and convenient reproducibility assessment of ASC-CM prior its use for different applications.

Nevertheless, we suggest not to focus reservedly on selected components but rather to aim at acquiring an overview of the great complexity of this promising cell-free therapeutic, whose strength relies precisely on the presence of a multitude of biologically active factors of different natures. Here, we propose multiple steps for secretome standardization, either providing an overlook of its composition by NTA and Raman spectroscopy or specifically focusing on the quantification of key molecules of different natures.

Data Availability

All data used to support the findings of this study are included within the supplementary information files and/or are uploaded in zenodo repository (https://doi.org/10.5281/zenodo.5211269) and/or are available from the corresponding author upon request.

Conflicts of Interest

The authors declare that there is no conflict of interest regarding the publication of this paper.

Acknowledgments

The authors would like to thank Dr. Marco Viganò, Dr. Giovanni Lombardi, and Dr. Marta Gomarasca for their precious help. This research was funded by the Italian Ministry of Health (grant numbers RC L1038 and RC L1039, IRCCS Istituto Ortopedico Galeazzi) and by the Department of Biomedical, Surgical and Dental Sciences, University of Milan (grant number RV_PRO_RIC16ABRIN_M).

Supplementary Materials

Supplementary Table 1: protein concentration (pg/ml) of factors quantified in all ASC-CM samples. Supplementary Table 2: list of factors undetectable in all ASC-CM samples. Supplementary Table 3: factors quantified in all ASC-CM samples, normalized on donor cell number, and ranked by coefficient of variation (CV). Supplementary Table 4: KEGG pathway enrichment analysis by STRING (FDR < 0.05). Supplementary Table 5: lipids quantified in all ASC-CM samples, normalized on donor cell number, and ranked by coefficient of variation (CV). Supplementary Table 6: lipids quantified in all ASC pellets, normalized on donor cell number, and ranked by coefficient of variation (CV). *(Supplementary Materials)*

References

[1] M. Wang, Q. Yuan, and L. Xie, "Mesenchymal stem cell-based immunomodulation: properties and clinical application," *Stem Cells International*, vol. 2018, Article ID 3057624, 12 pages, 2018.

[2] X. L. Fan, Y. Zhang, X. Li, and Q. L. Fu, "Mechanisms underlying the protective effects of mesenchymal stem cell-based therapy," *Cellular and Molecular Life Sciences*, vol. 77, no. 14, pp. 2771–2794, 2020.

[3] Y. Shi, Y. Wang, Q. Li, K. Liu, J. Hou, and C. Shao, "Immunoregulatory mechanisms of mesenchymal stem and stromal cells in inflammatory diseases," *Nature Reviews. Nephrology*, vol. 14, no. 8, pp. 493–507, 2018.

[4] R. E. Delanois, J. I. Etcheson, N. Sodhi et al., "Biologic therapies for the treatment of knee osteoarthritis," *The Journal of Arthroplasty*, vol. 34, no. 4, pp. 801–813, 2019.

[5] A. Andrzejewska, S. Dabrowska, B. Lukomska, and M. Janowski, "Mesenchymal stem cells for neurological disorders," *Advanced Science*, vol. 8, no. 7, p. 2002944, 2021.

[6] M. Gnecchi, H. He, N. Noiseux et al., "Evidence supporting paracrine hypothesis for Akt-modified mesenchymal stem cell-mediated cardiac protection and functional improvement," *The FASEB Journal*, vol. 20, no. 6, pp. 661–669, 2006.

[7] A. I. Caplan, "What's in a name?," *Tissue Engineering. Part A*, vol. 16, no. 8, pp. 2415–2417, 2010.

[8] H. Tjalsma, H. Antelmann, J. D. Jongbloed et al., "Proteomics of protein secretion by Bacillus subtilis: separating the "secrets" of the secretome," *Microbiology and Molecular Biology Reviews*, vol. 68, no. 2, pp. 207–233, 2004.

[9] C. R. Harrell, M. G. Jankovic, C. Fellabaum et al., "Molecular mechanisms responsible for anti-inflammatory and immunosuppressive effects of mesenchymal stem cell-derived factors," *Advances in Experimental Medicine and Biology*, vol. 1084, pp. 187–206, 2019.

[10] A. Gualerzi, S. A. A. Kooijmans, S. Niada et al., "Raman spectroscopy as a quick tool to assess purity of extracellular vesicle preparations and predict their functionality," *Journal of extracellular vesicles*, vol. 8, no. 1, 2019.

[11] S. Niada, C. Giannasi, A. Gualerzi, G. Banfi, and A. T. Brini, "Differential proteomic analysis predicts appropriate applications for the secretome of adipose-derived mesenchymal stem/stromal cells and dermal fibroblasts," *Stem Cells International*, vol. 2018, Article ID 7309031, 11 pages, 2018.

[12] S. Niada, C. Giannasi, C. Magagnotti, A. Andolfo, and A. T. Brini, "Proteomic analysis of extracellular vesicles and conditioned medium from human adipose-derived stem/stromal cells and dermal fibroblasts," *Journal of Proteomics*, vol. 232, 2020.

[13] C. Carlomagno, C. Giannasi, S. Niada, M. Bedoni, A. Gualerzi, and A. T. Brini, "Raman fingerprint of extracellular vesicles and conditioned media for the reproducibility assessment of cell-free therapeutics," *Frontiers in Bioengineering and Biotechnology*, vol. 9, 2021.

[14] S. Niada, C. Giannasi, M. Gomarasca, D. Stanco, S. Casati, and A. T. Brini, "Adipose-derived stromal cell secretome reduces TNFα-induced hypertrophy and catabolic markers in primary human articular chondrocytes," *Stem Cell Research*, vol. 38, p. 101463, 2019.

[15] C. Giannasi, S. Niada, C. Magagnotti, E. Ragni, A. Andolfo, and A. T. Brini, "Comparison of two ASC-derived therapeutics in an in vitro OA model: secretome versus extracellular vesicles," *Stem Cell Research & Therapy*, vol. 11, no. 1, p. 521, 2020.

[16] A. T. Brini, G. Amodeo, L. M. Ferreira et al., "Therapeutic effect of human adipose-derived stem cells and their secretome in experimental diabetic pain," *Scientific Reports*, vol. 7, no. 1, p. 9904, 2017.

[17] G. Amodeo, S. Niada, G. Moschetti et al., "Secretome of human adipose-derived mesenchymal stem cell relieves pain and neuroinflammation independently of the route of administration in experimental osteoarthritis," *Brain, Behavior, and Immunity*, vol. 94, pp. 29–40, 2021.

[18] S. Casati, C. Giannasi, M. Minoli et al., "Quantitative lipidomic analysis of osteosarcoma cell-derived products by UHPLC-MS/MS," *Biomolecules*, vol. 10, no. 9, 2020.

[19] B. S. Park, W. S. Kim, J. S. Choi et al., "Hair growth stimulated by conditioned medium of adipose-derived stem cells is enhanced by hypoxia: evidence of increased growth factor secretion," *Biomedical Research*, vol. 31, no. 1, pp. 27–34, 2010.

[20] R. Seetharaman, A. Mahmood, P. Kshatriya, D. Patel, and A. Srivastava, "Mesenchymal stem cell conditioned media ameliorate psoriasis vulgaris: a case study," *Case Reports in Dermatological Medicine*, vol. 2019, Article ID 8309103, 5 pages, 2019.

[21] L. Jia, Q. Xi, H. Wang et al., "miR-142-5p regulates tumor cell PD-L1 expression and enhances anti-tumor immunity," *Biochemical and Biophysical Research Communications*, vol. 488, no. 2, pp. 425–431, 2017.

[22] E. Ragni, C. Perucca Orfei, P. De Luca et al., "Inflammatory priming enhances mesenchymal stromal cell secretome potential as a clinical product for regenerative medicine approaches through secreted factors and EV-miRNAs: the example of joint disease," *Stem Cell Research & Therapy*, vol. 11, no. 1, p. 165, 2020.

[23] E. Mendez-Enriquez and E. A. García-Zepeda, "The multiple faces of CCL13 in immunity and inflammation," *Inflammopharmacology*, vol. 21, no. 6, pp. 397–406, 2013.

[24] G. A. McQuibban, J. H. Gong, J. P. Wong, J. L. Wallace, I. Clark-Lewis, and C. M. Overall, "Matrix metalloproteinase processing of monocyte chemoattractant proteins generates CC chemokine receptor antagonists with anti-inflammatory properties in vivo," *Blood*, vol. 100, no. 4, pp. 1160–1167, 2002.

[25] P. Singh, K. B. Marcu, M. B. Goldring, and M. Otero, "Phenotypic instability of chondrocytes in osteoarthritis: on a path to hypertrophy," *Annals of the New York Academy of Sciences*, vol. 1442, no. 1, pp. 17–34, 2019.

[26] A. B. Blom, S. M. Brockbank, P. L. van Lent et al., "Involvement of the Wnt signaling pathway in experimental and human osteoarthritis: prominent role of Wnt-induced signaling protein 1," *Arthritis and Rheumatism*, vol. 60, no. 2, pp. 501–512, 2009.

[27] R. Yasuhara, Y. Ohta, T. Yuasa et al., "Roles of _β_ -catenin signaling in phenotypic expression and proliferation of articular cartilage superficial zone cells," *Laboratory Investigation*, vol. 91, no. 12, pp. 1739–1752, 2011.

[28] B. Kovács, E. Vajda, and E. E. Nagy, "Regulatory effects and interactions of the Wnt and OPG-RANKL-RANK signaling at the bone-cartilage interface in osteoarthritis," *International journal of molecular sciences*, vol. 20, no. 18, p. 4653, 2019.

[29] M. Chayanupatkul and S. Honsawek, "Soluble receptor for advanced glycation end products (sRAGE) in plasma and synovial fluid is inversely associated with disease severity of knee osteoarthritis," *Clinical Biochemistry*, vol. 43, no. 13-14, pp. 1133–1137, 2010.

[30] M. M. Steenvoorden, T. W. Huizinga, N. Verzijl et al., "Activation of receptor for advanced glycation end products in osteoarthritis leads to increased stimulation of chondrocytes and synoviocytes," *Arthritis and Rheumatism*, vol. 54, no. 1, pp. 253–263, 2006.

[31] G. D. Kalliolias and L. B. Ivashkiv, "TNF biology, pathogenic mechanisms and emerging therapeutic strategies," *Nature Reviews Rheumatology*, vol. 12, no. 1, pp. 49–62, 2016.

[32] M. Feldmann, "Development of anti-TNF therapy for rheumatoid arthritis," *Nature Reviews. Immunology*, vol. 2, no. 5, pp. 364–371, 2002.

[33] S. O. Adegbola, K. Sahnan, J. Warusavitarne, A. Hart, and P. Tozer, "Anti-TNF therapy in Crohn's disease," *International journal of molecular sciences*, vol. 19, no. 8, p. 2244, 2018.

[34] P. Wojdasiewicz, Ł. A. Poniatowski, and D. Szukiewicz, "The role of inflammatory and anti-inflammatory cytokines in the pathogenesis of osteoarthritis," *Mediators of Inflammation*, vol. 2014, Article ID 561459, 19 pages, 2014.

[35] Z. Yao, P. Chen, S. Wang, G. Deng, Y. Hu, and Q. Lin, "Reduced PDGF-AA in subchondral bone leads to articular cartilage degeneration after strenuous running," *Journal of Cellular Physiology*, vol. 234, no. 10, pp. 17946–17958, 2019.

[36] X. Y. Guo, F. X. Duan, J. Chen et al., "Subcutaneous administration of PDGF-AA improves the functional recovery after spinal cord injury," *Frontiers in Neuroscience*, vol. 13, p. 6, 2019.

[37] S. Casati, C. Giannasi, S. Niada, R. F. Bergamaschi, M. Orioli, and A. T. Brini, "Bioactive lipids in MSCs biology: state of the art and role in inflammation," *International Journal of Molecular Sciences*, vol. 22, no. 3, p. 1481, 2021.

[38] K. Nishitani, H. Ito, T. Hiramitsu et al., "PGE2 inhibits MMP expression by suppressing MKK4-JNK MAP kinase-c-JUN pathway via EP4 in human articular chondrocytes," *Journal of Cellular Biochemistry*, vol. 109, no. 2, pp. 425–433, 2010.

[39] M. Attur, H. E. Al-Mussawir, J. Patel et al., "Prostaglandin E2 exerts catabolic effects in osteoarthritis cartilage: evidence for signaling via the EP4 receptor," *Journal of Immunology*, vol. 181, no. 7, pp. 5082–5088, 2008.

[40] M. H. Pillinger, P. B. Rosenthal, S. N. Tolani et al., "Cyclooxygenase-2-derived E prostaglandins down-regulate matrix metalloproteinase-1 expression in fibroblast-like synoviocytes via inhibition of extracellular signal-regulated kinase activation," *Journal of Immunology*, vol. 171, no. 11, pp. 6080–6089, 2003.

Dissemination of result

Publications

- Giannasi C, Niada S, Della Morte E, **Casati S**, Orioli M, Gualerzi A, Brini AT. Towards secretome standardization: identifying key ingredients of MSC-derived therapeutic cocktail. Stem Cells Int. 2021. doi: 10.1155/2021/3086122
- **Casati S**, Giannasi C, Niada S, Bergamaschi RF, Orioli M, Brini AT. Bioactive lipids in MSCs biology: state of the art and role in inflammation. Int. J. Mol. Sci. 2021.doi.org/10.3390/ijms22031481
- **Casati S**, Giannasi C, Minoli M, Niada S, Ravelli A, Angeli I, Ottria R, Ciuffreda P, Orioli M, Brini AT. Quantitative Lipidomic Analysis of Osteosarcoma Cell-Derived Products by UHPLC-MS/MS. Biomolecules. 2020. doi: 10.3390/biom10091302.
- Niada S, Giannasi C, Gomarasca M, Stanco D, **Casati S**, Brini AT. Adipose-derived stromal cell secretome reduces TNFα-induced hypertrophy and catabolic markers in primary human articular chondrocytes. Stem Cell Res. 2019. doi.org/10.1016/j.scr.2019.101463

Meeting reports

Talk (speaker*):

- **Casati S***, Niada S. Analisi lipidomica del secretoma di cellule mesenchimali stromali (MSC) e applicazione in un modello di osteoartrosi in vitro. 1° Incontro Galeazzi Round Robin 2021. IRCCS Istituto Ortopedico Galeazzi. Milan, Italy. 2021 May 20

Poster:

- Giannasi C, Niada S, Della Morte E, **Casati S**, Gualerzi A, Brini A.T. Identification of stable features and key ingredients of a cell-free therapeutic derived from Mesenchymal Stem/Stromal Cells. StemNet. Padua, Italy. 2021 Sep 22-24
- Della Morte E, Giannasi C, Niada S, **Casati S**, Brini AT. Study of cell-free treatments for osteoarthritis from Adipose-derived Stem/Stromal Cells: secretome versus extracellular vesicles. StemNet. Padua, Italy. 2021 Sep 22-24
- Giannasi C, Niada S, **Casati S**, Brini AT. Adipose-derived Stem/Stromal Cell secretome, containing both soluble factors and extracellular vesicles, exerts chondroprotective effects in vitro. ISEV. Kyoto, Japan. 2019 Apr 24-28

- Niada S, Giannasi C, **Casati S**, Brini AT. Adipose-derived Stem/Stromal Cell secretome blunts TNFα-induced hypertrophy on human primary articular chondrocytes. Gruppo Italiano Staminali Mesenchimali (GISM). Genoa, Italy. 2019 Apr 4-5

Summary of the research for the general public

Italian: Questo progetto di ricerca ha riguardato lo studio di alcune classi lipidiche bioattive nel secretoma di cellule mesenchimali stromali e nella successiva valutazione della loro funzione biologica in un modello cellulare di osteoartrosi (OA). L'utilizzo di tecniche analitiche avanzate per la determinazione di queste molecole ha permesso la loro quantificazione in concentrazioni dell'ordine dei pico-nanogrammi. I lipidi sono stati principalmente ricercati nel prodotto di secrezione, cosiddetto secretoma, di alcune cellule mesenchimali stromali, isolate da midollo spinale e da tessuto adiposo di derivazione umana. Tale approccio ha consentito una parziale caratterizzazione dei lipidi contenuti all'interno del secretoma e, in secondo, luogo la definizione della loro concentrazione. Tali evidenze sono state fondamentali per studiare l'attività biologica di due molecole lipidiche riscontrate nel secretoma, il 2-arachinoilglicerolo (2AG) e l'N-palmitoiletanolammina (PEA), in un modello cellulare di OA ottenuto mediante la stimolazione di condrociti primari con uno stimolo infiammatorio. I risultati ottenuti mostrano un effetto pro-infiammatorio del 2AG e un possibile effetto anti-infiammatorio del PEA.

English: This research project involved the study of some bioactive lipid classes in the secretome of mesenchymal stem/stromal cells and the evaluation of their biological function in a cellular model of osteoarthritis (OA). Advanced analytical techniques were used for the determination of lipids, providing their quantification of pico-nanograms concentrations. The lipids were mainly assessed in the secretome of mesenchymal stem/stromal cells, isolated from the human bone marrow or adipose tissue. This approach allowed a partial characterization of the lipids contained within the secretome and, secondly, the definition of their concentration. These findings were crucial to study the biological activity of two lipids found in the secretome, 2-arachinoylglycerol (2AG) and N-palmitoylethanolamine (PEA), in a model of OA obtained by the primary chondrocyte treatment with an inflammatory stimulus. The results showed a potential pro-inflammatory effect of 2AG and a possible anti-inflammatory effect of PEA.